frontiers | Research Topics

Flavors and nutrition in beverages: Formation mechanisms, interactions, and stabilizations

Edited by
Wenjiang Dong, Predrag Putnik, Yuan Liu and Ye Liu

Published in
Frontiers in Nutrition

ISSN 1664-8714
ISBN 978-2-8325-3961-3
DOI 10.3389/978-2-8325-3961-3

About Frontiers

Frontiers is more than just an open access publisher of scholarly articles: it is a pioneering approach to the world of academia, radically improving the way scholarly research is managed. The grand vision of Frontiers is a world where all people have an equal opportunity to seek, share and generate knowledge. Frontiers provides immediate and permanent online open access to all its publications, but this alone is not enough to realize our grand goals.

Frontiers journal series

The Frontiers journal series is a multi-tier and interdisciplinary set of open-access, online journals, promising a paradigm shift from the current review, selection and dissemination processes in academic publishing. All Frontiers journals are driven by researchers for researchers; therefore, they constitute a service to the scholarly community. At the same time, the *Frontiers journal series* operates on a revolutionary invention, the tiered publishing system, initially addressing specific communities of scholars, and gradually climbing up to broader public understanding, thus serving the interests of the lay society, too.

Dedication to quality

Each Frontiers article is a landmark of the highest quality, thanks to genuinely collaborative interactions between authors and review editors, who include some of the world's best academicians. Research must be certified by peers before entering a stream of knowledge that may eventually reach the public - and shape society; therefore, Frontiers only applies the most rigorous and unbiased reviews. Frontiers revolutionizes research publishing by freely delivering the most outstanding research, evaluated with no bias from both the academic and social point of view. By applying the most advanced information technologies, Frontiers is catapulting scholarly publishing into a new generation.

What are Frontiers Research Topics?

Frontiers Research Topics are very popular trademarks of the *Frontiers journals series*: they are collections of at least ten articles, all centered on a particular subject. With their unique mix of varied contributions from Original Research to Review Articles, Frontiers Research Topics unify the most influential researchers, the latest key findings and historical advances in a hot research area.

Find out more on how to host your own Frontiers Research Topic or contribute to one as an author by contacting the Frontiers editorial office: frontiersin.org/about/contact

Flavors and nutrition in beverages: Formation mechanisms, interactions, and stabilizations

Topic editors

Wenjiang Dong — Chinese Academy of Tropical Agricultural Sciences, China
Predrag Putnik — University North, Croatia
Yuan Liu — Shanghai Jiao Tong University, China
Ye Liu — Beijing Technology and Business University, China

Citation

Dong, W., Putnik, P., Liu, Y., Liu, Y., eds. (2023). *Flavors and nutrition in beverages: Formation mechanisms, interactions, and stabilizations*. Lausanne: Frontiers Media SA. doi: 10.3389/978-2-8325-3961-3

Table of contents

04 Evaluating the effect of lactic acid bacteria fermentation on quality, aroma, and metabolites of chickpea milk
Panling Zhang, Fengxian Tang, Wenchao Cai, Xinxin Zhao and Chunhui Shan

17 Roasting treatments affect oil extraction rate, fatty acids, oxidative stability, antioxidant activity, and flavor of walnut oil
Huankang Li, Jiajia Han, Zhongkai Zhao, Jinhu Tian, Xizhe Fu, Yue Zhao, Changqing Wei and Wenyu Liu

30 Metabolomic fingerprinting based on network analysis of volatile aroma compounds during the forced aging of Huangjiu: Effects of dissolved oxygen and temperature
Na Wang, Lili Zhang, Xuejiao Ren, Shuang Chen and Zhen Zhang

42 Impact of tea leaves categories on physicochemical, antioxidant, and sensorial profiles of tea wine
Chun Zou, De-Quan Chen, Hua-Feng He, Yi-Bin Huang, Zhi-Hui Feng, Jian-Xin Chen, Fang Wang, Yong-Quan Xu and Jun-Feng Yin

50 Formation mechanism and functional properties of walnut protein isolate and soy protein isolate nanoparticles using the pH-cycle technology
Yixin Dai, Ying Xu, Chunhe Shi, Ye Liu and Shuang Bi

65 Adding functional properties to beer with jasmine tea extract
De-Quan Chen, Chun Zou, Yi-Bin Huang, Xuan Zhu, Patrizia Contursi, Jun-Feng Yin and Yong-Quan Xu

79 Vinegar: A potential source of healthy and functional food with special reference to sugarcane vinegar
Gan-Lin Chen, Feng-Jin Zheng, Bo Lin, Yu-Xia Yang, Xiao-Chun Fang, Krishan K. Verma and Li-Fang Yang

89 Chemical composition and anti-cholesterol activity of tea (*Camellia sinensis*) flowers from albino cultivars
Ying Gao, Zhen Han, Yong-Quan Xu and Jun-Feng Yin

98 Headspace solid-phase microextraction coupled with gas chromatography-mass spectrometry (HS-SPME-GC-MS) and odor activity value (OAV) to reveal the flavor characteristics of ripened Pu-erh tea by co-fermentation
Yaru Zheng, Chunhua Zhang, Dabing Ren, Ruoxue Bai, Wenting Li, Jintao Wang, Zhiguo Shan, Wenjiang Dong and Lunzhao Yi

109 Unraveling the difference in flavor characteristics of *Huangjiu* fermented with different rice varieties using dynamic sensory evaluation and comprehensive two-dimensional gas chromatography–quadrupole mass spectrometry
Haiyan Yu, Qiaowei Li, Wei Guo, Lianzhong Ai, Chen Chen and Huaixiang Tian

frontiers | Frontiers in Nutrition

TYPE Original Research
PUBLISHED 05 December 2022
DOI 10.3389/fnut.2022.1069714

OPEN ACCESS

EDITED BY
Ye Liu,
Beijing Technology and Business University, China

REVIEWED BY
Yuyun Lu,
National University of Singapore, Singapore
Amit Kumar Rai,
Institute of Bioresources and Sustainable Development, India

*CORRESPONDENCE
Chunhui Shan
972338194@qq.com

SPECIALTY SECTION
This article was submitted to Food Chemistry, a section of the journal Frontiers in Nutrition

RECEIVED 14 October 2022
ACCEPTED 21 November 2022
PUBLISHED 05 December 2022

CITATION
Zhang P, Tang F, Cai W, Zhao X and Shan C (2022) Evaluating the effect of lactic acid bacteria fermentation on quality, aroma, and metabolites of chickpea milk.
Front. Nutr. 9:1069714.
doi: 10.3389/fnut.2022.1069714

Evaluating the effect of lactic acid bacteria fermentation on quality, aroma, and metabolites of chickpea milk

Panling Zhang, Fengxian Tang, Wenchao Cai, Xinxin Zhao and Chunhui Shan*

School of Food Science, Shihezi University, Shihezi, China

Legumes are an attractive choice for developing new products since their health benefits. Fermentation can effectively improve the quality of soymilk. This study evaluated the impact of *Lactobacillus plantarum* fermentation on the physicochemical parameters, vitamins, organic acids, aroma substances, and metabolites of chickpea milk. The lactic acid bacteria (LAB) fermentation improved the color, antioxidant properties, total phenolic content, total flavonoid content, lactic acid content, and vitamin B6 content of raw juice. In total, 77 aroma substances were identified in chickpea milk by headspace solid-phase microextraction with gas chromatography/mass spectrometry (HS-SPME-GC-MS); 43 of the 77 aroma substances increased after the LAB fermentation with a significant decrease in beany flavor content ($p < 0.05$), improving the flavor of the soymilk product. Also, a total of 218 metabolites were determined in chickpea milk using non-targeted metabolomics techniques, including 51 differentially metabolites (28 up-regulated and 23 down-regulated; $p < 0.05$). These metabolites participated in multiple metabolic pathways during the LAB fermentation, ultimately improving the functional and antioxidant properties of fermented soymilk. Overall, LAB fermentation can improve the flavor, nutritional, and functional value of chickpea milk accelerating its consumer acceptance and development as an animal milk alternative.

KEYWORDS

lactic acid bacteria fermentation, soymilk functional properties, soymilk antioxidants, soymilk flavors, soymilk metabolites

Introduction

With growing health awareness, consumers are now selecting healthy food products, such as soymilk enjoyed widespread interest (1, 2). Soy grains are rich in nutrients such as proteins, vitamins, and minerals, which can be extracted in water as soymilk. Also, soymilk is a preferred choice for those who are lactose intolerant, allergic to milk protein,

or vegetarian (3). And soymilk is an ideal food to prevent some diseases, such as high blood pressure, high blood cholesterol. Moreover, Soybean and soy products are rich in nutrients, especially fermented soy products (fermented soymilk), which have health benefits such as: antioxidant effect, anticancer effect, and anti-inflammatory effect due to the presence of bioactive substances (4–6). And fermented soy products can also used as potential source of functional foods and bioactive peptides for developing nutritional products (7). Lactic acid bacteria (LAB) fermentation can improve the nutritional and functional values of soymilk (8). *Lactobacillus plantarum* bacteria grow well in soymilk, produce some bioactive peptides and reduce soy oligosaccharides in a strain-specific manner (9). *Lactobacillus plantarum* fermentation improves the antioxidant activity of soymilk food products (10). The soymilk fermented with *L. plantarum* was also found to lower the concentration of total cholesterol, triglyceride and low-density lipoprotein cholesterol in serum (11). And, compared to fresh soymilk, the concentrations of the characteristic flavor compounds for fermented soymilk using *L. plantarum* increased, while the contents of beany substances were decreased like hexanal, 2-pentylfuran, and 2-pentanone (12).

Although the effect of LAB fermentation on soybean products has been extensively investigated, little is known about the same for chickpeas, which can be a potential substitute of soymilk for its nutritional and organoleptic properties (2). Chickpeas (*Cicer arietinum L.*), one of the oldest and most widely consumed beans, are enriched in proteins (21–25%), fiber, and minerals. Also, chickpeas have high levels of resistant starch and amylose, which may reduce the onset of type II diabetes and hypertension. Chickpea milk is often regarded as an attractive milk substitute (13, 14).

Food flavor is one of the most decisive features of consumer acceptance (15, 16). Headspace solid-phase microextraction with gas chromatography/mass spectrometry (HS-SPME-GC-MS) has been widely adopted in environment samples, biology samples, especially food samples for odor analysis, quality classification, pesticide residue determination (17, 18). The displeasing beany flavor of soy products limits their consumption (9). The lactic acid bacteria fermentation significantly reduces the beany flavor of soymilk. Moreover, LAB fermentation can provide characteristic flavor to fermented soymilk by producing active reductases and unique flavor substances (19). Furthermore, LAB fermentation can convert certain off-favor aldehydes into corresponding alcohols and acids with fruity and sweet notes (20).

Lactic acid bacteria fermentation involves complex chemistry modulating the quality attributes of fermented foods by producing small molecule metabolites, which can be possibly tailored to achieve specific nutrition and flavor needs (21). Metabolomics, with high objectivity and reliability, offers a comprehensive and quantitative overview of metabolites in biological systems (22). Metabolomics is often used to assess critical metabolites related to food quality (23). Untargeted metabolomics examines a wide range of metabolites in a sample without a previous understanding and can also be used to describe the metabolism of a whole microorganism (24). Therefore, the same method can be used to determine the fermentation characteristics of chickpea milk.

So far, although many studies have examined the functional properties of fermented soy foods, the systematic descriptions of their quality, flavor, and metabolites are scarce, especially of the fermented chickpea milk. *Lactobacillus plantarum* can better adapt to growth-limiting substrates such as organic acids, polyphenols, etc. Therefore, *L. plantarum* fermentation can be a good choice for chickpea milk. Here, we investigated the effect of *L. plantarum* fermentation on physicochemical parameters, cell viability, and antioxidant properties of chickpea milk. Also, variations in organic acid and vitamins were determined by HPLC. The post-fermentation changes in flavor substances and metabolites were analyzed by headspace solid-phase microextraction with gas chromatography/mass spectrometry (HS-SPME-GC-MS) as well as untargeted metabolomics analysis via ultra high performance liquid chromatography/mass spectrometry (UHPLC-MS). Our results uncover the qualitative changes in fermented chickpea milk, which may be used to study its functional properties in the future.

Materials and methods

Preparation of chickpea milk

Chickpeas (Shihezi Market, Xinjiang, China) were soaked overnight in water (1:5 bean: water, m/v). The next day, removing moldy and insect-infested chickpeas, one part of the soaked beans was crushed in six parts of water (2) with heat processing for 30 min by mixer grinder (Joyoung, JYL-Y921, China). Then the soy drink was separated from solid residue using sterile gauze, eliminating impurities to make soymilk with fine taste and homogeneous texture. About 250 mL of soymilk sample was prepared by boiling for 10 min to confirm pasteurization.

Fermentation of chickpea milk

The commercial strain *L. plantarum* (LP-56) was obtained from CINOBIO-TEC Co., Ltd. (Shanghai, China), and preserved at −20°C. The lyophilized strain powder was dissolved in sterile distilled water (1:50, w/v) (25), which was used to inoculate (0.07%, w/v) chickpea milk at 10 log CFU/mL (cell count at activation), as determined by spread plate method. The fermentation was performed for 24 h at 37°C (9). Samples were collected in triplicates at 0 and 24 h.

Determination of physicochemical indices

In total, 1 mL of sample was added with 9 mL of saline (0.9%, w/v) and then serially diluted with saline multiple times in the same ratio. 1 mL of respective dilution was plated onto a Petri dish containing about 15 mL of the MRS agar medium. The inoculated Petri dish was incubated at 37°C for 48 h and the bacterial count was estimated as described previously (26).

$$N = \frac{\sum C}{(n1+0.1n2)\,d} \quad (1)$$

Where N = the number of microorganisms in the sample, ΣC = microbial total number, n_1 = the number of plates for the first dilution; n_2 = the number of plates for the second dilution; d = dilution factor.

The β-glucosidase activity was determined as described previously with some modifications (27). Took 0.1 mL of fermented soymilk, added 0.2 mL of sodium phosphate buffer (0.1 mol/L, pH 7.0) containing 5 mM *p*-NPG (*p*-nitrophenyl-β-D-glucoside) and put it into a 37°C water bath for 30 min. Then 0.5 mL of 1 mol/L $NaCO_3$ solution (4°C) was added to terminate the reaction, followed by centrifugal treatment (8,000 r/min, 30 min, 4°C), and the supernatant was taken to determine the absorbance value at 400 nm. Control group was inactivated with boiling water for 5 min instead of heating with water bath 37°C for 30 min. One unit of β-glucosidase activity is defined as the amount of enzyme required to catalyze the formation of 1 μmol of ρ-nitrophenol per minute under the assay conditions. Standard curve: $y = 0.1028x - 0.0078$, $r^2 = 0.9999$.

The sample color evaluation was performed with a colorimeter to obtain the L^*, a^*, and b^* values.

The total protein and total fat contents were determined spectrophotometrically following the Chinese National Standard GB5009.5-2016 and GB5009.6-2016, respectively. The method details are mentioned in **Supplementary Text 1**.

Determination of functional components

The total phenolic content (TPC) was determined using the Folin-Ciocalteu colorimetric method by measuring absorbance at 765 nm (26). This value denotes mg gallic acid equivalent (GAE) per mL of soymilk. The total flavonoid content (TFC) was determined using the aluminum nitrate colorimetric method by measuring absorbance at 508 nm (28). This value denotes mg rutin equivalent (RE) per mL of soymilk. The method details are in **Supplementary Text 2**.

Determination of antioxidant activity

The DPPH (2,2-diphenyl-1-picrylhydrazyl) radical cation ($DPPH^+$) scavenging activity of the samples was estimated spectrophotometrically at 517 nm as described previously with some modifications (29). The control group used methanol in place of the $DPPH^+$ solution, while the blank samples had deionized water. The calculation was performed as follows:

$$DPPH^+ \textit{ radical scavenging rate } (\%) = \frac{A2-A1}{A0} \times 100\% \quad (2)$$

Where A_2, A_1, and A_0 are the absorbance of experimental, control, and blank samples, respectively.

The ABTS [2,2′-azino-bis(3-ethyl-benzothiazoline)-6-sulphonic acid] radical cation ($ABTS^+$) scavenging activity of the samples was estimated by spectrophotometry at 734 nm as reported previously with some modifications (30). In control samples, absolute ethanol replaced the $ABTS^+$ solution. The hydroxyl radical cation (OH^-) scavenging activity was analyzed spectrophotometrically at 510 nm (31). In control samples, deionized water replaced the ethanol-salicylic acid, $FeSO_4$, and H_2O_2 solutions, while the blank samples had deionized water. The calculation was performed as follows:

$$\textit{Radical scavenging rate } (\%) = (1 - \frac{A2-A1}{A0}) \times 100\% \quad (3)$$

Where A_2, A_1, and A_0 are the absorbance of experimental, control, and blank samples, respectively.

Determination of vitamin B5 and B6 contents

Following the China National Standard GB5009.210-2016, vitamin B5 content was estimated by high performance liquid chromatography (HPLC) equipped with an ultraviolet spectrophotometric detector (Shimadzu, LC-2010, Japan). The HPLC conditions were as follows: chromatographic column, C18 column (4.6 mm × 250 mm, 5 μm); mobile phase, potassium dihydrogen phosphate solution (0.02 mol/L): acetonitrile (95:5); flow rate, 1 mL/min; column temperature, 30°C; detection wavelength, 210 nm; injection volume, 20 μL. The vitamin B5 standard solutions were 0, 2, 4, 8, 16, and 32 μg/mL ($y = 106295x - 13160$, $r^2 = 0.998$).

Following the China National Standard GB5009.154-2016, vitamin B6 content was also estimated by HPLC equipped with a fluorescence detector (Shimadzu, LC-2010, Japan) under the following conditions: chromatographic column: C18 column (4.6 mm × 250 mm, 5 μm); mobile phase: methanol 50 mL, sodium octane sulfonate 2 g, and triethylamine 2.5 mL were dissolved in 1,000 mL ultrapure water of

pH 3.0 ± 0.1 adjusted with glacial acetic acid; detection wavelength: excitation 293 nm, emission 395 nm; injection volume: 20 μL. The vitamin B6 standard solutions were 0, 0.1, 0.2, 0.4, 0.6, and 1.0 μg/mL (y = 6000000x – 154981, r^2 = 0.995).

Determination of lactic and citric acid contents

Analysis of organic acids was performed as follows (32): the sample was centrifuged and the obtained supernatant was filtered using a 0.45 μm membrane filter. 20 μL of the filtered sample was injected into a Waters 2998 HPLC system with a C18 column (4.6 mm × 250 mm, 5 μm) and diode-array detector (DAD). The conditions were as follows: mobile phase, 0.1% phosphoric acid + methanol (97 + 3, v/v); elution, isometric; column temperature, 40°C; detection wavelength, 210 nm. The standard solutions were 0, 4, 10, 20, 40, 100, 200, and 400 μg/mL (lactic acid: y = 243.07x + 163.46, r^2 = 0.999; citric acid: y = 591.87x + 170.28, r^2 = 0.999).

Headspace solid-phase microextraction with gas chromatography-mass spectrometry analysis

In total, 5 mL of the sample was placed in a 20 mL headspace vial and equilibrated on a magnetic stirrer for 20 min at 60°C. An SPME fiber 50/30 μm carboxyene/dimethicone/divinylbenzene (CAR/PDMS/DVB) was extended through the needle and exposed in the vial and adsorbed in the headspace for 30 min. Afterward, the fiber was immediately injected into the GC inlet and desorbed at 250°C for 3 min. The samples were measured by GC-MS (Agilent 8890-7000D, USA) and the analysis of volatile compounds was performed in the splitless injection mode on an Agilent 19091N-133 with an HP-INNO Wax column (30 m × 0.25 mm, 0.25 μm). High-purity helium was the carrier gas at a constant flow rate of 1 mL/min. The GC oven was set to 40°C for 3 min, ramped to 82°C at 2°C/min, then to 103°C at 1°C/min, 124°C at 7°C/min, 138°C at 2°C/min, and finally 220°C at 10°C/min to hold for 3 min. Qualitative analysis of volatile compounds was identified by matching the National Institute of Standards and Technology database (NIST17.L) and retention index (RI).

UHPLC/MS analysis

Analysis of metabolites by UHPLC/MS (Thermo Scientific, Thermo Fisher Scientific Inc., Waltham, MA, USA) according to the previous method with some modifications (33). Sample preparation: 20 mg sample was extracted with 400 μL of acetonitrile: methanol solution (1:1, v:v) containing 0.02 mg/mL of L-2-chlorophenylalanine (internal standard); Frozen tissue was ground for 6 min at −10°C and 50 Hz; Cryogenic ultrasonic extraction was performed for 30 min at 5°C and 40 KHz; The samples were incubated at −20°C for 30 min and then centrifuged for 15 min at 13.000 × *g* and 4°C, Also, 20 μL of supernatant from each sample was separately mixed with the quality control (QC) sample. A QC sample was run after every 5-15 analytical samples to test the stability of the whole detection process.

Chromatographic conditions were as follows: column: ACQUITY UPLC HSS T3 (100 mm × 2.1 mm i.d., 1.8 μm; Waters, Milford, MA, USA); mobile phase A: 95% water : 5% acetonitrile (containing 0.1% formic acid), mobile phase B: 47.5% acetonitrile : 47.5% isopropanol : 5% water (contains 0.1% formic acid); flow rate: 0.40 mL/min; injection volume: 2 μL; column temperature: 40°C. The gradient elution condition was: 95% A and 5% B, 0.1 min; 75% A and 25% B, 2 min; 100% B, 9 min; 100% B, 13 min; 100% A, 13.1 min; 100%, 16 min.

Mass spectrometry conditions were as follows: Samples were electrosprayed/ionized, and MS signals were collected in the negative ion scanning mode. Scan type (m/z): 70–1,050; Sheath gas flow rate (arb): 40; Aux gas flow rate (arb): 10; Heater temp (°C): 400; Capillary temp (°C): 320; Spray voltage (–) (V): −2,800; S-Lens RF Level: 50; Normalized collision energy (eV): 20, 40, 60; Resolution (Full MS): 70000; Resolution (MS2): 17500.

Statistical analysis

All samples were tested in triplicates. Significant differences between data were identified by ANOVA Tukey's test. Origin 9.8.5 was used for plotting the bar charts, stacked histograms, etc. Heatmaps were plotted by R Version 3.6.3 to analyze the changes. Adobe Illustrator 2020 was used to map the metabolic pathways.

Results and discussion

Analysis of the physicochemical indicators of RJ and *Lactobacillus plantarum fermented juice*

Food color is a critical indicator of food quality (34). The mean L^*, a^*, and b^* values of different samples are shown in **Figure 1A**. Compared with RJ (raw juice), the change in b^* and a^* values indicated a significant color change of LPFJ (*L. plantarum* fermented juice), however, the L^* value did not change much ($p < 0.05$). The LAB fermentation changed the color of chickpea milk to more red and yellow colors.

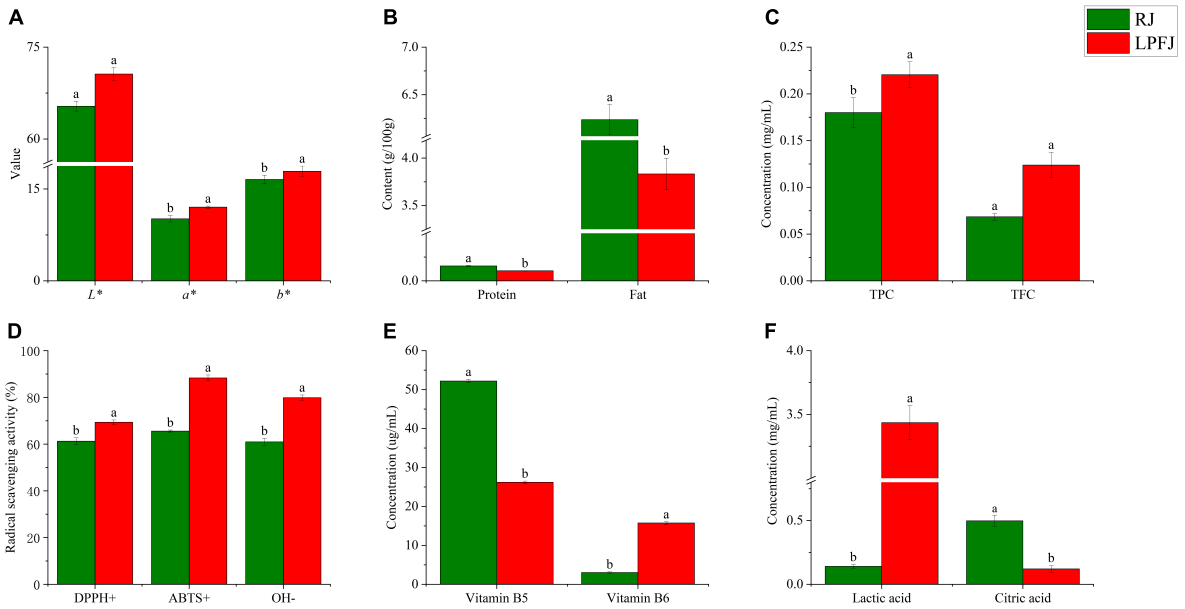

FIGURE 1
Analysis of the physicochemical indicators of RJ and *Lactobacillus plantarum* fermented juice (LPFJ). Post-LAB fermentation change in panel **(A)** color properties of chickpea milk L^* (brightness), a^* (red-green), and b^* (yellow and blue), **(B)** protein and fat contents, and functional indicators including **(C)** TPC and TFC, **(D)** radical scavenging activity, **(E)** vitamin B5 and vitamin B6 contents, and **(F)** lactic and citric acids contents. Values marked with different superscript letters indicate statistically significant differences ($p < 0.05$). RJ, raw juice; LPFJ, *L. plantarum* fermented juice; TPC, total phenol content; TFC, total fat content.

Also, after fermentation, both total protein and total fat contents showed a downward trend (**Figure 1B**, $P < 0.05$). The decrease in total protein content may be because LAB promoted protein degradation during fermentation to meet the bacterial needs for nitrogen-containing substances (35). The lactic acid bacteria-degraded proteins are easily absorbed by the body; the formed ACE (angiotensin-converting enzyme) inhibiting peptides have anti-cardiovascular disease and blood pressure-lowering activities (36). Regarding the total fat content, its decrease may be due to the content of linoleic and linolenic acid decreased (37). The linolenic acid in soymilk positively correlates with the content of hexanal, which produces beany flavor (38). Therefore, LAB fermentation should reduce the beany flavor of chickpea milk. Hence, a decrease in total protein and total fat contents improved human digestion/absorption and the flavor of LPFJ.

The post-fermentation change in microorganism number is significantly increased ($p < 0.05$). The results indicated that LAB had good growth in chickpea milk and rapidly accumulated after 24 h of fermentation, reaching 8.87 $\log_{10}$CFU/mL. Consistently, past research has also demonstrated that LABs grew better in soymilk with microbiological counts ranging from 5.7 to 10.4 $\log_{10}$CFU/mL (39). Overall, chickpea milk is a suitable fermentation substrate with enough nutrients for the good growth of LAB.

As shown in **Figures 1C,D**, LAB fermentation significantly enhanced the TPC and DPPH+, ABTS+, and OH− scavenging capacity of LPFJ ($p < 0.05$), indicating a positive effect. However, TFC did not change much ($p \geq 0.05$). Increased phenolic content can be attributed to the production of β-galactosidase during LAB fermentation, which catalyzes the release of phenolic compounds from bound sugars increasing antioxidant activity (40). Also, there could be other microbial transformations and depolymerization of compounds (41). Next, a small increase in TFC may be because LAB promote the release of flavonoids by producing enzymes and acids. *Lactobacillus plantarum* has been shown to increase TFC during fermentation (42).

Hydrolysis of glucosides through enzymatic processes using β-glucosidase to increase their bioavailability in soy-based products, and probiotic micro-organisms have been found to possess β-glucosidase (43, 44). The results showed a significant increase in β-glucosidase activity measured after fermentation ($p < 0.05$), reaching 28.13 mU/mL. Remarkably, the higher β-glucosidase activity in fermented soymilk indicates that the strain converts glycosidic soy isoflavones to glycosidic soy isoflavones faster, and the antioxidant capacity is enhanced (27, 44, 45). Subsequently, we utilized three different methods to assess the antioxidant properties of LPFJ (**Figure 1D**). The enhancement of antioxidant capacity indicates the accumulation of antioxidant compounds, such as phenolic compounds, flavonoids, and superoxide dismutase (SOD) (46). The lactic acid bacteria-fermented fruit and vegetable juices also show an increase in free radical scavenging and antioxidant activity (47, 48). Compared with RJ, LPFJ showed a significant increase in

antioxidant activity, which may promote its health benefits in daily use (49).

Besides having abundant proteins, chickpeas are also rich in vitamins and minerals, especially vitamins B5 and B6 (50). Here, we found that the content of vitamin B5 decreased and the content of vitamin B6 increased significantly in LPFJ after LAB fermentation ($p < 0.05$; Figure 1E). Consistently, past research has also indicated that LAB fermentation can increase the

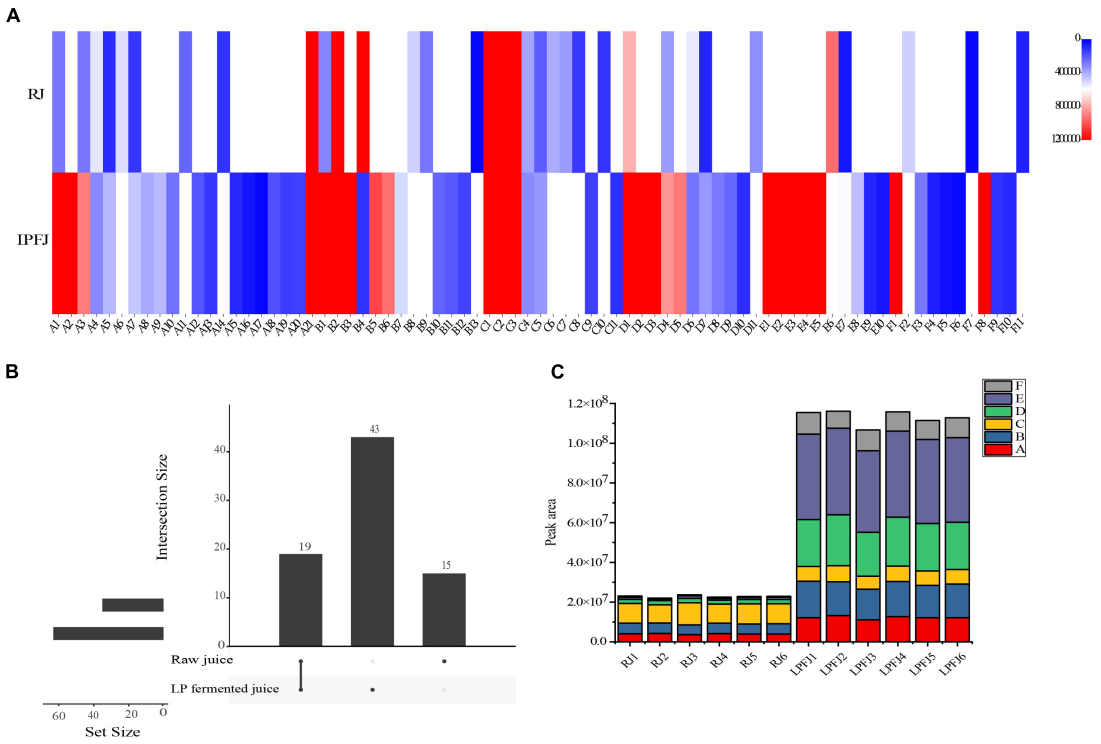

FIGURE 2
Change in aroma profiles of RJ and *Lactobacillus plantarum* fermented juice (LPFJ). **(A)** Content of aroma substances: the degree of redness and blueness indicate the higher and lower content, respectively. **(B)** Quantity of aroma substances: the value represents the type and a larger value indicates the sample richness of that substance. **(C)** A stacked histogram of volatile contents: A-alcohol; B-aldehyde; C-ester; D-acid; E-ketone; and F-others. RJ, raw juice; LPFJ, *L. plantarum* fermented juice.

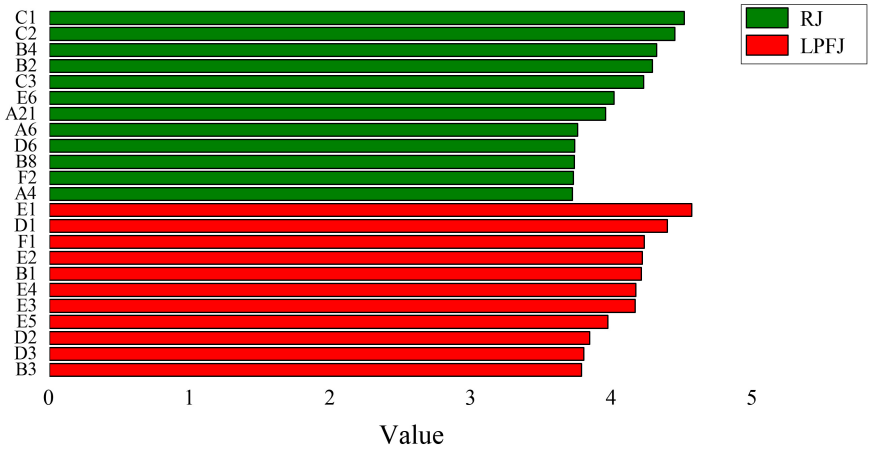

FIGURE 3
Linear discrimination analysis and the Kruskal-walls test to find significantly different aroma species (LDA score). A volatile compound with an LDA score > 3.7 was considered a significantly different species and a biomarker of soymilk fermentation. RJ, raw juice; LPFJ, *L. plantarum* fermented juice.

contents of vitamin B6 in soymilk (51). The lactic acid bacterias are considered the biological factories for vitamin B production, and utilization (52). During LAB fermentation, lactic acid, a major organic acid in fermented beverages, increases (53). Meanwhile, the content of citric acid, which is an intermediate metabolite of the tricarboxylic acid cycle (TCA cycle), shows a dynamic change. The TCA cycle is the pivot for the liaison and transformation of key substances, such as sugar, lipid, protein, and even nucleic acids. Therefore, we measured the change in contents of lactic and citric acids (**Figure 1F**). Lactic acid production is not limited to sugars and citric acid as it may also originate from the conversion of amino acids (54). Here too, the lactic acid content increased and the citric acid content decreased in LPFJ.

Change in aroma profiles of RJ and *Lactobacillus plantarum* fermented juice

Types, content, and relevance of aroma substances in RJ and *Lactobacillus plantarum* fermented juice

The post-fermentation change in aroma compounds was determined by HS-SPME–GC/MS; in total, 77 aroma compounds were measured, containing 21 alcohols, 13 aldehydes, 11 esters, 10 ketones, 11 acids, and 11 others (**Figure 2A** and **Supplementary Table 2**). Aroma compounds followed a kinetic trend during the fermentation. There were 19 common substances, while 43 new substances were produced in LPFJ, and 15 substances were present only in RJ (**Figure 2B**). This indicated that LAB fermentation transformed substances in RJ producing a series of new flavor substances in LPFJ (55).

Figure 2A (A1–A21) shows the significant change in alcohols after LAB fermentation ($p < 0.05$); the enzyme activity in LPFJ increased by nearly 50%, while the half-life decreased (56). This significantly improved the total alcohol content in LPFJ. The lactic acid bacteria fermentation produces more alcohol substances. Hexanol (A2) is a typical feature of legume flavor compounds, with a fruity aromatic aroma; 1-nonanol (A14) has a slightly pleasant aroma of rose and orange. The production and accumulation of these substances improved the flavor of fermented soymilk (57). Also, 1-octen-3-ol (A1) is a common volatile organic compound in fermented soy products, which is generated by unsaturated fatty acid metabolism (58).

The main aldehyde and ketone substances in soymilk were acetone, 2-butanone, 3-methyl-butyraldehyde, and hexanal. The flavor substances and soy protein can bind hydrophobically, and their binding constants increase with the number of carbon chains (59). This complicates the elimination of beany flavor

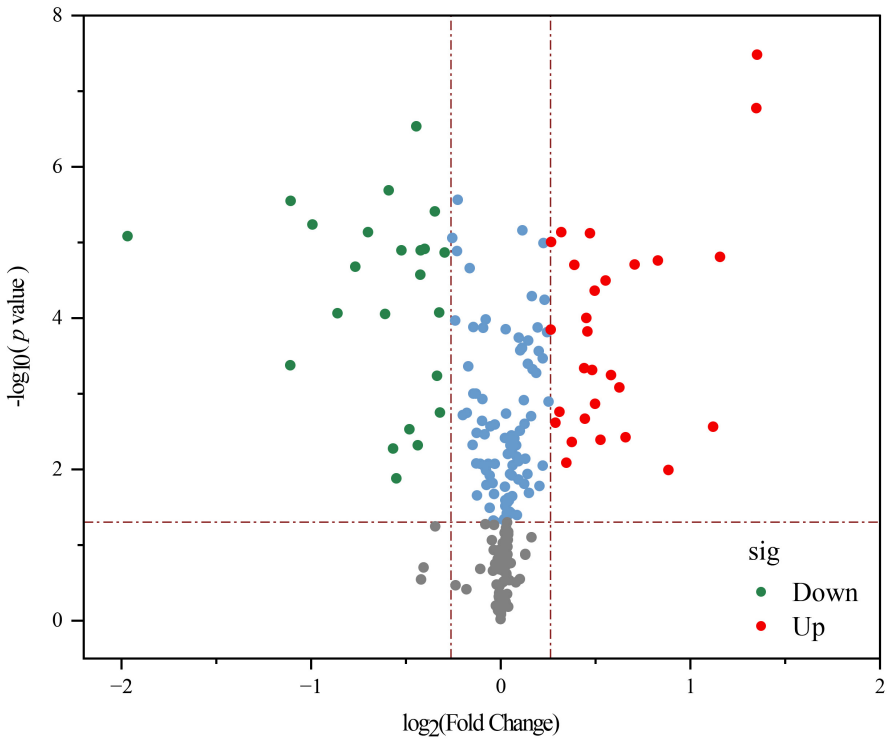

FIGURE 4
A volcano plot showing differential non-volatile metabolites between RJ and *Lactobacillus plantarum* fermented juice (LPFJ). Red and green indicate up-and down-regulated metabolites.

during the fermentation. Our results showed that the content of hexanal (B4) decreased significantly after LAB fermentation ($p < 0.05$; **Figure 2A** and **Supplementary Table 2**). Hexanal could have been converted to hexanoic acid eliminating the beany flavor and improving the flavor of chickpea milk (60). Also, there were high levels of benzaldehyde (B2), 3-hydroxybutanal (B13), acetone (E6), and others in RJ. Meanwhile, levels of certain substances increased in LPFJ, most are ketones. These can be attributed to amino acids degradation by microbial metabolism (61, 62). Furthermore, the increased content of octaldehyde (B5) added a certain fruity flavor to LPFJ. Also, the reduction in acetone with special odors (spicy and sweet) greatly improved the flavor of the beverage increasing consumer demand for taste.

Typically, some acids undergo esterification to form esters, which provide a fruity or floral aroma and contribute to the mild and pleasant flavors of fermented foods (63). As shown in **Figure 2C**, the total content of esters did not change much, however, a general trend showed the production of new substances and the decrease/disappearance of old ones (**Figure 2A**). Notably, the flavor of LPFJ would have improved due to the peach aroma of 2-phenylethyl acetate (C11) and the pineapple aroma of 2-phenylethyl caproate (C9) produced after fermentation. And, LAB fermentation also increased the acid content in chickpea milk, especially acetic and nonanoic acids.

Next, we performed correlation analyses between the flavor substances (**Supplementary Figure 1**). We found significant positive linear correlations between alcohols and aldehydes, and aldehydes and acids ($p < 0.05$). Additionally, both alcohols and acids had a significant negative correlation with esters ($p < 0.05$). Typically, alcohols and acids undergo esterification and therefore have a negative correlation (63). Also, aldehydes and ketones showed a negative correlation with esters. Furthermore, LAB fermentation led to obvious differences in the types of flavor and specific substances between LPFJ and RJ. The changes in the relative content of each component directly affect the flavor of chickpea milk, such as the decrease in beany flavor after LAB fermentation.

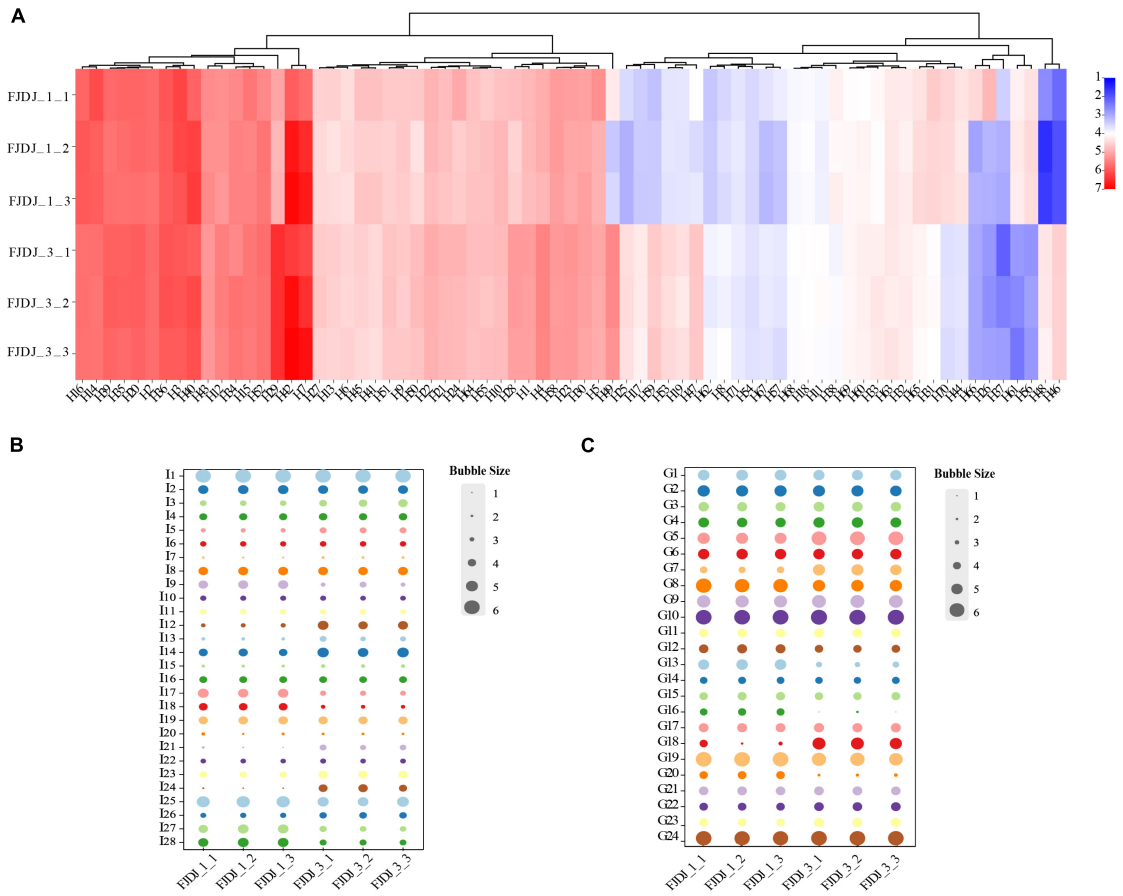

FIGURE 5
Key metabolites in RJ and *Lactobacillus plantarum* fermented juice (LPFJ). Content changes of **(A)** lipids and lipid-like molecules, **(B)** amino acids, peptides, and analogs, and **(C)** carbohydrates and carbohydrate conjugates. FJDJ1-1, FJDJ1-2, FJDJ1-2 belong to RJ; FJDJ3-1, FJDJ3-2, and FJDJ3-2 belong to LPFJ.

Key aroma compounds in RJ and *Lactobacillus plantarum* fermented juice

The key aroma compounds are the main components of fermented chickpea milk, which determine the aroma characteristics and form the unique flavor of fermented chickpea milk. We found clear enrichment of a few aroma substances to different levels in LPFJ. Most aldehydes were abundant in RJ (**Figure 3**). The key aroma substances in RJ were mainly hexanal (B4), benzaldehyde (B2), 1,4-butanediol (A6), etc. Some of these have a grassy, bitter almond flavor. The main compounds in LPFJ were ketones [2-heptanone (E1), 2-nonanone (E3), etc.] and acids [acetic acid (D1), 3-methyl-butanoic acid (D2), hexanoic acid (D3)]. Also, a flavor substance with a faint "smelly foot smell" was produced in LPFJ. Based on existing literature, this substance could be isovaleric acid, which is a common characteristic flavor component in fermented soybean products (64). Besides, LPFJ had some special substances with relatively high content, such as (E)-2-heptenal (B1), (E)-2-octenal (B3), etc. (E)-2-heptenal has a little fatty aroma; 2-heptanone and 2-nonanone have a fruity and creamy aroma. Acetoin (E2) improves the overall sensory acceptability of fermented soymilk (65). Due to carbonyl compounds could be converted by lactic acid bacterial metabolism into further well-known odor substances, like ketones, esters, or organic acids (66). So, post-fermentation, the good aroma substance increased in LPFJ, while the beany flavor weakened, improving the total flavor of the beverage.

Metabolite analysis: Untargeted metabolomics

Types, classification, and differential metabolites in RJ and *Lactobacillus plantarum* fermented juice

Based on the untargeted metabolomic approach, the comprehensive changes in metabolites were analyzed to identify differential metabolites between RJ and LPFJ. In total, 218 metabolites were detected by UHPLC (**Supplementary Figure 2**). The levels of substances changed significantly during fermentation ($p < 0.05$), indicating a mutual transformation of substances. All metabolites detected in RJ and LPFJ were

FIGURE 6
Metabolic pathways analysis. **(A)** Kyoto Encyclopedia of Genes and Genomes (KEGG) metabolite statistics; **(B)** schematic diagram of the metabolic pathway for the selected metabolites.

matched with the human metabolome database (HMDB). The changed metabolites belonged to nine primary classifications, 32 secondary classifications, and 51 tertiary classifications, and some were not identified. The dynamic changes in metabolite contents between RJ and LPFJ are shown in **Supplementary Figure 3**. At the level of primary classification, the metabolites were organoheterocyclic compounds (oxygenates 11.9%), lipids and lipid-like molecules (32.6%), organic acids and derivatives (17.9%), and so on. The majority of organic acids and derivatives were amino acids, peptides, and analogs (71.8%); organic oxygenates were composed of carbohydrates and carbohydrate conjugates (92.3%). Also, a significant increase in the content of phenylpropanoids and polyketides, lipids, and lipid-like molecules, and the total content of metabolites was observed in LPFJ ($p < 0.05$), indicating the role of LAB fermentation.

A volcano diagram shows the overall distribution of significantly different metabolites ($p < 0.05$) in **Figure 4**. Based on threshold criteria $p < 0.05$ and FC (fold change) ≥ 1.2, we found 28 up-regulated and 23 down-regulated metabolites in LPFJ after fermentation. The up-regulated metabolites were pyridoxine (vitamin B6), indole acetaldehyde, 5-L-glutamyl-L-alanine, 5-hydroxy-indole-acetaldehyde, and others. Notably, the increase in vitamin B6 is consistent with the results in **Figure 1E**. The down-regulated substances were xanthosine, vanilloside, D-glucarate, and others. Based on the Kyoto Encyclopedia of Genes and Genomes (KEGG) pathway descriptions, indole acetaldehyde and 5-hydroxy-indole-acetaldehyde participate in amino acid metabolism; 5-L-glutamyl-L-alanine is involved in other amino acid metabolism; Xanthosine is involved in nucleotide metabolism, biosynthesis of other secondary metabolites and membrane metabolism; D-Glucarate is involved in carbohydrate metabolism.

Key metabolites in RJ and *Lactobacillus plantarum* fermented juice

Legumes are rich in proteins and carbohydrates and are an excellent source of unsaturated fatty acids (50). The change in these substances indicated that LAB fermentation effectively worked in soymilk, improving its digestion, absorption, nutritional, and functional qualities (67). Carbohydrates in fermented beverages can promote colon health (68). Therefore, we next analyze the change in these metabolites (**Figure 5**).

The content of fatty acids changed in LPFJ during LAB fermentation (**Figure 6A**). There were 71 key metabolites, of which, 50 increased including 13 with a significant increase ($p < 0.05$), such as 9,10,13-trihydroxystearic acid (H25), 2-hydroxyhexadecanoic acid (H47), 7-methylinosine (H62), and so on. Studies have shown that the acid compounds generated during fermentation enhance the taste, flavor, and texture of the fermented product (68). In total, 21 metabolite decreased after fermentation, including 13 with a significant decrease ($p < 0.05$). Among them, PE (16:0/0:0) (H45) is an important phospholipid that constitutes biological membranes, mainly in the brain, nerves, microorganisms, and soybeans. It plays an important role in signal transduction and maintenance of life functions. LysoPC [18:2 (9Z, 12Z)] (H14) functions in lipid signaling by acting on the lysophospholipid receptor (LPL-R). There were also some substances involved in oleic and linoleic acid metabolism. Oleic and stearic acids are regarded as health-promoting substances for their preventive effects against high blood pressure and cardiovascular diseases (33).

The increase in peptides and amino acids is a result of soy protein hydrolysis by extracellular proteases of LAB. Similarly, we found an increase in the contents of amino acids, peptides, and analogs, including 9 with a significant increase ($p < 0.05$; **Figure 5B**). In general, LAB-fermented products are rich in beneficial peptides and amino acids (69). And study showed that *L. plantarum* has a high potential for peptide production (9). Notably, the contents of L-glutamine (I12), *N*-formylmethionine (I21), 5-L-glutamyl-L-alanine (I24), allysine (I26), and others almost doubled in LPFJ. Based on the KEGG database, these metabolites are involved in alanine, aspartate, and glutamate metabolism; the biosynthesis of arginine; protein digestion and absorption; metabolism of cysteine and methionine; metabolism of glutathione; degradation of lysine, etc. Additionally, there is the possibility that some peptides may provide a bitter taste to fermented products.

Change in carbohydrate content was observed throughout the fermentation process (**Figure 5C**). Carbohydrate metabolism produces intermediate products that are components of the bacterial cell structure, as well as provide energy for bacterial growth and survival. *L. plantarum* bacterium harbors multiple sugar metabolic pathways that can metabolize various sugars (70, 71). During the LAB fermentation, some carbohydrates such as ribonolactone (G5), ribitol (G7), and dulcitol (G22) increased significantly, while some such as jasmolone glucoside (G13), galactinol (G19), D-glucarate (G20) decreased ($p < 0.05$). Notably, galactinol is a common component of the cottonseed glycoconjugate family and participates in the biosynthesis of oligosaccharides. The beany flavor and high levels of nondigestible oligosaccharides are the key issues limiting the consumer acceptance of soy products. A decrease in galactinol can reduce the biosynthesis of oligosaccharides enhancing the digestibility of LPFJ.

Metabolic pathways analysis

In **Figure 6A**, partial metabolites were engaged in 37 metabolic pathways belonging to seven categories, such as organismal systems, human diseases, cellular processes, metabolism, and so on. These metabolic pathway categories were searched against the KEGG database. Among them, carbohydrate metabolism (19 metabolites), lipid metabolism (10 metabolites), amino acid metabolism (22 metabolites), biosynthesis of other secondary metabolites (10 metabolites), and membrane transport (10 metabolites) were the main

metabolic pathways during the fermentation. Up to 22 kinds of metabolites were associated with amino acid metabolism. The lactic acid bacteria degrade proteins and peptides to meet the needs of bacterial growth (35). Additionally, certain peptides work on target sites for specific functions, such as antioxidant and anti-hypertension activities (72, 73). In summary, KEGG metabolite analysis revealed the diversity of metabolic pathways in LPFJ during LAB fermentation.

The levels of glutathione and L-glutamate decreased significantly after fermentation ($p < 0.05$; **Figure 6B**). Glutathione is broken down into *N*-formylmethionine and L-glutamate and oxidized. Glutamate, cysteine, and glycine are synthesized into glutathione, which is part of almost every cell in body (**Figure 6B**). Subsequently, glutamate is transformed into α-ketoglutarate (α-KG) by glutamate dehydrogenase (GDH), which is a part of the TCA cycle (**Figure 6B**). Glutathione is the richest non-protein thiol compound in all organisms (74). It has critical functions with antioxidant properties such as preventing cellular damage caused by various oxidative stressors, detoxification of pathogens, and immune enhancer (74, 75). Moreover, glutamate participates in many important metabolic reactions in animals, plants, and microorganisms. Therefore, an increase in glutathione improves the antioxidant capacity and other functional properties of fermented chickpea milk.

Conclusion

In this study, chickpea milk was fermented using LP-56. The lactic acid bacteria fermentation improved the physicochemical characteristics, antioxidant activity, and other functional properties of fermented chickpea milk. Also, the content of beany substance was reduced improving the flavor of the final product. The increase in the content of acid and other substances improved the overall taste of LPFJ. Notably, 51 differential metabolites were identified between RJ and LPFJ that participate in multiple metabolic pathways providing the specific sensory and functional characteristics to LPFJ. An increase in glutathione metabolism also played an extremely important role. Our study uncovered the effect of LAB fermentation on chickpea milk in terms of flavor and functional properties, which may help the development and commercialization of fermented chickpea milk. We should next assess the changes in micronutrients (such as peptides) and identify their effect on the functional properties of LPFJ.

Data availability statement

The original contributions presented in this study are included in this article/**Supplementary material**, further inquiries can be directed to the corresponding author.

Author contributions

PZ: conceptualization, methodology, investigation, and writing—original draft. WC: investigation and software. XZ: investigation. FT: supervision. CS: project administration and funding acquisition. All authors contributed to the article and approved the submitted version.

Funding

This work was supported by Science and Technology Innovation Talent Program of Xinjiang Production and Construction Corps grant number (2020CB025).

Acknowledgments

The rigorous and responsible reviewers have also contributed considerably to the improvement and publication of this manuscript.

Conflict of interest

The authors declare that the research was conducted in the absence of any commercial or financial relationships that could be construed as a potential conflict of interest.

Publisher's note

Supplementary material

The Supplementary Material for this article can be found online at: https://www.frontiersin.org/articles/10.3389/fnut.2022.1069714/full#supplementary-material

SUPPLEMENTARY FIGURE 1
Correlation between substances: red is positive correlation, blue is negative correlation; the size of the circle represents the degree of correlation ($p < 0.05$).

SUPPLEMENTARY FIGURE 2
Heatmap of hierarchical clustering analysis of differential abundant metabolites in RJ and LPFJ.

SUPPLEMENTARY FIGURE 3
Sankey plot of the changes of non-volatile metabolites in RJ and LPFJ based on HMDB super class.

References

1. Jeske S, Zannini E, Arendt EK. Past, present and future: the strength of plant-based dairy substitutes based on gluten-free raw materials. *Food Res Int.* (2018) 110:42–51. doi: 10.1016/j.foodres.2017.03.045

2. Wang S, Chelikani V, Serventi L. Evaluation of chickpea as alternative to soy in plant-based beverages, fresh and fermented. *LWT.* (2018) 97:570–2. doi: 10.1016/j.lwt.2018.07.067

3. Undhad T, Hati S, Makwana S. Significance of storage study on ACE inhibitory, antioxidative, antimicrobial activities, and biotransformation of isoflavones of functional fermented soy-based beverage. *J Food Proc Preserv.* (2021) 45:e15062. doi: 10.1111/jfpp.15062

4. Chourasia R, Padhi S, Chiring Phukon L, Abedin MM, Singh SP, Rai AK. A potential peptide from soy cheese produced using *Lactobacillus delbrueckii* WS4 for effective inhibition of SARS-CoV-2 main protease and S1 glycoprotein. *Front Mol Biosci.* (2020) 7:601753. doi: 10.3389/fmolb.2020.601753

5. Do Prado FG, Binder Pagnoncelli MG, De Melo Pereira GV, Karp SG, Soccol CR. Fermented soy products and their potential health benefits: a review. *Microorganisms.* (2022) 10:1606. doi: 10.3390/microorganisms10081606

6. Padhi S, Chourasia R, Kumari M, Singh SP, Rai AK. Production and characterization of bioactive peptides from rice beans using *Bacillus subtilis*. *Bioresour Technol.* (2022) 351:126932. doi: 10.1016/j.biortech.2022.126932

7. Chourasia R, Chiring Phukon L, Minhajul Abedin M, Sahoo D, Kumar Rai A. Production and characterization of bioactive peptides in novel functional soybean chhurpi produced using *Lactobacillus delbrueckii* WS4. *Food Chem.* (2022) 387:132889–132889. doi: 10.1016/j.foodchem.2022.132889

8. Frias J, Song YS, Martinez-Villaluenga C, De Mejia EG, Vidal-Valverde C. Immunoreactivity and amino acid content of fermented soybean products. *J Agric Food Chem.* (2008) 56:99–105. doi: 10.1021/jf072177j

9. Singh BP, Vij S. Growth and bioactive peptides production potential of *Lactobacillus plantarum* strain C2 in soy milk: a LC-MS/MS based revelation for peptides biofunctionality. *LWT.* (2017) 86:293–301. doi: 10.1016/j.lwt.2017.08.013

10. Liu T-H, Chiang W-T, Cheng M-C, Tsai T-Y. Effects of germination black soy milk fermented with *Lactobacillus plantarum* TWK10 on anti-oxidative and Anti-melanogenesis. *Appl Sci.* (2021) 12:277. doi: 10.3390/app12010277

11. Wang ZL, Bao Y, Zhang Y, Zhang JC, Yao GQ, Wang SQ, et al. Effect of soymilk fermented with *Lactobacillus plantarum* P-8 on lipid metabolism and fecal microbiota in experimental hyperlipidemic rats. *Food Biophys.* (2013) 8:43–9. doi: 10.1007/s11483-012-9282-z

12. Li CC, Li W, Chen XH, Feng MQ, Rui X, Jiang M, et al. Microbiological, physicochemical and rheological properties of fermented soymilk produced with exopolysaccharide (EPS) producing lactic acid bacteria strains. *LWT.* (2014) 57:477–85. doi: 10.1016/j.lwt.2014.02.025

13. Osorio-Diaz P, Agama-Acevedo E, Mendoza-Vinalay M, Tovar J, Bello-Perez LA. Pasta added with chickpea flour: chemical composition, in vitro starch digestibility and predicted glycemic index. *Cienc Tecnol Aliment.* (2008) 6:6–12. doi: 10.1080/11358120809487621

14. Fu YH, Zhang FC. Changes in isoflavone glucoside and aglycone contents of chickpea yoghurt during fermentation by *Lactobacillus bulgaricus* And *Streptococcus thermophilus*. *J Food Proc Preserv.* (2013) 37:744–50. doi: 10.1111/j.1745-4549.2012.00713.x

15. Cai WC, Xue YA, Wang YR, Wang WP, Shu N, Zhao HJ, et al. The fungal communities and flavor profiles in different types of high-temperature Daqu as revealed by high-throughput sequencing and electronic senses. *Front Microbiol.* (2021) 12:784651. doi: 10.3389/fmicb.2021.784651

16. Cai WC, Xue YA, Tang FX, Wang YR, Yang SY, Liu WH, et al. The depth-depended fungal diversity and non-depth-depended aroma profiles of pit mud for strong-flavor Baijiu. *Front Microbiol.* (2022) 12:789845. doi: 10.3389/fmicb.2021.789845

17. Pico Y, Alfarhan AH, Barcelo D. How recent innovations in gas chromatography-mass spectrometry have improved pesticide residue determination: an alternative technique to be in your radar. *Trac Trends Analy Chem.* (2020) 122:115720. doi: 10.1016/j.trac.2019.115720

18. Xu XX, Wu BB, Zhao WT, Pang XL, Lao F, Liao XJ, et al. Correlation between autochthonous microbial communities and key odorants during the fermentation of red pepper (*Capsicum annuum* L.). *Food Microbiol.* (2020) 91:103510. doi: 10.1016/j.fm.2020.103510

19. Blagden TD, Gilliland SE. Reduction of levels of volatile components associated with the "Beany" flavor in soymilk by Lactobacilli and Streptococci. *J Food Sci.* (2005) 70:M186–9.

20. Tangyu M, Fritz M, Aragao-Borner R, Ye LJ, Bogicevic B, Bolten CJ, et al. Genome-based selection and application of food-grade microbes for chickpea milk fermentation towards increased l-lysine content, elimination of indigestible sugars, and improved flavour. *Microb Cell Fact.* (2021) 20:109. doi: 10.1186/s12934-021-01595-2

21. Gao YX, Hou LZ, Gao J, Li DF, Tian ZL, Fan B, et al. Metabolomics approaches for the comprehensive evaluation of fermented foods: a review. *Foods.* (2021) 10:2294. doi: 10.3390/foods10102294

22. Park MK, Kim YS. Mass spectrometry based metabolomics approach on the elucidation of volatile metabolites formation in fermented foods: a mini review. *Food Sci Biotechnol.* (2021) 30:881–90. doi: 10.1007/s10068-021-00917-9

23. Peng JY, Ma LQ, Kwok LY, Zhang WY, Sun TS. Untargeted metabolic footprinting reveals key differences between fermented brown milk and fermented milk metabolomes. *J Dairy Sci.* (2022) 105:2771–90. doi: 10.3168/jds.2021-20844

24. Schrimpe-Rutledge AC, Codreanu SG, Sherrod SD, Mclean JA. Untargeted metabolomics strategies-challenges and emerging directions. *J Am Soc Mass Spectr.* (2016) 27:1897–905. doi: 10.1007/s13361-016-1469-y

25. Liu YY, Sheng J, Li JJ, Zhang PL, Tang FX, Shan CH. Influence of lactic acid bacteria on physicochemical indexes, sensory and flavor characteristics of fermented sea buckthorn juice. *Food Biosci.* (2022) 46:101519. doi: 10.1016/j.fbio.2021.101519

26. Sheng J, Shan CH, Liu YY, Zhang PL, Li JJ, Cai WC, et al. Comparative evaluation of the quality of red globe grape juice fermented *by Lactobacillus acidophilus* and *Lactobacillus plantarum*. *Int J Food Sci Technol.* (2022) 57:2235–48. doi: 10.1111/ijfs.15568

27. Lee KH, Kim SH, Woo KS, Kim HJ, Choi HS, Kim YH, et al. Functional beverage from fermented soymilk with improved amino nitrogen, beta-glucosidase activity and aglycone content using *Bacillus subtilis* starter. *Food Sci Biotechnol.* (2016) 25:1399–405. doi: 10.1007/s10068-016-0218-0

28. Guo Y, Li YR, Zhang S, Wu XJ, Jiang LY, Zhao QH, et al. The effect of total flavonoids of *Epimedium* on granulosa cell development in laying hens. *Poult Sci.* (2020) 99:4598–606. doi: 10.1016/j.psj.2020.05.032

29. Cai WC, Tang FX, Shan CH, Hou QC, Zhang ZD, Dong Y, et al. Pretreatment methods affecting the color, flavor, bioactive compounds, and antioxidant activity of jujube wine. *Food Sci Nutr.* (2020) 8:4965–75. doi: 10.1002/fsn3.1793

30. Xiao Y, Xing GL, Rui X, Li W, Chen XH, Jiang M, et al. Enhancement of the antioxidant capacity of chickpeas by solid state fermentation with *Cordyceps militaris* SN-18. *J Funct Foods.* (2014) 10:210–22. doi: 10.1016/j.jff.2014.06.008

31. Sun J, Zhong X, Sun D, Cao X, Yao F, Shi L, et al. Structural characterization of polysaccharides recovered from extraction residue of ginseng root saponins and its fruit nutrition preservation performance. *Front Nutr.* (2022) 9:934927. doi: 10.3389/fnut.2022.934927

32. Cai WC, Wang YR, Hou QC, Zhang ZD, Tang FX, Shan CH, et al. Rice varieties affect bacterial diversity, flavor, and metabolites of Zha-Chili. *Food Res Int.* (2021) 147:110556. doi: 10.1016/j.foodres.2021.110556

33. Zha MS, Li KN, Zhang WY, Sun ZH, Kwok LY, Menghe B, et al. Untargeted mass spectrometry-based metabolomics approach unveils molecular changes in milk fermented by *Lactobacillus plantarum* P9. *LWT.* (2021) 140:110759. doi: 10.1016/j.lwt.2020.110759

34. Cai WC, Tang FX, Guo Z, Guo X, Zhang Q, Zhao XX, et al. Effects of pretreatment methods and leaching methods on jujube wine quality detected by electronic senses and HS-SPME-GC-MS. *Food Chem.* (2020) 330:127330. doi: 10.1016/j.foodchem.2020.127330

35. Cai W, Tang F, Wang Y, Zhang Z, Xue Y, Zhao X, et al. Bacterial diversity and flavor profile of Zha-Chili, a traditional fermented food in China. *Food Res Int.* (2021) 141:110112. doi: 10.1016/j.foodres.2021.110112

36. Donkor ON, Henriksson A, Vasiljevic T, Shah NP. alpha-Galactosidase and proteolytic activities of selected probiotic and dairy cultures in fermented soymilk. *Food Chem.* (2007) 104:10–20. doi: 10.1016/j.foodchem.2006.10.065

37. Kang JY, Kim MJ, Moon JS, Lee DK, Lee KH, Shin HS, et al. Producing functional soy-based yogurt incubated with *Bifidobacterium longum* SPM1205 isolated from healthy adult Koreans. *FASEB J.* (2012) 26:2944.

38. Yuan SH, Chang SKC. Selected odor compounds in soymilk as affected by chemical composition and lipoxygenases in five soybean materials. *J Agric Food Chem.* (2007) 55:426–31. doi: 10.1021/jf062274x

39. Singh BP, Vij S. alpha-Galactosidase activity and oligosaccharides reduction pattern of indigenous lactobacilli during fermentation of soy milk. *Food Biosci.* (2018) 22:32–7. doi: 10.1016/j.fbio.2018.01.002

40. Mantzourani I, Kazakos S, Terpou A, Alexopoulos A, Bezirtzoglou E, Bekatorou A, et al. Potential of the probiotic *Lactobacillus plantarum* ATCC 14917 strain to produce functional fermented pomegranate juice. *Foods.* (2019) 8:4. doi: 10.3390/foods8010004

41. Chu SC, Chen CS. Effects of origins and fermentation time on the antioxidant activities of kombucha. *Food Chem.* (2006) 98:502–7. doi: 10.1016/j.foodchem.2005.05.080

42. Xiao Y, Wang LX, Rui X, Li W, Chen XH, Jiang M, et al. Enhancement of the antioxidant capacity of soy whey by fermentation with *Lactobacillus plantarum* B1-6. *J Funct Foods.* (2015) 12:33–44. doi: 10.1016/j.jff.2014.10.033

43. Rekha CR, Vijayalakshmi G. Bioconversion of isoflavone glycosides to aglycones, mineral bioavailability and vitamin B complex in fermented soymilk by probiotic bacteria and yeast. *J Appl Microbiol.* (2010) 109:1198–208. doi: 10.1111/j.1365-2672.2010.04745.x

44. Hati S, Ningtyas DW, Khanuja JK, Prakash S. β-Glucosidase from almonds and yoghurt cultures in the biotransformation of isoflavones in soy milk. *Food Biosci.* (2020) 34:100542. doi: 10.1016/j.fbio.2020.100542

45. Chien H-L, Huang H-Y, Chou C-C. Transformation of isoflavone phytoestrogens during the fermentation of soymilk with lactic acid bacteria and bifidobacteria. *Food Microbiol.* (2006) 23:772–8. doi: 10.1016/j.fm.2006.01.002

46. Hur SJ, Lee SY, Kim YC, Choi I, Kim GB. Effect of fermentation on the antioxidant activity in plant-based foods. *Food Chem.* (2014) 160:346–56. doi: 10.1016/j.foodchem.2014.03.112

47. Kim NJ, Jang HL, Yoon KY. Potato juice fermented with *Lactobacillus casei* as a probiotic functional beverage. *Food Sci Biotechnol.* (2012) 21:1301–7. doi: 10.1007/s10068-012-0171-5

48. Marazza JA, Nazareno MA, De Giori GS, Garro MS. Enhancement of the antioxidant capacity of soymilk by fermentation with *Lactobacillus rhamnosus*. *J Funct Foods.* (2012) 4:594–601. doi: 10.1016/j.jff.2012.03.005

49. Yang XX, Zhou JC, Fan LQ, Qin Z, Chen QM, Zhao LM. Antioxidant properties of a vegetable-fruit beverage fermented with two *Lactobacillus plantarum* strains. *Food Sci Biotechnol.* (2018) 27:1719–26. doi: 10.1007/s10068-018-0411-4

50. Kaur R, Prasad K. Technological, processing and nutritional aspects of chickpea (*Cicer arietinum*) – a review. *Trends Food Sci Technol.* (2021) 109:448–63. doi: 10.1016/j.tifs.2021.01.044

51. Li H, Yan L, Wang J, Zhang Q, Zhou Q, Sun T, et al. Fermentation characteristics of six probiotic strains in soymilk. *Ann Microbiol.* (2012) 62:1473–83. doi: 10.1007/s13213-011-0401-8

52. Zhu YY, Thakur K, Feng JY, Cai JS, Zhang JG, Hu F, et al. B-vitamin enriched fermented soymilk: a novel strategy for soy-based functional foods development. *Trends Food Sci Technol.* (2020) 105:43–55. doi: 10.1016/j.tifs.2020.08.019

53. Li C, Rui X, Zhang YH, Cai FY, Chen XH, Jiang M. Production of tofu by lactic acid bacteria isolated from naturally fermented soy whey and evaluation of its quality. *LWT.* (2017) 82:227–34. doi: 10.1016/j.lwt.2017.04.054

54. Yvon M, Rijnen L. Cheese flavour formation by amino acid catabolism. *Int Dairy J.* (2001) 11:185–201. doi: 10.1016/s0958-6946(01)00049-8

55. Liang HP, He Z, Wang XY, Song G, Chen HY, Lin XP, et al. Effects of salt concentration on microbial diversity and volatile compounds during suancai fermentation. *Food Microbiol.* (2020) 91:103537. doi: 10.1016/j.fm.2020.103537

56. Liu Y, Chen H, Chen W, Zhong Q, Zhang G, Chen W. Beneficial effects of tomato juice fermented by *Lactobacillus plantarum* and *Lactobacillus casei*: antioxidation, antimicrobial effect, and volatile profiles. *Molecules.* (2018) 23:2366. doi: 10.3390/molecules23092366

57. Chen RH, Chen WX, Chen HM, Zhang GF, Chen WJ. Comparative evaluation of the antioxidant capacities, organic acids, and volatiles of papaya juices fermented by *Lactobacillus acidophilus* and *Lactobacillus plantarum*. *J Food Qual.* (2018) 2018:9490435. doi: 10.1155/2018/9490435

58. Lee SM, Kim SB, Kim YS. Determination of key volatile compounds related to long-term fermentation of soy sauce. *J Food Sci.* (2019) 84:2758–76. doi: 10.1111/1750-3841.14771

59. Wang K, Arntfield SD. Binding of carbonyl flavours to canola, pea and wheat proteins using GC/MS approach. *Food Chem.* (2014) 157:364–72. doi: 10.1016/j.foodchem.2014.02.042

60. Tsangalis D, Shah NP. Metabolism of oligosaccharides and aldehydes and production of organic acids in soymilk by probiotic bifidobacteria. *Int J Food Sci Technol.* (2004) 39:541–54. doi: 10.1111/j.1365-2621.2004.00814.x

61. Zhuang K, Wu N, Wang X, Wu X, Wang S, Long X, et al. Effects of 3 feeding modes on the volatile and nonvolatile compounds in the edible tissues of female Chinese mitten crab (*Eriocheir sinensis*). *J Food Sci.* (2016) 81:S968–81. doi: 10.1111/1750-3841.13229

62. Cai W, Wang Y, Wang W, Shu N, Hou Q, Tang F, et al. Insights into the aroma profile of sauce-flavor Baijiu by GC-IMS combined with multivariate statistical analysis. *J Analy Methods Chem.* (2022) 2022:4614330. doi: 10.1155/2022/4614330

63. Chen Y, Li P, Liao LY, Qin YY, Jiang LW, Liu Y. Characteristic fingerprints and volatile flavor compound variations in Liuyang douchi during fermentation via HS-GC-IMS and HS-SPME-GC-MS. *Food Chem.* (2021) 361:130055. doi: 10.1016/j.foodchem.2021.130055

64. Peng XY, Li X, Shi XD, Guo ST. Evaluation of the aroma quality of Chinese traditional soy paste during storage based on principal component analysis. *Food Chem.* (2014) 151:532–8. doi: 10.1016/j.foodchem.2013.11.095

65. Zheng Y, Fei YT, Yang Y, Jin ZK, Yu BN, Li L. A potential flavor culture: *Lactobacillus harbinensis* M1 improves the organoleptic quality of fermented soymilk by high production of 2,3-butanedione and acetoin. *Food Microbiol.* (2020) 91:103540. doi: 10.1016/j.fm.2020.103540

66. Zhang X, Tian WL, Xie BJ, Sun ZD. Insight into the influence of lactic acid bacteria fermentation on the variations in flavor of chickpea milk. *Foods.* (2022) 11:2445. doi: 10.3390/foods11162445

67. Gao Y, Li D, Tian Z, Hou L, Gao J, Fan B, et al. Metabolomics analysis of soymilk fermented by *Bacillus subtilis* BSNK-5 based on UHPLC-Triple-TOF-MS/MS. *LWT.* (2022) 160:113311. doi: 10.1016/j.lwt.2022.113311

68. Azi F, Tu C, Meng L, Zhiyu L, Cherinet MT, Ahmadullah Z, et al. Metabolite dynamics and phytochemistry of a soy whey-based beverage bio-transformed by water kefir consortium. *Food Chem.* (2021) 342:128225. doi: 10.1016/j.foodchem.2020.128225

69. Ghosh D, Chattoraj DK, Chattopadhyay P. Studies on changes in microstructure and proteolysis in cow and soy milk curd during fermentation using lactic cultures for improving protein bioavailability. *J Food Sci Technol Mysore.* (2013) 50:979–85. doi: 10.1007/s13197-011-0421-1

70. De Vries MC, Vaughan EE, Kleerebezem M, De Vos WM. *Lactobacillus plantarum*- survival, functional and potential probiotic properties in the human intestinal tract. *Int Dairy J.* (2006) 16:1018–28. doi: 10.1016/j.idairyj.2005.09.003

71. Cai WC, Wang YR, Ni H, Liu ZJ, Liu JM, Zhong JA, et al. Diversity of microbiota, microbial functions, and flavor in different types of low-temperature Daqu. *Food Res Int.* (2021) 150:110734. doi: 10.1016/j.foodres.2021.110734

72. Power O, Jakeman P, Fitzgerald RJ. Antioxidative peptides: enzymatic production, in vitro and in vivo antioxidant activity and potential applications of milk-derived antioxidative peptides. *Amino Acids.* (2013) 44:797–820. doi: 10.1007/s00726-012-1393-9

73. Garcia-Tejedor A, Sanchez-Rivera L, Castello-Ruiz M, Recio I, Salom JB, Manzanares P. Novel antihypertensive lactoferrin-derived peptides produced by *Kluyveromyces marxianus*: gastrointestinal stability profile and in vivo angiotensin i-converting enzyme (ACE) inhibition. *J Agric Food Chem.* (2014) 62:1609–16. doi: 10.1021/jf4053868

74. Kobayashi J, Sasaki D, Hara KY, Hasunuma T, Kondo A. Metabolic engineering of the L-serine biosynthetic pathway improves glutathione production in *Saccharomyces cerevisiae*. *Microb Cell Fact.* (2022) 21:153. doi: 10.1186/s12934-022-01880-8

75. Wangsanut T, Pongpom M. The role of the glutathione system in stress adaptation, morphogenesis and virulence of pathogenic *Fungi*. *Int J Mol Sci.* (2022) 23:10645. doi: 10.3390/ijms231810645

frontiers | Frontiers in Nutrition

TYPE Original Research
PUBLISHED 04 January 2023
DOI 10.3389/fnut.2022.1077081

OPEN ACCESS

EDITED BY
Wenjiang Dong,
Chinese Academy of Tropical Agricultural Sciences, China

REVIEWED BY
Zhou Qi,
Chinese Academy of Agricultural Sciences (CAAS), China
Wanpeng Xi,
Southwest University, China

*CORRESPONDENCE
Changqing Wei
✉ wcq_food@shzu.edu.cn
Wenyu Liu
✉ 1538805022@qq.com

†These authors have contributed equally to this work

SPECIALTY SECTION
This article was submitted to Food Chemistry, a section of the journal Frontiers in Nutrition

RECEIVED 22 October 2022
ACCEPTED 21 November 2022
PUBLISHED 04 January 2023

CITATION
Li H, Han J, Zhao Z, Tian J, Fu X, Zhao Y, Wei C and Liu W (2023) Roasting treatments affect oil extraction rate, fatty acids, oxidative stability, antioxidant activity, and flavor of walnut oil. *Front. Nutr.* 9:1077081. doi: 10.3389/fnut.2022.1077081

Roasting treatments affect oil extraction rate, fatty acids, oxidative stability, antioxidant activity, and flavor of walnut oil

Huankang Li[1†], Jiajia Han[1†], Zhongkai Zhao[2], Jinhu Tian[3], Xizhe Fu[1], Yue Zhao[1], Changqing Wei[1,4*] and Wenyu Liu[1*]

[1]School of Food Science and Technology, Shihezi University, Shihezi, China, [2]College of Life Sciences and Technology, Xinjiang University, Ürümqi, China, [3]College of Biosystems Engineering and Food Science, Zhejiang University, Hangzhou, China, [4]Key Laboratory of Xinjiang Phytomedicine Resource and Utilization of Ministry of Education, Shihezi University, Shihezi, China

Introduction: The quality of pressed walnut oil can be improved by moderate roasting treatment.

Methods: This study compared physicochemical characteristics and antioxidant ability of walnut oils pressed from differently roasted pretreated walnuts, analyzed the correlation among these indicators by using Pearson correlation coefficient and correlation coefficient heatmap, and evaluated the volatile organic compounds (VOCs) of walnut oil under optimal pretreatment roasting conditions using headspace-gas chromatography-ion mobility spectrometry (HS-GC-IMS).

Results: Hierarchical cluster analysis (HCA) and principal component analysis (PCA) were able to remarkably distinguish walnut oil produced by different roasting processes. In addition, correlation analysis showed that there was a significant impact among indicators. There were 73 VOCs were identified in the optimum roasted treated walnut oil, consisting of 30 aldehydes, 13 alcohols, 11 ketones, 10 esters, 5 acids, 2 oxygen-containing heterocycles, 1 nitrogen-containing heterocycle and 1 other compound. GC-IMS results showed that aldehydes contributed significantly to the volatile flavor profile of walnut oil, especially (E)-2-heptenal, (E)-2-pentenal and hexenal.

Discussion: The properties of walnut oil based on varying roasting pretreatment of walnut kernels were significantly differentiated. Roasting at 120°C for 20 min is a suitable pretreatment roasting condition for pressing walnut oil. Roasting at 120°C for 20 min is a suitable pretreatment roasting condition for pressing walnut oil.

KEYWORDS

walnut oil, roasting treatment, physicochemical characteristics, antioxidant capacity, correlation analysis, volatile organic compounds, HS-GC-IMS

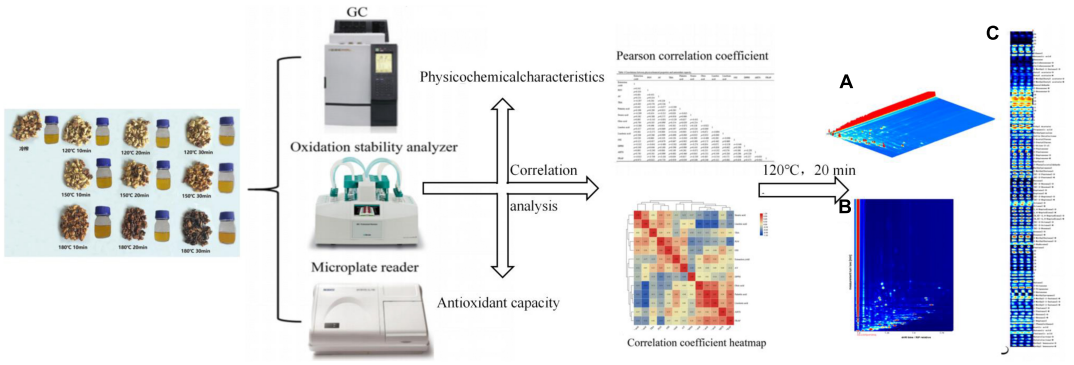

GRAPHICAL ABSTRACT

The physicochemical properties and antioxidant capacity of walnut oil obtained by pressing walnut kernels after different roasting times and temperatures were compared, and the correlations between these indicators were analyzed using Pearson correlation coefficients and correlation coefficient heat maps, and the volatile organic compounds of walnut oil under optimal pretreatment roasting conditions were evaluated using headspace-gas chromatography-ion mobility spectrometry.

1. Introduction

Walnut is a perennial deciduous tree of the genus Juglans, and with almonds, cashews and hazelnuts are known as the four dried fruits. At present, there are 21 species of walnut, which are widespread in the West Indies, southern Europe, Asia, Central America, North America, and western South America (1). The global walnut cultivation area reaches about 1.3 million hectares. Turkey, the United States, and China are the three major walnut producing countries, with the combined area and production of walnuts accounting for 69.22 and 81.32% of the world total, respectively (2). The main production areas of walnut in China include Yunnan Province (880,000 tons), Xinjiang Uygur Autonomous Region (440,000 tons), Sichuan Province (300,000 tons), Shaanxi Province (200,000 tons), Hebei Province (120,000 tons) and Guizhou Province (90,000 tons). Xinjiang's unique climatic conditions have created the excellent quality of Xinjiang walnuts. Hetian, Kashi, and Aksu are the three major walnut producing areas in Xinjiang of China, which main varieties include Zha No. 343, Xinfeng, Wen 185, Xinzaofeng, Xinxin No. 2. Walnuts contain large amounts of monounsaturated fatty acids (MUFAs) and polyunsaturated fatty acids (PUFAs), with an oil content of 60–70% (3). The ratio of ω-6: ω-3 PUFAs in walnut oil is generally 4:1, which is in line with the optimal ratio proposed by the World Health Organization (WHO) and the Food and Agriculture Organization of the United Nations (FAO). The flavonoids in walnut oil can relieve headache, tinnitus, dizziness, and other symptoms. The rich phospholipids in walnut oil can enhance cell activity, promote hematopoiesis, and protect brain nerves. Walnut oil is also rich in vitamin E, which plays an important role in scavenging free radicals and delaying aging (4, 5). However, the high content of unsaturated fatty acids in walnut oil can make it prone to oxidation, resulting in a short shelf life (6). In recent years, with the increasing interest in fats and oils from a health and nutritional perspective, consumers have become increasingly interested in unrefined vegetable oils, especially cold-pressed obtained (7). Cold pressing is the use of mechanical force to produce oil at a temperature below 60°C, such as poppy seed oil, pumpkin oil and rapeseed oil (8–12). Additionally, roasting is a pretreatment method for nut kernels before the oil extraction, which can effectively improve the flavor in the oil (13). Antioxidant activity and phenolic content of nuts such as peanuts, hazelnuts and cashews as affected by roasting treatment (14, 15). Chandrasekara and Shahidi treated the cashew at low and high temperatures, respectively, which confirmed that with the increase of roasting temperature, their antioxidant activity would also increase (16). The highest activity was achieved when nuts were roasted at 130°C for 33 min. This implied that the antioxidant effect of processed foods would be enhanced by Maillard reaction products generated during heat treatment (17). In addition, the fatty acid composition of walnut and hazelnut changed after the roasting treatment (18, 19). Lin et al. researched show that roasting enhanced the content of linoleic acid, oleic acid, and linolenic acid (20). In summary, moderate roasting may also cause changes in the physicochemical properties and antioxidant capacity of walnut oil. However, most of the researches focus on the change of properties caused by the roasting process, but the correlation between these properties has been insufficiently studied. Therefore, this study aimed to investigate and elucidate the correlation between the antioxidant capacity and physicochemical properties of walnut oil.

Odor is one of the typical characteristics of vegetable oil flavor, which is an important index to judge the quality of plant oil. It is an important factor in affecting consumer choice. The flavor of plant oils depends on the variety, ripeness degree, environmental condition, growing region, storage, and processing techniques (21–23). Processing technique can significantly affect the concentrations of major volatile components, and thus causing different flavors in plant oils (24). Headspace gas chromatography-ion mobility spectrometry (HS-GC-IMS) is a recent instrumentation technique for

the separation and detection of volatile organic compounds (VOCs) in mixed analytes (25). GC is widely applied to the measurement of volatiles. IMS has been applied mainly in airport security and military applications in the quick identification of chemical narcotics, explosives and warfare agents owing to its high sensitivity (26). Simultaneously, IMS has also been demonstrated valuable in other applications, like interior and exterior environmental quality control, food and pharmaceutical quality control, and respiratory disease monitoring (27–29). Specifically, IMS is developing extremely well in the food industry to examine information concerning food origin, food raw materials, food quality and food aroma (30–33). Therefore, HS-GC-IMS was utilized for the rapid identification of VOCs in walnut oil obtained from the suitable pretreatment roasting conditions determined in this research.

Pretreatment of walnut kernels through different roasting temperatures and durations will affect the physicochemical characteristics, antioxidant capacity and flavor of walnut oil. Walnut oil was prepared by the cold pressing method, using walnut kernels at various roasting temperatures (120, 150, and 180°C) and different durations (10, 20, and 30 min) in this paper. The fatty acid, physicochemical characteristics, free radical scavenging capacity and oxidative stability index (OSI) of the oils were investigated. Then, correlation analysis was performed on these indicators by the Pearson correlation coefficient and the correlation coefficient heatmap. HS-GC-IMS was utilized for the rapid identification of VOCs in walnut oil obtained from the determined suitable pretreatment roasting conditions. These results have significant implications for improving research and guiding the market.

2. Materials and methods

2.1. Walnut samples collection

The walnut samples were the Wen 185 walnuts from Aletai, Xinjiang, China. These walnuts were picked up in the Xinjiang Autonomous Region in 2019–2020.

2.2. Chemicals

Palmitic, stearic, oleic, linoleic, and linolenic acid standards, 2,2-Diphenyl-1-picrylhydrazyl (DPPH), 2,2′-Azino-bis (3-ethylbenzothiazoline-6-sulfonic acid) diammonium salt (ABTS) and 2,4,6-Tris (2-pyridyl)-1,3,5-triazine (TPTZ) were purchased from Sigma-Aldrich Inc. (St. Louis, MO). Sigma-Aldrich Chemical Co., Ltd. (Shanghai, China). Additional solvents and reagents were purchased from Tianjin Fuyu Fine Chemical Co. (Tianjin, China).

2.3. Walnut oil preparation

2.3.1. Roasting temperature and duration

The walnut kernels were divided at random into 30 groups of 300 g for each part, of which 27 portions were applied in roasting, and the remaining 3 were used as blank controls. The roasting temperature was set to 120, 150, and 180°C, and the roasting durations was set to 10, 20, and 30 min. A total of nine different groups of roasting treatments were carried out, with three parallel treatments in each group. Each sample is baked in the electric oven (K1H, Guangdong Galanz Microwave and Electrical Appliances Manufacturing Co., Ltd., China). The roasted walnuts were cooled to ambient temperature, stored in a sealed plastic bag, and placed in a 4°C refrigerator pending the next stage of experimentation.

2.3.2. Sample preparation

Walnut kernels were transferred to a screw press (ZY-22A, Wenzhou Hongkuo Technology Co., Ltd., China). The temperature in the press is 30°C, and the oil output temperature was 30 ± 2°C. The turbid oil was centrifuged at 8,000 r/min for 20 min, and then the supernatant oil was directly transferred to a 100 mL dark bottle for sealing storage, pending further experiments.

2.4. Determination of fatty acid

2.4.1. Fatty acid methyl esterification

The fatty acid methyl esterification (FAME) preparation followed the prior procedure except for some modifications (20). The crude walnut oil (200 mg) with 8 mL of 2% NaOH (prepared with methanol) refluxed in a water bath at 80 ± 1°C until the oil droplets disappeared, then 7 mL 15% BF_3 (made by methanol) was added to the conical flask and reacted for 2 min to completely derivatize the methyl ester. For the purification of methyl ester, 20 mL of hexane and 3 mL of saturated NaCl solution were added. The hexane extracted FAME products were dried with anhydrous Na_2SO_4 and then filtered through a 0.22 μm filter before being analyzed by GC.

2.4.2. GC analysis

The fatty acid was analyzed using a GC-2014 gas chromatograph (Shimadzu, Kyoto, Japan) and a HP-INNOWAX capillary column (0.25 μm, 30 m × 0.25 mm, Agilent, USA).

The operating conditions were as follows: nitrogen with a linear velocity of 1.0 mL/min as carrier gas, the flame ionization detector (FID) (Thermo Fisher), the sampler temperature was 240°C, injection mode was no split, injection volume was 1.0 μL, the chromatographic column adopted a gradient temperature increase, kept at 140°C for 2 min, then increased the temperature to 180°C at 5°C/min and held for 5 min,

and finally increased to 230°C at 5°C/min to maintain 6 min. The fatty acid composition was analyzed by comparing the retention time on the chromatogram of the sample and the FAME standard, and the fatty acid content was expressed as a relative percentage.

2.5. Determination of physicochemical properties

2.5.1. Determination of peroxide value

A mixture of 2 mL of oil sample, 1 mL of saturated potassium iodide solution and 30 mL of chloroform-glacial acetic acid (2:3, v/v) was added sequentially to a 250 mL conical flask, shaken for 0.5 min and allowed to stand for 3 min. Subsequently, 100 mL of distilled water was added to the conical flask and the mixture was titrated to light yellow with 0.001 mol/L of $Na_2S_2O_3{\cdot}5H_2O$, 1 mL of starch indicator was added and the titration was continued until the blue color of the solution disappeared.

2.5.2. Determination of acid value

The mixture of 50 mL 95% ethanol and 0.5 mL phenolphthalein indicator was heated to a slight boil in a 95°C water bath and titrated to red in 0.1 mol/L NaOH solution while hot. Twenty grams of oil sample was added, and the reaction was continued to be heated to a slight boil in a 95°C water bath and titrated to a slight red color.

2.5.3. Determination of 2-thiobarbituric acid

The thiobarbituric acid (TBA) reagent was 200 mg of 2-TBA with 1-butanol to 100 mL volumetric flask. After 12–15 h at room temperature, it was filtered and the filtrate was placed in a refrigerator at 4°C for use. After the 200 mg of oil sample was made up to 25 mL with 1-butanol, 5 mL of the mixture was mixed with TBA regent and allowed to stand in a water bath at 95°C for 2 h. The absorbance was measured at 530 nm with the spectrophotometer (T600, Beijing Puxi General Instrument Co., Ltd., Beijing, China).

2.6. Determination of antioxidant capacity

2.6.1. DPPH radical assay

The measurement was performed based on a modified reported method (34). Dissolve 5 g of walnut oil in 20 mL of methanol and mix, keep shaking and extract for 30 min at 50°C, centrifuge at low temperature (8,000 r/min) for 5 min. The supernatant was aspirated and the extraction process was repeated 4 times and the combined supernatant was polarized. Mix 1 mL of the polar substances with 1 mL of 1 mM DPPH (prepared with methanol), react in the dark at room temperature for 30 min. The absorbance of the reaction solution and the blank were measured at 517 nm. Meanwhile, different concentrations of Vitamin E (V_E) solutions were used instead of the sample as a control test. The results were showed as the equivalent of V_E.

2.6.2. Ferric reducing antioxidant power assay

The Ferric reducing antioxidant power (FRAP) method was performed according to the previous procedure with some modifications (35). The extraction of polar components of walnut oil was the same as that of DPPH. FRAP reagent was prepared by mixing 20 mmol/L $FeCl_3{\cdot}6H_2O$ solution, 10 mmol/L TPTZ solution (40 mmol/L HCl), and 0.1 mol/L sodium acetate buffer solution (pH 3.6) in a ratio of 1:1:10. The oil polar substance (200 μL) was dissolved into FRAP reagent (2 mL) and fixed to 10 mL with deionized water and reacted at 37°C for 10 min. Dissolve 27.802 mg $FeSO_4{\cdot}7H_2O$ into 100 mL with distilled water to configure 1 mmol/L $FeSO_4$ solution. After dilution, different concentration gradients of $FeSO_4$ and FRAP reagent were reacted to obtain $FeSO_4$ standard curve. The absorbance of the reaction solution and the blank were measured at 593 nm. Meanwhile, different concentrations of V_E solutions were used as control tests instead of the samples, and the results were expressed as the equivalent of V_E.

2.6.3. ABTS radical assay

ABTS was determined using the reported method with slight modifications (36). The extraction of polar components of walnut oil was the same as the extraction method in DPPH. The ABTS working solution was prepared by mixing 7 mmol/L ABTS and 2.45 mmol/L potassium persulfate solution in equal amounts, and placed in the dark at room temperature for 12–16 h. The ABTS working solution was diluted with ethanol to an absorbance of 0.700 ± 0.020 at 734 nm for analysis. The 200 μL of oil polar components and 4 mL of ABTS radical solution were mixed in the dark at room temperature for 20 min. The absorbance of the reaction solution and the blank were measured at 734 nm. Meanwhile, different concentrations of V_E solutions were used as control tests instead of the samples, and the results were expressed as the equivalent of V_E.

2.6.4. Oxidative stability index

The OSI was measured by the 892 professional Rancimat oil oxidation stability analyzer (Metrohm China Co., Ltd., Beijing, China) at 110°C and 20 L/h airflow. Use 5 g walnut oil for the measurement. High temperature and excessive air can accelerate the oxidation of glycerol fatty acid esters and produce volatile organic acids. The air brought volatile organic acids into a conductive chamber and changed the conductivity of water. The time period before the conductivity increases sharply (OSI time) was measured by continuously measuring the conductivity of the conductive chamber.

2.7. HS-GC-IMS analysis

The GC-IMS instrument (FlavourSpec®, the G.A.S. Department of Shandong Hai Neng Science Instrument Co., Ltd., Shandong, China) is equipped with a syringe and an automatic headspace research sampler unit. The sample entered the instrument with the carrier gas, passed through the gas chromatographic column for the initial separation, and then entered the ion transfer tube. Through the action of the reverse drift gas, it migrated to the Faraday disc for detection and realized the secondary separation.

In this study, 2.0 g sample of walnut oil sample was accurately weighed into a 20 mL headspace glass sampling vial and incubated at 500 rpm, 80°C for 20 min. Subsequently, 200 μL of headspace was automatically injected into the injector (85°C) Separation of VOCs was performed by the gas chromatographic column MXT-5 capillary column (15 m × 0.53 mm, 60°C) and the carrier gas consisted of 99.99% pure nitrogen. The programmed nitrogen flow rate was: 2 mL/min for 2 min; increased to 100 mL/min within the 2–20 min. The drift tube was maintained at 45°C under N_2 as a drift gas at 150 mL/min. the total running time was 30 min.

Retention indices (National Institute of Standards and Technology database) and drift times (IMS database) were used to perform qualitative analysis of VOCs in the sample.

2.8. Statistical analysis

Statistical analyses were carried out using Unscrambler version 9.7 (CAMO ASA, Oslo, Norway), Origin 2018 Pro (Originlab, Northampton, MA, USA) and SPSS 25.0 (IBM, Armonk, NY, USA). Correlation analysis was performed out by Pearson correlation coefficient and *t*-test. Chemometrics [principal component analysis (PCA) and Hierarchical cluster analysis (HCA)] were used to analyze the obtained data. The samples were determined three times and the results were recorded as mean ± standard deviation.

3. Results and discussion

3.1. Effect of roasting on oil extraction rate and fatty acid composition of walnut oil

The crude oil yields ranged from 41.48 to 54.41% from roasted walnut kernels. The oil yield of the roasted sample was significantly higher than that of the unroasted sample (41.48%) (**Figure 1**). The roasting treatment caused a series of changes in the walnut kernels, including destroying oil cells, promoting protein denaturation, reducing oil viscosity, which were suitable for squeezing oil and increasing oil yield. The oil extraction yield of walnut kernels increases with the extension of roasting time. The highest oil yield was obtained for the sample roasted at 120°C for 30 min compared to the other samples.

Table 1 shows the fatty acid compositions of walnut oil pressed from roasted walnut kernels under different roasting conditions. In all samples studied, the main fatty acids identified were linoleic acid (C18:2) (50.74–62.65%), oleic acid (C18:1) (13.33–20.88%), linolenic acid (C18:3) (12.39–17.59%), palmitic acid (C16:0) (7.08–9.41%), and stearic acid (C18:0) (1.22–2.44%). PUFAs were the primary fatty acids, with 68.33–77.06%, and the second were MUFAs, with 13.33–20.88%. Linoleic acid was the main fatty acid in walnut oil. The lowest content of linoleic acid was found in samples baked at 120°C for 30 min, and the highest content of linoleic acid was found in walnut oil baked at 150°C for 30 min.

The roasting treatment did not affect the composition of fatty acids in walnut oil, but the fatty acid content varied slightly after roasting. Moderate roasting can increase the content of unsaturated fatty acids (oleic acid and linoleic acid) and saturated fatty acids (palmitic acid), especially the sample roasted 120°C for 30 min. The results of Vaidya and Eun showed that there was no significant difference in the fatty acid composition of walnut oil obtained from roasted and unroasted walnut kernels, without considering the effect of roasting time and temperature (37). It is reported that the SFA content in perilla oil slightly increased after roasting treatment (38). Lin et al., reported that with the extension of temperature and duration, the content of unsaturated fatty acids and saturated fatty acids in almond kernel oil increased (20).

3.2. Physicochemical characteristics

Table 2 lists the physicochemical characteristics of the walnut oil. Walnut oil had a low acid value (AV) (0.12–0.37 mg NaOH/g), indicating that the roasting treatment did not promote the formation of free fatty acids in walnut oil. POV characterizes the degree of oil rancidity by measuring the oxidation products of the oil (4). The results revealed that the POV increased from 1.77 mmol/kg (120°C, 10 min) to 3.98 mmol/kg (180°C, 30 min) with increasing roasting temperature and time. Significant increase in POV indicated that the roasting treatment promoted the production of peroxides and hydroperoxides in walnut oil. However, the POV results still meet the standards for commercial edible vegetable oils (≤10 mmol/kg). TBA is directed to the oxidation products unsaturated fatty acid aldehydes, which are used to characterize the degree of oxidation in different oxidation stages. The resulting TBA values after roasting ranged from 0.0268 to 0.0318. Roasting at 120°C for 30 min, 150°C for 30 min and 180°C for 10 min had the lowest degree of oxidation at the corresponding temperature.

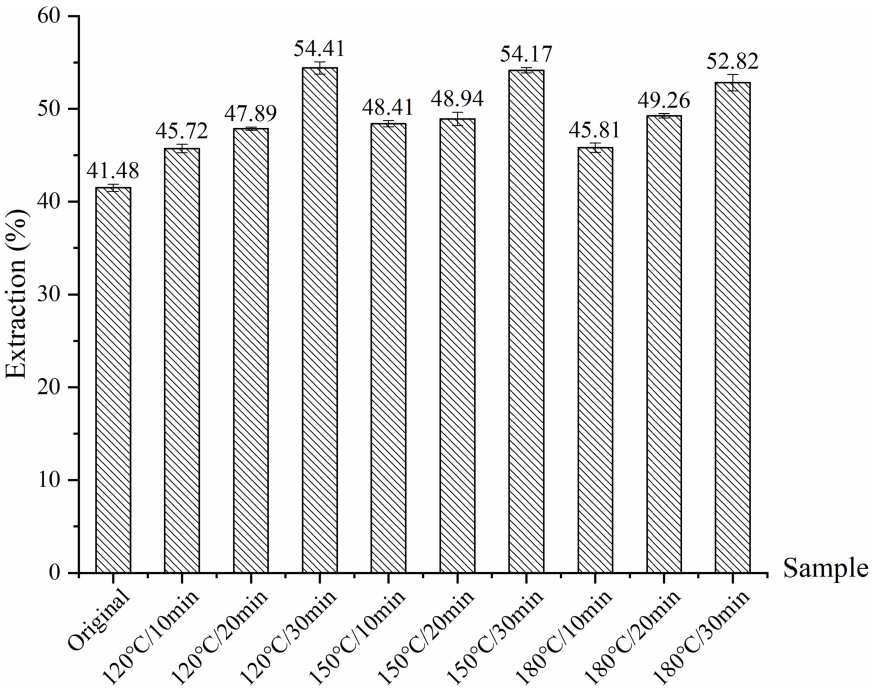

FIGURE 1
Extraction yields for walnut kernels roasted with different temperature and duration.

TABLE 1 Fatty acid composition (%) of walnut oil by roasted walnut kernels with different temperature and duration.

Sample		Palmitic acid	Stearic acid	Oleic acid	Linoleic acid	Linolenic acid	SFA	MUFA	PUFA
Original		7.08 ± 0.08^{c}	2.43 ± 0.03^{a}	15.79 ± 0.08^{bc}	62.31 ± 0.11^{a}	12.40 ± 0.08^{d}	9.51 ± 0.12^{cd}	15.79 ± 0.08^{bc}	74.71 ± 0.19^{ab}
120°C	10 min	7.99 ± 0.13^{bc}	1.26 ± 0.25^{c}	17.97 ± 0.05^{ab}	58.87 ± 0.35^{b}	13.94 ± 0.09^{cd}	9.24 ± 0.38^{d}	17.97 ± 0.05^{ab}	72.80 ± 0.43^{bc}
	20 min	8.70 ± 0.06^{ab}	1.57 ± 0.02^{bc}	19.02 ± 0.09^{ab}	54.03 ± 0.45^{c}	16.69 ± 0.40^{ab}	10.28 ± 0.04^{ab}	19.02 ± 0.09^{ab}	70.72 ± 0.06^{cd}
	30 min	9.41 ± 0.13^{a}	1.39 ± 0.08^{c}	20.88 ± 0.18^{a}	50.74 ± 0.28^{d}	17.59 ± 0.25^{a}	10.80 ± 0.22^{a}	20.88 ± 0.18^{a}	68.33 ± 0.04^{d}
150°C	10 min	8.84 ± 0.36^{ab}	1.67 ± 0.01^{abc}	18.73 ± 0.33^{ab}	55.68 ± 0.70^{c}	15.10 ± 0.74^{bc}	10.51 ± 0.37^{ab}	18.73 ± 0.33^{ab}	70.77 ± 0.04^{cd}
	20 min	7.41 ± 0.24^{c}	1.22 ± 0.25^{c}	16.28 ± 1.19^{bc}	60.92 ± 2.09^{a}	14.18 ± 0.91^{cd}	8.63 ± 0.01^{e}	16.28 ± 1.19^{bc}	75.10 ± 1.18^{ab}
	30 min	8.14 ± 1.19^{bc}	1.89 ± 0.67^{abc}	13.82 ± 3.01^{c}	62.65 ± 1.07^{a}	13.50 ± 1.43^{cd}	10.02 ± 0.51^{bc}	13.82 ± 3.01^{c}	76.16 ± 2.50^{a}
180°C	10 min	7.15 ± 0.11^{c}	2.33 ± 0.01^{ab}	15.91 ± 0.02^{bc}	61.57 ± 0.06^{a}	13.06 ± 0.02^{cd}	9.48 ± 0.11^{cd}	15.91 ± 0.02^{bc}	74.62 ± 0.08^{ab}
	20 min	7.82 ± 1.03^{bc}	1.80 ± 0.72^{abc}	13.33 ± 3.42^{c}	62.46 ± 0.93^{a}	14.61 ± 2.18^{bcd}	9.61 ± 0.31^{cd}	13.33 ± 3.42^{c}	77.06 ± 3.11^{a}
	30 min	7.10 ± 0.13^{c}	2.44 ± 0.00^{a}	16.62 ± 0.07^{bc}	61.45 ± 0.07^{a}	12.39 ± 0.01^{d}	9.54 ± 0.13^{cd}	16.62 ± 0.07^{bc}	73.84 ± 0.06^{abc}

Values (mean ± SD, $n = 3$) in the same column followed by a different letter are significantly different ($p < 0.05$).

3.3. Analysis of antioxidant capacity

Table 3 lists the free radical scavenging ability (FRAP, ABTS, and DPPH) and OSI of walnut oil under different roasting conditions. The oxidation process of the walnut oil can be accelerated by exposing the walnut oil to 110°C and the air at a flow rate of 20 L/h (39). The oxidative stability of walnut oil was characterized by measuring the length of the induction time from the induction period to the oxidation period. The OSI of walnut oil ranged from 4.53 to 5.57 h, indicating that roasting caused increasing OSI of the oil. In the FRAP assay, the results ranged from 88.19 to 119.45 μmol TE/kg. For ABTS, the results were in the range of 14.76–95.48 μmol TE/kg. The DPPH results varied from 1.84 to 45.45 μmol TE/kg. Moderate roasting treatment could lead to a significant increase ($p < 0.05$) in the antioxidant activity of walnut oil. Roasting of kernels at 120°C for 20 min resulted in a significant increase ($p < 0.05$) in the ABTS and FRAP test values compared to those of others sample, while the highest value of DPPH appeared at 120°C for 10 min.

TABLE 2 Peroxide value, acid value, and thiobarbituric acid of walnut oil by roasted walnut kernels with different temperature and duration.

Sample		POV (mmol/kg)	AV (mg NaOH/g)	TBA
Original		1.59 ± 0.09^{i}	0.12 ± 0.25^{e}	0.0313 ± 0.0019^{b}
120°C	10 min	1.77 ± 0.05^{h}	0.23 ± 0.23^{cd}	0.0315 ± 0.0006^{b}
	20 min	1.93 ± 0.02^{g}	0.23 ± 0.21^{cd}	0.0318 ± 0.0005^{b}
	30 min	2.00 ± 0.02^{g}	0.20 ± 0.10^{d}	0.0268 ± 0.0010^{d}
150°C	10 min	2.34 ± 0.04^{f}	0.29 ± 0.17^{b}	0.0285 ± 0.0006^{c}
	20 min	2.57 ± 0.06^{e}	0.37 ± 0.10^{a}	0.0303 ± 0.0010^{b}
	30 min	2.71 ± 0.07^{d}	0.21 ± 0.15^{d}	0.0270 ± 0.0000^{d}
180°C	10 min	3.58 ± 0.09^{c}	0.19 ± 0.10^{d}	0.0270 ± 0.0000^{d}
	20 min	3.83 ± 0.05^{b}	0.26 ± 0.31^{bc}	0.0355 ± 0.0013^{a}
	30 min	3.98 ± 0.12^{a}	0.34 ± 0.53^{a}	0.0318 ± 0.0009^{b}

Values (mean ± SD, $n = 3$) in the same column followed by a different letter are significantly different ($p < 0.05$). POV (mmol/kg) = (volume consumed by the sample-volume consumed by the blank) × concentration of $Na_2S_2O_3 \cdot 5H_2O$ × 1,000/(2 × quality of oil sample). AV (mg NaOH/g) = volume consumed by the titrant × concentration of NaOH × 39.996/quality of oil sample. TBA = (50 × absorbance of the tested solution/sample weight) × 100%.

TABLE 3 Oxidative stability index (h) and free radical scavenging capacity (μmol TE/L) of walnut oil by roasted walnut kernels with different temperature and duration.

Sample		OSI	DPPH	ABTS	FRAP
Original		4.53 ± 0.31^{c}	29.19 ± 3.21^{b}	30.00 ± 0.72^{d}	101.41 ± 2.86^{c}
120°C	10 min	4.68 ± 0.12^{c}	45.45 ± 2.37^{a}	14.76 ± 0.42^{h}	106.13 ± 1.61^{b}
	20 min	5.34 ± 0.30^{ab}	12.91 ± 1.57^{d}	95.48 ± 0.83^{a}	119.45 ± 1.22^{a}
	30 min	4.77 ± 0.13^{c}	18.56 ± 1.39^{c}	26.44 ± 0.72^{e}	102.31 ± 0.66^{c}
150°C	10 min	4.78 ± 0.24^{c}	13.59 ± 1.42^{d}	21.44 ± 0.72^{f}	109.07 ± 0.26^{b}
	20 min	4.69 ± 0.23^{c}	18.55 ± 1.55^{c}	29.76 ± 0.83^{d}	100.10 ± 1.46^{cd}
	30 min	5.57 ± 0.20^{a}	31.89 ± 2.16^{b}	38.80 ± 0.42^{b}	106.85 ± 2.23^{b}
180°C	10 min	5.14 ± 0.08^{b}	19.44 ± 0.68^{c}	15.24 ± 0.42^{h}	88.19 ± 0.16^{e}
	20 min	5.45 ± 0.19^{ab}	4.55 ± 1.78^{e}	19.76 ± 1.10^{g}	96.99 ± 2.93^{d}
	30 min	5.41 ± 0.13^{ab}	1.84 ± 0.68^{e}	36.68 ± 0.42^{c}	91.19 ± 3.23^{e}

Values (mean ± SD, $n = 3$) in the same column followed by a different letter are significantly different ($p < 0.05$).

The results of free radicals scavenging capacity and OSI indicated that the roasting treatment can strengthen the antioxidant capacity of walnut oil. The research results of Aleksander et al. on the antioxidant capacity of rapeseed oil prepared after roasting are consistent with this study (40). The antioxidant activity of Sacha Inchi oil is also improved by roasting Sacha Inchi (*Plukenetia Volubilis L.*) seeds (41). Plants contain many phenolic compounds with antioxidant capacity in the combined form (42). The roasting treatment may destroy these phenolic compounds in the form of covalent bonding, and release the phenolic compounds in free form. The marked enhancement in the antioxidant capacity of the oil after roasting treatment may be attributed to the degradation of some heat-insensitive antioxidant components to produce heat-resistant antioxidant components and the formation of some antioxidants with potential antioxidant activity by Maillard reaction (17, 43).

3.4. PCA and HCA

Principal component analysis aims to use mathematical dimensionality reduction methods to transform multiple variables into a small number of new variables using orthogonal changes, thereby using new variables to reflect the main characteristics of things in a smaller dimension. Thirteen variables were employed for statistically evaluating including extraction yield, physicochemical characteristics, and antioxidant capacity (**Figure 2A**).

We note that the first two component scores consider 92% (component 1 = 71% and component 2 = 21%) of the total variation. Component 1 exhibits positive loading mainly with ABTS, FRAP, linolenic acid, OSI, palmitic acid, and negative loading with linoleic acid. The main contributors to principal component 2 are DPPH, POV, FRAP, AV, OSI, stearic acid, and extraction yield. The figure showed that the sample roasted at 120°C for 20 min can be clearly distinguished from

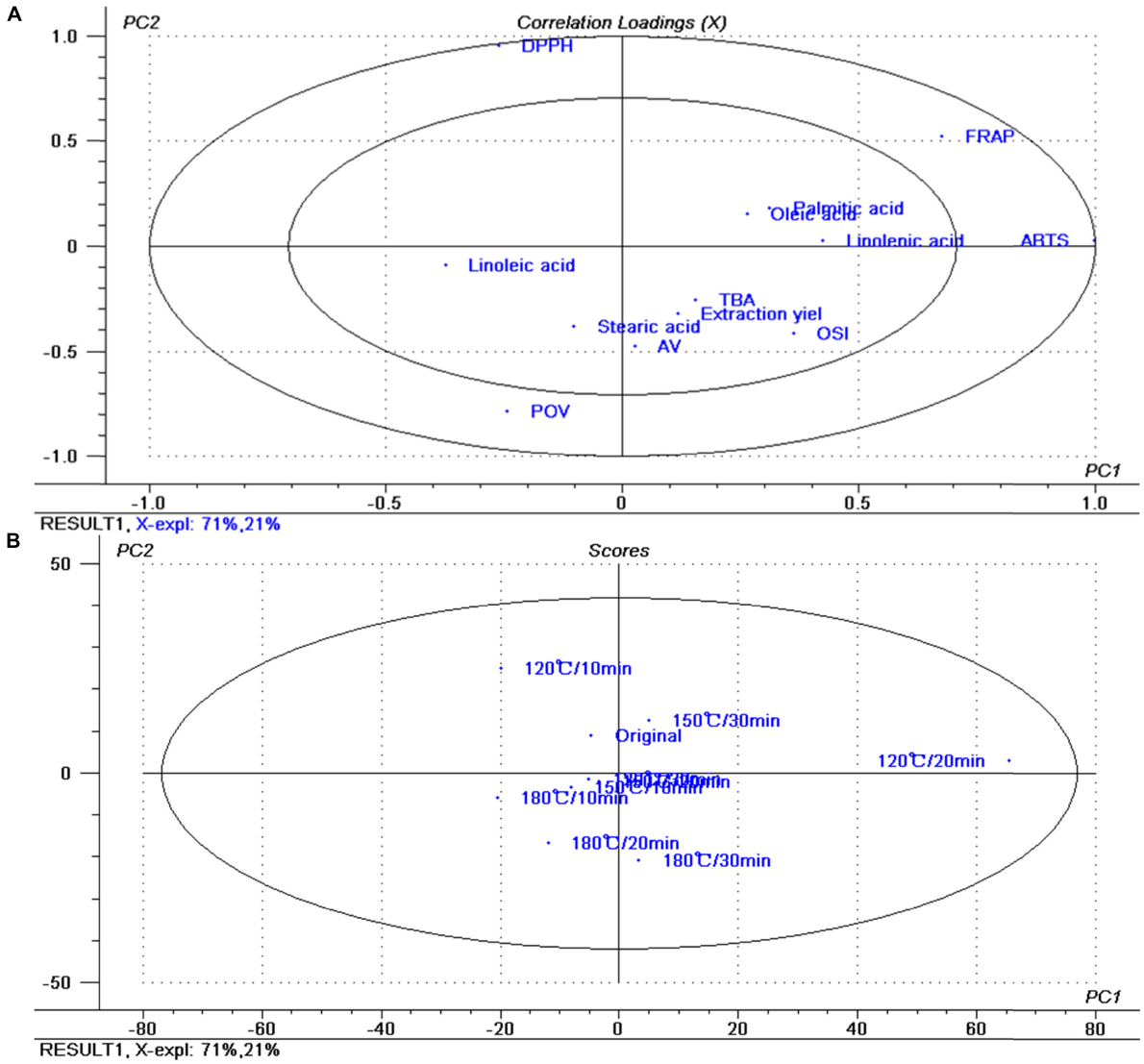

FIGURE 2
Principal component analysis of the data. **(A)** Loadings plot. **(B)** Scores plot.

other samples (Figure 2B). According to the above research, considering that the samples roasted at 120°C for 20 min have better antioxidant capacity, this roasting treatment is a suitable pretreatment roasting condition for pressing walnut oil.

Hierarchical cluster analysis is a type of clustering algorithm. It uses Euclidean distance to calculate the distance (similarity) between different data points and sequentially combines the two closest data points to generate a hierarchical nested clustering tree (Figure 3). The smaller the distance between data points, the higher the similarity. These results show that walnut oil samples have a clear tendency to aggregate. The tree structure of the cluster analysis was divided into two main parts when the 10-distance threshold was chosen. The sample roasted at 120°C for 20 min can be clearly distinguished from other samples. In summary, we can conclude that the sample roasted at 120°C for 20 min is the better processing condition.

3.5. Correlations between indicators of walnut oils

Heatmap is a common visualization method in scientific research papers. The correlation of samples is often displayed in the form of correlation heatmap. In summary, any value that characterizes the correlation can be plotted using a correlation heatmap. The depth of color in the correlation heatmap can clearly show the strength of the correlation among indicators (Figure 4). The red color represents a positive correlation, blue

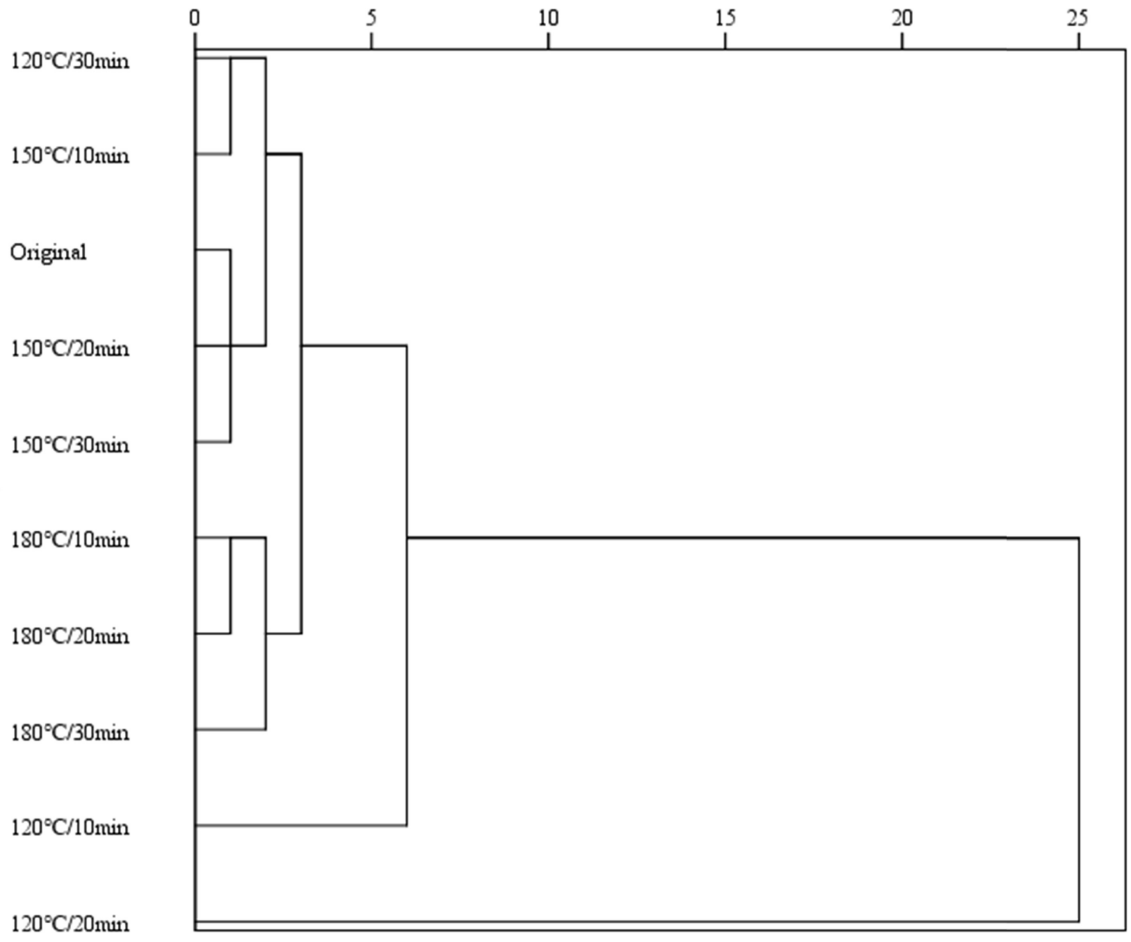

FIGURE 3
Hierarchical cluster analysis of walnut oil.

color represents a negative correlation. Palmitic acid had a significant positive correlation with linolenic acid (r = 0.905, $p < 0.01$), oleic acid (r = 0.657, $p < 0.05$) and FRAP (r = 0.657, $p < 0.05$), and a significant negative correlation with linoleic acid (r = –0.871, $p < 0.01$). POV showed a significant positive correlation with OSI (r = 0.663, $p < 0.05$), and a significant negative correlation with DPPH (r = –0.641, $p < 0.05$) and FRAP (r = –0.709, $p < 0.05$). Linolenic acid was significant negative correlated with stearic acid (r = –0.673, $p < 0.05$) and linoleic acid (r = –0.894, $p < 0.01$), and positively correlated with oleic acid (r = 0.672, $p < 0.05$). Linoleic acid displayed a significant negative correlation on oleic acid (r = –0.922, $p < 0.01$). FRAP exhibited a significant positive correlation on ABTS (r = 0.650, $p < 0.05$). There is no significant relationship between the rest. At the same time, these indicators can be divided into two categories through cluster analysis. The first category includes TBA, stearic acid, linoleic acid, POV, and OSI. The other category includes DPPH, extraction yield, AV, palmitic acid, oleic acid, linolenic acid, ABTS, and FRAP.

3.6. HS-GC-IMS analysis

Volatiles of walnut oil (120°C, 20 min) were plotted in 3D topography (**Figure 5A**). The X, Y, and Z axis in 3D spectrum correspond to ion drift identification time, gas chromatography retention time and quantitative peak height, respectively. **Figure 5B** shows the gas-phase ion mobility profiles of volatile compounds from walnut oil. The vertical coordinate is the retention time (s) of the compound, and the horizontal coordinate is the ion migration time (ms). Each point on the spectrum represents a volatile compound, with red representing high concentration and white representing low concentration, and the darker the color indicates the higher concentration of the volatile compound. The results of the qualitative analysis of volatile compounds using the NIST database and IMS database integrated with the software are shown in **Supplementary Table**. A total of 73 volatile compounds were detected, including 30 aldehydes, 13 alcohols, 11 ketones, 10 esters, 5 acids, 2 oxygen-containing heterocycles, 1 nitrogen-containing heterocycle and

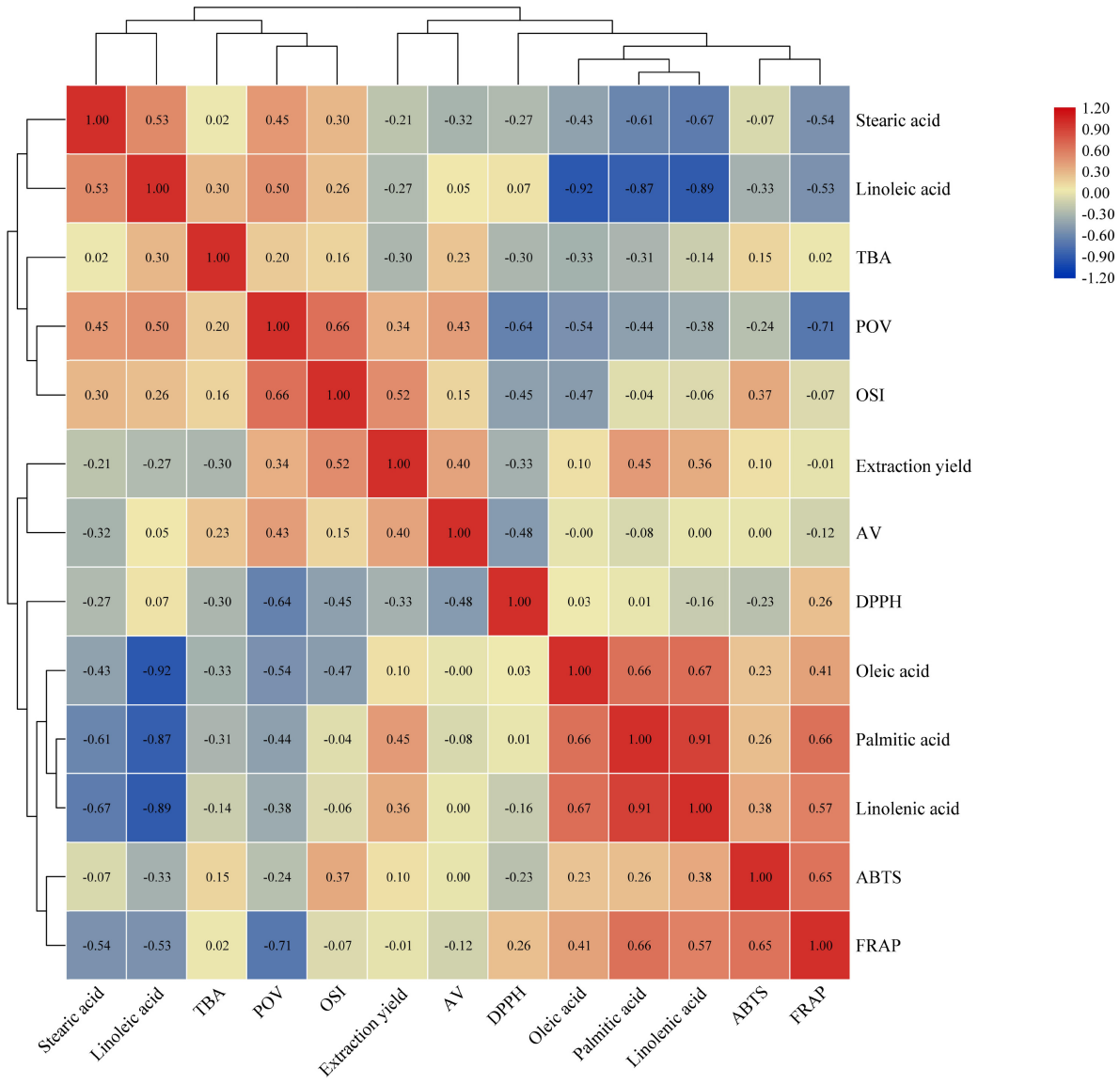

FIGURE 4
Correlation heatmap between walnut oil indicators.

1 other compound. Figure 5C shows the fingerprint profile, each row of the figure represents the peak intensity of all volatile compounds in the walnut oil sample, and each column represents the peak intensity of a volatile compound in the walnut oil sample. Dimer or polymer formation in the ionized region is associated with high proton affinity of the volatile compound and results in a varying drift time in contrast to the monomeric form, so that some compounds can produce two peak signals, including dimer (D) and monomer (M), as observed in GC-IMS (44).

Aldehydes are mainly derived from the cleavage of free radicals of lipid molecules. The peroxides generated by auto-oxidation of lipids decompose to form alkoxy radicals and hydroxyl radicals, which further cleave to form volatile organic compounds such as aldehydes, alkenes and alcohols (45, 46). Aldehydes have aromatic characteristics such as clear, fruity, and fatty aromas, and their detection concentration is high and the aroma threshold is low, which is the main aroma presenting substance of walnut oil. Among them, (*E*)-2-heptenal, (*E*)-2-pentenal and hexanal were the aldehydes with the highest peak intensity in the pretreated walnut oil at 120°C, 20 min. (*E*)-2-heptenal had a green, herbal or cucumber aroma and was a high-concentration volatile compound in cooked white quinoa samples (47). (*E*)-2-Pentenal was considered as a potential marker for linolenic acid-based vegetable oils (48). Hexanal was derived from 13-hydroperoxides formed by the autoxidation

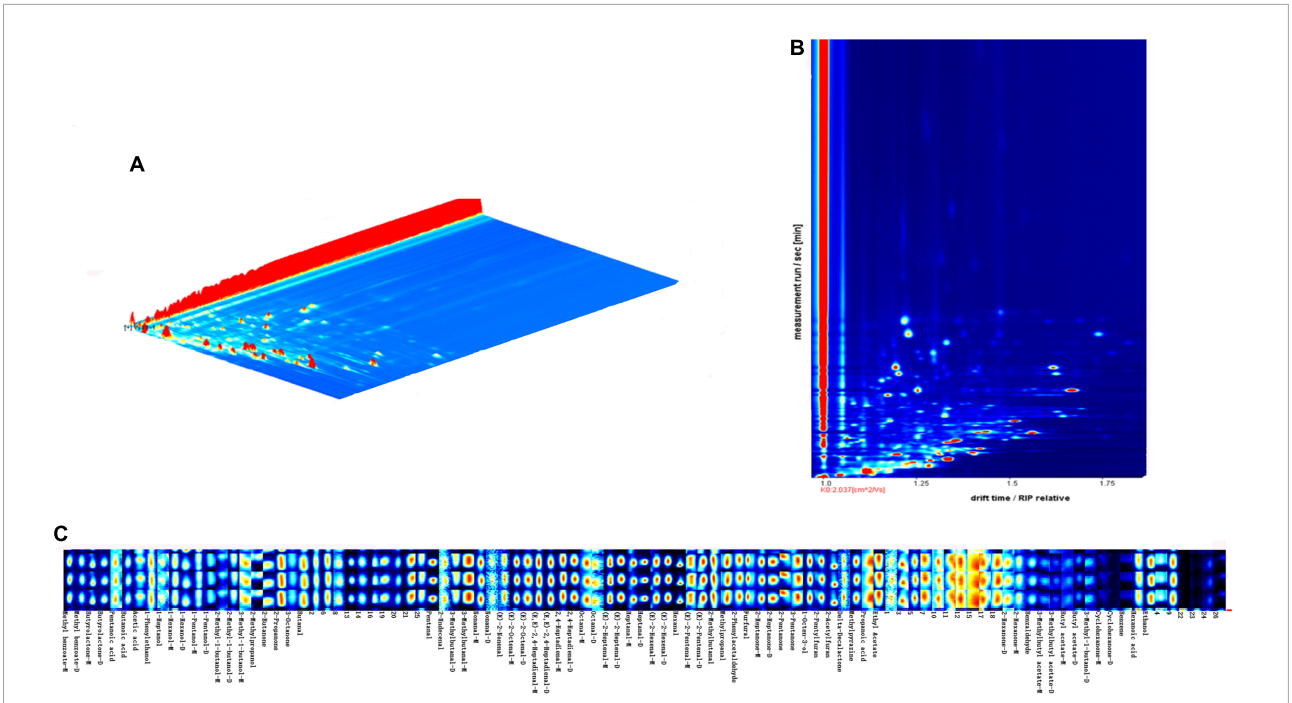

FIGURE 5
3D topography **(A)**, 2D-topographic plots **(B)** and fingerprinting of VOCs **(C)** of walnut oil under optimal roasting treatment (120°C, 20 min).

of linoleic acid and was directly related to the formation of off-flavors from the oxidation of oils and fats (49, 50). Ketones are produced through lipid degradation, Maillard reaction and interaction between these two reactions. In addition, ketones have a comparatively high-odor threshold, contributing to a minor flavor impact on food (51). 2-Acetone was the volatile compound with the highest peak intensity in walnut oil (5,480). The ester and aldehyde with the highest peak areas in walnut oil were ethyl acetate (pineapple flavor) and ethanol (sweetness), respectively, which were considered potential markers of yogurt flavor quality (52).

4. Conclusion

In this work, we investigated the effects of roasting treatment on the physicochemical properties, antioxidant capacity and correlation between indicators of walnut oil, and further measured the flavor substances of walnut oil under optimal roasting treatment. Linoleic acid (62.31% of the crude oil) and oleic acid (12.40% of crude oil) were the predominant fatty acids in the oil extracted from walnut kernels without roasted. Moderate roasting could increase the content of unsaturated fatty acids (oleic acid and linoleic acid) and saturated fatty acids (palmitic acid), especially the sample roasted 120°C for 30 min. As the roasting temperature and duration increases, it caused a statistically significant increase in POV relative to the control sample. PCA and HCA could distinguish walnut oil from different roasting treatments, and the result showed that roasting at 120°C for 20 min was a suitable pretreatment roasting condition for pressing walnut oil. There were significant influences among indicators. POV had a significant positive correlation with OSI ($r = 0.633$, $p < 0.05$), and a significant negative correlation with DPPH ($r = -0.641$, $p < 0.05$) and FRAP ($r = -0.709$, $p < 0.05$). Palmitic acid had a significant positive correlation on FRAP ($r = 0.657$, $p < 0.05$). Antioxidant capacity (OSI, DPPH, and FRAP) could be guided by the correlation between POV and palmitic acid. The study also rapidly identified VOCs in walnut oil obtained under suitable pretreatment roasting conditions. Aldehydes with clear, fruity, and fatty aromas were considered as the main aroma-presenting substances of walnut oil.

Data availability statement

The original contributions presented in this study are included in the article/**Supplementary material**, further inquiries can be directed to the corresponding authors.

Author contributions

HL: conceptualization, methodology, formal analysis, and writing—original draft. JH: formal analysis,

writing—original draft, and writing—review and editing. ZZ and JT: writing—review and editing, resources, and supervision. XF: supervision and writing—review and editing. YZ: writing—review and editing. CW and WL: funding acquisition, resources, and supervision. All authors contributed to the article and approved the submitted version.

Funding

This work was supported by the Major Science and Technology Research Project of Xinjiang Autonomous Region (Grant no. 2022A020009-2).

Conflict of interest

The authors declare that the research was conducted in the absence of any commercial or financial relationships that could be construed as a potential conflict of interest.

Publisher's note

All claims expressed in this article are solely those of the authors and do not necessarily represent those of their affiliated organizations, or those of the publisher, the editors and the reviewers. Any product that may be evaluated in this article, or claim that may be made by its manufacturer, is not guaranteed or endorsed by the publisher.

Supplementary material

The Supplementary Material for this article can be found online at: https://www.frontiersin.org/articles/10.3389/fnut.2022.1077081/full#supplementary-material

References

1. Aradhya, M, Potter D, Gao F, Simon C. Molecular phylogeny of Juglans (*Juglandaceae*): a biogeographic perspective. *Tree Genet Genomes.* (2007) 3:363–78. doi: 10.1007/s11295-006-0078-5

2. Wang P, Zhong L, Yanga H, Zhu F, Hou X, Wu C, et al. Comparative analysis of antioxidant activities between dried and fresh walnut kernels by metabolomic approaches. *LWT Food Sci Technol.* (2022) 155:112875. doi: 10.1016/j.lwt.2021.112875

3. Zhou Y, Fan W, Chu F, Pei D. Improvement of the flavor and oxidative stability of walnut oil by microwave pretreatment. *J Am Oil Chem Soc.* (2016) 93:1563–72. doi: 10.1007/s11746-016-2891-9

4. Gharibzahedi S, Mousavi S, Hamedi M, Khodaiyan F. Determination and characterization of kernel biochemical composition and functional compounds of Persian walnut oil. *J Food Sci Technol.* (2014) 51:34–42. doi: 10.1007/s13197-011-0481-2

5. Pereira J, Oliveira I, Sousa A, Ferreira I, Bento A, Estevinho L. Bioactive properties and chemical composition of six walnut (*Juglans regia L.*) cultivars. *Food Chem Toxicol.* (2008) 46:2103–11. doi: 10.1016/j.fct.2008.02.002

6. Rébufa C, Artaud J, Le Dréau Y. Walnut (*Juglans regia L.*) oil chemical composition depending on variety, locality, extraction process and storage conditions: a comprehensive review. *J Food Compos Anal.* (2022) 110:104534. doi: 10.1016/j.jfca.2022.104534

7. Mildner-Szkudlarz S, Różańska M, Siger A, Kowalczewski P, Rudzińska M. Changes in chemical composition and oxidative stability of cold-pressed oils obtained from by-product roasted berry seeds. *LWT Food Sci Technol.* (2019) 111:541–7. doi: 10.1016/j.lwt.2019.05.080

8. Rękas A, Wroniak M, Rusinek R. Influence of roasting pretreatment on high-oleic rapeseed oil quality evaluated by analytical and sensory approaches. *Int J Food Sci Technol.* (2015) 50:2208–14. doi: 10.1111/ijfs.12884

9. Mikołajczak N, Tańska M, Ogrodowska D. Phenolic compounds in plant oils: a review of composition, analytical methods, and effect on oxidative stability. *Trends Food Sci Technol.* (2021) 113:110–38. doi: 10.1016/j.tifs.2021.04.046

10. Siger A, Michalak M. The long-term storage of cold-pressed oil from roasted rapeseed: effects on antioxidant activity and levels of canolol and tocopherols. *Eur J Lipid Sci Technol.* (2015) 118:1030–41. doi: 10.1002/ejlt.201500183

11. Potoènik T, Rak Cizej M, Košir I. Influence of seed roasting on pumpkin seed oil tocopherols, phenolics and antiradical activity. *J Food Compos Anal.* (2018) 69:7–12. doi: 10.1016/j.jfca.2018.01.020

12. EmÝR D, AydenÝZ B, Yilmaz E. Effects of roasting and enzyme pretreatments on yield and quality of cold-pressed poppy seed oils. *Turk J Agric For.* (2015) 39:260–71. doi: 10.1002/jsfa.1904

13. Parker J. Thermal generation or aroma. In: Parker JK, Elmore JS, Methven L editors. *Flavour Development, Analysis and Perception in Food and Beverages.* Sawston: Woodhead publishing (2015). p. 151–85. doi: 10.1016/B978-1-78242-103-0.00008-4

14. Chang S, Alasalvar C, Bolling B, Shahidi F. Nuts and their co-products: the impact of processing (roasting) on phenolics, bioavailability, and health benefits – A comprehensive review. *J Funct Foods.* (2016) 26:88–122. doi: 10.1016/j.jff.2016.06.029

15. Vinson J, Cai Y. Nuts, especially walnuts, have both antioxidant quantity and efficacy and exhibit significant potential health benefits. *Food Funct.* (2012) 3:134–40. doi: 10.1039/c2fo10152a

16. Chandrasekara N, Shahidi F. Effect of roasting on phenolic content and antioxidant activities of whole cashew nuts, kernels, and testa. *J Agric Food Chem.* (2011) 59:5006–14. doi: 10.1021/jf2000772

17. Dewanto V, Wu X, Adom K, Liu R. Thermal processing enhances the nutritional value of tomatoes by increasing total antioxidant activity. *J Agric Food Chem.* (2002) 50:3010–4. doi: 10.1021/jf0115589

18. Gao P, Liu R, Jin Q, Wang X. Effects of processing methods on the chemical composition and antioxidant capacity of walnut (*Juglans regia L.*) oil. *LWT Food Sci Technol.* (2021) 135:109958. doi: 10.1016/j.lwt.2020.109958

19. Belviso S, Dal Bello B, Giacosa S, Bertolino M, Ghirardello D, Giordano M, et al. Chemical, mechanical and sensory monitoring of hot air- and infrared-roasted hazelnuts (*Corylus avellana L.*) during nine months of storage. *Food Chem.* (2017) 217:398–408. doi: 10.1016/j.foodchem.2016.08.103

20. Lin J, Liu S, Hu C, Shyu Y, Hsu C, Yang D. Effects of roasting temperature and duration on fatty acid composition, phenolic composition, Maillard reaction degree and antioxidant attribute of almond (*Prunus dulcis*) kernel. *Food Chem.* (2016) 190:520–8. doi: 10.1016/j.foodchem.2015.06.004

21. Angerosa F, Servili M, Selvaggini R, Taticchi A, Esposto S, Montedoro G. Volatile compounds in virgin olive oil: occurrence and their relationship with the quality. *J Chromatogr A.* (2004) 1054:17–31. doi: 10.1016/s0021-9673(04)01298-1

22. Kandylis P, Vekiari A, Kanellaki M, Grati Kamoun N, Msallem M, Kourkoutas Y. Comparative study of extra virgin olive oil flavor profile of Koroneiki variety (*Olea europaea* var. *Microcarpa alba*) cultivated in Greece and Tunisia

during one period of harvesting. *LWT Food Sci Technol.* (2011) 44:1333–41. doi: 10.1016/j.lwt.2010.12.021

23. Yu P, Yang Y, Zhou Q, Jia X, Zheng C, Zhou Q, et al. Identification of volatile sulfur-containing compounds and the precursor of dimethyl sulfide in cold-pressed rapeseed oil by GC–SCD and UPLC–MS/MS. *Food Chem.* (2022) 367:130741. doi: 10.1016/j.foodchem.2021.130741

24. Wei C, Xi W, Nie X, Liu W, Wang Q, Yang B, et al. Aroma characterization of flaxseed oils using headspace solid-phase microextraction and gas chromatography-olfactometry. *Eur J Lipid Sci Technol.* (2013) 115:1032–42. doi: 10.1002/ejlt.201200397

25. Cavanna D, Zanardi S, Dall'Asta C, Suman M. Ion mobility spectrometry coupled to gas chromatography: a rapid tool to assess eggs freshness. *Food Chem.* (2019) 271:691–6. doi: 10.1016/j.foodchem.2018.07.204

26. Babis J, Sperline R, Knight A, Jones D, Gresham C, Denton M. Performance evaluation of a miniature ion mobility spectrometer drift cell for application in hand-held explosives detection ion mobility spectrometers. *Anal Bioanal Chem.* (2009) 395:411–9. doi: 10.1007/s00216-009-2818-5

27. Li Q, Li R, Cao G, Wu X, Yang G, Cai B, et al. Direct differentiation of herbal medicine for volatile components by a multicapillary column with ion mobility spectrometry method. *J Sep Sci.* (2015) 38:3205–8. doi: 10.1002/jssc.201500402

28. Arnanthigo Y, Anttalainen O, Safaei Z, Sillanpää M. Sniff-testing for indoor air contaminants from new buildings environment detecting by aspiration-type ion mobility spectrometry. *Int J Ion Mobility Spectrom.* (2016) 19:15–30. doi: 10.1007/s12127-016-0189-0

29. Mochalski P, Wiesenhofer H, Allers M, Zimmermann S, Guntner A, Pineau N, et al. Monitoring of selected skin- and breath-borne volatile organic compounds emitted from the human body using gas chromatography ion mobility spectrometry (GC-IMS). *J Chromatogr B Analyt Technol Biomed Life Sci.* (2018) 1076:29–34. doi: 10.1016/j.jchromb.2018.01.013

30. Pu D, Zhang H, Zhang Y, Sun B, Ren F, Chen H, et al. Characterization of the aroma release and perception of white bread during oral processing by gas chromatography-ion mobility spectrometry and temporal dominance of sensations analysis. *Food Res Int.* (2019) 123:612–22. doi: 10.1016/j.foodres.2019.05.016

31. Li M, Yang R, Zhang H, Wang S, Chen D, Lin S. Development of a flavor fingerprint by HS-GC-IMS with PCA for volatile compounds of *Tricholoma matsutake* singer. *Food Chem.* (2019) 290:32–9. doi: 10.1016/j.foodchem.2019.03.124

32. Arroyo-Manzanares N, Martin-Gomez A, Jurado-Campos N, Garrido-Delgado R, Arce C, Arce L. Target vs spectral fingerprint data analysis of Iberian ham samples for avoiding labelling fraud using headspace - gas chromatography-ion mobility spectrometry. *Food Chem.* (2018) 246:65–73. doi: 10.1016/j.foodchem.2017.11.008

33. Mackey P, Whitaker M. Diabetes mellitus and hyperglycemia management in the hospitalized patient. *J Nurse Pract.* (2015) 11:531–7. doi: 10.1016/j.nurpra.2015.02.016

34. Liu S, Lin J, Wang C, Chen H, Yang D. Antioxidant properties of various solvent extracts from lychee (*Litchi chinenesis Sonn.*) flowers. *Food Chem.* (2009) 114:577–81. doi: 10.1016/j.foodchem.2008.09.088

35. Gao P, Jin J, Liu R, Jin Q, Wang X. Chemical compositions of Walnut (*Juglans regiaL.*) oils from different cultivated regions in China. *J Am Oil Chem Soc.* (2018) 95:825–34. doi: 10.1002/aocs.12097

36. Re R, Pellegrini N, Proteggente A, Pannala A, Yang M, Rice-Evans C. Antioxidant activity applying an improved ABTS radical cation decolorization assay. *Free Radical Biol Med.* (1999) 26:1231–7. doi: 10.1016/S0891-5849(98)00315-3

37. Vaidya B, Eun J. Effect of roasting on oxidative and tocopherol stability of walnut oil during storage in the dark. *Eur J Lipid Sci Technol.* (2013) 115:348–55. doi: 10.1002/ejlt.201200288

38. Zhao T, Hong S, Lee J, Lee J, Kim I. Impact of roasting on the chemical composition and oxidative stability of *Perilla* oil. *J Food Sci.* (2012) 77:C1273–8. doi: 10.1111/j.1750-3841.2012.02981.x

39. Gunstone F. *Edible Oil and Fat Products: Chemistry, Properties, and Health Effects. Fereidoon Shahidi. Bailey's Industrial Oil and Fat Products*. (Vol. 1), New York, NY: John Wiley & Sons (2005).

40. Aleksander Siger M, Lampart-Szczapa E. The content and antioxidant activity of phenolic compounds in cold-pressed plant oils. *J Food Lipids.* (2007) 15:137–49. doi: 10.1111/j.1745-4522.2007.00107.x

41. Cisneros F, Paredes D, Arana A, Cisneros-Zevallos L. Chemical composition, oxidative stability and antioxidant capacity of oil extracted from roasted seeds of Sacha-inchi (*Plukenetia volubilis L.*). *J Agric Food Chem.* (2014) 62:5191–7. doi: 10.1021/jf500936j

42. Lee S, Kim J-H, Jeong S-M, Kim D, Ha J, Nam K, et al. Effect of far-infrared radiation on the antioxidant activity of rice hulls. *J Agric Food Chem.* (2003) 51:4400–3. doi: 10.1021/JFO300285

43. Nicoli M, Anese M, Parpinel M. Influence of processing on the antioxidant properties of fruit and vegetables. *Trends Food Sci Technol.* (1999) 10:94–100. (99)00023-0 doi: 10.1016/s0924-2244

44. Chen Y, Li P, Liao L, Qin Y, Jiang L, Liu Y. Characteristic fingerprints and volatile flavor compound variations in Liuyang Douchi during fermentation via HS-GC-IMS and HS-SPME-GC-MS. *Food Chem.* (2021) 361:130055. doi: 10.1016/j.foodchem.2021.130055

45. Sun X, Wang Y, Li H, Zhou J, Han J, Wei C. Changes in the volatile profile, fatty acid composition and oxidative stability of flaxseed oil during heating at different temperatures. *LWT Food Sci Technol.* (2021) 151:112137. doi: 10.1016/j.lwt.2021.112137

46. Yang Y, Yu P, Sun J, Jia Y, Wan C, Zhou Q, et al. Investigation of volatile thiol contributions to rapeseed oil by odor active value measurement and perceptual interactions. *Food Chem.* (2022) 373:131607. doi: 10.1016/j.foodchem.2021.131607

47. Yang X, Zhu K, Guo H, Geng Y, Lv W, Wang S, et al. Characterization of volatile compounds in differently coloured *Chenopodium quinoa* seeds before and after cooking by headspace-gas chromatography-ion mobility spectrometry. *Food Chem.* (2021) 348:129086. doi: 10.1016/j.foodchem.2021.129086

48. Hu Q, Zhang J, He L, Xing R, Yu N, Chen Y. New insight into the evolution of volatile profiles in four vegetable oils with different saturations during thermal processing by integrated volatolomics and lipidomics analysis. *Food Chem.* (2022) 403:134342. doi: 10.1016/j.foodchem.2022.134342

49. Fullana A, Carbonell-Barrachina AA, Sidhu S. Volatile aldehyde emissions from heated cooking oils. *J Sci Food Agric.* (2004) 84:2015–21.

50. Xu Y, Bi S, Zhou Q, Dai Y, Zhou Q, Liu Y, et al. Identification of aroma active compounds in walnut oil by monolithic material adsorption extraction of RSC18 combined with gas chromatography-olfactory-mass spectrometry. *Food Chem.* (2023) 402:134303. doi: 10.1016/j.foodchem.2022.134303

51. Wang Y, Tang X, Luan J, Zhu W, Xu Y, Yi S, et al. Effects of ultrasound pretreatment at different powers on flavor characteristics of enzymatic hydrolysates of cod (*Gadus macrocephalus*) head. *Food Res Int.* (2022) 159:111612. doi: 10.1016/j.foodres.2022.111612

52. Zhang Y, Lin Q, Zhong H, Zeng Y. Identification and source analysis of volatile flavor compounds in paper packaged yogurt by headspace solid-phase microextraction-gas chromatography-mass spectrometry. *Food Packag Shelf Life.* (2022) 34:100947. doi: 10.1016/j.fpsl.2022.100947

frontiers | Frontiers in Nutrition

TYPE Original Research
PUBLISHED 16 January 2023
DOI 10.3389/fnut.2023.1114880

OPEN ACCESS

EDITED BY
Ye Liu,
Beijing Technology and Business University, China

REVIEWED BY
Baoqing Zhu,
Beijing Forestry University, China
Shuang Bi,
Beijing Technology and Business University, China

*CORRESPONDENCE
Shuang Chen
✉ shuangchen@jiangnan.edu.cn
Zhen Zhang
✉ zzjinzhou@126.com

SPECIALTY SECTION
This article was submitted to Food Chemistry, a section of the journal Frontiers in Nutrition

RECEIVED 03 December 2022
ACCEPTED 02 January 2023
PUBLISHED 16 January 2023

CITATION
Wang N, Zhang L, Ren X, Chen S and Zhang Z (2023) Metabolomic fingerprinting based on network analysis of volatile aroma compounds during the forced aging of Huangjiu: Effects of dissolved oxygen and temperature.
Front. Nutr. 10:1114880.
doi: 10.3389/fnut.2023.1114880

Metabolomic fingerprinting based on network analysis of volatile aroma compounds during the forced aging of Huangjiu: Effects of dissolved oxygen and temperature

Na Wang[1], Lili Zhang[1], Xuejiao Ren[1], Shuang Chen[2]* and Zhen Zhang[1]*

[1]School of Food and Health, Jinzhou Medical University, Jinzhou, Liaoning, China, [2]State Key Laboratory of Food Science and Technology, Key Laboratory of Industrial Biotechnology of Ministry of Education and School of Biotechnology, Jiangnan University, Wuxi, Jiangsu, China

Introduction: Huangjiu is an important Chinese alcoholic beverage, usually prepared from rice. Although its unique flavor improves with prolonged storage in traditional pottery jars, knowledge of the aging mechanism, necessary for commercialization of an optimum product, remains unclear.

Methods: Here, volatile aroma compounds from forced aged samples exposed to different temperatures and oxygen treatments were measured by GC/MS. After retention time alignment and normalization, the peak vectors were compared over storage time using Pearson's correlation, and a correlation network was established. Marker compounds, representative of traditionally aged Huangjiu, were then monitored and compared to similar compounds in the forced aged product.

Results and discussion: Correlation network analysis revealed the following: Temperature had little effect on most aroma compounds; alcohols, acids, and esters all increased with increasing dissolved oxygen, while polyphenols, lactones, and ketones were readily oxidized; aldehydes (e.g., furfural and benzaldehyde) were highly dependent on both temperature and dissolved oxygen. Dynamic changes in the targeted aging-markers showed that a higher initial oxygen concentration intensified the "aging-aroma" of Huangjiu in the early and middle stages of storage. Consequently, careful control of oxygen supplementation and storage temperature could be beneficial in controlling the desirable flavor of Huangjiu in the artificially aged product.

KEYWORDS

Huangjiu (Chinese rice wine), aroma, forced aging, temperature, dissolved oxygen, metabolomics, network analysis

1. Introduction

Huangjiu, or Chinese rice wine, as a typical fermented rice wine, is known as Chinese national wine, and "Pottery storage, and more aging, more flavors" is one of its most typical characteristics. Although this well-known phrase "more aging, more flavors" is not completely true for all Huangjius (1, 2), the practice proved that there are significant differences between storage in pottery and stainless-steel tank, and this typical "more aging, more flavors" for Huangjiu can be generally characterized only by stored in pottery, not in stainless-steel tank (1, 3, 4). However, it is why?

The unique flavor of traditional Huangjiu is believed to develop during storage over several years in pottery jars. However, to meet increased demand for alcoholic beverages (5, 6), a relatively short-term industrial storage in stainless-steel tank must be instead of the

long-term storage in pottery jars for Huangjiu. Therefore, industrial processes are required for the accelerated flavor development of Huangjiu during storage in stainless-steel tanks.

Temperature and dissolved oxygen are recognized as important storage parameters for Huangjiu (2, 4, 7, 8). It is reported that compared with storage in stainless steel, pottery jars have a better oxygen permeability, and their higher thermal mass is less susceptible to changes in ambient temperature so as to keep a stable and suitable temperature of 5–20°C (1, 2), but the model system studies, including oxygen permeability, are still lacking. Moreover, although changes in volatile aroma compounds, amino acids, sensory characteristics, and developments in analytical methods associated with the aging of Huangjiu have been reported (1–4, 7–17), the overall mechanism has not been studied in detail.

Correspondingly, the effects of temperature and dissolved oxygen, as two key factors of Maillard and oxidation flavor reactions in alcoholic beverages (18), have been studied in e.g., red wine, sake, and beer. Among these studies, forced aging simulations combined with kinetics, chemiomics, flavoromics, sensomics, and metabolomics etc. (18–28), have helped to clarify the aging mechanism and regulation of key aroma compounds (e.g., sotolon, vanillin, benzaldehyde, anthocyanins, ferulic acid, and sulfides) (22, 25, 29–34) in different alcoholic beverages. As the demand for high quality products increases, artificial aging is an attractive technology (35–39). However, to realize its potential, a clear understanding of aging mechanisms and product stability during artificial aging is a prerequisite for the commercialization of the process.

While metabolomics is concerned with characterizing the metabolome (22), metabolomics can be defined as the measurement of time-related changes (usually in a smaller set of metabolites) due to an intervention. To date, metabolomics has been successfully applied to the age-dependent characterization of Huangjiu (14) and other wines (9, 30, 40–43). Additionally, network analysis has proved to be a convenient method for visualizing and identifying key relationships between aroma compounds during the aging of some alcoholic beverages (23, 44, 45).

Here, a system was developed to investigate the effects of temperature and dissolved oxygen on the volatile aroma compounds of Huangjiu during forced aging. The aim was to use network analysis and volatile compound data obtained from the analysis of processed samples using headspace-solid phase microextraction (HS-SPME)-GC/MS to obtain information about the mechanisms of aroma formation during the forced aging of Huangjiu. Aging markers identified in previous studies of Huangjiu aged in pottery jars (14–16) provided a useful reference for metabonomic fingerprinting. The results from this small-scale simulation provide a theoretical reference for the development of the commercial aging of Huangjiu in large-scale stainless-steel tanks.

2. Materials and methods

2.1. Chemicals and materials

All chemicals were of analytical reagent grade: Anhydrous sodium sulfate, sodium chloride, lactic acid, and sodium hydroxide were purchased from China National Pharmaceutical Group Corp. (Shanghai, China). 2-Octanol [internal standard (IS)], methanol, ethanol, dichloromethane, and all other reagents were from Sigma-Aldrich (Shanghai) Trading Co., Ltd., (Shanghai, China). Pure water (>18.18 MΩ cm, 25°C) was obtained from a Milli-Q purification system (Millipore, Bedford, MA, USA).

Young samples of Huangjiu from the same production year were obtained from Zhejiang Guyuelongshan Huangjiu Co., Ltd. (Shaoxing, China). The characteristics of each sample were as follows: Total sugars (glucose), 3.92 g/L; alcohol, 17.2 % (v/v); total acids (lactic acid), 5.86 g/L; sugar solids, 20.90 g/L; dissolved oxygen [O_2] before the oxygen treatment, 1.8–2.5 mg/L (OX-Y dissolved oxygen sensor, Shanghai Chunye Instrument Technology Co., Ltd., China); and pH 3.5–4.0.

2.2. Forced aging

A summary of the experimental procedure used for the forced aging of Huangjiu was given in Figure 1. Two regimes of seven groups were kept for 70 days, and all samples were prepared in duplicate, where the setting of temperature and dissolved oxygen referred to and was modified from the existed researches on beer and other wines (19–21, 25).

Based on this forced-aging protocol, all samples in condition (I) were placed in a magnetic stirring water-bath with four different temperatures of 20, 30, 40, and 50°C, and no oxygen was added ($0O_2$) during this forced-aging 70 days (19–21). Correspondingly, all samples in condition (II) kept a constant 37°C temperature (25). Meanwhile, samples for condition (II) were labeled 1, 3, and $5O_2$, where 1–5 denotes the number of oxygen treatments. Oxygen saturation was achieved by stirring the sample for ∼1 h until the oxygen concentration reached 8–9 mg/L (OX-Y oxygen sensor) (19–21): $1O_2$ was saturated on day 35; $3O_2$ was saturated on days zero, 28, and 56; $5O_2$ was saturated on days zero, 14, 28, 42, and 56 (Figure 1). All apparatus was cleaned and sterilized prior to use. Pyrex GL 45 media bottles were each filled with Huangjiu (each sample 500 mL), GL45 screw cap twin hose connectors, stainless steel vent pipes, hoses, and clamps were fitted, and the samples were placed in a constant temperature water bath at 90°C for 30 min to sterilize the media. When cool, samples 3 and $5O_2$ were subjected to oxygen saturation, all vent pipe hoses were clamped, and the samples were treated according to the conditions given in Figure 1.

Samples taken at predetermined times were stored at −20°C until required for analysis. To reduce the GC/MS analytical burden, samples from the duplicate batch were selected at random and used as a crosscheck validation. Prior to analysis, all samples were subjected to a simple odor test to verify that the Huangjiu was viable. Additionally, the initial volume of 500 mL would be less and less with sampling, so we took a cross-sample in duplicate samples every other week to reduce the influence of sampling on the sample volume reduction.

2.3. HS-SPME-GC/MS analysis of volatile compounds

The forced-aging experimental protocol was performed in duplicate for practical reason and some samples were analyzed by GC/MS on the replicate trial. Referring to our existed studies (14, 46), two milliliters of Huangjiu samples, 8 mL of pure water with 3 g of sodium chloride and 10 μl of IS (2-O, 68.344 ppm) were mixed into 20 mL screw-capped vial for GC/MS analysis. An automatic

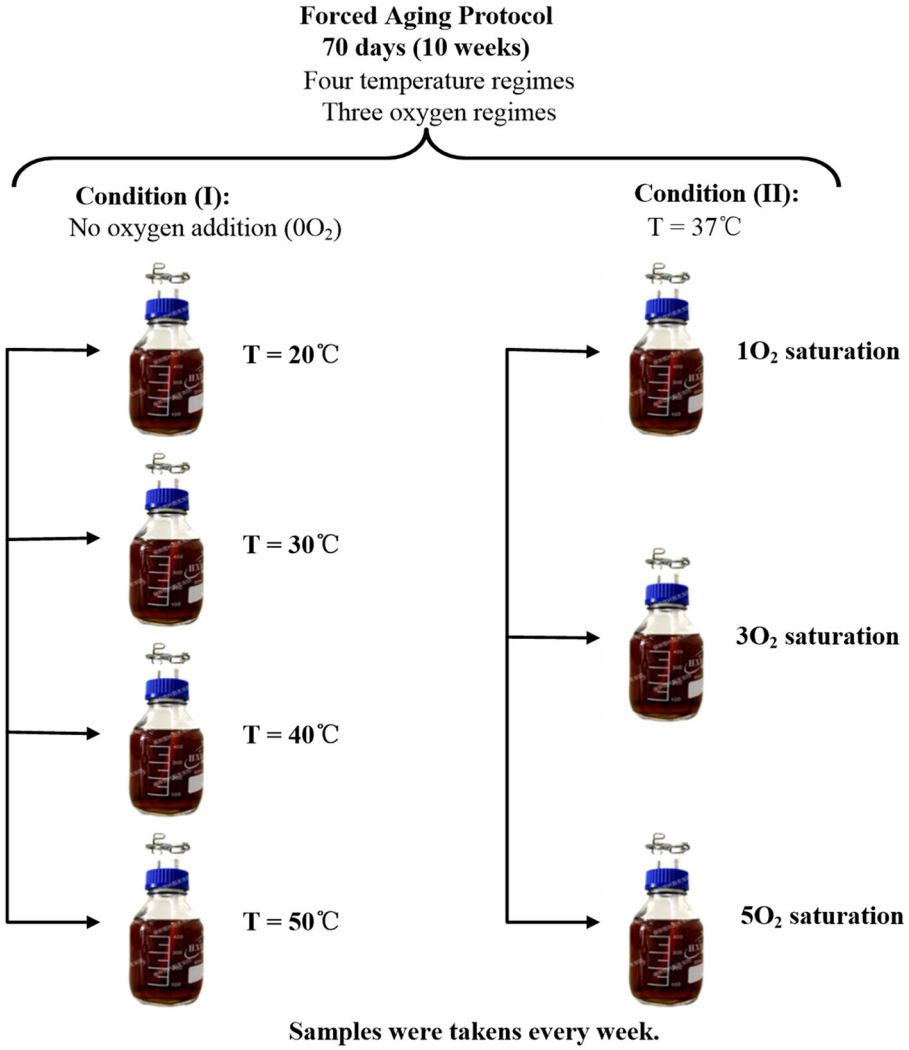

FIGURE 1
Summary of the forced aging procedure for Huangjiu: All samples were prepared in duplicate; the volume of each sample was 500 mL.

headspace (HS) sampling system with an Agilent GC68905975MSD was used for extraction of volatile compounds in samples, and DBFFAP column was used for the separations. The oven temperature was initially held at 50°C for 2 min, then raised at 5°C/min to 230°C for 15 min. Data acquisition was in the selective ion monitoring (SIM) mode (ionization energy = 70 eV).

2.4. Data analysis

2.4.1. Pre-processing

Feature detection, retention time (RT) correction, and preliminary statistical analyses were carried out using XCMS online (XCMSOnline version 2.2.5; XCMS version 1.47.3; CAMERA version 1.26.0, the Scripps Center for Metabolomics, La Jolla, CA; https://xcmsonline.scripps.edu). Raw data conversion, GC/MS spectra processing, set parameters, etc., were described in Yu et al. (9). All chromatograms were simultaneously analyzed under the same conditions. From seven different conditions of the forced aging procedure (Figure 1), the multi-group job was selected, and the seven groups were classified.

2.4.2. Optimization of candidate features

Using the extracted features from XCMS-online software as the Y-Variable, a bivariate Pearson's correlation was performed. The marked significant Y-variables, which were the optimized candidate features based on a false discovery rate≤ 0.05, were selected as candidate features for network analysis and qualitative and quantitative analyses. To further simplify these analyses and delete the corresponding features of the IS and ethanol, the m/z and RT of all extracted features were compared in METLIN (https://metlin.scripps.edu) and the NIST 05 library on the GC/MS workstation (Agilent Technologies Inc., USA).

2.4.3. Identification and quantification of candidate features in network analysis

The identification of candidate features in network analysis directly referred to the existing our study (14): The aligned matrix (/.xlsx) from XCMS-Oline software (https://xcmsonline.scripps.edu) consists of all the exported metabolite features-putative identifications through METLIN standard database matching, which are defined as ions with unique m/z and RT values

(Supplementary material). Finally, MS features were validated by (i) crosschecking their presence in the raw data, (ii) comparing their features with those present in the NIST 05 (matching degree %) and NIST 98 MS library (http://webbook.nist.gov), and (iii) comparing with the existing identifications (14–17, 46).

Finally, all identified volatile compounds, including unknowns, were directly quantified using HS-SPME-GC/MS.

2.5. Statistical methods

Bivariate Pearson's correlation was carried out using IBM SPSS Statistics for Windows, version 19.0 (IBM Corp., Armonk, NY USA). Network analysis of the optimized candidate features was performed with Gephi version 0.9.2 (https://gephi.org/) using the Fruchterman–Reingold algorithm. All box plots and PCA sores plots were exported directly from XCMS-online software. Data trends were graphed with OriginPro 8.5.0 SR1 (The OriginLab Corporation, USA).

3. Results and discussion

3.1. Preliminary analysis of untargeted SPME-GC/MS-based metabolomics

A total of 149 candidate features were extracted from the raw HS-SPME-GC/MS data (Supplementary material) of all 140 Huangjiu samples after pre-processing. Meanwhile, a preliminary analysis of PCA was directly exported from XCMS-online software based on 149 candidate features and 140 Huangjiu samples, and the PCA result (Figure 2) showed that samples 3 and $5O_2$ from condition (II) could be distinguished from all other forced aging treatments based on the first two principal components, PC1 and PC2, representing 57.53 and 15.91% of the total variation, respectively. Compared with all samples from condition (II), 10 samples from condition (I) also showed a wider distribution, and these preliminary results implied that the different temperatures in condition (I) had a significant effect on the aging time (increase or decrease) of Huangjiu, but frequent oxygenation [e.g., 3 and $5O_2$ in condition (II)] promoted changes in the volatile aging compounds. However, this PCA result was to be verified and improved.

3.2. Network analysis fingerprinting

Based on the PCA result above, in order to verify the influence of temperature and dissolved oxygen in our experiment further, we decided to further use network analysis method to quickly extract and identify compounds with similar trends under different conditions.

Following repeated comparison and screening (*m/z* and RT) of the 149 candidate features using the METLIN and NIST 05 databases, peaks due to the IS (2-octanol) and ethanol were deleted. A bivariate Pearson's correlation and network analysis of the remaining 112 characteristic peaks were then used to determine the characteristic peaks and markers for the effects of oxygen and temperature on volatile compounds during the forced aging.

Figure 3 showed the network analysis map obtained from untargeted GC/MS data: The 112 characteristic peaks were represented as nodes, while the magnitude of the associations could be visualized from the densities of the interconnecting edges; the nodes were divided into four regions (A–D), each representing those characteristic peaks with significant positive correlations and similar changes during this forced aging. Although these characteristic peaks in the same color region had the significant positive correlations and similar changes during this forced aging, they could come from different compounds.

Based on the preliminary identification and quantification of some nodes, network analysis was used to further visualize the relationships and differences among all volatile aging compounds present in each region (A-D), as well as changes in their concentrations over time (Figures 4–7).

3.2.1. Correlation network analysis of region A

As shown in Figure 4, about 69% of all the candidate features in region A were identified as alcohols (e.g., 2- and 3-methylbutanol, 2-methylpropanol), followed by ethyl acetate, ethyl lactate, ethyl hexanoate, and acetic acid. Some common characteristics and trends were observed for samples from conditions (I) and (II). For example, the content of 2-methylpropanol, 3-methylbutanol, ethyl lactate, and acetic acid was significantly higher in sample treatments 3 and $5O_2$ compared with $1O_2$. Oxygen supplementation at week 5 (day 35, $1O_2$) showed an increase in marker compounds, which then decreased in the latter stages of storage. In contrast, the four different temperatures of condition (I) had little effect on the amount of volatile aroma compounds. Hence, the results suggested that amounts of the volatile marker compounds in region A were dependent on dissolved oxygen and not readily oxidized.

Previously we found that amounts of 2- and 3-methylbutanol and 2-methypropanol showed significant decreasing trends during the aging of Huangjiu, and these compounds were representative aging markers, especially for the short-aged wine (14–16). Here, 3-methylbutanol and 2-methylpropanol showed some association with 3 and $5O_2$, but the decreasing trend fluctuated greatly, especially in sample $5O_2$. In a study on the aroma of fortified wine, a high initial oxygen concentration increased the concentration of aroma compounds during aging (21). Based on these findings, we speculated that the interval and frequency of oxygenation during aging could increase overall alcohol production. Since a higher oxygenation frequency also increased the concentration of other aroma compounds, we proposed that its introduction in the early stage of aging would be beneficial for the flavor of Huangjiu.

The organic acids in wine can be formed from the oxidation of alcohols and aldehydes and the hydrolysis of esters, while amounts of 2- and 3-methylbutanol, 2-methylpropanol, acetic acid, ethyl acetate, ethyl hexanoate, ethyl lactate mainly originated from the raw materials and fermentation process of Huangjiu. Consequently, the concentrations of these flavor compounds during fermentation can determine their individual reactivities (23). Since the hydrolysis of esters largely determined concentrations of the corresponding organic acids and alcohols in the aging process, it was reasonable to assume that the above three alcohols, acetic acid, and three ethyl esters occurred in the same environment of region A.

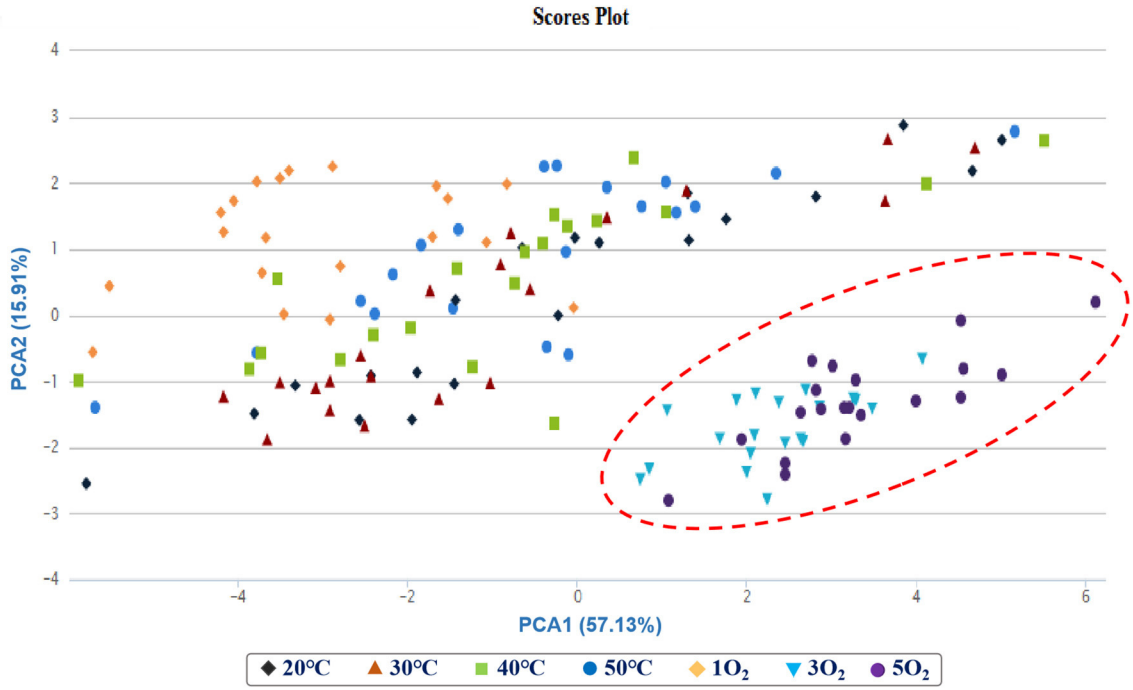

FIGURE 2
PCA scores plot obtained from the untargeted SPME-GC/MS data for the forced aging samples.

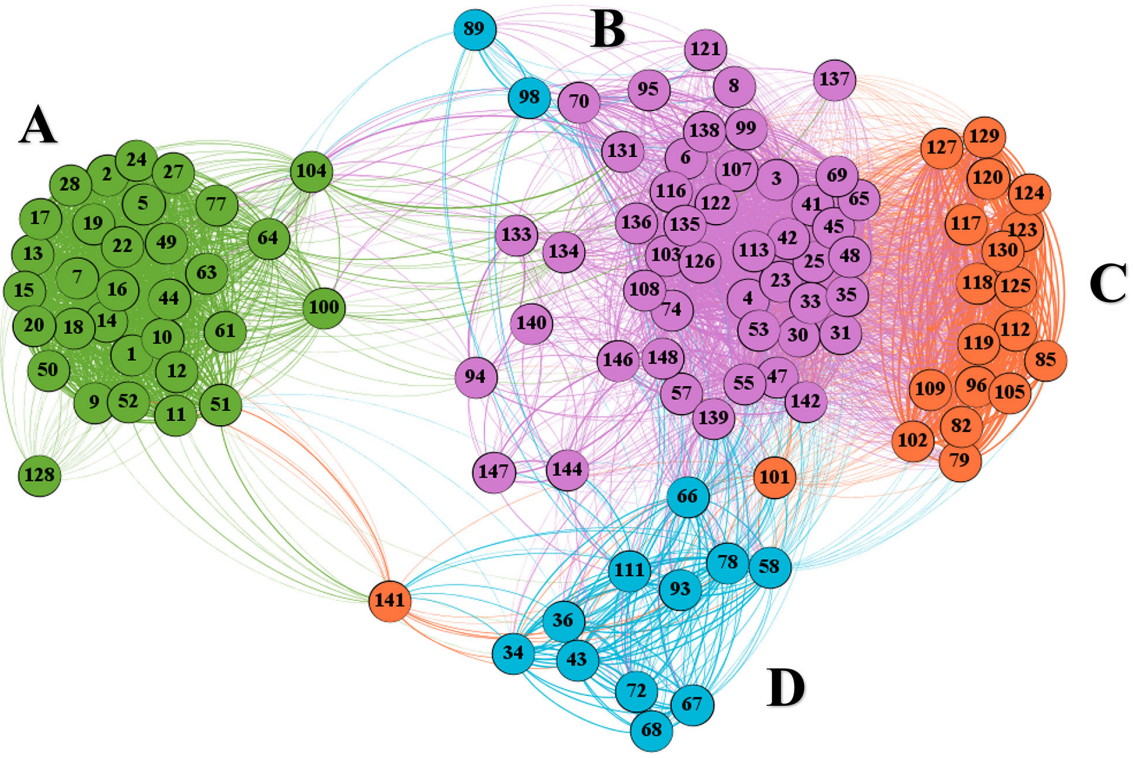

FIGURE 3
(A–D) Network analysis shows the correlated characteristic peaks obtained from the untargeted GC/MS data: The nodes represent the characteristic peaks, while the different densities of the connecting edges indicate the relative strength of the associations. The number is the code of characteristic peaks, and the different color regions represent different conditions (temperature and oxygenation) with time.

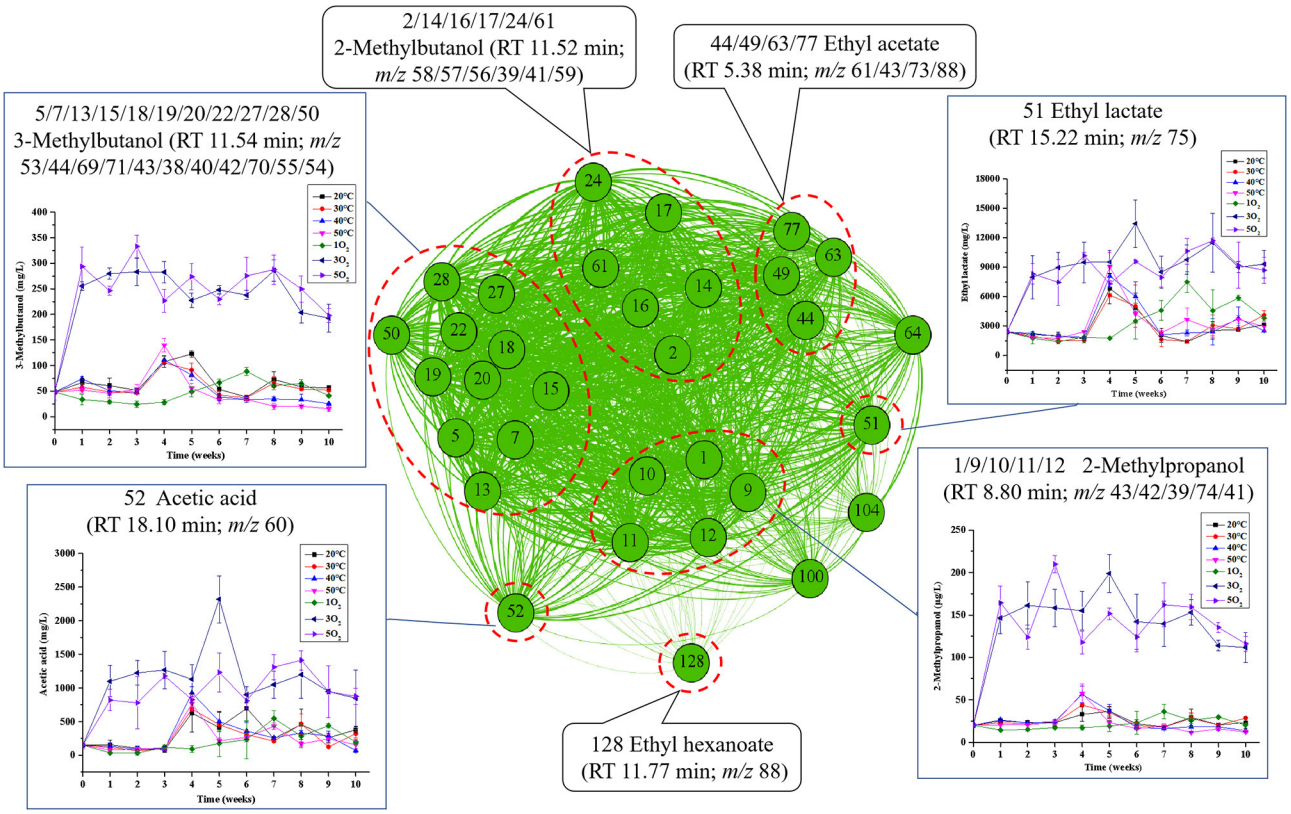

FIGURE 4
Network analysis map showing the associations between the characteristic peaks in region A: Inset charts show changes in the concentrations of marker compounds for each treatment condition (temperature and oxygenation) with time. The nodes represent the characteristic peaks, while the different densities of the connecting edges indicate the relative strength of the associations in this region. The number in front is the code of characteristic peaks, corresponding with those in Figure 3, and the number in the back is the observed features (m/z).

3.2.2. Correlation network analysis of region B

Most of the candidate features in region B were identified as phenethyl alcohol, with lesser amounts of γ-non-alactone, ethyl palmitate, 2,4-dimethylphenol, phenethyl acetate, and other unknowns (Figure 5). Contrary to region A, the interval and frequency of oxygenation (3 and $5O_2$) decreased the concentration of these volatile aroma compounds.

Many phenolic compounds have antioxidant properties and are readily oxidized during aging. Correspondingly, the content of 2,4-dimethylphenol following $1O_2$ supplementation was significantly higher than that with 3 and $5O_2$, suggesting that a higher initial concentration of dissolved oxygen increased the oxidation of phenolic compounds during aging. The presence of both phenethyl acetate and phenethyl alcohol in the same region also indicated that the ester was mainly derived from the reaction of the parent alcohol with acetic acid.

The fatty acid ester ethyl palmitate is readily hydrolyzed to palmitic acid and ethanol in an acidic environment (47). Previously we reported that the relatively high concentration of ethyl palmitate in young Huangjiu decreased throughout the aging process, while the total acid content showed the opposite trend (14, 16).

Since the volatile compounds (including unknowns) in region B were readily oxidized, dissolved oxygen had a greater influence on the aging aroma of Huangjiu than temperature.

3.2.3. Correlation network analysis of region C

Compared with the box-plots derived from the untargeted GC/MS data (Figure 6), all the candidate features in region C were pre-confirmed as the same component (RT 29.47–29.48 min). The identity of the unknown could not be confirmed because of the limited mass accuracy of the single quadrupole mass spectrometer used. Inspection of the inset box plots of Figure 6 shows that the abundance of some unknown compounds (i.e., nodes 79, 105, and 130) approached zero at 3 and $5O_2$ in condition (II). This implied that the molecular species were easily oxidized, and the aroma compounds in region C had similar characteristics to those of region B.

3.2.4. Correlation network analysis of region D

As shown in Figure 7, benzaldehyde was the most abundant volatile compound, followed by an unknown and furfural. Benzaldehyde can be formed by the oxygenation of its parent alcohol, which could account for the higher concentrations of the aldehyde found in samples 3 and $5O_2$ compared with $1O_2$. The highest concentration of benzaldehyde and the most significant change occurred in samples at 50°C and $5O_2$, respectively, which agreed with the reported oxygen and temperature dependence of benzaldehyde (and sotolon) during Port wine aging (23). The identification of benzaldehyde may also be useful in unraveling the connection between the Maillard mechanism and oxidation during

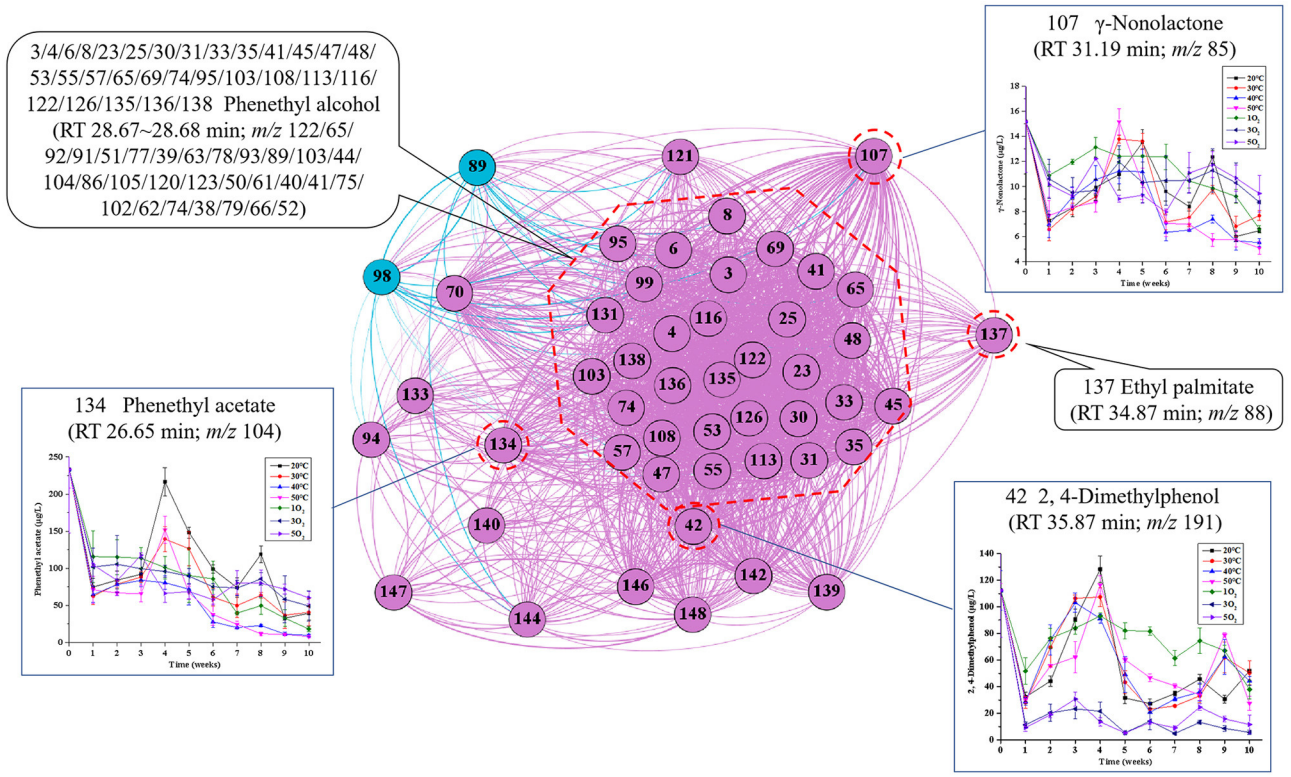

FIGURE 5
Network analysis map showing the associations between the characteristic peaks in region B: Inset charts show changes in the concentrations of marker compounds for each treatment condition (temperature and oxygenation) with time. The nodes represent the characteristic peaks, while the different densities of the connecting edges indicate the relative strength of the associations in this region. The number in front is the code of characteristic peaks, corresponding with those in Figure 3, and the number in the back is the observed features (m/z).

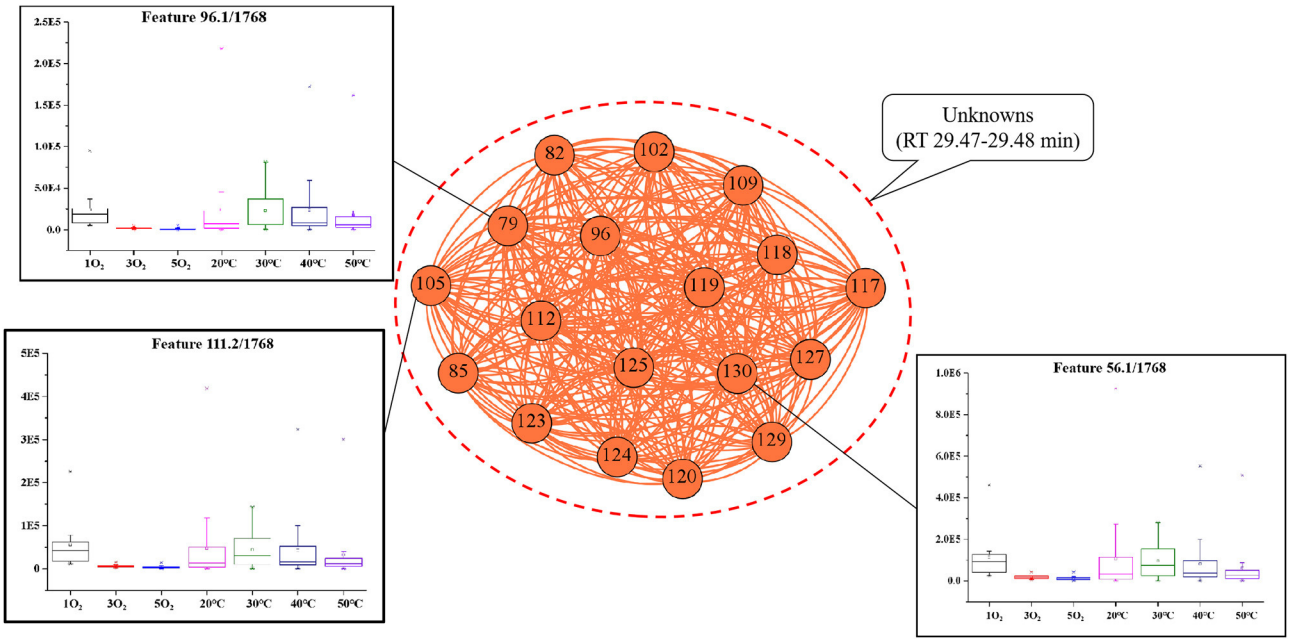

FIGURE 6
Network analysis map showing the associations between the characteristic peaks in region C: Inset box plots show the abundance for each treatment condition (temperature and oxygenation). The nodes represent the characteristic peaks, while the different densities of the connecting edges indicate the relative strength of the associations in this region. The number in front is the code of characteristic peaks, corresponding with those in Figure 3, and the number in the back is the observed features (m/z).

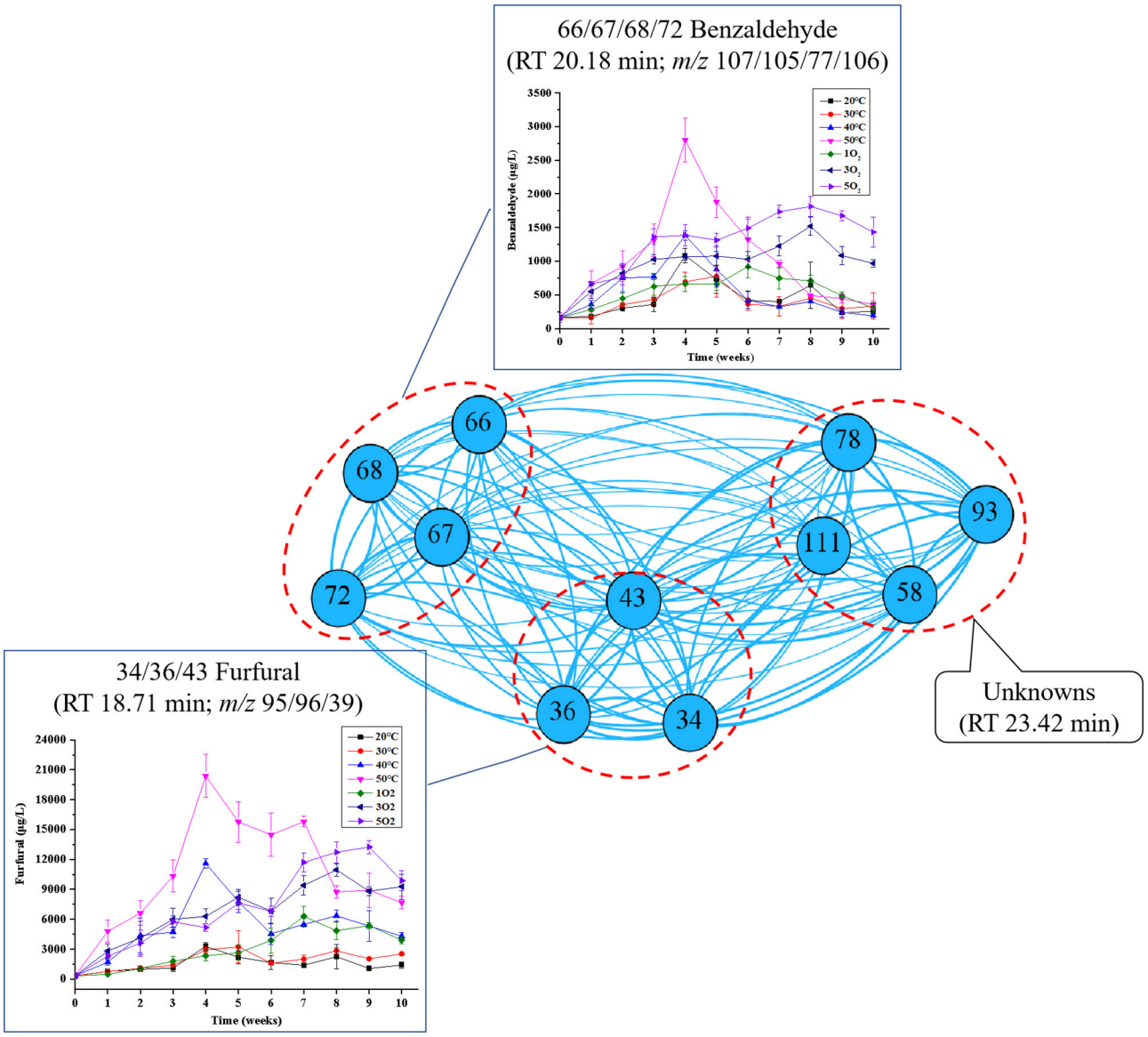

FIGURE 7
Network analysis map showing the associations between the characteristic peaks in region D: Inset charts show changes in the concentrations of marker compounds for each treatment condition (temperature and oxygenation). The nodes represent the characteristic peaks, while the different densities of the connecting edges indicate the relative strength of the associations in this region. The number in front is the code of characteristic peaks, corresponding with those in Figure 3, and the number in the back is the observed features (m/z).

the aging of Huangjiu. Temperature also had a significant effect on the formation of furfural in region D during aging.

Maillard reactions are regarded as the major pathways of furan formation. Furans are responsible for the key "caramel-like" aroma in aged wine (17), and their formations are believed to occur *via* Maillard reactions and oxidation (21, 23). The aldehyde substituted furan, furfural, is a common flavor compound in wine, and its formation was shown to be significantly affected by temperature during the aging of a fortified wine (21). Here the concentration of furfural increased with increasing temperature (40 and 50°C) and dissolved oxygen (3 and $5O_2$). Although the effect of condition (II) was much less than that of condition (I), furfural showed a strong association between time and dissolved oxygen (r values: 0.826**, 0.802**, and 0.819** at 1, 3, and $5O_2$, respectively). Hence, dissolved oxygen may also play an important role in the formation of furfural.

3.2.5. Network analysis fingerprinting: Summary of effects

Temperature had little effect on the aging-aromas in regions A, B, and C, but the alcohols, acids, and esters in region A were highly dependent on oxygen. Although they were not easily oxidized, their concentrations increased with increasing dissolved oxygen. In contrast, the polyphenols, lactones, ketones, and unknowns in regions B and C were easily oxidized, and their concentrations were significantly affected by dissolved oxygen. The effects of both temperature and dissolved oxygen on the formation of the key marker compounds, furfural, and benzaldehyde, in region D, confirmed the importance of these parameters during the aging of Huangjiu (15, 17). The interval and frequency of oxygenation also increased their concentrations.

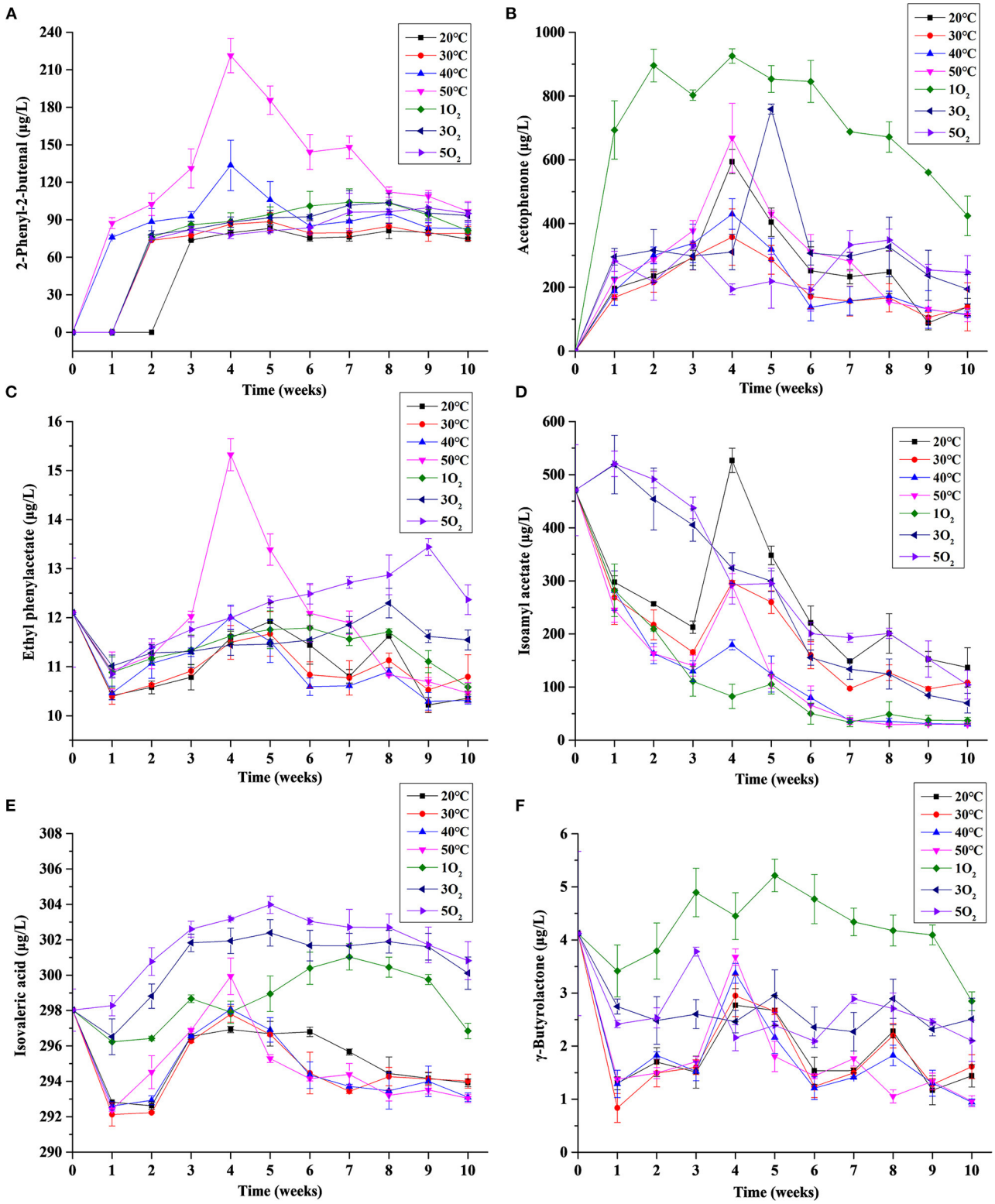

FIGURE 8
Effects of temperature and dissolved oxygen on the concentrations of key marker compounds during the forced aging of Huangjiu: **(A)** 2-Phenyl-2-butenal; **(B)** acetophenone; **(C)** ethyl phenylacetate; **(D)** isoamyl acetate; **(E)** isovaleric acid (3-methylbutanoic acid); and **(F)** γ-butyrolactone at different conditions.

3.3. Effects of dissolved oxygen and temperature on key aging-markers during the forced-aging of Huangjiu

To compare the effects of forced-aging with the natural process, six aging-markers (2-phenyl-2-butenal, ethyl phenylacetate, 3-methylbutyric acid, acetophenone, isoamyl acetate, and γ-butyrolactone) were selected from previous investigations of Huangjiu (14–16). Although these compounds could not be extracted by the untargeted GC/MS-based network analysis method used in this study, they were considered to be important markers for the aging status of Huangjiu (15, 16).

Figure 8 showed the influence of temperature and dissolved oxygen on the key marker compounds in Huangjiu.

3.3.1. Aromatic marker compounds

The aromatic compounds (2-phenyl-2-butenal, ethyl phenylacetate, acetophenone; Figures 8A–C) showed an initial increasing trend for most conditions during the forced aging process. These compounds, together with benzaldehyde, are characteristic markers of the long-aged product (10–15 years) (14–16) and are, therefore, indicators of high-quality Huangjiu. However, the concentration of these markers all decreased after 4 or 5 weeks for samples under condition (I), and this trend increased with increasing temperature (Figures 8A–C). In the presence of oxygen, the initial increasing trend persisted until weeks 8–9 (especially 3 and $5O_2$). Compared with the traditional aging in pottery jars, the decrease in the three aromatic aging-markers after 4 or 5 weeks under the condition (I) represented the largest difference. This difference could be attributed to insufficient dissolved oxygen and poor oxygen permeability in the forced aging process.

In addition, the trends for each treatment condition showed that the effect of temperature on 2-phenyl-2-butenal and ethyl phenylacetate was greater than that of dissolved oxygen (Figure 8A), and so was ethyl phenylacetate, while dissolved oxygen had a greater effect on acetophenone, phenethyl alcohol, and phenethyl acetate (Figure 5).

3.3.2. Non-aromatic marker compounds

The overall decreasing trends in the concentrations of isoamyl acetate showed a spiked increase for the condition (I) sample at week 4, the magnitude of which decreased with increasing temperatures (Figure 8D), and this agreed with a previous investigation of Huangjiu (15). Higher initial concentrations of isoamyl acetate, and a greater decreasing trend, were observed in samples subject to increased oxygenation (2 and $3O_2$), and this mirrored the behavior of 3-methlybutaol and acetic acid in region A of network analysis (Figure 4).

The highest amounts of isovaleric acid (Figure 8E) were also found in samples with the highest oxygenation treatments. This was similar to the behavior of compounds in region A of network analysis, and its effect was greater than that of temperature. Hence, isoamyl acetate and isovaleric acid, together with the volatile compounds identified in region A of network analysis (Figure 4), constitute potential markers for the forced aging process of Huangjiu.

3.3.3. Lactone marker compounds

Lactones are cyclic organic esters of the corresponding carboxylic acids, and their formations in wine are reported to be sensitive to temperature (23). Here a slightly higher concentration of γ-butyrolactone (Figure 8F) existed at 50°C compared with the other temperature treatments. This followed the behavior of γ-non-olactone (Figure 5), but the trends were not clear. The concentration of γ-butyrolactone was highest at $1O_2$ (Figure 8F), compared with 3 and $5O_2$, indicating that the lactone was readily oxidized during the forced aging process. Hence dissolved oxygen had a greater influence on γ-butyrolactone than temperature. However, the regulation of dissolved oxygen on a commercial scale, and optimization of γ-butyrolactone and γ-non-olactone formation, may require development.

3.3.4. Other marker compounds

Although the key marker compounds ethyl butyrate and ethyl 3-methylbutyrate were expected, they were only detected in some samples at 50°C, and their concentrations were very low. Consequently, their absence/low concentration suggests that the forced aging procedure may require further development/validation.

4. Conclusions

Metabonomic fingerprinting based on network analysis of untargeted GC/MS volatile compound data, and quantitative analysis of targeted marker compounds, was successfully applied to determine the effects of dissolved oxygen and temperature on the forced aging aroma of Huangjiu. Alcohols, acids, and esters all increased with increasing dissolved oxygen, while polyphenols, lactones, and ketones were readily oxidized; aldehydes (e.g., furfural and benzaldehyde) were highly dependent on both temperature and dissolved oxygen. Dynamic changes of six marker compounds during the laboratory scale forced aging of Huangjiu identified potential limitations in aroma generation for the product stored in large-scale stainless-steel tanks. Higher initial concentrations of oxygen, together with supplementation in the middle stages, favored the generation of stronger aging aromas. While higher temperatures promoted the concentration of some key marker compounds, this observation required verification and optimization on a commercial scale. Consequently, here the model system was to be further developed, including a further study on the kinetics of the identified aging markers, but this study would provide a theoretical reference for the development of high quality Huangjiu using modern production methods.

Data availability statement

The original contributions presented in the study are included in the article/Supplementary material, further inquiries can be directed to the corresponding authors.

Ethics statement

Ethical review and approval were waived for this study, because Huangjiu samples used in the study are consumed in daily life.

Author contributions

NW: methodology, data curation, and writing—original draft preparation. SC and NW: writing—review and editing. LZ, XR, and ZZ: supervision and resources. NW, LZ, XR, and ZZ: project administration and funding acquisition. All authors have read and agreed to the published version of the manuscript.

Funding

This research was supported by the Doctoral Start-up Foundation of Liaoning Province (No. 2022-BS-322) and the 2021 Basic Scientific Research Project of Liaoning Provincial Education Department (Key Project; No. LJKZ0802).

Acknowledgments

The authors would like to thank all the panelists in this study. Meanwhile, the authors would like to express their gratitude to EditSprings (https://www.editsprings.cn) for the expert linguistic services provided.

Conflict of interest

The authors declare that the research was conducted in the absence of any commercial or financial relationships that could be construed as a potential conflict of interest.

Publisher's note

Supplementary material

The Supplementary Material for this article can be found online at: https://www.frontiersin.org/articles/10.3389/fnut.2023.1114880/full#supplementary-material

References

1. Wang YX. Elementary introduction of storematurity of yellow rice wine. *Liquor Making Sci Technol.* (1999) 3:66–7.

2. Yang GJ. Aging of Chinese rice wine. *Liquor Making Sci Technol.* (2006) 6:74–6.

3. Luo SM, Ni B, Zhang QW. Effects of different storage methods on the flavor and organic acids of Huangjiu. *Liquor Making Sci Technol.* (2021) 2021:78–84. doi: 10.13746/j.njkj.2020198

4. Hu J, Chi GH. Investigation on the orignal of aging-aromas in Huangjiu. *Liquor Making Sci Technol.* (2012) 2:30–2.

5. Li ZF, Kong HC, Liu YF, Liu YF, Chen J. Future foods: Opportunity and challenge. *J Chin Inst Food Sci Technol.* (2022) 22:1–13. doi: 10.16429/j.1009-7848.2022.04.001

6. Davis KF, Gephart JA, Emery KA, Leach AM, Galloway JN, D'Odorico P. Meeting future food demand with current agricultural resources. *Global Environ Chang.* (2016) 39:125–32. doi: 10.1016/j.gloenvcha.2016.05.004

7. Han X, Mao J, Huang GD. Effect of trace ventilation on flavoring substances and free amino acids in Chinese rice wine during storage. *Food Sci.* (2013) 34:123–7.

8. Zhou XD, Wang RQ, Shen QT, Zhu YY, Wu YH, Tian RG. Study on the transfer rate of oxygen in pottery jar of Shaoxing-rice wine. *Acta Agri Boreali-occidentalis Sinica.* (2016) 25:950–4.

9. Yu H, Zheng D, Xie T, Xie J, Tian H, Ai L, et al. Comprehensive two-dimensional gas chromatography mass spectrometry-based untargeted metabolomics to clarify the dynamic variations in the volatile composition of Huangjiu of different ages. *J Food Sci.* (2022) 87:1563–74. doi: 10.1111/1750-3841.16047

10. Yang Y, Ai L, Mu Z, Liu H, Yan X, Ni L, et al. Flavor compounds with high odor activity values (OAV >1) dominate the aroma of aged Chinese rice wine (Huangjiu) by molecular association. *Food Chem.* (2022) 383:132370. doi: 10.1016/j.foodchem.2022.132370

11. Wei Z, Zhang J, Shao W, Wang J. Fabrication and application of three-dimensional nanocomposites modified electrodes for evaluating the aging process of Huangjiu (Chinese rice wine). *Food Chem.* (2022) 372:131158. doi: 10.1016/j.foodchem.2021.131158

12. Ma Y, Guo S, Zhang J, Xu Y, Wang D. Kinetic modeling of ethyl carbamate formation from urea in Huangjiu during storage. *Food Control.* (2021) 129:108249. doi: 10.1016/j.foodcont.2021.108249

13. Xu JF, Zhang FJ. Changes of aroma substances, taste characteristics and surface tension during the aging process of Chinese rice wine. *China Brew.* (2018) 1:41–4. doi: 10.11882/j.issn.0254-5071.2018.01.009

14. Wang N, Chen S, Zhou ZM. Age-dependent characterization of volatile organic compounds and age discrimination in Chinese rice wine using an untargeted GC/MS-based metabolomic approach. *Food Chem.* (2020) 325:126900. doi: 10.1016/j.foodchem.2020.126900

15. Wang N, Zhou ZM, Chen S. Aging status characterization of Chinese rice wine based on key aging-marker profiles combined with principal components analysis and partial least-squares regression. *Eur Food Res Technol.* (2020) 246:1283–96. doi: 10.1007/s00217-020-03488-x

16. Wang N, Chen S, Zhou ZM. Characterization of volatile organic compounds as potential aging markers in Chinese rice wine using multivariable statistics. *J Sci Food Agric.* (2019) 99:6444–54. doi: 10.1002/jsfa.9923

17. Chen S, Wang CC, Qian MC, Li Z, Xu Y. Characterization of the key aroma compounds in aged Chinese rice wine by comparative aroma extract dilution analysis, quantitative measurements, aroma recombination, and omission studies. *J Agric Food Chem.* (2019) 67:4876–84. doi: 10.1021/acs.jafc.9b01420

18. Martins RC, Lopes VV, Silva Ferreira AC. Port wine oxidation management: A chemoinformatics approach. *Am J Enol Viticult.* (2009) 60:389A.

19. Oliveira CM, Barros AS, Silva Ferreira AC, Silva AMS. Influence of the temperature and oxygen exposure in red Port wine: A kinetic approach. *Food Res Int.* (2015) 75:337–47. doi: 10.1016/j.foodres.2015.06.024

20. Silva HOE, Pinho PGD, Machado BP, Hogg T, Marques JC, Camara JS, et al. Impact of forced-aging process on Madeira wine flavor. *J Agric Food Chem.* (2008) 56:11989–96. doi: 10.1021/jf802147z

21. Martins RC, Monforte AR, Silva Ferreira AC. Port wine oxidation management: A multiparametric kinetic approach. *J Agric Food Chem.* (2013) 61:5371–9. doi: 10.1021/jf4005109

22. Castro CC, Martins RC, Teixeira JA, Silva Ferreira AC. Application of a high-throughput process analytical technology metabolomics pipeline to Port wine forced ageing process. *Food Chem.* (2014) 143:384–91. doi: 10.1016/j.foodchem.2013.07.138

23. Monforte AR, Jacobson D, Silva Ferreira AC. Chemiomics: Network reconstruction and kinetics of Port wine aging. *J Agric Food Chem.* (2015) 63:2576–81. doi: 10.1021/jf5055084

24. Azevedo J, Pinto J, Teixeira N, Oliveira J, Cabral M, Guedes de Pinho P, et al. The impact of storage conditions and bottle orientation on the evolution of phenolic and volatile compounds of vintage Port wine. *Foods.* (2022) 11:2770. doi: 10.3390/foods11182770

25. Ferreira IM, Freitas F, Pinheiro S, Mourão MF, Guido LF, Gomes da Silva M. Impact of temperature during beer storage on beer chemical profile. *LWT.* (2022) 154:112688. doi: 10.1016/j.lwt.2021.112688

26. Martínez A, Vegara S, Herranz-López M, Martí N, Valero M, Micol V, et al. Kinetic changes of polyphenols, anthocyanins and antioxidant capacity in forced aged hibiscus ale beer. *J Inst Brew.* (2017) 123:58–65. doi: 10.1002/jib.387

27. Pons-Mercadé P, Giménez P, Gombau J, Vilomara G, Conde M, Cantos A, et al. Oxygen consumption rate of lees during sparkling wine (Cava) aging; influence of the aging time. *Food Chem.* (2021) 342:128238. doi: 10.1016/j.foodchem.2020.128238

28. Ugliano M. Oxygen contribution to wine aroma evolution during bottle aging. *J Agric Food Chem.* (2013) 61:6125–36. doi: 10.1021/jf400810v

29. Isogai A, Kanda R, Hiraga Y, Iwata H, Sudo S. Contribution of 1,2-dihydroxy-5-(methylsulfinyl)pentan-3-one (DMTS-P1) to the formation of dimethyl trisulfide (DMTS) during the storage of Japanese sake. *J Agric Food Chem.* (2010) 58:7756–61. doi: 10.1021/jf100707a

30. Zhang XK, Lan YB, Huang Y, Zhao X, Duan CQ. Targeted metabolomics of anthocyanin derivatives during prolonged wine aging: Evolution, color contribution and aging prediction. *Food Chem.* (2021) 339:127795. doi: 10.1016/j.foodchem.2020.127795

31. Isogai A, Kanda R, Hiraga Y, Nishimura T, Iwata H, Goto-Yamamoto N. Screening and identification of precursor compounds of dimethyl trisulfide (DMTS) in Japanese sake. *J Agric Food Chem.* (2008) 57:189–95. doi: 10.1021/jf802582p

32. Monforte AR, Martins SIFS, Silva Ferreira AC. Discrimination of white wine ageing based on untarget peak picking approach with multi-class target coupled with machine learning algorithms. *Food Chem.* (2021) 352:129288. doi: 10.1016/j.foodchem.2021.129288

33. Isogai A. Aroma compounds responsible for the aging of sake and their formation mechanism. *J Society Brew Japan.* (2009) 104:847–57. doi: 10.6013/jbrewsocjapan.104.847

34. Canas S, Anjos O, Caldeira I, Belchior AP. Are the furanic aldehydes ratio and phenolic aldehydes ratios reliable to assess the addition of vanillin and caramel to the aged wine spirit? *Food Control.* (2019) 95:77–84. doi: 10.1016/j.foodcont.2018.07.048

35. Ma T, Wang J, Wang H, Zhao Q, Zhang F, Ge Q, et al. Wine aging and artificial simulated wine aging: Technologies, applications, challenges, and perspectives. *Food Res Int.* (2022) 153:110953. doi: 10.1016/j.foodres.2022.111079

36. Santos MC, Nunes C, Rocha MA, Rodrigues A, Rocha SM, Saraiva JA, et al. High pressure treatments accelerate changes in volatile composition of sulphur dioxide-free wine during bottle storage. *Food Chem.* (2015) 188:406–14. doi: 10.1016/j.foodchem.2015.05.002

37. Carvalho MJ, Pereira V, Pereira AC, Pinto JL, Marques JC. Evaluation of wine colour under accelerated and oak-cask ageing using CIELab and chemometric approaches. *Food Bioprocess Technol.* (2015) 8:2309–18. doi: 10.1007/s11947-015-1585-x

38. Del Alamo M, Nevares I, Gallego L, Fernandez de Simon B, Cadahia E. Micro-oxygenation strategy depends on origin and size of oak chips or staves during accelerated red wine aging. *Anal Chim Acta.* (2010) 660:92–101. doi: 10.1016/j.aca.2009.11.044

39. Caldeira I, Vitória C, Anjos O, Fernandes TA, Gallardo E, Fargeton L, et al. Wine spirit ageing with Chestnut Staves under different micro-oxygenation strategies: Effects on the volatile compounds and sensory profile. *Appl Sci.* (2021) 11:3991. doi: 10.3390/app11093991

40. Gao Y, Hou L, Gao J, Li D, Tian Z, Fan B, et al. Metabolomics approaches for the comprehensive evaluation of fermented foods: A review. *Foods.* (2021) 10:2294. doi: 10.3390/foods10102294

41. Pinto J, Oliveira AS, Azevedo J, Freitas VD, Lopes P, Roseira I, et al. Assessment of oxidation compounds in oaked Chardonnay wines: A GC–MS and 1H NMR metabolomics approach. *Food Chem.* (2018) 257:120–7. doi: 10.1016/j.foodchem.2018.02.156

42. Arapitsas P, Ugliano M, Perenzoni D, Angeli A, Pangrazzi P, Mattivi F. Wine metabolomics reveals new sulfonated products in bottled white wines, promoted by small amounts of oxygen. *J Chromatogr A.* (2016) 1429:155–65. doi: 10.1016/j.chroma.2015.12.010

43. Mu Y, Su W, Yu XT, Mu YC, Jiang L, Wang HL. Untargeted metabolomics based on GC-TOF-MS reveals the optimal pre-fermentation time for black glutinous rice wine. *Int J Food Prop.* (2019) 22:2033–46. doi: 10.1080/10942912.2019.1705481

44. Jacobson D, Monforte AR, Silva Ferreira AC. Untangling the chemistry of Port wine aging with the use of GC-FID, multivariate statistics, and network reconstruction. *J Agric Food Chem.* (2013) 61:2513–21. doi: 10.1021/jf3046544

45. Fang C, Du H, Jia W, Xu Y. Compositional differences and similarities between typical Chinese baijiu and western liquor as revealed by mass spectrometry-based metabolomics. *Metabolites.* (2018) 9:2. doi: 10.3390/metabo9010002

46. Chen S, Xu Y, Qian MC. Aroma characterization of Chinese rice wine by gas chromatography-olfactometry, chemical quantitative analysis, and aroma reconstitution. *J Agric Food Chem.* (2013) 61:11295–302. doi: 10.1021/jf4030536

47. Qiu XJ. Influencing factors and formation mechanism of higher fatty acid ethyl ester in soy-flavor liquor. *Stand Qual Light Ind.* (2019) 163:78–80.

frontiers | Frontiers in Nutrition

TYPE Original Research
PUBLISHED 07 February 2023
DOI 10.3389/fnut.2023.1110803

OPEN ACCESS

EDITED BY
Wenjiang Dong,
Chinese Academy of Tropical Agricultural Sciences, China

REVIEWED BY
Yuyun Lu,
National University of Singapore, Singapore
Qin Li,
Hunan Agricultural University, China

*CORRESPONDENCE
Yong-Quan Xu
✉ yqx33@126.com
Jun-Feng Yin
✉ yinjf@tricaas.com

SPECIALTY SECTION
This article was submitted to Food Chemistry, a section of the journal Frontiers in Nutrition

RECEIVED 29 November 2022
ACCEPTED 13 January 2023
PUBLISHED 07 February 2023

CITATION
Zou C, Chen D-Q, He H-F, Huang Y-B, Feng Z-H, Chen J-X, Wang F, Xu Y-Q and Yin J-F (2023) Impact of tea leaves categories on physicochemical, antioxidant, and sensorial profiles of tea wine. *Front. Nutr.* 10:1110803. doi: 10.3389/fnut.2023.1110803

Impact of tea leaves categories on physicochemical, antioxidant, and sensorial profiles of tea wine

Chun Zou[1], De-Quan Chen[1,2], Hua-Feng He[3], Yi-Bin Huang[1,4], Zhi-Hui Feng[1], Jian-Xin Chen[1], Fang Wang[1], Yong-Quan Xu[1]* and Jun-Feng Yin[1]*

[1]Tea Research Institute Chinese Academy of Agricultural Sciences, National Engineering Research Center for Tea Processing, Key Laboratory of Tea Biology and Resources Utilization, Ministry of Agriculture, Hangzhou, China, [2]Graduate School of Chinese Academy of Agricultural Sciences, Beijing, China, [3]School of Pharmacy, Jining Medical University, Jining, China, [4]College of Tea Science, Guizhou University, Guiyang, China

Introduction: Tea is the main raw material for preparing tea wine.

Methods: In this research, four types of tea wine were prepared using different categories of tea leaves, including green tea, oolong tea, black tea, and dark tea, and the comparative study looking their physicochemical, sensorial, and antioxidant profiles were carried out.

Results: The dynamic changes of total soluble solids, amino acids and ethanol concentrations, and pH were similar in four tea wines. The green tea wine (GTW) showed the highest consumption of total soluble solids and amino acids, and produced the highest concentrations of alcohol, malic, succinic, and lactic acid among all tea wines. The analysis of volatile components indicated the number and concentration of esters and alcohols increased significantly after fermentation of tea wines. GTW presented the highest volatile concentration, while oolong tea wine (OTW) showed the highest number of volatile compounds. GTW had the highest total catechins concentration of 404 mg/L and the highest ABTS value (1.63 mmol TEAC/mL), while OTW showed the highest DPPH value (1.00 mmol TEAC/mL). Moreover, OTW showed the highest score of sensory properties.

Discussion: Therefore, the types of tea leaves used in the tea wine production interfere in its bioactive composition, sensorial, and antioxidant properties.

KEYWORDS

tea wine, organic acids, volatile components, catechins, antioxidant activity, sensory properties

1. Introduction

Tea wine is an alcoholic drink with tea as the main raw material (1). It combines the fragrance of tea and mellow of wine, which has a unique and attractive flavor (2, 3). Moreover, there are many potential benefits of tea wine for human health, including immunity improvement, neuroprotective effect, antioxidant effect, and antimicrobial efficacy (4–6). Therefore, tea wine has attracted a wide attention of researchers and consumers in recent years (7).

In tea wine fermentation, sugar is supplemented as carbon source, while tea is not only used as nitrogen source, but also provides flavor and functional components for tea wine (8, 9). According to different fermentation degrees (10), tea leaves have the categories of green tea (non-fermented), oolong tea (semi-fermented), black tea (full-fermented), and dark tea

(post-oxidized with microorganisms). The major polyphenolic catechins are largely retained in green tea, while they are enzymatically oxidized or metabolized by microorganisms to catechin polymers in black tea or dark tea. The major polyphenolic catechins (11), including (−)-epigallocatechin (EGC), (−)-epicatechin (EC), (−)-epicatechin gallate (ECG), (−)-epigallocatechin gallate (EGCG), (+)-catechin (C), (−)-catechin gallate (CG), (−)-gallocatechin (GC), (−)-gallocatechin gallate (GCG), are known to possess antioxidant activity (3). Moreover, the sensory properties and aroma compounds in various categories of tea are also different (12). Therefore, the effects of tea categories on the properties of tea wine need to be clarified.

In this study, four types of tea wine, including black tea wine (BTW), green tea wine (GTW), oolong tea wine (OTW), and dark tea wine (DTW) were prepared using different categories of tea leaves. The aim of this research was to investigate the effects of categories of tea leaves on the physicochemical, antioxidant, and sensorial profile of tea wines.

2. Materials and methods

2.1. Reagents and materials

Black tea (Keemun), green tea (Longjing), oolong tea (*Tieguanyin*), and dark tea (Pu-erh) were purchased from Yifutang Co. (Hangzhou, China), Longguan Co. (Hangzhou, China), Mingjuhui Co. (Quanzhou, China), and Xinyihao Co. (Kunming, China), respectively. Lyophilized yeast powder was purchased from Angel Yeast Co., Ltd. (Yichang, China). Sucrose was purchased from Jingtang Co. (Beijing, China).

Standards of organic acids (gluconic, succinic, citric, and gallic acid) and catechins (EGC, EC, ECG, EGCG, C, CG, GC, and GCG) were purchased from Sigma-Aldrich Shanghai Trading Co., Ltd. (Shanghai, China). Methanol and acetonitrile of high performance liquid chromatograph (HPLC) grade were purchased from Merck Co. (Darmstadt, Germany). All the other chemicals were of analytical grade and purchased from Sinopharm Chemical Reagent Co., Ltd. (Shanghai, China).

2.2. Tea wine production

The sugared tea infusion was prepared as the following steps: 225 g sucrose was dissolved in 1.5 L water. The solution was sterilized at 121°C for 15 min, and then 9 g of tea leaves were added and extracted at 90°C for 20 min. After extraction, the tea leaves were removed and the sugared tea infusion was transferred into a sterilized glass jar, which was cooled down to room temperature before inoculation.

For yeast strain recovery, 0.75 g lyophilized yeast powder was added into a 5% sucrose solution, and maintained at 35°C for 20 min. Subsequently, the recovered yeast was inoculated into the sugared tea infusion, and then tea wine fermentation was carried out at 28°C for 20 days (13).

2.3. Determination of total soluble solids contents

The total soluble solids content (TSSC) of tea wine were determined using a refractometer (RX-007a, Atago Co., Ltd., Japan).

2.4. Determination of ethanol

The ethanol concentration was determined using a biosensor analyzer (Jinan Yanhe Biotechnology Co., Ltd., Jinan, China). The biosensor analyzer was calibrated with the alcohol standard solution before measurement. If the alcohol concentration of sample was higher than 0.4 g/L, the sample should be diluted. Twenty-five microliters sample was sucked accurately using a micro sampler, and injected into the biosensor analyzer for enzyme reaction. After reaction, the test result will be displayed on the screen.

2.5. Determination of amino acids

The concentration of amino acids in tea wine was determined using a spectrophotometer by the ninhydrin method (14) at 540 nm. Glutamic acid was used as the standard.

2.6. Determination of pH

The pH value of tea wine was determined using a pH meter (SG2, Mettler-Toledo Instruments Co., Ltd., Shanghai, China).

2.7. Determination of organic acids and catechins

Organic acids (malic, succinic, lactic, and gluconic acid) were analyzed using a HPLC equipped with an Agilent ZORBAX® SB-C18 column (4.6 × 150 mm, 5 μm) and a UV-DAD detector (15). The mobile phase was a mixture of methanol and 1 g/L phosphoric acid (3:97). The detection wavelength was set at 220 nm. The column temperature and flow rate were maintained at 28°C and 1 ml/min, respectively.

Catechins (EGC, EC, ECG, EGCG, C, CG, GC, and GCG) were analyzed using a HPLC equipped with a Waters Symmetry C18 column (4.6 × 250 mm, 5 μm) and a UV-DAD detector (16). The detection wavelength was set at 280 nm. The mobile phase A was formed with 2% acetic acid, and the mobile phase B was 100% acetonitrile. The following elution gradient program was adopted: 0–16 min, 6.5% B; 16–25 min, 15% B; and 25–30 min, 6.5% B. The flow rate and column temperature were maintained at 1 ml/min and 35°C, respectively.

2.8. Analysis of volatiles

The tea wine samples were pretreated by headspace solid-phase microextraction (HS-SPME) using a SPME stable flex fiber (50/30 μm, PDMS/DVB/CAR) for the headspace experiments (17). One hundred milliliter of sample and 100 μl of internal standard (10 μg/ml ethyl caprate) were mixed and placed in a 150-ml sealed glass vial. After equilibration and stabilization for at 50°C 5 min, the SPME fiber was used for the absorption of volatiles for 40 min. After absorption, the volatiles were desorbed in a gas chromatography–mass spectrometry (GC–MS) injector at 220°C for 5 min.

The volatiles were analyzed with an Agilent 6890N GC equipped with 5975B mass selective detector. A DB-5MS (60 m × 0.25 mm × 0.25 μm) capillary column was used for the separation. The GC inlet temperature

was set at 220°C. The carrier gas was set at 1.5 ml/min of high purity helium (99.999%). The temperature was programmed as follows: 50°C for 2 min, raised to 80°C at 3°C/min, held at 80°C for 2 min, then raised to 180°C at 5°C/min, held for 1 min, and finally raised to 230°C at 10°C/min and held for 2 min. For MS analysis, the electronic energy of the EI mode and the temperature of the ion source were set at 70 eV and 230°C, respectively. The mass scan range was 50–500 *m*/*z*. The volatile compounds were identified based on the National Institute of Standards and Technology (NIST) database library.

2.9. Analysis of antioxidant activity

The 1,1-diphenyl-2-picrylhydrazyl (DPPH) and 2,2′-azinobis-3-ethylbenzthiazoline-6-sulfonic acid (ABTS) assays were used to analyze the antioxidant capacity of tea wines, using trolox as a standard.

The DPPH assay was carried out as follows: 3 ml of DPPH solution (200 μM) and 1.5 ml of sample were mixed, and then setted in a dark place at room temperature for 30 min. Subsequently, the decrease in absorbance at 515 nm was measured.

The ABTS assay was conducted as follows: 7 mM ABTS solution and 2.45 mM potassium persulfate solution were mixed and kept in the dark for 12–16 h. The mixture should be diluted to an absorbance of 0.70 ± 0.02 at 734 nm before use. One milliliter of sample and 4 ml of ABTS diluted solution were mixed and kept for 6 min in a dark at room temperature. The decrease in absorbance at 734 nm was measured.

2.10. Analysis of sensory properties

The sensory properties of tea wines were scored by a trained team of eight panelists (four men and four women, 23–50 years old) from the Tea Research Institute of the Chinese Academy of Agricultural Sciences. Based on their preference, the panelists gave the scores for taste, odor, appearance, and overall acceptability. A scoring range of 1–9 was used, which indicated (1) extreme disliking, (2) great disliking, (3) moderate disliking, (4) slight disliking, (5) neither liking nor disliking, (6) slight liking, (7) moderate liking, (8) great liking, and (9) extreme liking.

2.11. Statistical analysis

All results were presented as mean ± standard deviation (SD) of three replicates. The level of statistical significance among the means was analyzed by one-way ANOVA using SPSS (version 18.0, SPSS Inc., Chicago, IL, United States).

3. Results and discussion

3.1. The changes of total soluble solids, amino acids, and ethanol concentrations during fermentation

The total soluble solids contents (TSSC) of all four tea wines were decreased with fermentation time (Figure 1A), and the TSSC of GTW showed the largest decline among all samples. The TSSC of GTW at 20 days reached 4.67°Bx, which was 22.3, 19.1, and 9.6% lower than that of BTW, OTW, and DTW, respectively. Similar range of TSSC at the end of wine fermentation was reported by Lu et al. (18) and Joshi et al. (8). Because sugar was the main contributor of the TSSC in tea wine (18), green tea might be more conducive to sugar consumption than the other three kinds of tea leaves.

Since there was no supplemental nitrogen source added in tea wine fermentation, amino acids in tea broth might be the main nitrogen source for cell growth and metabolism. As shown in Figure 1B, the amino acid concentrations of all four types of tea wine rapidly decreased during the first 2 days, and remained at a low level (<34 mg/L) after that. The initial amino acid concentration of GTW was 150 mg/L, which was the highest among all samples. Therefore, high amino acid concentration in tea broth might promote sugar consumption in tea wine fermentation. Similar results were found in the fermentation of soy whey alcohol (19) and wine (20).

Ethanol is an important metabolite of tea wine. As shown in Figure 1C, the ethanol concentrations of all four tea wines were increased with fermentation time. The ethanol concentration of GTW at 20 days was 8.5%ABV, which was 1.31-fold, 1.16-fold, and 1.01-fold than that of BTW, OTW, and DTW, respectively. This indicated that the alcohol yield of GTW was significantly higher than that of BTW under the similar initial sugar concentration, and similar results could be found in previous studies (21, 22).

The dynamic changes of total soluble solids, amino acids, and ethanol concentrations were similar in four tea wines. Compared to the other three tea wines, GTW had the highest consumption of TSSC and amino acids, and produced the highest alcohol concentration. Therefore, green tea was found more conducive to yeast fermentation and alcohol production compared to the other three tea leaves. As a non-oxidized tea, green tea retained more nutrients during tea processing, such as amino acids and vitamins (23), which might promote the degree of tea wine fermentation. Similar results (14, 24) were found in other fermented products with different tea leaves as raw materials.

3.2. The changes of pH and organic acids concentrations during fermentation

The changes of pH showed similar trends in four tea wines (Figure 2A). In the first 4 days, the pH of tea wines dropped rapidly to 3.08–3.28, and then slowly decreased and maintained at about 3. The main reason for the decrease of pH was probably due to the accumulation of organic acids during tea wine fermentation (25).

The changes in concentrations of organic acids during the tea wine fermentation were shown in Figures 2B–E. Malic, succinic, lactic, and gluconic acid were the main organic acids found in tea wines, which showed different trends during the fermentation process. The concentrations of malic acid increased rapidly in the first 6 days, and thereafter increased slowly in all tea wines except DTW, which decreased after 12 days. It reached a maximal concentration of 1.39 g/L in BTW and GTW at day 20, which was 1.11-fold and 1.49-fold than that of OTW and DTW, respectively. The concentrations of succinic acid in all types of tea wines increased with prolonged fermentation time, and reached to the maximum of 1.15 g/L in GTW at day 20, which was 1.97-fold, 1.3-fold, and 2.16-fold than that of BTW, OTW, and DTW, respectively. The concentrations of lactic acid increased slowly in the

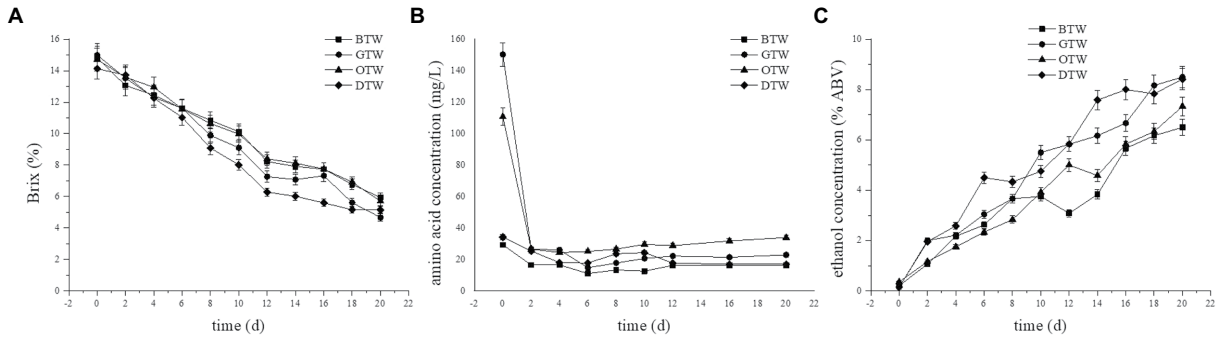

FIGURE 1
The changes of total soluble solids **(A)**, amino acids **(B)**, and ethanol **(C)** concentrations during the fermentation of tea wines.

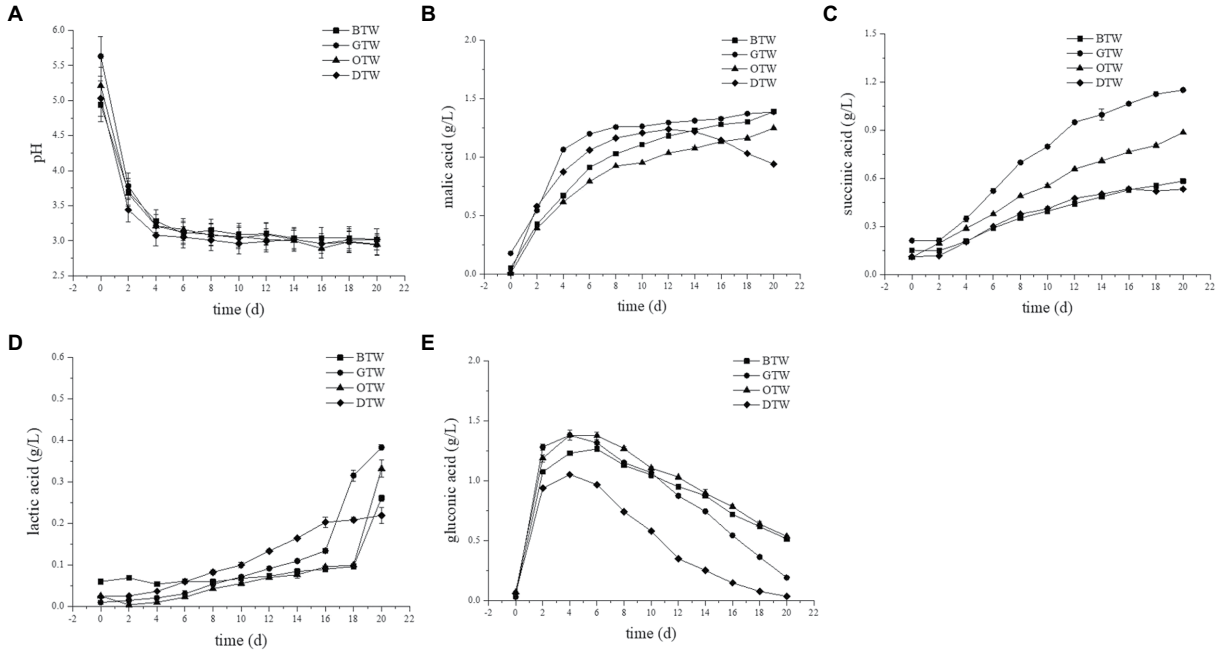

FIGURE 2
The changes of pH **(A)**, malic **(B)**, succinic **(C)**, lactic **(D)**, and gluconic **(E)** acid concentrations during the fermentation of tea wines.

first and middle period, and increased rapidly in the last few days. The concentration of lactic acid was relatively low, and reached to the maximum of 0.38 g/L in GTW at day 20. The concentrations of gluconic acid increased rapidly in the first 4 days, and then gradually decreased in a low range (0.19–0.54 g/L).

After fermentation, GTW showed the highest concentration of malic, succinic, and lactic acid among all tea wines, while BTW had the highest concentration of gluconic acid. The highest concentration of organic acids accumulated in GTW may because its raw materials can promote yeast fermentation. The sensory quality of each organic acid is different (26). Malic acid shows smooth tartness and gluconic acid has mild, soft, and refreshing taste. However, lactic acid presents acrid taste, and succinic acid has slightly bitterness in aqueous solutions. Therefore, the difference of organic acids contents might affect the sensory properties of each tea wines. Moreover, some studies found that the formation of organic acids can improve the antibacterial activity of tea wine (27).

3.3. Analysis of volatile components in tea wines

The volatile compounds of all tea wines were detected by HS-SPME-GC-MS. There were 80 compounds were putatively identified, which was listed in "Supplementary material." As shown in Figures 3A,B, there were six groups of volatiles identified, including esters, alkenes, alcohols, aldehydes, ketones, and aromatics. After 20 days of fermentation, the aromatics concentrations of four tea wines significantly increased to 10.2–14.7 μg/L from a low level (1.93–3.70 μg/L), especially in esters and alcohols. However, the concentrations of aldehydes significantly decreased after fermentation. Moreover, the number of volatile compounds in all tea wines increased significantly compared to the related tea broth before fermentation. The aromatics concentration of GTW was the highest among four tea wines, while OTW showed the highest number of volatile compounds-34, which was 1.42-fold, 1.42-fold, and 1.17-fold than that of BTW, GTW, and DTW, respectively.

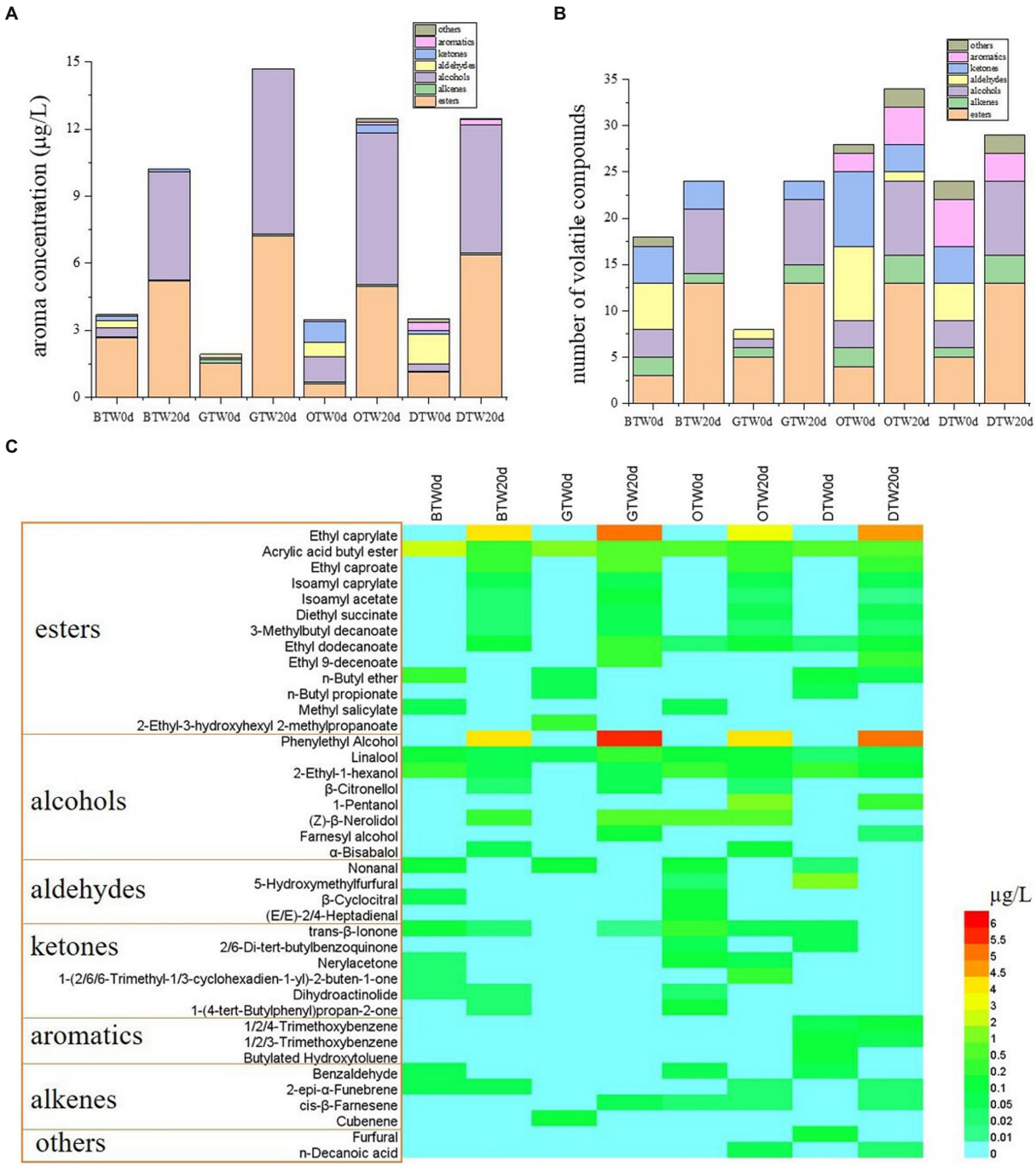

FIGURE 3
The aroma concentration **(A)**, the number of volatile compounds **(B)**, and the heatmap **(C)** of tea wines.

The heatmap of the top 40 compounds ranking their relative concentrations was constructed to visualize the critical metabolites changes of all tea wines (Figure 3C). There were plenty of new esters produced in all tea wines after fermentation, including ethyl caprylate, ethyl caproate, isoamyl caprylate, isoamyl acetate, diethyl succinate, and 3-methylbutyl decanoate. Among them, ethyl ester octanoic acid presented the highest concentration that ranged from 3.82–5.22 μg/L. In terms of alcohols, phenylethyl alcohol was newly produced in all tea wines after fermentation, of which the concentration ranged from 4.22–5.98 μg/L. Moreover, most aldehydes could not be detected after fermentation, which remained a relatively low level of initial concentration.

In general, the number and concentration of esters and alcohols increased significantly after fermentation, while most aldehydes disappeared in tea wines. Ethyl caprylate and phenylethyl alcohol had the highest concentration among all esters and alcohols produced in all tea wines. As reported (28), ethyl caprylate is found as an important aroma contribution of Baijiu, which is generally regarded as fragrant contributor. Phenylethyl alcohol is an aromatic alcohol with rose-like fragrance, usually formed in yeast fermentation (29). Therefore, the

accumulation of ethyl caprylate and phenylethyl alcohol might effectively improve the aroma quality of tea wine.

3.4. Analysis of catechins and antioxidant activity

As important active components and antioxidants in tea wine, catechins were determined by HPLC and the results were shown in Table 1. The concentration of total catechins in GTW was 404 mg/L, which was 26.5-fold, 1.8-fold, and 64.7-fold than that of BTW, OTW, and DTW, respectively. The concentrations of epi form of catechins (EC, EGC, ECG, and EGCG) in GTW was the highest among all tea wines, while OTW showed the highest concentrations of non-epi form (GC, C, CG, and GCG) in all samples. Eight catechins could be detected in GTW and OTW, while GC, EGC, and EC were not detected in BTW, and GC, EGC, and EGCG were not detected in DTW. The catechin concentrations in BTW and DTW were much lower than those in GTW and OTW. Because black tea is full-fermented tea and dark tea is post-oxidized tea, the catechins were oxidized or degraded in tea processing (30).

TABLE 1 The concentrations of catechins in tea wine samples (mg/L).

	BTW	GTW	OTW	DTW
GC	N.D.	31.3 ± 0.6^{b}	50.2 ± 4.2^{a}	N.D.
EGC	N.D.	6.6 ± 0.5^{b}	14.4 ± 0.8^{a}	N.D.
C	3.4 ± 0^{c}	19.6 ± 1.2^{a}	6.4 ± 0.5^{b}	1.8 ± 0^{d}
EC	N.D.	2.8 ± 0.6^{b}	6.1 ± 0.1^{a}	2.1 ± 0.1^{c}
EGCG	3.9 ± 0^{c}	160 ± 2^{a}	92.6 ± 1.1^{b}	N.D.
GCG	1.5 ± 0.2^{c}	105 ± 6^{a}	34.0 ± 1.4^{b}	0.3 ± 0^{d}
ECG	5.0 ± 0^{c}	68.3 ± 1.8^{a}	22.0 ± 0.8^{b}	1.8 ± 0.2^{d}
CG	1.5 ± 0.1^{c}	10.9 ± 0.5^{a}	2.0 ± 0.2^{b}	0.2 ± 0^{d}
Non-epi	3.4 ± 0^{d}	60.3 ± 2.9^{b}	77.2 ± 5.6^{a}	3.9 ± 0.1^{c}
epi	11.9 ± 0.3^{c}	343 ± 10^{a}	151 ± 3.5^{b}	2.3 ± 0.2^{d}
Total	15.2 ± 0.3^{c}	404 ± 13^{a}	228 ± 9.1^{b}	6.2 ± 0.4^{d}

Data are means (±SD) of three replicates. Different letters (a, b, c, d) in the same row indicate significant differences between mean values ($p < 0.05$). N.D., not detected.

The antioxidant ability of tea wines was analyzed by two different antioxidant evaluation assays of ABTS and DPPH scavenging abilities, and the results were shown in Figure 4. The antioxidant activities determined by ABTS and DPPH assay were decreased significantly in all four types of tea wines at day 20 compared to that of day 0. The reason for the decline of antioxidant activities may be that some antioxidant substances, such as tea polyphenols, were degraded in tea wine fermentation. Similar results were reported in previous research (31, 32).

The effects of tea varieties on antioxidant activities of tea wines were compared. GTW presented the highest ABTS value (1.63 mmol TEAC/ml), which was 5.69-fold, 1.49-fold, and 3.90-fold than that of BTW, OTW, and DTW, respectively. However, OTW showed the highest DPPH value (1.00 mmol TEAC/ml), which was 5.02-fold, 1.15-fold, and 3.89-fold than that of BTW, GTW, and DTW, respectively. The antioxidant abilities of GTW and OTW were much higher than those of BTW and DTW. It was probably due to the higher concentrations of catechins in GTW and OTW, which were mainly responsible for antioxidant activities. Many researchers (33, 34) have reported the similar results.

3.5. Evaluation of sensory properties

As shown in Figure 5, the sensory attribute of taste, odor, appearance, and overall acceptability for four types of tea wines were evaluated. The score for taste of OTW was 6.72, which was 4.7, 29.6, and 3.4% higher than that of BTW, GTW, and DTW, respectively. GTW showed the lowest score for taste, probably because the highest concentration of organic acids accumulated, which caused the tea wine to be too sour and taste incongruous. The score for odor of OTW was 7.71, which was 11.6, 10.2, and 31.4% higher than that of BTW, GTW, and DTW, respectively. This may because OTW has the highest number of volatile compounds and the second highest aromatics concentrations.

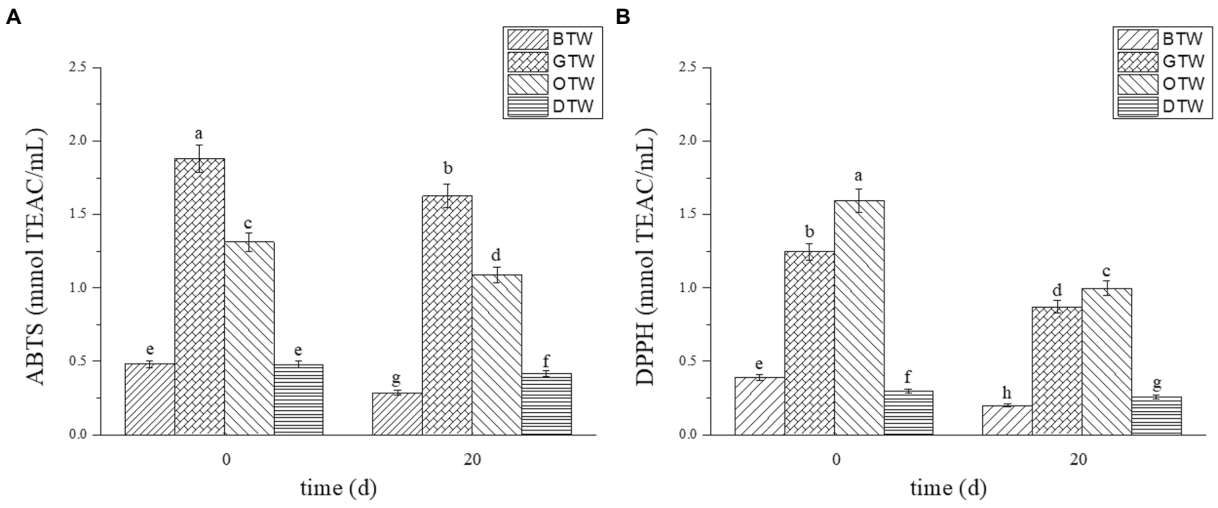

FIGURE 4
The antioxidant evaluation assays of ABTS **(A)** and DPPH **(B)** scavenging abilities on tea wines. Different letters (a, b, c, d, e, f, g, h) in the same column indicate significant differences between the mean values ($p<0.05$).

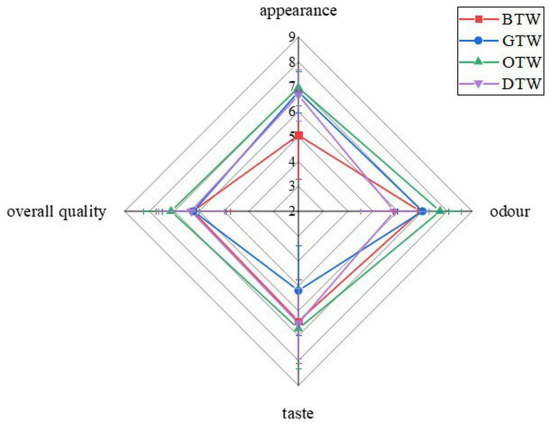

FIGURE 5
The sensory property evaluation on tea wines.

The score for appearance of OTW was 6.97, which was 37.8, 2.5, and 4.5% higher than that of BTW, GTW, and DTW, respectively.

As OTW showed the highest score in taste, odor, and appearance, the score for overall acceptability of OTW was also the highest in all samples, which was 7.13. Therefore, oolong tea is the most suitable for the production of tea wine in terms of flavor. As reported (35, 36), oolong tea was found to be more suitable for many fermented foods than other tea leaves due to its flavor improvement.

4. Conclusion

In this research, the effects of tea leaves categories on the physicochemical, antioxidant, and sensorial profile of tea wines were investigated. The dynamic changes of total soluble solids, amino acids and ethanol concentrations, and pH were similar in four tea wines. The GTW showed the highest consumption of total soluble solids and amino acids, and produced the highest concentrations of alcohol, malic, succinic, and lactic acid among all tea wines, which indicated that green tea may promote the degree of tea wine fermentation. The number and concentration of esters and alcohols increased significantly after fermentation, while most aldehydes disappeared in tea wines. Ethyl caprylate and phenylethyl alcohol had the highest concentration among all esters and alcohols produced in all tea wines, which might effectively improve the aroma quality of tea wine. GTW presented the highest volatile concentration, while oolong tea wine (OTW) showed the highest number of volatile compounds. GTW had the highest total catechins concentration of 404 mg/L and the highest ABTS value (1.63 mmol TEAC/ml), while OTW showed the highest DPPH value (1.00 mmol TEAC/ml). Moreover, OTW showed the highest score in taste, odor, appearance, and overall acceptability, which indicated that oolong tea is the most suitable for the production of tea wine in terms of flavor. Therefore, the types of tea leaves used in the tea wine production interfere in its bioactive composition, sensorial, and antioxidant properties. This study provides guidance for the selection of tea leaves as the raw materials in the tea wine production.

Data availability statement

The raw data supporting the conclusions of this article will be made available by the authors, without undue reservation.

Author contributions

CZ: conceptualization, formal analysis, investigation, data curation, writing – original draft, and funding acquisition. D-QC and H-FH: formal analysis, investigation, and data curation. Y-BH and Z-HF: investigation and data curation. J-XC and FW: investigation. Y-QX and J-FY: writing – review and editing, supervision, funding acquisition, and project administration. All authors contributed to the article and approved the submitted version.

Funding

This research was supported by the National Natural Science Foundation of China (32002094), the Key Research and Development Program of Zhejiang (2022C02033), the China Agriculture Research System of MOF and MARA (CARS-19) and the Innovation Project for Chinese Academy of Agricultural Sciences (CAAS-ASTIP-TRI).

Conflict of interest

The authors declare that the research was conducted in the absence of any commercial or financial relationships that could be construed as a potential conflict of interest.

Publisher's note

Supplementary material

The Supplementary material for this article can be found online at: https://www.frontiersin.org/articles/10.3389/fnut.2023.1110803/full#supplementary-material

References

1. Li, Y, Zhang, S, and Sun, Y. Measurement of catechin and gallic acid in tea wine with HPLC. *Saudi J Biol Sci*. (2020) 27:214–21. doi: 10.1016/j.sjbs.2019.08.011

2. Qin, Y, Yuan, ZJ, Yang, FY, and Yu, YG. Development of a new type of Anhua black tea and its application: black tea wine. *J Food Process Preserv*. (2022) 46:15862. doi: 10.1111/jfpp.15862

3. Anaya, JA, Alvarez, I, Garcia, MJ, and Lizama, V. Application of green tea extract and catechin on the polyphenolic and volatile composition of Monastrell red wines. *Int J Food Sci Technol*. (2022) 57:6097–111. doi: 10.1111/ijfs.15970
4. Xu, X, Ma, WL, Hu, SN, Qian, ZY, Shen, C, and Mao, J. Neuroprotective effects of Chinese rice wine fermented with Fu brick tea on H2O2-induced PC12 cells. *FASEB J*. (2021) 35. doi: 10.1096/fasebj.2021.35.S1.01966
5. Xia, YR, Wang, XT, Sun, HC, and Huang, XM. Proton-coupled electron transfer of catechin in tea wine: the enhanced mechanism of anti-oxidative capacity. *RSC Adv*. (2021) 11:39985–93. doi: 10.1039/d1ra07769d
6. Kumar, V, Joshi, VK, Thakur, NS, Sharma, N, and Gupta, RK. Effect of artificial ageing using different wood chips on Physico-chemical, sensory and antimicrobial properties of apple tea wine. *Braz Arch Biol Technol*. (2020) 63:20180413. doi: 10.1590/1678-4324-2020180413
7. Bayoi, JR, Vandi, Y, Foundikou, BY, and Etoa, FX. Traditional processing, physicochemical property, phytochemical content, and microbiological and sensory quality of the yellow "tea Lemi" wine made in the far-north of Cameroon. *J Food Qual*. (2021) 2021:1–12. doi: 10.1155/2021/6634747
8. Joshi, VK, and Kumar, V. Influence of different sugar sources, nitrogen sources and inocula on the quality characteristics of apple tea wine. *J Inst Brew*. (2017) 123:268–76. doi: 10.1002/jib.417
9. Kumar, V, Joshi, VK, Thakur, NS, Kumar, S, Gupta, RK, Sharma, N, et al. Bioprocess optimization for production of apple tea wine: influence of different variables on the quality attributes. *J Food Meas Char*. (2022) 16:1528–39. doi: 10.1007/s11694-021-01262-5
10. Liang, S, Granato, D, Zou, C, Gao, Y, Zhu, Y, Zhang, L, et al. Processing technologies for manufacturing tea beverages: from traditional to advanced hybrid processes. *Trends Food Sci Technol*. (2021) 118:431–46. doi: 10.1016/j.tifs.2021.10.016
11. Ye, JH, Ye, Y, Yin, JF, Jin, J, Liang, YR, Liu, RY, et al. Bitterness and astringency of tea leaves and products: formation mechanism and reducing strategies. *Trends Food Sci Technol*. (2022) 123:130–43. doi: 10.1016/j.tifs.2022.02.031
12. Feng, ZH, Li, YF, Li, M, Wang, YJ, Zhang, L, Wan, XC, et al. Tea aroma formation from six model manufacturing processes. *Food Chem*. (2019) 285:347–54. doi: 10.1016/j.foodchem.2019.01.174
13. Zhao, XY, Xu, HD, and Yang, RX. Optimization of fermentation conditions of green tea wine and changes in its Main components during fermentation. *Food Sci*. (2014) 35:169–75. doi: 10.7506/spkx1002-6630-201405034
14. Zou, C, Li, RY, Chen, JX, Wang, F, Gao, Y, Fu, YQ, et al. Zijuan tea- based kombucha: physicochemical, sensorial, and antioxidant profile. *Food Chem*. (2021) 363:130322. doi: 10.1016/j.foodchem.2021.130322
15. Li, RY, Xu, YQ, Chen, JX, Wang, F, Zou, C, and Yin, JF. Enhancing the proportion of gluconic acid with a microbial community reconstruction method to improve the taste quality of Kombucha. *LWT-Food Sci Technol*. (2022) 155:112937. doi: 10.1016/j.lwt.2021.112937
16. Cao, QQ, Zou, C, Zhang, YH, Du, QZ, Yin, JF, Shi, J, et al. Improving the taste of autumn green tea with tannase. *Food Chem*. (2019) 277:432–7. doi: 10.1016/j.foodchem.2018.10.146
17. Zeng, L, Fu, YQ, Huang, JS, Wang, JR, Jin, S, Yin, JF, et al. Comparative analysis of volatile compounds in Tieguanyin with different types based on HS-SPME-GC-MS. *Foods*. (2022) 11:1530. doi: 10.3390/foods11111530
18. Lu, YY, Peh, JCH, Lee, PR, and Liu, SQ. Modulation of grape wine flavor via the sequential inoculation of Williopsis saturnus and Saccharomyces cerevisiae. *Food Biotechnol*. (2017) 31:245–63. doi: 10.1080/08905436.2017.1369434
19. Chua, JY, Tan, SJ, and Liu, SQ. The impact of mixed amino acids supplementation on *Torulaspora delbrueckii* growth and volatile compound modulation in soy whey alcohol fermentation. *Food Res Int*. (2021) 140:109901. doi: 10.1016/j.foodres.2020.109901
20. Su, Y, Heras, JM, Gamero, A, Querol, A, and Guillamon, JM. Impact of nitrogen addition on wine fermentation by S. cerevisiae strains with different nitrogen requirements. *J Agric Food Chem*. (2021) 69:6022–31. doi: 10.1021/acs.jafc.1c01266
21. Li, JF, Zhou, Y, Zhou, F, Wang, RR, and Fang, L. Study on optimized technical parameters of the liquid fermented green tea wine. *J Tea Sci*. (2011) 36:66–9. doi: 10.1097/RLU.0b013e3181f49ac7
22. Zou, CL, Zhou, HX, and Chen, S. Preparation of fermented black tea wine. *China Brew*. (2017) 36:180–3. doi: 10.11882/j.issn.0254-5071.2017.02.039
23. Jiang, H, Yu, F, Qin, L, Zhang, N, Cao, Q, Schwab, W, et al. Dynamic change in amino acids, catechins, alkaloids, and gallic acid in six types of tea processed from the same batch of fresh tea (*Camellia sinensis* L.) leaves. *J Food Compos Anal*. (2019) 77:28–38. doi: 10.1016/j.jfca.2019.01.005
24. Najgebauer-Lejko, D, Zmudzinski, D, Ptaszek, A, and Socha, R. Textural properties of yogurts with green tea and Pu-erh tea additive. *Int J Food Sci Technol*. (2014) 49:1149–58. doi: 10.1111/ijfs.12411
25. Kim, JH, and Kim, MY. Development of citrus wine with green tea. *Life Sci J*. (2013) 10:1176–80.
26. Tran, T, Grandvalet, C, Verdier, F, Martin, A, Alexandre, H, and Tourdot-Marechal, R. Microbiological and technological parameters impacting the chemical composition and sensory quality of kombucha. *Compr Rev Food Sci Food Saf*. (2020) 19:2050–70. doi: 10.1111/1541-4337.12574
27. Kumar, V, Joshi, VK, Vyas, G, Thakur, NS, and Sharma, N. Process optimization for the preparation of apple tea wine with analysis of its sensory and physico-chemical characteristics and antimicrobial activity against food-borne pathogens. *Forum Nutr*. (2016) 15:111–21. doi: 10.17470/NF-016-1030-2
28. Wang, Z, Wang, Y, Zhu, TT, Wang, J, Huang, MQ, Wei, JW, et al. Characterization of the key odorants and their content variation in *Niulanshan baijiu* with different storage years using flavor sensory omics analysis. *Food Chem*. (2022) 376:131851. doi: 10.1016/j.foodchem.2021.131851
29. Wagner, K, and Rapp, A. Influence of yeasts on the formation of 2-phenylethanol during the alcoholic fermentation. *Deut Lebensm*. (1999) 95:304–9.
30. Zhao, C, Li, C, Liu, S, and Lei, Y. The Galloyl Catechins contributing to Main antioxidant capacity of tea made from *Camellia sinensis* in China. *Sci World J*. (2014) 2014:1–11. doi: 10.1155/2014/863984
31. Wang, R, Sun, J, Lassabliere, B, Yu, B, and Liu, SQ. Biotransformation of green tea (*Camellia sinensis*) by wine yeast *Saccharomyces cerevisiae*. *J Food Sci*. (2020) 85:306–15. doi: 10.1111/1750-3841.15026
32. Li, JF, Zhou, F, and Zhang, JP. Study on phenol content and influence factors of the liquid fermented green tea wine. *Sci Technol Food Ind*. (2012) 33:208–11. doi: 10.13386/j.issn1002-0306.2012.10.072
33. Bilge, G, and Ozdemir, KS. Synchronous fluorescence spectroscopy combined with chemometrics for determination of total phenolic content and antioxidant activity in different tea types. *J Sci Food Agric*. (2020) 100:3741–7. doi: 10.1002/jsfa.10413
34. Degirmencioglu, N, Yildiz, E, Sahan, Y, Guldas, M, and Gurbuz, O. Impact of tea leaves types on antioxidant properties and bioaccessibility of kombucha. *J Food Sci Technol*. (2021) 58:2304–12. doi: 10.1007/s13197-020-04741-7
35. Swiader, K, Florowska, A, Konisiewicz, Z, and Chen, YP. Functional tea-infused set yoghurt development by evaluation of sensory quality and textural properties. *Foods*. (2020) 9:1848. doi: 10.3390/foods9121848
36. Rong, L, Peng, LJ, Ho, CT, Yan, SH, Meurens, M, Zhang, ZZ, et al. Brewing and volatiles analysis of three tea beers indicate a potential interaction between tea components and lager yeast. *Food Chem*. (2016) 197:161–7. doi: 10.1016/j.foodchem.2015.10.088

frontiers | Frontiers in Nutrition

TYPE Original Research
PUBLISHED 10 February 2023
DOI 10.3389/fnut.2023.1135048

OPEN ACCESS

EDITED BY
Ken Ng,
University of Melbourne, Australia

REVIEWED BY
Zhongjiang Wang,
Northeast Agricultural University, China
Bin Yu,
MANE SEA Pte Ltd., Singapore

*CORRESPONDENCE
Ye Liu
✉ liuyecau@126.com
Shuang Bi
✉ bishuang@btbu.edu.cn

SPECIALTY SECTION
This article was submitted to Food Chemistry, a section of the journal Frontiers in Nutrition

RECEIVED 31 December 2022
ACCEPTED 30 January 2023
PUBLISHED 10 February 2023

CITATION
Dai Y, Xu Y, Shi C, Liu Y and Bi S (2023) Formation mechanism and functional properties of walnut protein isolate and soy protein isolate nanoparticles using the pH-cycle technology. *Front. Nutr.* 10:1135048. doi: 10.3389/fnut.2023.1135048

Formation mechanism and functional properties of walnut protein isolate and soy protein isolate nanoparticles using the pH-cycle technology

Yixin Dai, Ying Xu, Chunhe Shi, Ye Liu* and Shuang Bi*

Beijing Engineering and Technology Research Center of Food Additives, Beijing Advanced Innovation Center for Food Nutrition and Human Health, School of Food and Health, Beijing Technology and Business University, Beijing, China

Walnut protein isolate (WPI) is a nutritious protein with poor solubility, which severely limits its application. In this study, composite nanoparticles were prepared from WPI and soy protein isolate (SPI) using the pH-cycle technology. The WPI solubility increased from 12.64 to 88.53% with a WPI: SPI ratio increased from 1: 0.01 to 1: 1. Morphological and structural analyses illustrated that interaction forces with hydrogen bonding as the main effect jointly drive the binding of WPI to SPI and that protein co-folding occurs during the neutralization process, resulting in a hydrophilic rigid structure. In addition, the interfacial characterization showed that the composite nanoparticle with a large surface charge enhanced the affinity with water molecules, prevented protein aggregation, and protected the new hydrophilic structure from damage. All these parameters helped to maintain the stability of the composite nanoparticles in a neutral environment. Amino acid analysis, emulsification capacity, foaming, and stability analysis showed that the prepared WPI-based nanoparticles exhibited good nutritional and functional properties. Overall, this study could provide a technical reference for the value-added use of WPI and an alternative strategy for delivering natural food ingredients.

KEYWORDS

walnut protein isolate, soy protein isolate, pH-cycle, nanoparticles, interaction, functional properties

1. Introduction

Recently, plant proteins have been applied as raw materials for nanoparticles due to several advantages, including easy surface modification, good biodegradability, biocompatibility, high targeting, and environmental protection (1). Some studies described that nanoparticles produced with proteins derived from plants are being widely used for the encapsulation and delivery of biomolecules, leading to an enhancement in the stability of nutrients and food shelf life (2–4).

It has been described that walnuts are a crucial source of proteins, and walnut protein isolate (WPI) has a high digestibility (85%) and a reasonable proportion of essential amino acids (5–7). In addition, some studies demonstrated that WPI exhibits anti-inflammatory, antioxidant, and blood pressure-lowering activities (5, 8). However, WPI contains a large amount of glutenin

(more than 70%), which leads to its low water solubility. The poor solubility of walnut limits its application of walnut in high value-added fields (9). Furthermore, the low solubility of WPI has been highly associated with its high surface hydrophobicity (10). For instance, hydrophobic regions commonly provide enough binding sites for many biological molecules (11). Therefore, proteins presenting low solubility and high surface hydrophobicity (such as zein, glutenin, gliadin, and rice proteins) were crucial raw materials for nanoparticles (12). Previous studies have shown that for insoluble proteins, it was possible to form nanoparticles by complexing other macromolecules, thus increasing the solubility of insoluble proteins and expanding their applications (13). Over the years, some researchers successfully prepared stable protein-based composite nanoparticles using zein and sodium caseinate as the raw material (14). In addition, some reports revealed that protein-based composite nanoparticles were prepared from hydrophobic rice protein and hydrophilic pea protein, or whey protein (15, 16), increasing the solubility of rice protein. Therefore, WPI could be useful as a nanoparticle component.

Moreover, the presence of other proteins, such as soy protein isolate (SPI), is also essential for preparing composite nanoparticles from insoluble proteins, including WPI. Due to the good biocompatibility and bioavailability of SPI (12), a previous study successfully obtained protein based composite nanoparticles containing scallop muscle protein and SPI, and the solubility of scallop muscle protein was significantly improved (17). Additionally, the other study prepared protein-based composite nanoparticles using rice protein and SPI, and a significant increase in the functional properties of the protein-based composite nanoparticles was detected compared to original rice protein. The solubility of rice protein in nanoparticles was enhanced (18). A recent study also demonstrated that protein-based composite nanoparticles prepared from wheat gluten protein and SPI presented an increase in the solubility of wheat gluten protein and its nutritional properties (19). Therefore, SPI could be useful as a nanoparticle component.

Numerous studies have focused on structural modifications of walnut proteins to improve their solubility. Based the purpose, several methods have been applied, including physical (20), chemical (21), and biological (22). However, physical methods consume a large amount of energy during the process, which results in high costs. For chemical methods, they exhibit potential safety hazards, and for biological methods they lead to a decrease in the nutritional, functional, and sensory properties of proteins. The pH-cycle technology is a low-energy, organic solvent-free, and simple method to prepare nanoparticles. In this technology, a non-covalent interaction of two biomacromolecules occur (by adjusting the pH of the environment in which the two biomacromolecules are located) resulting in the burial of hydrophobic and the exposure of hydrophilic groups to obtain hydrophilic nanoparticles stable in neutral water systems (23). In previous studies, the pH-cycle technology overcomes the poor solubility of insoluble proteins and improves the biological functions after the co-assembly of proteins obtained from different sources into hydrophilic nanoparticles (14). The pH-cycle technology could improve the solubility of insoluble proteins and maintain the protein structure compared to the traditional methods described above, and this technology could help to retain nutritional properties and physiological activities with low damage to nutrients, meeting the needs of green, low-cost, easy operation, high-efficiency, safety, and has high commercialization potential (24). Since WPI contains many hydrophobic groups, in this study, the pH-cycle technology was performed to treat walnut proteins to obtain nanoparticles and eventually improve their functional properties. To date, the interaction mechanism between WPI and SPI-forming nanoparticles under the pH-cycle technology remains unclear, and the applicability of nanoparticles prepared using WPI and SPI in bioactive ingredients delivery has not been investigated.

Therefore, this study had three main aims. Firstly, this study aimed to perform a co-assembly between WPI and SPI into hydrophilic nanoparticles to enhance the WPI water solubility. Secondly, this study also tried to understand potential alterations in the protein structure and investigate the mechanism of interaction between WPI and SPI. Finally, several biological properties of the protein nanoparticles, including the foaming and emulsification, were measured, and the amino acid composition was determined to assess the performance of their functional and nutritional properties. This research has a broad prospect of contributing to the development of flavor-enhanced beverages and functional beverages with high nutritional value and helping the development of beverage processing industry. Overall, this study could help to develop soluble hydrophilic nanoparticles and expand their application in the commercial food industry. Furthermore, this research work could provide a new strategy for the solubilization of hydrophobic plant proteins, which can improve their applicability and acceptability in the industry and among consumers.

2. Materials and methods

2.1. Materials

In this study, the walnuts were purchased from the Winsuk County Woody Grain and Oil Forestry (Xinjiang, China). The soybean meal was acquired from Shandong Yuwang Group (Shandong, China). The 2 × Laemmli sample buffer, colored pre-stained proteins molecular weight standards, and pre-prepared gels were purchased from Shanghai Biyuntian Biotechnology Co., Ltd. (Shanhai, China). Methanol, ethanol and acetonitrile were purchased from MREDA Technology Co., Ltd. (HPLC grade, Beijing, China). Hydrochloric acid (HCl) and sodium hydroxide (NaOH) were purchased from Sinopharm Chemical Reagent Co., Ltd (analytical grade, Shanghai, China).

2.2. Sample preparation

2.2.1. Extraction of WPI

In this study, WPI was prepared according to a previous methodology with slight modifications (25). Briefly, the walnut kernels were degreased using a customized oil press (Shandong Changjian Hydraulic Equipment Co., Ltd., Shandong, China), and then mixed with a hexane solution (1:10, w/v) overnight. After drying, the defatted walnut meal was crushed using a JYS-M01 grinder (Jiu Yang Co., Ltd., Shandong, China) and passed through a 100-mesh sieve. Then, the powder was mixed with ultrapure water (1:40, w/v), and the pH of the mixture was adjusted to pH 12 with 1 M NaOH and stirred for 2 h at room temperature. Obtained samples were centrifuged (HITACHI CR220, Tokyo, Japan) at 10000 × *g* and 4°C for 20 min. After centrifuging the supernatant was collected.

After the pH of the supernatant was adjusted to pH 4.5 by 1 M HCl, and centrifuged at 10,000 × *g* and 4°C for 20 min to collect the precipitates. Finally, the precipitates were washed three times with ultrapure water (adjusted to pH 7 and dialyzed for 48 h). The samples were dried using an Alpha 2–4 Freeze Dryer (Christ, Osterode, Germany) to obtain powdered WPI. The proteins and moisture contents of WPI were 89.56 ± 0.48% (N × 5.3) and 4.24 ± 0.03%, respectively.

2.2.2. Extraction of SPI

In this study, the SPI was prepared following a previous method with slight modifications (26). Briefly, soybean meal was mixed overnight with hexane (1:10, w/v) for degreasing. After the defatted soybean meal was crushed and sieved through 100 mesh. After, the powder was mixed with ultrapure water (1:20, w/v), the pH of the mixture was adjusted to pH 9 with 1M NaOH, stirred for 2 h at room temperature, and after centrifugation at 10,000 × *g* and 4°C for 20 min, the supernatant was collected. Then, the pH of the supernatant was adjusted pH 4.5 by 1 M HCl, and centrifuged at 10,000 × *g* and 4°C for 20 min to collect the precipitates. The precipitates were washed three times with ultrapure water (adjusted to pH 7 and dialyzed for 48 h), and freeze-dried to obtain a SPI powder. Finally, the proteins and moisture contents of SPI were 92.48 ± 0.26% (N × 6.25) and 4.6 ± 0.05%, respectively.

2.2.3. Preparation of composite nanoparticles with WPI and SPI

To prepare the composite nanoparticles, the SPI was dissolved in WPI suspensions (1% w/v), and several protein mixtures were obtained from different WPI/SPI ratios (WPI: SPI ratios between 1:0.01 and 1:1, w/w). Then, the pH of the protein mixture was adjusted to 12 using 1 M NaOH to ensured full dissolution. After magnetic stirring for 1.5 h, the pH of the protein mixture was adjusted to 7 using 0.1 M HCl, and the solution was centrifuged at 5000 × *g* for 10 min to collect the supernatant and precipitate. Next, the supernatant was dialyzed for 24 h to obtain solution of composite nanoparticles. A part of solution was kept and used in each parameter analysis, and the remaining solution was lyophilized to perform a sodium dodecyl sulfate-polyacrylamide gel electrophoresis (SDS-PAGE) and amino acid analyses. On the other hand, the precipitate was lyophilized to do the SDS-PAGE and solubility evaluation. Unless otherwise specified, solutions of composite nanoparticles, WPI and SPI were used for the samples used in the subsequent determination of each parameter.

2.3. SDS-PAGE analysis

In this study, analysis of protein subunits by SDS-PAGE. The SDS-PAGE analysis was performed according to a previous report with slight modifications (27). In this study, the samples were prepared in a loading buffer containing 0.1 M Dithiothreitol (DTT) and incubated in a water bath at 95°C for 10 min. The electrophoretic gel was run at 120 V for 80 min after 10 uL of sample was loaded to electrophoretic gel. Then, the electrophoretic separation gel was stained with a Coomassie brilliant blue staining solution for 120 min, and the excess dye solutions were removed with the Coomassie brilliant blue destaining solution. Finally, the protein bands were photographed by the chemical gel imaging system Bio-Rad (Bio-Rad, Hercules, USA).

2.4. Nitrogen solubility index (NSI)

In this study, the solubility of proteins was determined using the NSI. After preparing the samples (as described in the section "2.2. Sample preparation"), the nitrogen content of the precipitated fraction was determined using the Kjeldahl method (28). The protein conversion factor was 5.3 and 6.25 for WPI and SPI, respectively. According to the SDS-PAGE results, no significant bands were detected in the SPI precipitated. Therefore, the NSI only referred to the WPI solubility. The NSI of WPI was calculated using the following Eq. 1:

$$NSI = \frac{P_{WPI} - P_{residue}}{P_{WPI}} \times 100 \quad (1)$$

Where P_{WPI} was the mass of initial WPI (g), $P_{residue}$ was the mass of residual protein (g).

2.5. Composite nanoparticles morphology

2.5.1. Transmission electron microscopy (TEM)

In this study, the micromorphological observations of composite nanoparticles were performed by TEM. The samples were diluted in ultrapure water to reach a protein concentration of 0.02% (w/v). After, the sample was added dropwise to a copper grid, dried, and analyzed using the Jem 2100F TEM (Jeol, Tokyo, Japan).

2.5.2. Atomic force microscopy (AFM)

In this study, the micromorphological observations of composite nanoparticles were performed by AFM. The samples were diluted with ultrapure water to obtain a final protein concentration of 0.0002% (w/v). After, 2.5 μL drops were placed on mica sheets and dried overnight at room temperature. Finally, the samples were used for the 5000II AFM (Hitachi, Tokyo, Japan) analysis.

2.6. Dynamic light scattering (DLS)

In this study, the particle size of composite nanoparticles were analyzed by DLS. DLS measurements were carried out by Nano-ZS90 (Malvern, Malvern, UK). The samples were diluted in ultrapure water to a final protein concentration of 0.1% (w/v) and were analyzed at 25°C. The refractive indices of the proteins and the dispersion medium were 1.450 and 1.330, respectively.

2.7. Fluorescence chromatography

In this study, the analysis of protein-protein interactions were performed by fluorescence chromatography. The samples were adjusted to a final protein concentration of 0.1% (w/v) with ultrapure water, and the intrinsic fluorescence spectra of complex nanoparticles were measured at room temperature using a FS5 fluorescence spectrometer (Edinburgh Instruments, Livingston, UK). An excitation wavelength of 280 nm was applied in this study, and the emission spectra was recorded between 300 and 400 nm. The theoretical fluorescence (Theor.) spectra were obtained by adding the fluorescence spectra of individual WPI and SPI with different concentrations in the samples, on the other hand, the experimental

fluorescence (Exp.) spectra corresponded to the fluorescence spectra of complexed nanoparticles (29). In this study, the significance of hydrogen bonding, hydrophobic interactions, and electrostatic interactions in the interaction between WPI and SPI was also evaluated. For that, WPI and SPI were dissolved in 36 mL of distilled water and processed according to the methodology described in the section "2.2. Sample preparation." Then, 4 mL of 0.1 M thiourea, SDS, and NaCl solutions (with a final concentration of 10 mM) were added to the protein samples. Next, the fluorescence spectra were collected using the same methodology used to prepare the previous samples.

Structural studies on composite nanoparticles were performed using the fluorescent probe ANS. This probe can specifically bind to the hydrophobic domain of the protein, being capable of detecting changes in the protein microenvironment. Briefly, the samples were diluted to a final protein concentration of 0.05% (w/v), then 10 μL of 8 M ANS was added to 4 mL of sample, and the reaction was completed kept in the dark for 15 min. Next, the samples were excited at 390 nm wavelength, and the fluorescence intensities were measured between 400 and 600 nm.

2.8. Circular dichroism (CD)

In this study, the analysis of protein secondary structure was performed by CD spectra. To determine the CD spectra of composite nanoparticles, a MOS-450 spectrometer (BioLogic Science Instruments, Ltd., Claix, France) was used. In this study, the samples were collected at different pH values during the pH-cycle process and diluted with ultrapure water. The wavelength range of far-UV CD was obtained between 190 and 250 nm, and the protein concentration was 0.05% (w/v). The near-UV CD was composed of wavelengths between 250 and 320 nm, and the protein concentration used was 0.01% (w/v). Distilled water was used as a blank solution for the determination.

2.9. Zeta-potential

In this study, the stability of composite nanoparticles were analyzed by zeta-potential. Zeta-potential measurements were carried out by Nano-ZS90 (Malvern, Malvern, UK). For this study, the samples were adjusted in ultrapure water to a final protein concentration of 0.1% (w/v) and analyzed at 25°C. The refractive indices of the proteins and the dispersion medium were 1.450 and 1.330, respectively.

2.10. Surface hydrophobic (H_0)

In this study, the stability of composite nanoparticles were analyzed by the H_0. The H_0 parameter was determined using the ANS fluorescent probe method (30). The samples were diluted with ultrapure water to obtain different protein concentrations ranging between 0.0125 and 0.1% (w/v). After 4 mL of the samples were mixed with 10 μL of 8 mmol/L ANS solution and placed in the dark for 15 min. Then, the fluorescence intensity of composite nanoparticles was determined by FS5 fluorescence spectrometer at excitation wavelength of 390 nm and an emission wavelength of 484 nm. In this study, the H_0 parameter was determined by the fluorescence intensity and protein concentration slope.

2.11. Amino acid analysis of composite nanoparticles

To determine the amino acid composition of the nanoparticles (g/100g protein), the proteins were hydrolyzed with hydrochloric acid. The co-assembled protein samples were placed into a sealed tube, and 10 ml of 6 mol/L hydrochloric acid solution was added. After neutralization with nitrogen, the tubes were sealed and hydrolyzed at 110 °C for 24 h. The supernatant was composed of a protein hydrolysate and determined by high-performance liquid chromatography. An Agilent 1200 liquid chromatograph equipped (Agilent Technologies Inc., Santa Clara, CA, USA) with a Zorbax Eclipse-AAA column (4.6 × 150 mm, 3.5 μm, Agilent Technologies Inc., Santa Clara, CA, USA) was employed to analyzing. The mobile phase was divided into phase A (pH 4.8, 0.04 mol/L NaH2PO4) and phase B (methanol: acetonitrile: ultrapure water (45:45:10 v/v/v)). The liquid phase conditions were as follows: flow rate, 1 mL/min; UV detection wavelength, 338 nm; injection volume, 1 mL; the column temperature was 40°C. The essential amino acid index (EAAI) was calculated according to formula 2 and corresponded to the geometric mean of the essential amino acid content and the corresponding amino acid content in the whole egg protein (31) (2):

$$EAAI = 100 \times \sqrt[n]{\frac{Lys_w}{Lys_s} \times \frac{Thr_w}{Thr_s} \times \ldots \times \frac{Val_w}{Val_s}} \quad (2)$$

Where the subscript w indicates the protein sample, *s* indicates the whole egg protein, and *n* indicates the number of amino acids.

2.12. Functional properties of composite nanoparticles

2.12.1. Emulsification capacity and stability of composite nanoparticles

In this study, the emulsification capacity and stability of composite nanoparticles were measured following a recent method with slight modifications (32). Briefly, the protein was mixed with deionized water to form a 1% (w/v) protein solution and stirred for 1 h to obtain complete hydration. Then, the protein solution was mixed with soybean oil to obtain an oil phase ratio of 0.25, followed by a 1 min homogenization at 20,000 r/min. After homogenization, 50 μL sample was mixed with 0.1% (w/v) SDS solution and diluted 100-fold. The UV absorbance of samples were measured using a UV-Vis spectrometer (Shimadzu UV-2600, Kyoto, Japan) at 500 nm (defined as A_0). The emulsifying activity index (EAI) was calculated using the following formula (3):

$$EAI\left(m^2/g\right) = \frac{2 \times 2.303 \times A_0 \times DF}{C \times (1-\alpha) \times 1000} \quad (3)$$

Where A_0 was the absorbance of emulsions at 0 min,c was the concentration of the protein used (g/mL), α was the oil volume ratio of the emulsion, and DF was the dilution multiple.

After 10 min, the sample was aspirated in the same method and added to the SDS solution to determine the UV absorbance value (designed as A_{10}). The emulsion stability index (ESI) was calculated

using the following formula (4):

$$ESI\,(min) = \frac{A_{10}}{A_0 - A_{10}} \times 10 \quad (4)$$

Where A_0 was the absorbance of emulsions at 0 min, and $A_0$was the absorbance of emulsions after 10 min.

2.12.2. Foaming and foaming stability of composite nanoparticles

In this study, the foaming and foaming stability of composite nanoparticles were evaluated using a previous report with slight modifications (33). Briefly, the protein was mixed with deionized water to form a 1% (w/v) protein solution and stirred for 1 h to obtain complete hydration, and homogenized at 20,000 r/min for 1 min. Then, the foam volume was read and defined as V_0. The homogenized sample was kept for 30 min, and after, the foam volume was measured again and defined as V_{30}. Finally, the foaming capacity (FC) and foaming stability (FS) were calculated using the following formulas (5, 6):

$$FC\,(\%) = \frac{V_0}{V} \times 100 \quad (5)$$

$$FS\,(\%) = \frac{V_{30}}{V_0} \times 100 \quad (6)$$

Where V was the initial volume before foaming, V_0 was the foam volume at 0 min after homogenization, and V_{30} was the foam volume at 30 min after homogenization.

2.13. Statistical analysis

At least three independent replicate experiments were performed for each determination of the sample to obtain the mean. Statistical results were expressed as mean ± standard deviation (SD) and analyzed using SPSS 20.0 software. Significant differences ($p < 0.05$) between groups were determined by one-way ANOVA variance.

3. Results and discussion

3.1. SDS-PAGE

In this study, WPI and SPI were co-solubilized at pH 12.0 and then neutralized and collected to prepare the soluble composite nanoparticles (Figure 1A). The results demonstrated that WPI aggregated and precipitated at the bottom in an aqueous solution before the SPI addition (Figure 1B). However, after adding SPI and using the pH-cycle technology, the resulting composite nanoparticles could dissolve in water (Figure 1B). Furthermore, composite nanoparticles with WPI: SPI = 1:0.5 and 1:1 still maintained colloidal stability in neutral water systems (Figure 1C).

As described above, the subunit information of the protein molecular weight was analyzed by the SDS-PAGE technology. The results obtained from the supernatants revealed that characteristic subunits of WPI and SPI were detected in composite nanoparticles. Furthermore, these subunit bands of SPI became more pronounced with the addition of SPI (Figure 2A, lanes 4–11). However, no characteristic subunit bands of SPI were observed in the SDS-PAGE performed with the precipitated fraction, indicating that only WPI was present after precipitation (Figure 2B, lanes 4–11). The composite nanoparticles in the supernatant retained the characteristic subunit bands of WPI and SPI after adding SPI and using the pH-cycle technology. These results suggest that most subunits of WPI and SPI were involved in the process of co-assembly to prepare composite nanoparticles and remained intact during the process. It has been described that conventional methods significantly degraded or removed most of the subunits of WPI, requiring a large quantity of energy and tedious labor and consequently leading to reduced applicability in the industry (34). This made the protocol significantly different from the conventional method. To investigate the changes in the solubility of walnut protein, the NSI was measured.

3.2. NSI

Studies described that protein solubility, a crucial functional property, could affect other several functional properties of proteins (35). The NSI of WPI in the composite nanoparticles was the percentage of WPI dissolved in solution relative to the initial WPI used in the reaction. Since the characteristic subunits of WPI were only present in the precipitate of composite nanoparticles (Figure 2B), the percentage of dissolved WPI can be obtained by calculating the difference between the total added amount and the content in precipitation. As shown in Figure 2C, the NSI of WPI with or without the pH-cycle treatment was approximately 20.09 and 12.64%, respectively. However, adding SPI induced an increase (30.71% at a WPI: SPI ratio of 1:0.01) in the NSI of WPI in the composite nanoparticles. Additionally, the NSI of WPI increased to 88.53% after adding SPI at a WPI: SPI ratio of 1:1, which was 7 times higher than in WPI nanoparticles without the pH-cycle treatment. Furthermore, the results showed that the WPI insolubility was significantly inhibited after the preparation of composite nanoparticles using the pH-cycle technology and adding SPI. On the other hand, most of the subunits in each protein were essentially unchanged in the composite nanoparticles (Figure 2A), demonstrating that the technology could improve the protein solubility and maintain molecular integrity. Since this study focused on WPI, SPI was added in an amount not exceeding WPI to avoid interferences with the structural analysis of composite nanoparticles. In this study, the morphological and structural properties of composite nanoparticles were evaluated to understand the formation mechanism of composite nanoparticles. The morphological of the composite nanoparticles were evaluated in the subsequent section.

3.3. Morphology of composite nanoparticles

The microscopic morphology of the protein and the composite nanoparticles can be visualized by TEM analysis. A significant aggregation was observed in TEM due to the high hydrophobicity of WPI (Figure 3A). Furthermore, an irregular aggregation was detected, leading to low protein solubility at pH 7.0, consistent with previous studies (36). On the other hand, SPI was well-dispersed in solution with uniform particle sizes at pH 7.0 (Figure 3B). Interestingly, the aggregation of proteins was reduced in the presence of the WPI/SPI = 1:0.1 ratio (Figure 3C). However, gradual, smaller, more dispersed, and homogeneous composite nanoparticles were

10.3389/fnut.2023.1135048

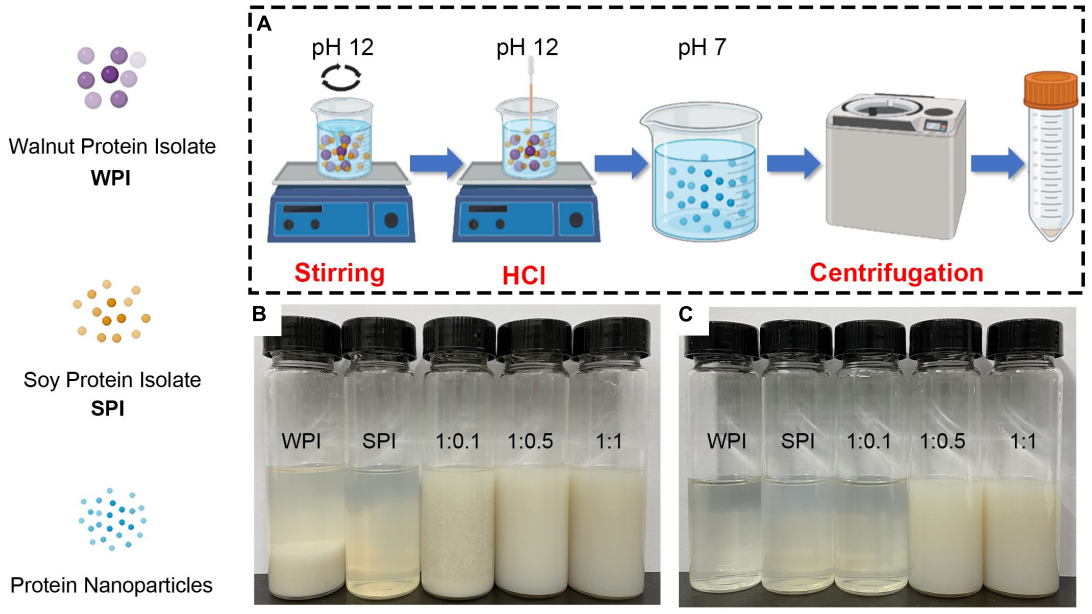

FIGURE 1
(A) Schematic illustration of the pH-cycle technique for fabricating protein-based composite nanoparticles with hydrophobic WPI and hydrophilic SPI. **(B)** Photographs of protein solutions and composite nanoparticles after the pH-cycle treatment. **(C)** Photographs of sample supernatants by centrifuging at 10,000 × *g* and 4°C for 20 min (1:0.1, 1:0.5, 1:1 represents walnut protein and soy protein isolate at the ratio of WPI:SPI = 1:0.1, 1:0.5, 1:1, respectively).

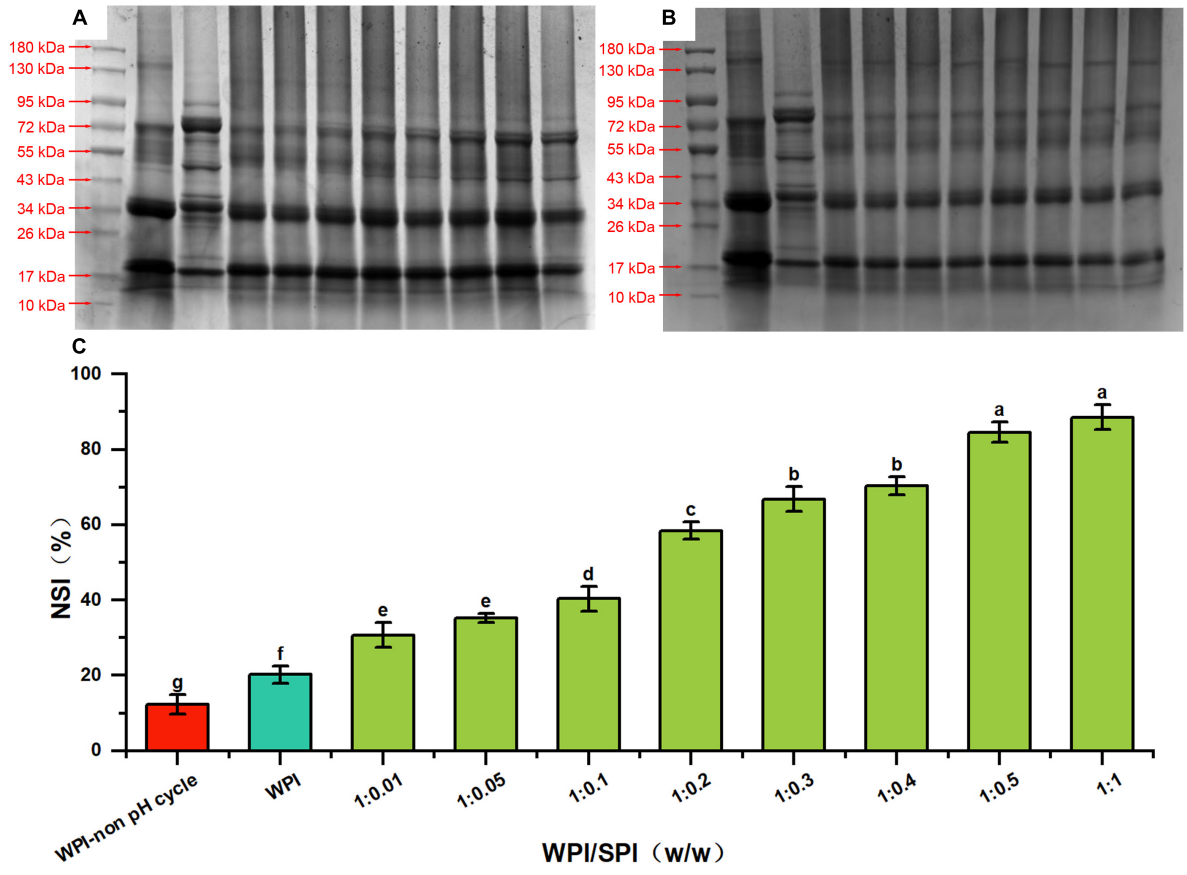

FIGURE 2
SDS-PAGE profiles of supernatant **(A)** and precipitates **(B)** of prepared composite nanoparticles, respectively (lane 1 is marker, lanes 2–10 are WPI, SPI, composite nanoparticles prepared by WPI: SPI = 1:0.01, 1:0.05, 1:0.1, 1:0.2, 1:0.3, 1:0.4, 1:0.5, and 1:1 (w/w), respectively). **(C)** Solubility of WPI in composite nanoparticles with WPI: SPI (w/w) from 1:0.01 to 1:1 by the pH-cycle technique (WPI represents walnut protein isolation solution without the pH-cycle treatment, control represents walnut protein isolation solution with the pH-cycle treatment).

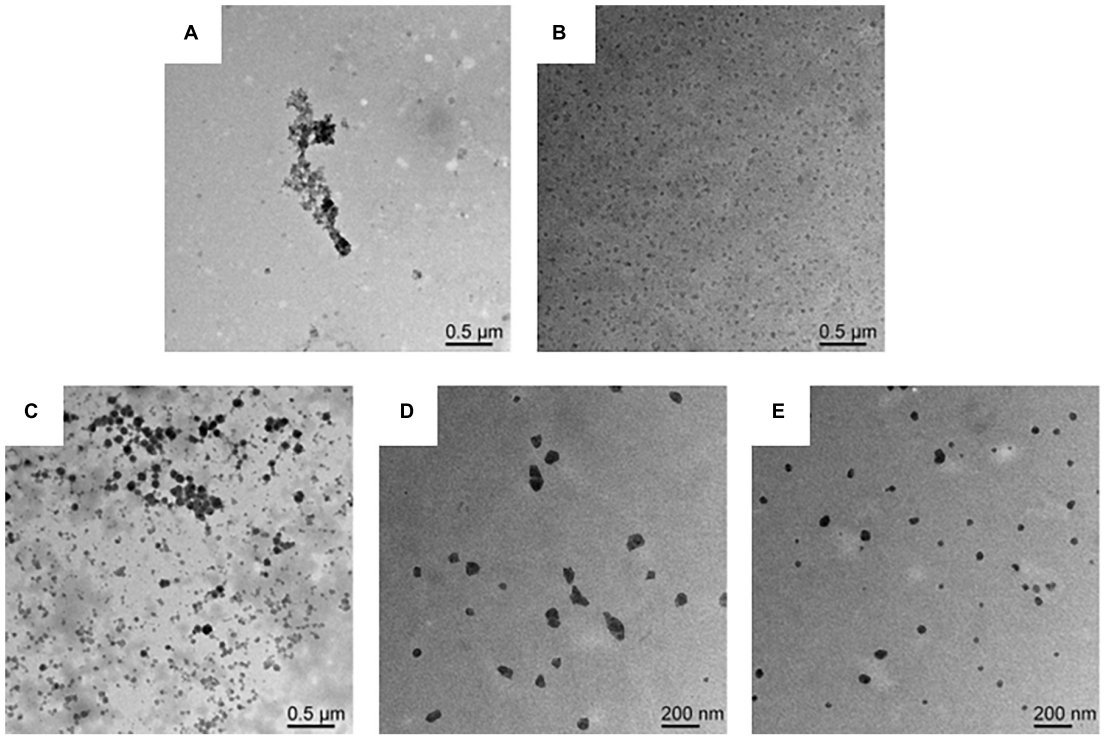

FIGURE 3
(A) Transmission electron microscopy (TEM) image of WPI solution. **(B)** TEM image of SPI solution. **(C)** TEM image of composite nanoparticles prepared by WPI: SPI (w/w) mass ratio of 1: 0.1. **(D)** TEM image of composite nanoparticles prepared by WPI: SPI (w/w) mass ratio of 1: 0.5. **(E)** TEM image of composite nanoparticles prepared by WPI: SPI (w/w) mass ratio of 1: 1.

obtained when the concentration of soy protein was enhanced (Figures 3D, E). To further investigate the structure of composite nanoparticles, AFM combined with the DLS technology was used. Therefore, the AFM results showed that an increase in SPI contributed to the dispersion of composite nanoparticles and the formation of uniform particles with a smaller size. These results agreed with the TEM results described above (Figure 4). The AFM results indicated that the composite nanoparticles collapse into nanoscale spherical structures on the mica sheet surface. The particle size of protein nanoparticles ranged between 80 and 250 nm, and a decrease was observed after adding SPI, which was in agreement with the TEM and AFM results (Figure 4D). Contrarily, the particle size was slightly larger than the size observed in TEM due to the crumpling of the sample that occurred during the drying pre-treatment in TEM. According to the microscopic and DLS analyses, it was possible to observe that when the two proteins interacted, a new protein structure was formed (30). To explore the mechanism behind the phenomenon of protein structure change, the structural properties of the composite nanoparticles were determined. The protein-protein interactions were elaborated.

3.4. Characterization of protein-protein interactions in composite nanoparticles

3.4.1. Quenching of fluorescence of WPI by SPI in composite nanoparticles

In this study, to understand the interaction between WPI and SPI, fluorescence spectroscopy was performed. The WPI and SPI contained aromatic amino acids of chromogenic groups, such as tryptophan, phenylalanine, after excitation at 280 nm wavelength, these amino acids promoted the generation of intrinsic fluorescence (37). It has been described that protein interactions are accompanied by the quenching of endogenous fluorescence, while the quenched forms of different proteins reflect the changes in several regions and action sites (38, 39). Therefore, some reports suggest that these changes in endogenous fluorescence intensity can be used as indirect evidence about protein interactions. In the current study, the endogenous fluorescence intensity decreased, and fluorescence quenching occurred after adding SPI (Figure 5A). These results indicate that the interaction between WPI and SPI occurred and formed a new structure after adding SPI and using the pH-cycle technology. Moreover, the Exp. and Theor. spectra were compared, and the results are shown in Supplementary Figure 1. Some authors described that this phenomenon was related to the electron-rich aromatic amino acid groups toward the electron-deficient amino acid groups (40, 41). In this study, after adding SPI, a higher difference was observed between Exp. and Theor. For example, the degree of quenching increased, indicating that SPI was involved in the formation of the new structure (Supplementary Figure 1). Additionally, a gradual increase in the difference between Exp. and Theor. occurred when the pH decreased, mainly when the ratio of WPI and SPI was 1:1 (Supplementary Figure 2). This result suggests that the molecular affinity between WPI and SPI increased during the pH-cycle treatment, leading to an enhancement in protein interactions and, consequently, leading to the generation of a new protein structure. On the other hand, the maximum fluorescence intensity of the proteins increased when the pH decreased,

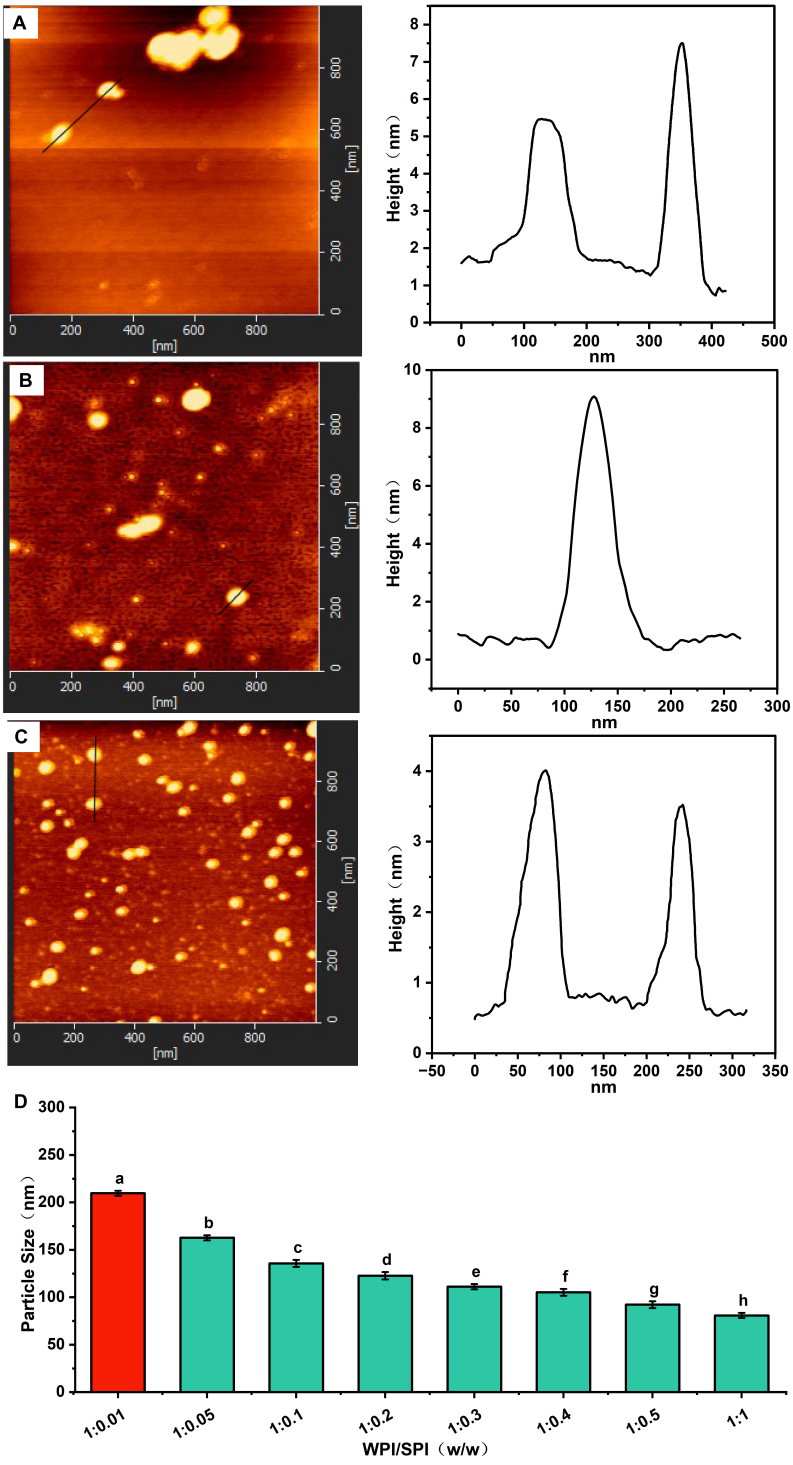

FIGURE 4
(A) Atomic force microscopy (AFM) image of composite nanoparticles prepared by WPI: SPI (w/w) mass ratio of 1: 0.1. **(B)** AFM image of composite nanoparticles prepared by WPI: SPI (w/w) mass ratio of 1: 0.5. **(C)** AFM image of composite nanoparticles prepared by WPI: SPI (w/w) mass ratio of 1: 1. **(D)** Particle size of composite nanoparticles with WPI: SPI (w/w) from 1:0.01 to 1:1.

indicating that the proteins underwent structural renaturation during the protonation process, leading to the formation of new structure (Figure 5B). Furthermore, increased fluorescence intensity was positively correlated with protein renaturation. Although the fluorescence intensity of the composite nanoparticles increased during the protonation process, this value remained lower compared to WPI, indicating that the structural renaturation of WPI could be inhibited by adding SPI (responsible for the increase in the WPI solubility).

In this study, the ANS probe was used to detect the folding and unfolding states of proteins since it can bind by hydrophobic interactions to the hydrophobic region of proteins, showing changes in microstructure and the surrounding environment polarity. For instance, after excitation at 390 nm wavelength, the fluorescence

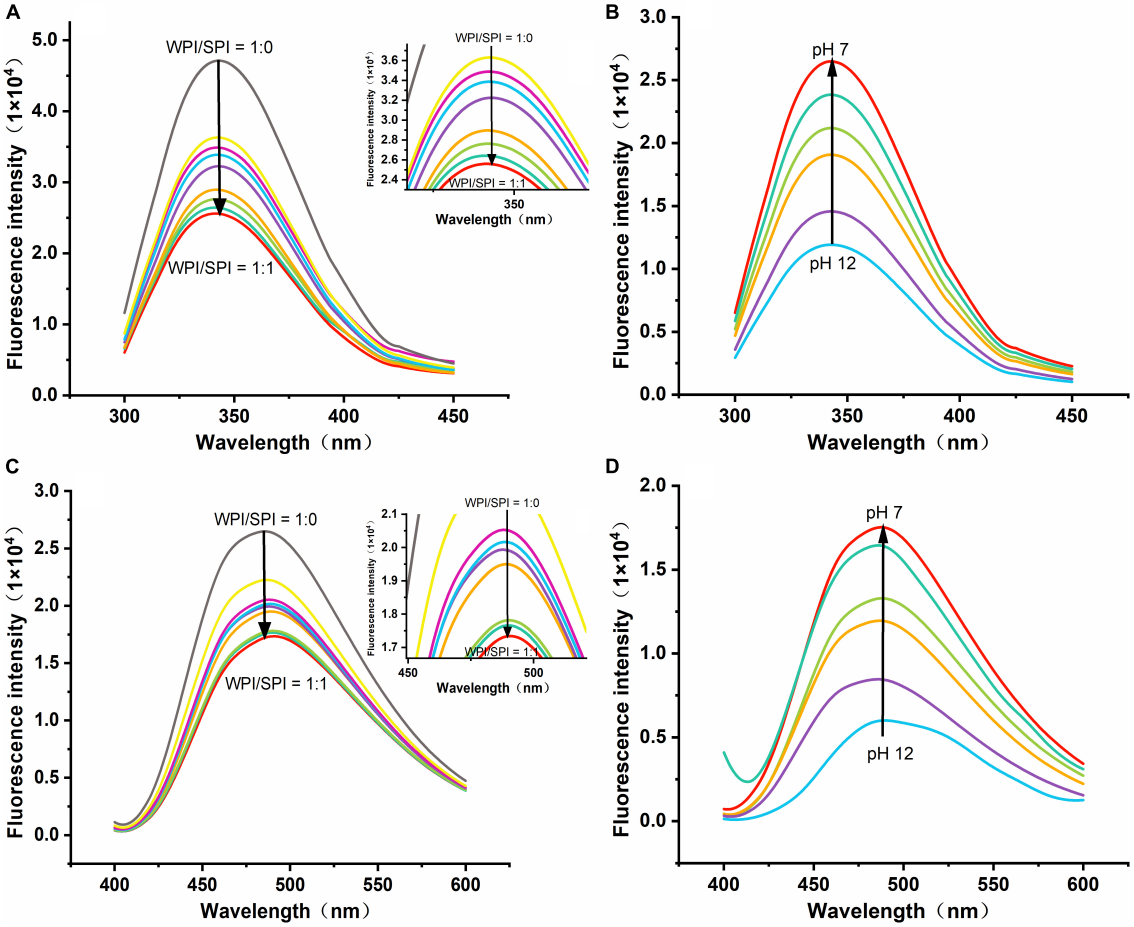

FIGURE 5
(A) Emission spectra of composite nanoparticles with WPI: SPI (w/w) from 1:0 to 1:1. **(B)** Emission spectra of composite nanoparticles (WPI: SPI = 1:1, w/w) at pH 12, 11, 10, 9, 8, and 7. **(C)** Emission spectra for ANS binding to composite nanoparticles with WPI: SPI (w/w) from 1:0 to 1:1. **(D)** Emission spectra for ANS binding to composite nanoparticles with WPI: SPI (WPI: SPI = 1:1, w/w) at pH 12, 11, 10, 9, 8, and 7.

intensity of ANS can reflect the protein folding, and a higher intensity could indicate the higher degree of folding (42, 43). The present study demonstrated that the fluorescence intensity decreased after adding a higher concentration of SPI, indicating that the two proteins interacted and formed a new structure (Figure 5C). Therefore, this result suggests that an interaction between WPI and SPI occurred, and the resulting structure limits the acid-induced refolding of WPI due to increased rigidity, promoting the forming of a new hydrophilic rigid structure in a neutral environment. These conditions could significantly inhibit the formation of hydrophobic regions of the nanoparticles and promote a significant anti-folding behavior. Additionally, at pH 12, when the protein structure was maximally unfolded, the fluorescence intensity of the composite nanoparticles was minimal (Figure 5D). With the pH-cycle technology was performed, the pH was decreased, the increase in fluorescence intensity indicated an increase in the ANS binding sites, further demonstrating to protein refolding.

3.4.2. Determination of type of interaction

This study also tried to determine the non-covalent interactions that are responsible for the interactions between WPI and SPI. For that, the same molar concentrations of SDS, NaCl, and thiourea were individually added to the protein mixture at pH 12. The role of hydrophobic, electrostatic interactions, and hydrogen bonding to promote the process of building and maintenance of a hydrophilic rigid structure of composite nanoparticles was determined using fluorescence intensity (44). The effects of above the block reagents on the molecular interactions/bonds of proteins are listed in Supplementary Table 1. The effect induced by the block reagents was contrary to the fluorescence quenching caused by protein-protein interactions. Furthermore, the fluorescence intensity of the samples in the presence of block reagents was higher than composite nanoparticles, indicating that the three types of non-covalent interactions/bonds could contribute to the formation of a hydrophilic and rigid protein structure (Figure 6A). In addition, the thiourea exhibited the most pronounced result compared to the other bond-disrupting agents, suggesting that hydrogen bonding was crucial for stabilizing the composite nanoparticles. The NSI of WPI in soluble composite nanoparticles was also measured after adding above block reagents. The results revealed that the NSI was significantly lower after adding thiourea and NaCl (Figure 6B), i.e., the absence of hydrogen bonding and electrostatic interactions restricted the interaction between WPI and SPI, inhibiting the WPI solubilization. In addition, after adding SDS, a slight increase was observed in the NSI compared to the other two groups. This result

suggests that SDS could act as a denaturant and inhibit the self-aggregation of WPI during the neutralization process.

3.4.3. Circular dichroism spectroscopy

Some studies described that the presence of amides in the protein backbone could generate CD signals susceptible to structural changes in proteins (45). In addition, the far-UV CD spectra region (comprised between 190 and 250 nm) gives information related to the protein secondary structure. The results in Figures 6C, D showed that the two proteins formed a different structure, supporting the previous hypothesis regarding the formation of a new protein structure. After adding SPI, an increase in the intensity was detected at 208 nm. However, no significant red-shift or blue-shift was observed in these samples, which led to alterations in the structure of the composite

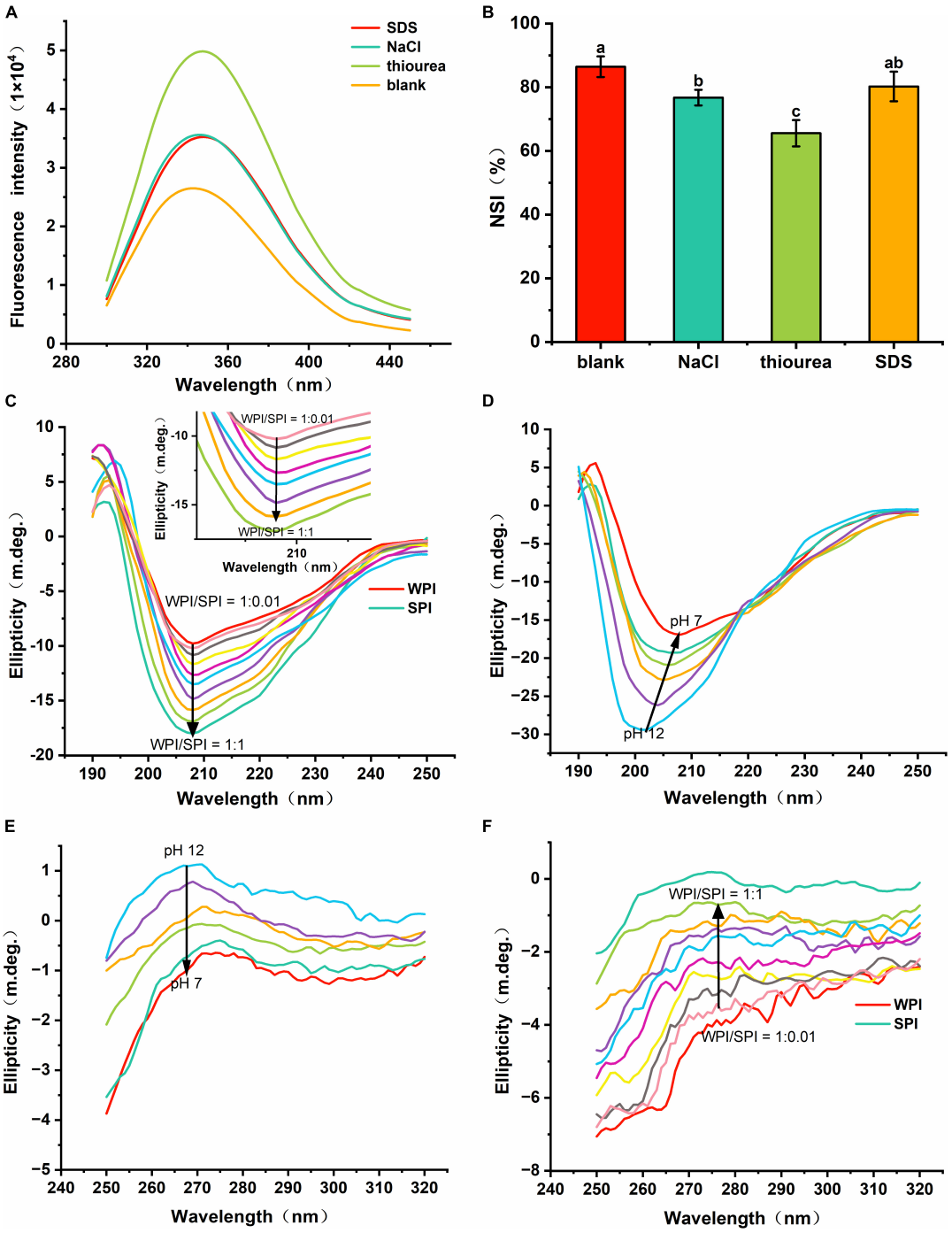

FIGURE 6
(A) Fluorescence spectra of composite nanoparticles WPI: SPI = 1:1 (w/w) with bond-disrupting agents added. **(B)** Nitrogen solubility index (NSI) of WPI with the addition of bond-disrupting agents (10 mM). **(C)** Far-UV CD spectra of composite nanoparticles with WPI/SPI (w/w) from 1:0.01 to 1:1. **(D)** Far-UV CD spectra of a representative composite nanoparticles (WPI: SPI = 1:1, w/w) prepared at pH 12, 11, 10, 9, 8, and 7. **(E)** Near-UV CD spectra of a representative composite nanoparticles (WPI: SPI = 1:1, w/w) prepared at pH 12, 11, 10, 9, 8, and 7. **(F)** Near-UV CD spectra of composite nanoparticles with WPI: SPI (w/w) from 1:0.01 to 1:1.

nanoparticles and differed from that of the WPI and SPI. Thus, these results suggest that the interaction between WPI and SPI could alter the protein structure, leading to the formation of highly hydrophilic composite nanoparticles. Also, a shift in the red signal occurred during the protonation (between pH 12.0 and pH 7.0) (Figure 6D). The above results showed that the protein structure expanded and exposed more charged groups at pH 12.0, and the strong repulsion between the internal groups of the protein expanded and extended the protein, leading to the generation of a stable structure (46). In the process of the pH-cycle technology performed, the protein could re-fold and aggregate due to the reduction in the number of charged groups in the protein surface. However, an enhancement in the folding resistance in WPI occurred after adding SPI. Thus, the composite nanoparticles could form the stable new hydrophilic rigid structure, under neutral conditions.

Furthermore, the aromatic amino acid residues were altered by the microenvironment in the near-UV region of the CD profile, reflecting the changes in the tertiary structure of the protein (47). In the near-UV CD spectrum (ranging between 250 and 320 nm), the CD signal at 275–282 nm was derived from the circular dichroism of Tyr (48, 49). Therefore, the near-UV CD signal of Tyr gradually increased when the pH decreased, indicating that the proteins were refolded (Figure 6E) (30). In addition, the wavelength at the maximum CD model was blue-shifted, indicating that more Try was encapsulated into the hydrophobic environment, which again demonstrated the refolding of the proteins. Moreover, when SPI was added, the near-UV CD signal gradually improved, significantly inhibiting the refolding of WPI (Figure 6F). Therefore, the interaction between WPI and SPI enhanced the anti-folding ability of WPI, forming a high-intensity hydrophilic structure, conferring strong hydrophilicity. Then, the interfacial properties of the nanoparticles were evaluated to understand their dispersion.

3.5. Interfacial properties of the composite nanoparticles

Some studies revealed that substances with good water solubility must be self-repelling and inhibit aggregation. Therefore, the hydrophobicity can modulate their physical stability, solubility, aggregation tendency, and adsorption behavior (50). Due to the macromolecular nature of proteins, surface hydrophobicity can significantly alter the protein function compared to the total hydrophobicity (51). In the present study, surface hydrophobicity and zeta-potential were used to investigate the surface properties of the composite nanoparticles. The results in Figure 7A showed that the surface hydrophobicity of the composite nanoparticles decreased after adding SPI. However, an opposite trend was observed in the absolute zeta-potential values (Figure 7B). This result indicates that the interaction between the two proteins can lead to a gradual increase in the anti-folding of WPI, which continuously inhibited the continuously inhibits the formation of hydrophobic groups and the exposure of charged protein groups, creating repulsive force on

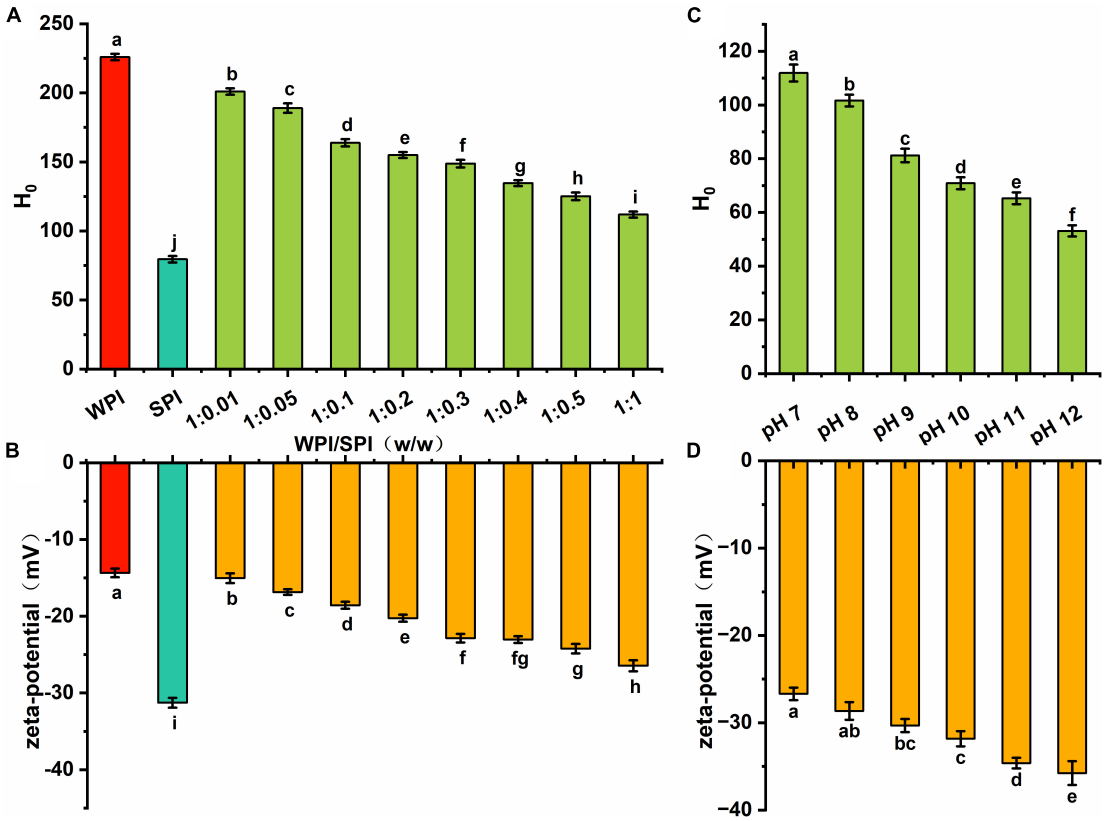

FIGURE 7
(A) The hydrophobicity of WPI, SPI and the composite nanoparticles at pH 7; **(B)** the zeta-potential of WPI, SPI and the composite nanoparticles at pH 7; **(C)** the hydrophobicity of the composite nanoparticles prepared at WPI: SPI ration of 1:1 at pH 12, 11, 10, 9, 8, and 7; **(D)** the zeta-potential of the composite nanoparticles prepared at WPI: SPI ration of 1:1 at pH 12, 11, 10, 9, 8, and 7.

TABLE 1 Amino acid composition of WPI-SPI nanoparticles.

Amino acid	WPI	SPI	WPI/SPI							
			1:0.01	1:0.05	1:0.1	1:0.2	1:0.3	1:0.4	1:0.5	1:1
GLU	22.28 ± 0.22^{a}	20.25 ± 0.39^{g}	22.06 ± 0.04^{ab}	21.99 ± 0.06^{ab}	21.79 ± 0.20^{bc}	21.52 ± 0.28^{cd}	21.54 ± 0.13^{cd}	21.27 ± 0.11^{de}	21.08 ± 0.18^{ef}	20.82 ± 0.21^{f}
ARG	14.80 ± 0.39^{a}	8.72 ± 0.15^{f}	14.20 ± 0.19^{b}	13.89 ± 0.24bc	13.80 ± 0.18^{bc}	13.65 ± 0.11^{cd}	13.52 ± 0.27^{cd}	13.31 ± 0.13^{d}	12.88 ± 0.17^{e}	12.59 ± 0.31^{e}
ASP	9.57 ± 0.21^{e}	13.36 ± 0.13^{a}	9.67 ± 0.12^{e}	9.87 ± 0.10^{e}	9.78 ± 0.18^{e}	10.70 ± 0.47^{d}	11.02 ± 0.33^{cd}	11.35 ± 0.15^{bc}	11.65 ± 0.45^{b}	11.52 ± 0.41^{bc}
SER	5.37 ± 0.10^{a}	4.16 ± 0.15^{g}	5.33 ± 0.18^{a}	5.21 ± 0.15^{ab}	5.11 ± 0.01^{bc}	5.05 ± 0.02^{bc}	4.93 ± 0.06^{cd}	4.82 ± 0.06^{de}	4.72 ± 0.06^{ef}	4.58 ± 0.06^{f}
GLY	4.75 ± 0.11^{a}	4.27 ± 0.11^{bc}	4.69 ± 0.17^{a}	4.71 ± 0.14^{a}	4.63 ± 0.19^{a}	4.59 ± 0.08^{a}	4.55 ± 0.35^{ab}	4.47 ± 0.11^{ab}	4.28 ± 0.05^{bc}	4.13 ± 0.09^{c}
LEU	7.74 ± 0.19^{d}	8.38 ± 0.32^{a}	7.73 ± 0.05^{d}	7.82 ± 0.03^{cd}	7.84 ± 0.07^{cd}	7.93 ± 0.11^{cd}	8.04 ± 0.08^{bc}	8.08 ± 0.07^{bc}	8.21 ± 0.02^{ab}	8.29 ± 0.22^{ab}
PHE	4.89 ± 0.13^{e}	6.32 ± 0.23^{a}	4.95 ± 0.04^{e}	5.35 ± 0.16^{d}	5.72 ± 0.22^{c}	5.75 ± 0.14^{c}	6.05 ± 0.02^{b}	6.13 ± 0.03^{ab}	6.16 ± 0.08^{ab}	6.24 ± 0.02^{ab}
VAL	4.79 ± 0.11^{a}	4.89 ± 0.11^{a}	4.80 ± 0.14^{a}	4.80 ± 0.15^{a}	4.81 ± 0.01^{a}	4.82 ± 0.18^{a}	4.82 ± 0.06^{a}	4.88 ± 0.11^{a}	4.84 ± 0.03^{a}	4.88 ± 0.09^{a}
ALA	4.69 ± 0.11^{a}	3.89 ± 0.05^{c}	4.67 ± 0.13^{a}	4.65 ± 0.06^{a}	4.66 ± 0.19^{a}	4.54 ± 0.15^{ab}	4.49 ± 0.07^{ab}	4.44 ± 0.06^{b}	4.39 ± 0.03^{b}	4.35 ± 0.08^{b}
ILE	4.24 ± 0.23^{a}	4.38 ± 0.22^{a}	4.26 ± 0.12^{a}	4.28 ± 0.08^{a}	4.28 ± 0.19^{a}	4.29 ± 0.11^{a}	4.31 ± 0.15^{a}	4.32 ± 0.07^{a}	4.33 ± 0.22^{a}	4.34 ± 0.02^{a}
THR	3.79 ± 0.16^{a}	3.65 ± 0.23^{a}	3.75 ± 0.03^{a}	3.75 ± 0.08^{a}	3.73 ± 0.04^{a}	3.71 ± 0.04^{a}	3.66 ± 0.08^{a}	3.65 ± 0.06^{a}	3.64 ± 0.02^{a}	3.63 ± 0.00^{a}
TYR	3.41 ± 0.11^{a}	3.46 ± 0.13^{a}	3.41 ± 0.08^{a}	3.42 ± 0.02^{a}	3.42 ± 0.00^{a}	3.42 ± 0.01^{a}	3.43 ± 0.02^{a}	3.43 ± 0.00^{a}	3.43 ± 0.01^{a}	3.42 ± 0.01^{a}
LYS	2.53 ± 0.17^{e}	6.22 ± 0.22^{a}	3.67 ± 0.31^{d}	3.71 ± 0.34^{cd}	3.79 ± 0.07^{cd}	3.83 ± 0.04^{cd}	3.96 ± 0.47^{bcd}	4.05 ± 0.12^{bcd}	4.14 ± 0.05^{bc}	4.29 ± 0.06^{b}
HIS	2.48 ± 0.26^{c}	2.85 ± 0.22^{a}	2.44 ± 0.01^{c}	2.48 ± 0.01^{c}	2.53 ± 0.13^{bc}	2.55 ± 0.32^{bc}	2.55 ± 0.00^{bc}	2.65 ± 0.01^{abc}	2.73 ± 0.05^{abc}	2.79 ± 0.10^{ab}
MET	1.53 ± 0.18^{a}	1.19 ± 0.12^{c}	1.39 ± 0.14^{ab}	1.34 ± 0.01^{bv}	1.31 ± 0.02^{bc}	1.34 ± 0.01^{bc}	1.30 ± 0.01^{bc}	1.23 ± 0.02^{bc}	1.22 ± 0.08^{c}	1.21 ± 0.05^{c}
CYS	0.86 ± 0.03^{a}	0.28 ± 0.02^{e}	0.47 ± 0.01^{b}	0.48 ± 0.00^{b}	0.42 ± 0.01^{c}	0.40 ± 0.06^{c}	0.35 ± 0.01^{d}	0.36 ± 0.01^{d}	0.34 ± 0.01^{d}	0.33 ± 0.00^{d}
EAAI	70.72 ± 1.61^{e}	78.25 ± 0.59^{a}	71.73 ± 1.52^{de}	72.34 ± 0.97^{cde}	72.60 ± 0.97^{cd}	72.93 ± 0.54^{bcd}	73.15 ± 0.72^{bcd}	73.57 ± 0.43^{bcd}	73.89 ± 0.99^{bc}	74.61 ± 0.57^{b}

Values are expressed as the percentage weight of the amino acid against protein weight. Different superscript letters indicate significant differences ($p < 0.05$).

10.3389/fnut.2023.1135048

the surface to improve the solubility and stability of the composite nanoparticles.

Additionally, this study investigated changes in the surface hydrophobicity and zeta-potential of the composite nanoparticles when the pH decreased. **Figure 7C** demonstrated that hydrophobic regions were continuously formed during the folding process. Furthermore, the surface hydrophobicity of composite nanoparticles was lower than in WPI, indicating that the interaction between WPI and SPI significantly inhibited the formation of hydrophobic regions and maintained the relative unfolding of the proteins conformation. The absolute values of zeta-potential continuously decreased with the decrease of pH, indicating that the charged groups exposed to pH 12 were encapsulated inside the complex structure (**Figure 7D**). The results showed that the decrease of surface hydrophobicity and the increase of net surface charge were crucial factors for good dispersion of the composite nanoparticles. Finally, the amino acid composition and functional properties were investigated.

3.6. Amino acid analysis of composite nanoparticles

WPI and SPI are considered excellent sources of amino acids for humans, being widely available in the diet (52), mainly WPI. The Food and Agriculture Organization of the United Nations and the World Health Organization (FAO/WHO) defined that nine essential amino acids are essential in dietary habits, including His, Ile, Leu, Lys Met + Cys, Phe + Tyr, Thr, Trp, and Val, to maintain normal body functions and health. For preschool children, the recommended levels of each amino acid are 19, 28, 66, 58, 25, 63, 34, 11, and 35 mg/g protein, respectively, and for adults, 16, 13, 19, 16, 17, 19, 9, 5, and 13 mg/g protein, respectively. The complex protein nanoparticles obtained in this study showed an impaired amino acid composition with EAAI values ranging from 71.73 to 74.61. On the other hand, SPI and WPI exhibited EAAI values of 70.72 and 78.25, respectively (**Table 1**). Therefore, it is possible to infer that the design of novel soluble protein complex structures composed of multiple proteins could be an effective strategy to obtain protein products with balanced nutritional composition and functionality.

3.7. Functional properties of composite nanoparticles

Under external energy input, proteins can reduce the oil-water interfacial tension and induce the formation of emulsions in oil-water mixtures. Moreover, the emulsification performance was closely related to the hydrophilic-hydrophobic balance of the molecular structure (20). Therefore, solubility and hydrophobicity are crucial parameters to modulate the emulsification effect when proteins are used as interfacial stabilizers. The EAI and ESI of WPI were significantly lower than in SPI, demonstrating the limitation of the lack of solubility on its ability to adsorb at the oil-water interface (**Supplementary Figures 3A, B**). Additionally, the solubility and surface hydrophobicity of WPI was improved by the interaction with SPI, and the EAI and ESI of the composite nanoparticles were significantly higher than in WPI (**Supplementary Figures 3A, B**). Moreover, the co-assembled structure was relatively unfolded, and the structure was rearranged to expose the internal groups capable of adsorbing to the surface of oil droplets. Therefore, an improvement in the hydrophilic-lipophilic balance of the protein particles could occur, leading to an increase in the EAI in WPI (53). This result showed that solubility is highly relevant for protein emulsification. The increase in ESI occurred due to the interaction of WPI and SPI, resulting in the formation of a new three-dimensional network spatial structure. Therefore, the protein contains all the proprieties to adhere to the oil droplet's surface. And the composite nanoparticles with a certain amount of surface charge are adsorbed to the oil-water interface to maintain the emulsion stability by the electrostatic repulsion between the interface-interface and then prevent the occurrence of oil droplet agglomeration (54).

Protein foaming properties can significantly alter the value for application in foamy foods, such as ice cream. Furthermore, some biological parameters, including protein solubility, molecular flexibility, hydrophobicity, and charge density, also significantly modulate the foaming ability (FA) (55). Additionally, changes in protein structure, size, and interactions could lead to alterations in the surface tension, viscoelasticity, and surface rheological properties and consequently affect the foaming stability (FS) (56). Taking this into account, the FA and FS parameters were evaluated in this study. The FA of the composite nanoparticles was significantly improved compared to WPI. However, the FS was boosted less (**Supplementary Figures 2C, D**). The results indicate that the interaction between WPI and SPI formed a new three-dimensional hydrophilic structure. The structure showed a relatively unfolded state, enhanced protein flexibility and solubility, and enhanced interaction between protein and water molecules, promoting protein adsorption at the liquid-air interface. All these changes could induce a significant improvement in the FA (57). Compared to WPI or SPI alone, the FS of the composite nanoparticles was enhanced because WPI and SPI interacted to form a new three-dimensional structure, exposing some of the hydrophobic groups. On the other hand, inter-protein forces were enhanced, resulting in rapid adsorption and formation of a stronger protein membrane at the air-water interface, enhancing the FS (55, 58). Overall, the composite nanoparticles showed improved functional properties compared to WPI or SPI alone.

4. Conclusion

In this study, soluble protein composite nanoparticles with a new hydrophilic rigid structure were successfully prepared by using pH cycling technology. The nanoparticles have an integrity of the protein primary structure. Furthermore, the structural changes between WPI and SPI were achieved by an interaction force with hydrogen bonding as the main effect, which significantly improved the anti-refolding property of protein, inhibited the acid-induce refolding, and formed a new high-strength hydrophilic structure. Under neutral conditions, the surface charged nature of the protein was maintained, resulting in an excellent water dispersion of the composite nanoparticles. Additionally, nutritional value and functional properties, such as EAI and FA of the proteins, were significantly enhanced during the pH-cycle treatment. Overall, this study can contribute to developing WPI-based nanoparticles with high nutritional value and functional properties. However, further studies are needed to evaluate the ability of the nanoparticles to improve bioavailability, control the essential oil release, and their applicability in the industry field.

Data availability statement

The raw data supporting the conclusions of this article will be made available by the authors, without undue reservation.

Author contributions

YD: conceptualization, methodology, investigation, and writing – original draft. YX: investigation and software. CS: investigation. SB: supervision. YL: project administration and funding acquisition. All authors contributed to the article and approved the submitted version.

Funding

This work was supported by the National Natural Science Foundation of China (31871821), the fund of Cultivation Project of Double First-Class Disciplines of Food Science and Engineering, and the Beijing Technology and Business University (BTBUKF202203).

Acknowledgments

We gratefully acknowledge the financial support from the National Natural Science Foundation of China (31871821), the fund of Cultivation Project of Double First-Class Disciplines of Food Science and Engineering, and the Beijing Technology and Business University (BTBUKF202203).

Conflict of interest

The authors declare that the research was conducted in the absence of any commercial or financial relationships that could be construed as a potential conflict of interest.

Publisher's note

Supplementary material

The Supplementary Material for this article can be found online at: https://www.frontiersin.org/articles/10.3389/fnut.2023.1135048/full#supplementary-material

References

1. Kianfar E. Protein nanoparticles in drug delivery: animal protein, plant proteins and protein cages, albumin nanoparticles. *J Nanobiotechnol.* (2021) 19:159. doi: 10.1186/s12951-021-00896-3

2. Yu X, Wu H, Hu H, Dong Z, Dang Y, Qi Q, et al. Zein nanoparticles as nontoxic delivery system for maytansine in the treatment of non-small cell lung Cancer. *Drug Delivery.* (2020) 27:100–9. doi: 10.1080/10717544.2019.1704942

3. Xu P, Qian Y, Wang R, Chen Z, Wang T. Entrapping curcumin in the hydrophobic reservoir of rice proteins toward stable antioxidant nanoparticles. *Food Chem.* (2022) 387:132906. doi: 10.1016/j.foodchem.2022.132906

4. Wang R, Wang T, Feng W, Wang Q, Wang T. Rice proteins and cod proteins forming shared microstructures with enhanced functional and nutritional properties. *Food Chem.* (2021) 354:129520. doi: 10.1016/j.foodchem.2021.129520

5. Liu D, Guo Y, Wu P, Wang Y, Golly M, Ma H. The necessity of walnut proteolysis based on evaluation after in vitro simulated digestion: ace inhibition and dpph radical-scavenging activities. *Food Chem.* (2020) 311:125960. doi: 10.1016/j.foodchem.2019.125960

6. Cai Y, Deng X, Liu T, Zhao M, Zhao Q, Chen S. Effect of xanthan gum on walnut protein/xanthan gum mixtures, interfacial adsorption, and emulsion properties. *Food Hydrocolloids.* (2018) 79:391–8. doi: 10.1016/j.foodhyd.2018.01.006

7. Sze-Tao KWC, Sathe SK. Walnuts (*Juglans Regia* L): proximate composition, protein solubility, protein amino acid composition and protein in vitro digestibility. *J Sci Food Agriculture.* (2000) 80:1393–401.

8. Liu D, Guo Y, Zhu J, Tian W, Chen M, Ma H. The necessity of enzymatically hydrolyzing walnut protein to exert antihypertensive activity based on in vitro simulated digestion and in vivo verification. *Food Funct.* (2021) 12:3647–56. doi: 10.1039/D1FO00427A

9. Mao X, Hua Y, Chen G. Amino acid composition, molecular weight distribution and gel electrophoresis of walnut (*Juglans Regia* L.) proteins and protein fractionations. *Int J Mol Sci.* (2014) 15:2003–14. doi: 10.3390/ijms15022003

10. Mao X, Hua Y. Composition, structure and functional properties of protein concentrates and isolates produced from walnut (*Juglans regia* L.). *Int J Mol Sci.* (2012) 13:1561–81. doi: 10.3390/ijms13021561

11. Tang C. Nanocomplexation of proteins with curcumin: from interaction to nanoencapsulation (a Review). *Food Hydrocolloids.* (2020) 109:106106. doi: 10.1016/j.foodhyd.2020.106106

12. Guan T, Zhang Z, Li X, Cui S, McClements D, Wu X, et al. Preparation, characteristics, and advantages of plant protein-based bioactive molecule delivery systems. *Foods.* (2022) 11:1562. doi: 10.3390/foods11111562

13. Wang T, Yang Y, Feng W, Wang R, Chen Z. Co-Folding of hydrophobic rice proteins and shellac in hydrophilic binary microstructures for cellular uptake of apigenin. *Food Chem.* (2020) 309:125695. doi: 10.1016/j.foodchem.2019.125695

14. Pan K, Zhong Q. Low energy, organic solvent-free co-assembly of zein and caseinate to prepare stable dispersions. *Food Hydrocolloids.* (2016) 52:600–6. doi: 10.1016/j.foodhyd.2015.08.014

15. Wang R, Xu P, Chen Z, Zhou X, Wang T. Complexation of rice proteins and whey protein isolates by structural interactions to prepare soluble protein composites. *LWT.* (2019) 101:207–13. doi: 10.1016/j.lwt.2018.11.006

16. Wang R, Li L, Feng W, Wang T. Fabrication of hydrophilic composites by bridging the secondary structures between rice proteins and pea proteins toward enhanced nutritional properties. *Food Funct.* (2020) 11:7446–55. doi: 10.1039/D0FO01182G

17. Wu C, Wang J, Na X, Wang Z, Xu X, Wang T. Inducing secondary structural interplays between scallop muscle proteins and soy proteins to form soluble composites. *Food Funct.* (2020) 11:3351–60. doi: 10.1039/C9FO03106E

18. Wang T, Xu P, Chen Z, Zhou X, Wang R. Alteration of the structure of rice proteins by their interaction with soy protein isolates to design novel protein composites. *Food Funct.* (2018) 9:4282–91. doi: 10.1039/C8FO00661J

19. He J, Wang R, Feng W, Chen Z, Wang T. Design of novel edible hydrocolloids by structural interplays between wheat gluten proteins and soy protein isolates. *Food Hydrocolloids.* (2020) 100:105395. doi: 10.1016/j.foodhyd.2019.105395

20. Zhu Z, Zhu W, Yi J, Liu N, Cao Y, Lu J, et al. Effects of sonication on the physicochemical and functional properties of walnut protein isolate. *Food Res Int.* (2018) 106:853–61. doi: 10.1016/j.foodres.2018.01.060

21. Yan C, Zhou Z. Solubility and emulsifying properties of phosphorylated walnut protein isolate extracted by sodium trimetaphosphate. *LWT.* (2021) 143:111117. doi: 10.1016/j.lwt.2021.111117

22. Jin F, Wang Y, Tang H, Regenstein J, Wang F. Limited hydrolysis of dehulled walnut (*Juglans regia* L.) proteins using trypsin: functional properties and structural characteristics. *LWT*. (2020) 133:110035. doi: 10.1016/j.lwt.2020.110035

23. Wang T, Chen X, Zhong Q, Chen Z, Wang R, Patel A. Facile and efficient construction of water-soluble biomaterials with tunable mesoscopic structures using all-natural edible proteins. *Adv Funct Mater.* (2019) 29:1901830. doi: 10.1002/adfm.201901830

24. Wang T, Wu J, Wang R, Zhong Q. Nanostructures self-assembled from food-grade molecules with ph-cycle as functional food ingredients. *Trends Food Sci Technol.* (2022) 120:36–47. doi: 10.1016/j.tifs.2022.01.010

25. Asadi M, Salami M, Hajikhani M, Emam-Djomeh Z, Aghakhani A, Ghasemi A. Electrospray production of curcumin-walnut protein nanoparticles. *Food Biophys.* (2021) 16:15–26. doi: 10.1007/s11483-020-09637-9

26. Ma X, Chen W, Yan T, Wang D, Hou F, Miao S, et al. Comparison of citrus pectin and apple pectin in conjugation with Soy Protein Isolate (SPI) under controlled dry-heating conditions. *Food Chem.* (2020) 309:125501. doi: 10.1016/j.foodchem.2019.125501

27. Laemmli U. Cleavage of structural proteins during the assembly of the head of bacteriophage T4. *Nature.* (1970) 227:680–5. doi: 10.1038/227680a0

28. Bradstreet R. Kjeldahl method for organic nitrogen. *Anal Chem.* (1954) 26:185–7. doi: 10.1021/ac60085a028

29. Shigemitsu H, Fujisaku T, Tanaka W, Kubota R, Minami S, Urayama K, et al. An adaptive supramolecular hydrogel comprising self-sorting double nanofibre networks. *Nat Nanotechnol.* (2018) 13:165–72. doi: 10.1038/s41565-017-0026-6

30. Wang T, Xu P, Chen Z, Wang R. Mechanism of structural interplay between rice proteins and soy protein isolates to design novel protein hydrocolloids. *Food Hydrocolloids.* (2018) 84:361–7. doi: 10.1016/j.foodhyd.2018.06.024

31. Zhao W, Xiang H, Liu Y, He S, Cui C, Gao J. Preparation of zein—soy protein isolate composites by Ph cycling and their nutritional and digestion properties. *LWT*. (2022) 159:113191. doi: 10.1016/j.lwt.2022.113191

32. Li K, Fu L, Zhao Y, Xue S, Wang P, Xu X, et al. Use of high-intensity ultrasound to improve emulsifying properties of chicken myofibrillar protein and enhance the rheological properties and stability of the emulsion. *Food Hydrocolloids.* (2020) 98:105275. doi: 10.1016/j.foodhyd.2019.105275

33. Zhu X, Zhan F, Zhao Y, Han Y, Chen X, Li B. Improved foaming properties and interfacial observation of sodium caseinate-based complexes: effect of carboxymethyl cellulose. *Food Hydrocolloids.* (2020) 105:105758. doi: 10.1016/j.foodhyd.2020.105758

34. Moghadam M, Salami M, Mohammadian M, Emam-Djomeh Z, Jahanbani R, Moosavi-Movahedi A. Physicochemical and bio-functional properties of walnut proteins as affected by trypsin-mediated hydrolysis. *Food Biosci.* (2020) 36:100611. doi: 10.1016/j.fbio.2020.100611

35. Cao Y, Mezzenga R. Food protein amyloid fibrils: origin, structure, formation, characterization, applications and health implications. *Adv Colloid Interface Sci.* (2019) 269:334–56. doi: 10.1016/j.cis.2019.05.002

36. Oboroceanu D, Wang L, Brodkorb A, Magner E, Auty M. Characterization of β-lactoglobulin fibrillar assembly using atomic force microscopy, polyacrylamide gel electrophoresis, and in situ fourier transform infrared spectroscopy. *J Agricultural Food Chem.* (2010) 58:3667–73. doi: 10.1021/jf9042908

37. Wang K, Luo S, Zhong X, Cai J, Jiang S, Zheng Z. Changes in chemical interactions and protein conformation during heat-induced wheat gluten gel formation. *Food Chem.* (2017) 214:393–9. doi: 10.1016/j.foodchem.2016.07.037

38. Eftink M, Ghiron C. Fluorescence quenching studies with proteins. *Anal Biochem.* (1981) 114:199–227.

39. Papadopoulou A, Green R, Frazier R. Interaction of flavonoids with bovine serum albumin: a fluorescence quenching study. *J Agricultural Food Chem.* (2005) 53:158–63. doi: 10.1021/jf048693g

40. Feitelson J. On the mechanism of fluorescence quenching. tyrosine and similar compounds. *J Phys Chem.* (1964) 68:391–7. doi: 10.1021/j100784a033

41. Yagai S. Supramolecularly engineered functional π-assemblies based on complementary hydrogen-bonding interactions. *Bull Chem Soc Japan.* (2015) 88:28–58. doi: 10.1246/bcsj.20140261

42. Gasymov O, Glasgow B. Ans fluorescence: potential to augment the identification of the external binding sites of proteins. *Biochim Biophys Acta (BBA)-Proteins Proteom.* (2007) 1774:403–11. doi: 10.1016/j.bbapap.2007.01.002

43. Semisotnov G, Rodionova N, Razgulyaev O, Uversky V, Gripas' A, Gilmanshin R. Study of the "Molten Globule" intermediate state in protein folding by a hydrophobic fluorescent probe. *Biopolymers: Orig Res Biomol.* (1991) 31:119–28. doi: 10.1002/bip.360310111

44. Nilsson L, Halle B. Molecular origin of time-dependent fluorescence shifts in proteins. *Proc Natl Acad Sci USA*. (2005) 102:13867–72. doi: 10.1073/pnas.0504181102

45. Ware W. Oxygen quenching of fluorescence in solution: an experimental study of the diffusion process. *J Phys Chem.* (1962) 66:455–8. doi: 10.1021/j100809a020

46. Artigues A, Iriarte A, Martinez-Carrion M. Acid-Induced reversible unfolding of mitochondrial aspartate aminotransferase. *J Biol Chem.* (1994) 269:21990–9. doi: 10.1016/0014-5793(94)00883-3

47. Kelly S, Price N. The use of circular dichroism in the investigation of protein structure and function. *Curr Protein Peptide Sci.* (2000) 1:349–84.

48. Kelly S, Price N. The application of circular dichroism to studies of protein folding and unfolding. *Biochim Biophys Acta-Protein Struct Mol Enzymol.* (1997) 1338:161–85. doi: 10.1016/s0167-4838(96)00190-2

49. Abedi E, Pourmohammadi K. Chemical modifications and their effects on gluten protein: an extensive review. *Food Chem.* (2021) 343:128398. doi: 10.1016/j.foodchem.2020.128398

50. Hu H, Wu J, Li-Chan E, Zhu L, Zhang F, Xu X, et al. Effects of ultrasound on structural and physical properties of Soy Protein Isolate (SPI) dispersions. *Food Hydrocolloids.* (2013) 30:647–55. doi: 10.1016/j.foodhyd.2012.08.001

51. Chandrapala J, Zisu B, Palmer M, Kentish S, Ashokkumar M. Effects of ultrasound on the thermal and structural characteristics of proteins in reconstituted whey protein concentrate. *Ultrasonics Sonochem.* (2011) 18:951–7. doi: 10.1016/j.ultsonch.2010.12.016

52. Friedman M. Food browning and its prevention: an overview. *J Agricultural Food Chem.* (1996) 44:631–53. doi: 10.1021/jf950394r

53. Zhang H, Zhao X, Chen X, Xu X. Thoroughly review the recent progresses in improving O/W interfacial properties of proteins through various strategies. *Front Nutrit.* (2022) 9:1043809. doi: 10.3389/fnut.2022.1043809

54. Khan S, Butt M, Sharif M, Sameen A, Mumtaz S, Sultan M. Functional properties of protein isolates extracted from stabilized rice bran by microwave, dry heat, and parboiling. *J Agricultural Food Chem.* (2011) 59:2416–20. doi: 10.1021/jf104177x

55. Li R, Cui Q, Wang G, Liu J, Chen S, Wang X, et al. Relationship between surface functional properties and flexibility of soy protein isolate-glucose conjugates. *Food Hydrocolloids.* (2019) 95:349–57. doi: 10.1021/acs.jafc.8b06713

56. Yang J, Roozalipour S, Berton-Carabin C, Nikiforidis C, van der Linden E, Sagis L. Air-Water interfacial and foaming properties of whey protein-sinapic acid mixtures. *Food Hydrocolloids.* (2021) 112:106467. doi: 10.1016/j.foodhyd.2020.106467

57. Zhu Y, Fu S, Wu C, Qi B, Teng F, Wang Z, et al. The investigation of protein flexibility of various soybean cultivars in relation to physicochemical and conformational properties. *Food Hydrocolloids.* (2020) 103:105709. doi: 10.1016/j.foodhyd.2020.105709

58. Hu A, Li L. Effects of ultrasound pretreatment on functional property, antioxidant activity, and digestibility of soy protein isolate nanofibrils. *Ultrason Sonochem.* (2022) 90:106193. doi: 10.1016/j.ultsonch.2022.106193

frontiers | Frontiers in Nutrition

TYPE Original Research
PUBLISHED 03 March 2023
DOI 10.3389/fnut.2023.1109109

OPEN ACCESS

EDITED BY
Ye Liu,
Beijing Technology and Business University, China

REVIEWED BY
Tao Yi,
Hong Kong Baptist University, Hong Kong SAR, China
Xuebo Song,
University of Florida, United States
Teodora Coldea,
University of Agricultural Sciences and Veterinary Medicine of Cluj-Napoca, Romania
Michael Rychlik,
Technical University of Munich, Germany

*CORRESPONDENCE
Yong-Quan Xu
✉ yqx33@126.com
Chun Zou
✉ zouchun@tricaas.com

SPECIALTY SECTION
This article was submitted to Food Chemistry, a section of the journal Frontiers in Nutrition

RECEIVED 27 November 2022
ACCEPTED 13 February 2023
PUBLISHED 03 March 2023

CITATION
Chen D-Q, Zou C, Huang Y-B, Zhu X, Contursi P, Yin J-F and Xu Y-Q (2023) Adding functional properties to beer with jasmine tea extract. *Front. Nutr.* 10:1109109. doi: 10.3389/fnut.2023.1109109

Adding functional properties to beer with jasmine tea extract

De-Quan Chen[1,2], Chun Zou[1]*, Yi-Bin Huang[1,3], Xuan Zhu[4], Patrizia Contursi[5], Jun-Feng Yin[1] and Yong-Quan Xu[1]*

[1]Tea Research Institute Chinese Academy of Agricultural Sciences, National Engineering Research Center for Tea Processing, Key Laboratory of Tea Biology and Resources Utilization, Hangzhou, China, [2]Graduate School of Chinese Academy of Agricultural Sciences, Beijing, China, [3]College of Tea Science, Guizhou University, Guiyang, China, [4]School of Food and Bioengineering, Zhejiang Gongshang University, Hangzhou, China, [5]Department of Biology, University of Naples Federico II, Naples, Italy

Hops provide the characteristic bitter taste and attractive aroma to beer; in this study, hops were replaced by jasmine tea extract (JTE) during late-hopping. The addition of JTE improved the beer foam stability 1.52-fold, and increased the polyphenol and organic acid contents. Linalool was the most important aroma compound in hopped (HOPB) and jasmine tea beer (JTB), but other flavor components were markedly different, including dimeric catechins, flavone/flavonol glycosides, and bitter acids and derivatives. Sensory evaluation indicated that addition of JTE increased the floral and fresh-scent aromas, reduced bitterness and improved the organoleptic quality of the beer. The antioxidant capacity of JTB was much higher than that of HOPB. The inhibition of amylase activity by JTB was 30.5% higher than that of HOPB. Functional properties to beer were added by substituting jasmine tea extract for hops during late hopping.

KEYWORDS

jasmine tea extract, hop, volatile components, brewing process, tea beer

1. Introduction

Beer is one of the most widely consumed alcoholic beverages worldwide; water, malt, hops, and yeast are the four main ingredients used in the production of beer (1). Beer production comprises several stages, namely, mashing, boiling, fermentation, maturation and solid liquid separations (wort separation, wort clarification, and rough beer clarification) (2). In recent years, consumer preference has increasingly emphasized the flavor and nutritional qualities of beer, which has increased interest and demand for craft beers (3). The main differences between craft and mass-produced beer are a more concentrated raw wort, the addition of a greater variety and quantity of hops, or the addition of other auxiliary flavor/nutritional ingredients, such as fruits, tea and natural plant extracts. The flavor of beer is influenced by the ingredients, particularly by auxiliary ingredients, the yeast, the brewing process and the fermentation conditions (4–7).

Hops (*Humulus lupulus* L.) are an essential ingredient in beer manufacturing, providing the characteristic bitter taste and attractive aroma of the final beverage (8). The main volatile component of hops is its essential oil, 80% of which is composed of myrcene, α-humulene, and β-caryophyllene (9), however, these volatiles contribute little to the beer aroma, because of their low water solubility and their tendency to oxidize and evaporate during heating and fermentation (10). Hops contain numerous bicyclic and tricyclic minor terpene hydrocarbons, the most important of which are the monoterpene alcohols, linalool and geraniol, as well as their isomers nerol and α-terpineol (11, 12), which impart floral, geranium-like, fresh, and citrus notes to beer (13), contribute to inhibiting beer spoilage bacteria, and improving taste and foam stability (11). There are three main ways of adding

hops (i.e., kettle, late, or dry hopping), late hopping and dry hopping have become key tools for brewers to impart beer with an intense hoppy aroma (12, 13). Late hopped beers have more pronounced hoppy and herbal aromas than early hopped ones, and late hopping increases the content of linalool and geraniol (14–16); delaying the addition of hops increases the geraniol content of the finished beer while avoiding conversion of geraniol to β-citronellol by the yeast (17).

Craft beer brewers often enrich the flavor of their beers by adding accessory ingredients, such as fruit, tea, and stevia to enhance consumer appeal. Addition of persimmon juice enhanced the antioxidant properties and consumer preference for the beer (18). The addition of white grape pomace increased the concentration of many volatile compounds in the beer, such as ethyl decanoate and ethyl dodecanoate, as well as increasing the phenolic content and antioxidant capacity (19). Addition of three types of tea (green, black, and oolong tea) increased the concentrations of tea volatile components, such as methyl salicylate, indole, and geraniol and its derivatives (20). Olive leaves have also been used in place of hops, to provide bitterness (21). Tea therefore has the potential to replace hops and provide the beer with a desirable, but unusual flavor.

The main objectives of this study were to enrich the flavor of beer by replacing hops with Jasmine tea extract (JTE) during late hopping and to investigate the effects of this on the quality of beer. This process modification has the potential to develop a novel application for tea and compensate for the scarcity of aromatic hops in China.

2. Materials and methods

2.1. Chemicals and standards

3-Nonanone (98%, Heowns, Tianjin, China), organic acid standards (oxalic acid, tartaric acid, malic acid, lactic acid, acetic acid, citric acid and succinic acid) were from Shanghai yuanye Bio-Technology Co., Ltd. Catechin standards (C, catechin; EC, epicatechin; GC, gallocatechin; CG, catechin gallate; EGC, epigallocatechin; CAF, caffeine; ECG, epicatechin gallate; EGCG, epigallocatechin gallate.) were from Sigma-Aldrich (Shanghai, China). *Saccharomyces cerevisiae* (lager yeast, s-33) was from Fermentis (Marquette-lez-Lille, France). 2,2-Diphenyl-1-picrylhydrazyl (DPPH), 2,2-azino-bis (3-ethylbenthiazoline-6-sulfonic acid (ABTS), and tripyridyl triazine (TPTZ) were from Sigma-Aldrich (Shanghai, China). All other chemicals and solvents used were of analytical grade, from local suppliers.

2.2. Brewing process

HOPB and JTB were produced in a 300 L pilot-scale brewing plant (Zhejiang Gongshang University). Pilsner-type (75 kg) and wheat (25 kg) malt was crushed using a two-roll mill and then transferred to a stainless-steel mashing vessel and mixed with water (45°C, 300 L). The process was initiated with the mash-in at 45°C (20 min), and the temperature was then gradually increased and maintained at 50°C (30 min), 65°C (40 min), 72°C (20 min) for maltose saccharification and 78°C (10 min) for enzyme inactivation, respectively. After complete mash conversion, the sweet wort was separated from the spent grains by lautering, then transferred to the kettle for boiling. The wort was boiled for 110 min with the addition of hops pellet (100 g, alfa-acid proportion: 13%) after 30 min and jasmine tea extract (360 g) after 100 min. The coarse break was separated through settling and the wort was cooled to about 40°C and transferred to the fermentation tank where the brewing yeast (150 g/L, activated for 30 min in sterile water) was added. After 7 days of primary fermentation at 20°C, the yeast slurry is drained from the bottom of the fermenter, followed by a temperature adjustment to 4°C and a closed venting valve for post-fermentation and maturation for 60 days, promptly sampling, storage (−80°C) and analysis. The control samples were brewed in the same way except for the addition of different ingredients at the late hopping stage. For the control sample, 150 g (alfa-acid proportion: 13%) of hops were added after 100 min of boiling.

2.3. Physicochemical analyses

Beer analysis was performed after maturation, following procedures in Chinese standard GB/T4928-2008. Color was determined by the spectrophotometric method (5.6.2) (Unico-2000, Unico, Shanghai, China); foam stability with a foam measuring cup (7.2); total acid content by titration with 0.1 mol/L NaOH; ethanol concentration was determined by quantitative distillation according to Dietz et al. (12). The alcohol concentration was determined with an SBA-40E biosensor (Shandong Biosensor Institute, China). Turbidity was determined using a HACH-TL2300 Turbidity Meter (HACH, Shanghai, China, detection limit = 0.001 NTU). A pH meter (FivrGo-2, Mettler Toledo, Shanghai, China) was used for pH measurements.

2.4. Characterization of tea catechins by HPLC

HPLC was used to analyze some targeted components, such as GA, GC, EGC, C, EC, EGCG, GCG, ECG, and caffeine, as described previously (22, 23). The HPLC (Agilent Technologies, Santa Clara, CA) was equipped with an Infinity binary pump, an autosampler, a column thermostat (set at 30°C), a diode array detector and an Agilent Zorbax SB-Aq C18 column (250 × 4.6 mm i.d., 5 μm). The mobile phases were 0.2% v/v aqueous formic acid (A) and methanol (B). The initial solvent was 5% B, which was ramped linearly to 20% B at 5 min, 25% B at 18 min, 42% B at 25 min, held for 7 min, then increased to 100% B at 40 min. The total run time was 40 min, the flow rate 1.0 ml/min, the injection volume 5 μl and the detection wavelength 278 nm.

TABLE 1 Basic physico-chemical parameters of the beer.

Items	HOPB	JTB
Color (EBC)	15.73 ± 1.17	15.12 ± 2.68
Turbidity (EBC)	2.89 ± 0.01	2.93 ± 0.03
Foam-stability (s)	347.67 ± 27.54[b]	528.00 ± 22.65[a]
Alcoholic content (%, v/v)	6.38 ± 0.21	6.63 ± 0.14
Diacetyl content (mg/L)	0.08 ± 0.01	0.06 ± 0.03
Total acids content (ml/100 ml)	3.35 ± 0.08[b]	3.75 ± 0.30[a]
Total polyphenols content (mg/L)	576.76 ± 4.86[b]	921.94 ± 1.55[a]
Total catechins content (mg/L)	8.71 ± 0.03[b]	302.39 ± 1.29[a]

Data are means (±SD) of three replicates.
EBC, European Brewery Convention units.
[a,b]Different letters in the same row indicate significant differences between mean values ($p < 0.05$).

TABLE 2 Content of catechin-like compounds in beer.

	JTB	HOPB
GA	25.24 ± 0.02[a]	N
GC	2.08 ± 0.04[a]	N
EGC	49.79 ± 3.10[a]	N
C	49.77 ± 3.19[a]	1.90 ± 0.03[b]
EGCG	62.02 ± 0.33[a]	N
EC	54.29 ± 0.43[a]	6.81 ± 0.05[b]
GCG	12.48 ± 2.07[a]	N
ECG	9.13 ± 1.39[a]	N
CG	37.58 ± 1.07[a]	N

Data are means (±SD) of three replicates.
N, not detected.
[a,b]Different letters in the same row indicate significant differences between mean values ($p < 0.05$).

2.5. Headspace-solid phase microextraction (HS-SPME) and GC-MS analysis of beer

The analysis was performed as described previously (24). Bottles of beer were maintained at 4°C to minimize loss of volatiles. Beer sample (4 ml), water (4 ml), internal standard (3-Nonanone, 20 μl, 9.8 mg/L) and NaCl (1 g) were added to 20 ml SPME headspace vials and sealed with a polytetrafluoroethylene (PTFE)-silicon septum. The septum covering the vial headspace was pierced with the needle containing the SPME fiber and retracted, and the fiber was exposed to the headspace for 30 min at 50°C, then inserted directly into the GC-MS injection port. The carrier gas was helium at a flow rate of 1 ml/min. Samples were analyzed on a DB-5MS UI column (30 m by 0.250-mm inside diameter by 0.25-μm film thickness, Agilent). The oven temperature was programmed as follows: initial temperature 35°C, held for 5 min, increased at 4°C/min to 130°C, held for 3 min, then at 5°C/min to 230°C, held for 5 min. Electron impact (EI) ionization was used at 70 eV, scanning from *m/z* 10 to 250. Background subtraction was performed on the raw GC-MS data using data processing software. The National Institute of Standards and Technology (NIST 14) database was used for qualitative analysis of the MS peaks corresponding to the chromatographic peak signals at different retention times (>70%). The peaks were quantified by comparison with the internal standard (3-Nonanone) to calculate the relative content of each substance and the data were imported into Simca-P software (Version 14.1, MKS Umetrics AB, Umeå, Sweden). The outputs were subjected to Orthogonal partial least squares-discriminant analysis (OPLS-DA). The variable importance in projection (VIP) value was used to evaluate data generated by OPLS-DA; only data with VIP values >1 were selected for further analysis.

2.6. Non-targeted metabolomics analysis

Non-targeted metabolomics analysis was carried out using UPLC-HRMS (Q-Exactive system, Thermo Fisher Scientific, Rockford, IL), as described previously (25) with some modifications. The column was an Acquity UPLC BEH C18 (100 nm × 2.1 mm; 1.7 μm, Waters, Manchester, UK). The mobile phases were aqueous, 0.1% v/v formic acid (A) and acetonitrile (B), and the linear elution gradient program was 0–1.0 min, 5% B; 2.0 min, 10% B; 6.0 min, 35% B; 8.5–9.5 min, 100% B; and 10.0–12.0 min, 5% B. The total analysis time was 12 min and the flow rate was 0.3 ml/min. The column and autosampler were set at 40 and 10°C, respectively.

Mass spectrometric analysis was performed with the Q-Exactive Orbitrap mass analyzer in negative ionization mode at a spray voltage of 3.0 kV. The capillary temperature and auxiliary gas heater temperature were both 300°C. The flow rates of sheath gas and auxiliary gas were set to 45 and 10 arbitrary units, respectively. The full scan MS/data-dependent MS/MS (ddMS2) mode was used, in which the resolution was 70,000 and 35,000 for full MS and ddMS2, respectively. The mass scan range was from *m/z* 66.7 to 1000.

All the samples were filtered through a 0.45 μm Millipore filter. The raw data acquired were processed on Compound Discoverer software (Version 3.0, Thermo Fisher) to obtain all the ion fragment information through peak picking and alignment. This information was used for partial least-squares discriminant analysis (PLS-DA) to screen for differential metabolites with VIP >1.2 and $p < 0.05$, which was performed on Simca-P v14.1. Thereafter, the Human Metabolome Database (http://www.hmdb.ca/), our laboratory's standards library and previous metabolomics studies (26, 27) were used for identification of the differential metabolites.

2.7. Total polyphenol content

The total phenolic content of beer was determined spectrophotometrically with Folin–Ciocalteu reagent (28). A calibration curve was plotted using gallic acid as standard. The beer samples were diluted with deionized water to adjust the concentration of phenolic compounds to the linear calibration

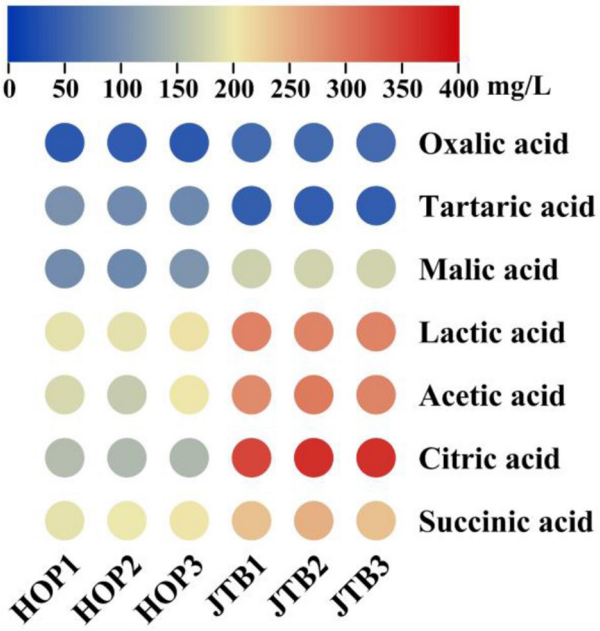

FIGURE 1
Heat map of seven organic acids.

range of gallic acid. Results were expressed as mg of gallic acid equivalent (GAE) per liter.

2.8. Antioxidant capacity

2.8.1. DPPH radical scavenging capacity

The DPPH radical scavenging capacity was determined as described previously (29, 30). The samples were appropriately diluted with ethanol, then sample (2 ml) was mixed with DPPH (2 ml, 0.2 mmol/L), then left to stand for 30 min at room temperature in the dark. The absorbance was measured with a spectrophotometer at 517 nm using quartz cuvettes (A_S). Ethanol was used as a blank control (A_0). DPPH radical scavenging capacity was calculated as:

$$\text{DPPH\%} = \frac{A_s - A_0}{A_s} \times 100$$

where A_0 is the absorbance of blank and A_S is the absorbance of the sample.

2.8.2. ABTS radical scavenging capacity

The ABTS radical scavenging capacity (ABTS%) was determined as described previously (31), with some modifications. The ABTS stock solution was made by mixing equal amounts of 14 mmol/L ABTS solution and 4.9 mmol/L potassium persulfate solution and stored for 14–16 h in the dark at room temperature to generate ABTS radicals, then diluted with methanol to achieve an absorbance of 0.75 ± 0.05 at 734 nm. Diluted ABTS radical solution (3.9 ml) was mixed with 0.1 ml of sample solution and left at room temperature in darkness for 6 min before reading its absorbance at 734 nm. Deionized water was used as the blank (A_0). ABTS% was calculated using the equation:

$$\text{ABTS\%} = \frac{A_S - A_0}{A_S} \times 100$$

where A_0 is the absorbance of the blank and A_S is the absorbance of the sample.

2.8.3. Ferric reducing antioxidant power

Ferric reducing antioxidant power (FRAP) assays were performed as described previously (32). The FRAP solution was prepared by mixing acetate buffer (300 mmol/L, pH 3.6), tripyridyltriazine (TPTZ 10 mmol/L) and $FeCl_3$ solution (20 mmol/L) in a ratio of 10:1:1 (v/v/v). An aliquot (100 μl) of sample solution was mixed with FRAP solution (3 ml) and incubated at 37°C for 10 min, then the absorbance at 593 nm was measured. Quantitation was achieved with reference to a standard curve of $FeSO_4$ (0.2–0.8 mmol/L) and results are expressed as millimoles (mmol) of Trolox per liter of beer.

2.9. α-Amylase inhibition assay

α-Amylase inhibition was determined as described previously (33), with minor modifications. Test samples (200 μl) were added to sodium phosphate buffer (300 μl, 0.02 M pH 6.9) containing 30 unit/ml porcine pancreatic α-amylase and preincubated at 37°C for 10 min. After preincubation, starch solution (300 μl, 0.5%) was added, then the reaction mixtures incubated at 37°C for 15 min. The reaction was stopped by adding 3,5-dinitrosalicylic acid reagent (600 μl), heating in a boiling water bath for 10 min, then cooling. After adding 900 μl of distilled water, the absorbance was measured at 540 nm. The α-amylase inhibitory activity was calculated as follows:

$$\text{Inhibitory activity (\%)} = [1 - (\text{OD}_{\text{test sample}} - \text{OD}_{\text{blank}}) / \text{OD}_{\text{control}}] \times 100$$

2.10. α-Glucosidase inhibition assay

The α-glucosidase inhibition was determined as described previously (34) with minor modifications. α-Glucosidase (100 μl, 70 U/ml, in 0.5 ml sodium acetate buffer, pH 5.0) was premixed with beer sample (0.5 ml) and incubated at 37°C for 15 min. *p*-Nitrophenyl-α-D-glucopyranoside (0.5 ml, 2.5 mmol/L) was added, then the mixture was incubated at 37°C for 15 min and stopped by adding sodium carbonate solution (1 ml 0.2 mol/L). The α-glucosidase activity was determined by measuring the release of *p*-nitrophenol at 405 nm. α-Glucosidase inhibition was calculated as follows:

$$\text{Inhibitory activity (\%)} = [1 - (\text{OD}_{\text{test sample}} - \text{OD}_{\text{blank}}) / \text{OD}_{\text{control}}] \times 100$$

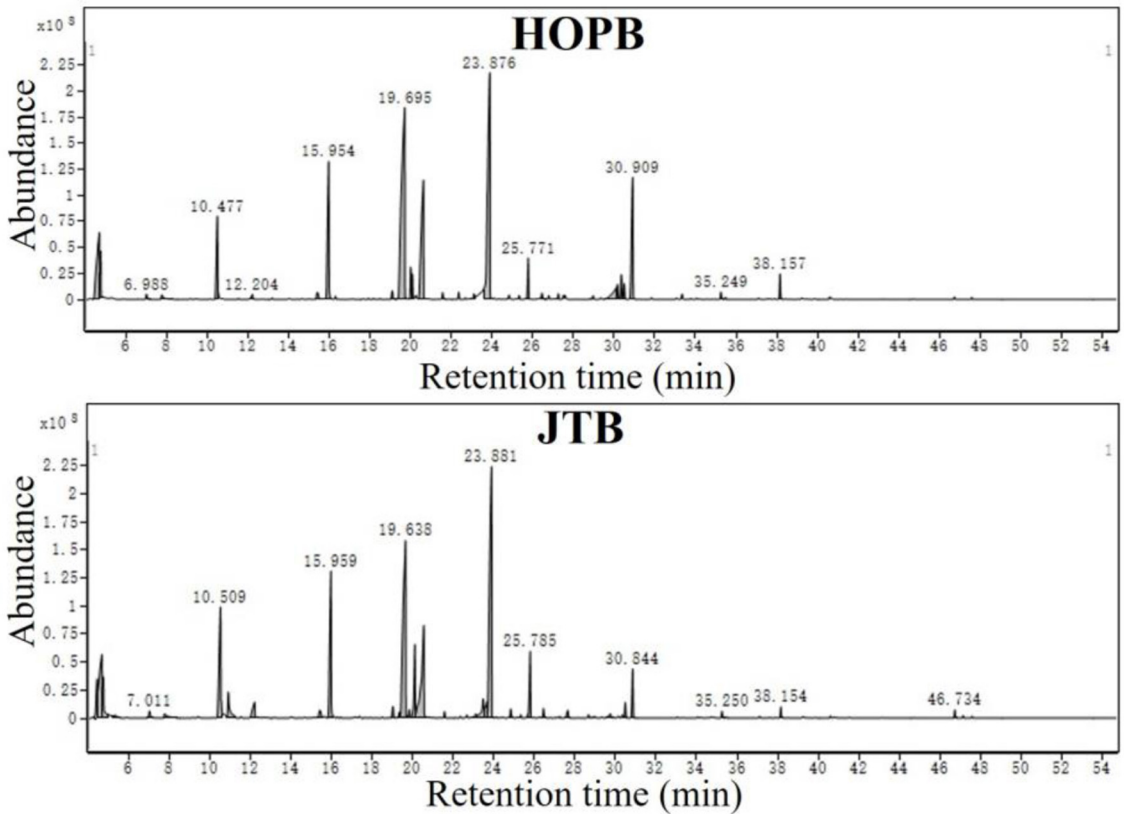

FIGURE 2
Total ion current (TIC) chromatograms of beer samples.

2.11. Sensory analysis

The beers were evaluated by 29 untrained tasters from the Tea Research Institute, Chinese Academy of Agricultural Sciences, aged between 20 and 59 years. For each taster, a 40 ml sample of the beer was served in a disposable, clear, acrylic glass. The tasters evaluated the aroma, taste, foam, appearance and overall score using a nine point hedonic scale form, where 1 = dislike strongly; 5 = neither like, nor dislike; and 9 = like strongly (35). A second four level scale (not sensed, faintly sensed, mildly sensed, and strongly sensed) was used to grade bitter and astringent tastes, and malty aroma, fruital aroma, floral aroma, and fresh-scent aroma. Training of tasters in grade evaluation prior to the experiment. All the participants (healthy and non-smokers from TRICAAS) were conducted considering the principle outlined in the Declaration of Helsinki, and informed written consent was obtained.

2.12. Statistical data analysis

The data are presented as the mean ± standard error of the mean. All experiments were carried out in triplicate. The results were analyzed with SPSS 18.0, using one-way analysis of variance to determine differences between sample groups, with $p < 0.05$ considered statistically significant.

3. Results and discussion

3.1. Physicochemical properties of beers

The effects of JTE on the physicochemical properties of the beers were compared (Table 1). JTE addition did not affect ($p > 0.05$) the color, turbidity and diacetyl content, however, it affected ($p < 0.05$) the contents of alcohol, total acids, total polyphenols, total catechins, and the foam-stability. The foam stability, alcohol concentration, total polyphenol concentration, and total catechin concentration of JTB were 528.0 ± 22.7 s, 6.6 ± 0.14% (v/v), 921.95 ± 1.6 mg/L, and 302.4 ± 1.3 mg/L, respectively, 1.52-, 1.04-, 1.6-, and 34.72-fold those of HOPB, respectively.

The catechin concentration of JTB was markedly higher than that of HOPB (Table 2), because of the high catechin concentration of JTE (17), and since catechins are the major JTE polyphenols, the polyphenol content of JTB was also significantly higher than that of HOPB. The foam stability of JTB was significantly higher, which may be related to its greater polyphenol content (18) and the foam-stabilizing effect of some polyphenols (36). Studies have shown that the type and content of polyphenols and catechins in beer are important factors affecting the antioxidant capacity and flavor stability of beer (37). In this study, it was found that beers with added tea extracts had stronger antioxidant capacity. Taken together, these results suggest that there is an association between JTE addition and beer quality.

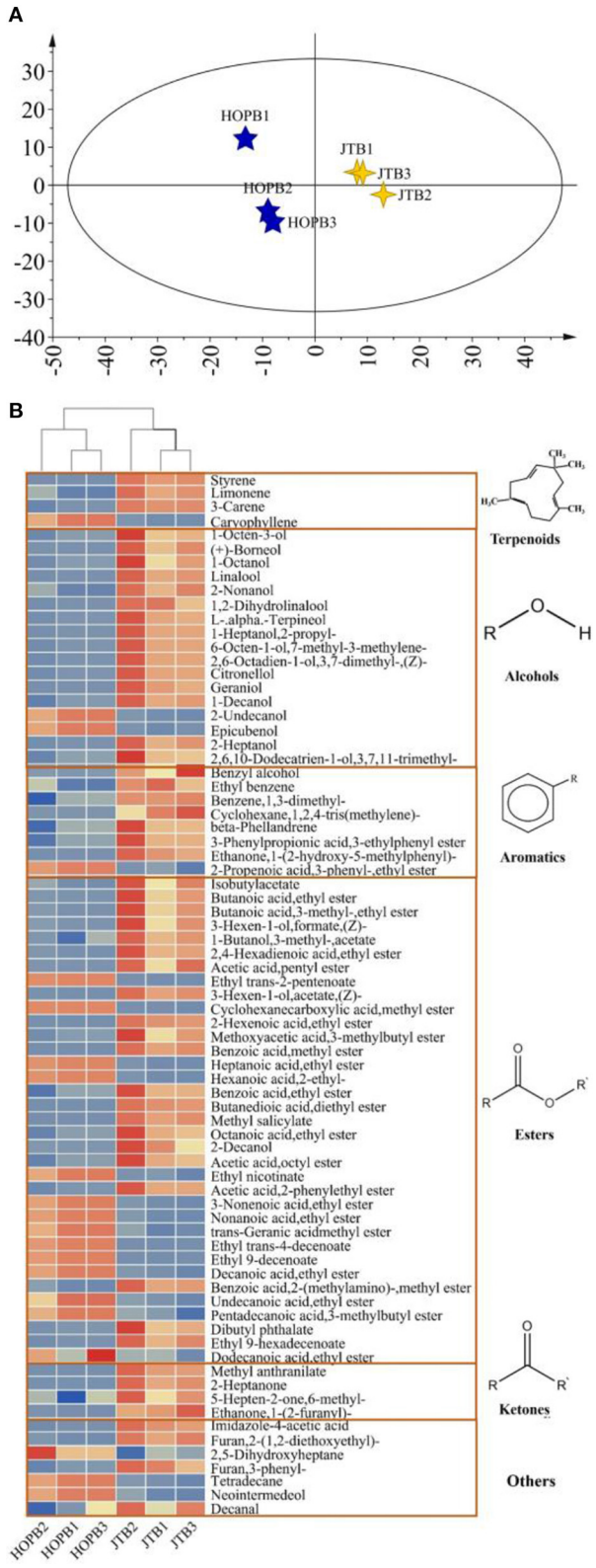

FIGURE 3
Differential volatiles analysis in beer samples. **(A)** Score plot from OPLS-DA model; **(B)** Heat map of the relative content of key difference volatile components.

3.2. Organic acid content and composition

Organic acids are important indicators of product quality and contribute to the organoleptic properties of beer, as well as being indicators of fermentation performance, so the organic acids (oxalic, tartaric, malic, lactic, acetic, citric, and succinic acid) in JTB and HOPB were determined (Figure 1). The total organic acid content of JTB (1445.38 mg/L), was 1.52-fold that of HOPB ($p < 0.05$). The main organic acids in both beers were lactic, acetic and citric acid and they differed significantly. The lactic, acetic and citric acid contents of JTB were 288.88 ± 1.02, 288.75 ± 7.34, and 356.44 ± 11.03 mg/L, respectively, 1.48-, 1.58- and 2.43-fold those of HOPB, respectively. The malic and succinic acid contents of JTB were 173.03 and 240.56 mg/L, 1.78- and 1.21-fold than those of HOPB, respectively. The tartaric acid content of JTB was significantly lower (0.44-fold) that of HOPB. The oxalic acid contents were similar, mainly because oxalic acid is primarily derived from the wort (38).

3.3. Analysis of volatile components

3.3.1. Identification of volatile compounds

The volatile compounds in the beers were determined by HS-SPME-GC-MS; the GC-MS total ion current (TIC) chromatograms are shown in Figure 2. A total of 519 compounds was putatively identified by comparison with the NIST 14 database, of which 231 compounds had a NIST 14 Best Match score >70. The main volatiles found were 2-methyl-1-butanol, 3-methyl-1-butanol, 3-methyl butanol acetate, hexanoic acid ethyl ester, phenylethyl alcohol, octanoic acid ethyl ester, 2-phenylethyl acetic acid ester, decanoic acid ethyl ester, and dodecanoic acid ethyl ester. These substances are mainly produced by the fermenting yeast (39).

3.3.2. Differential analysis of volatile compounds

OPLS-DA was used to compare the volatile profiles of the beers (Figure 3). The OPLS-DA score plot (Figure 3A) showed a clear difference between JTB and HOPB. To determine the most important differential volatile compounds between the beers, their VIP values were determined; with limits of VIP >1 and $p < 0.05$, 75 key volatile compounds were screened out. There were 17 alcohols, 36 esters, three ketones, four terpenes, eight aromatics and seven other compounds. Volatile esters were found to be the main differential components distinguishing the two beers. Esters are formed by a condensation reaction between alcohols and carboxylic acids, impart a fruity flavor to the beer and can strongly influence its overall flavor and style (40). A heat-map of the 75 key volatiles was plotted to visualize the differences between the beers (Figure 3B; red: content > mean, blue: content < mean) and a hierarchical cluster analysis (HCA) was performed to analyze clustering in the flavor profiles. As can be seen from the Figure 3B, the content of most volatiles in JTB is higher than that in HOPB. Cluster analysis enables a good classification of the same type of beer into one category.

TABLE 3 Main odor-active compounds (ROVA≥1) in HOPB and JTB samples.

ON	Compound	CAS	Threshold (μg/L)	HOPB (μg/L)	JTB (μg/L)	ROAV-HOPB	ROAV-JTB
1	Linalool	78-70-6	6	494.07	2211.11	82.35	368.52
2	Methyl anthranilate	134-20-3	3	0.78	221.54	<1	73.85
3	1-Butanol, 3-methyl-, acetate	123-92-2	210	3145.33	9608.58	14.98	45.76
4	1-Decanol	112-30-1	5	108.02	223.85	21.6	44.77
5	Hexanoic acid ethyl ester	51-79-6	230	7403.34	10029.19	32.19	43.61
6	Decanal	112-31-2	5	74.99	213.57	15	42.71
7	Acetic acid, 2-phenylethyl ester	103-45-7	210	3373.96	7265.75	16.07	34.6
8	Citronellol	68916-43-8	8	96.42	231.92	12.05	28.99
9	Octanoic acid, ethyl ester	106-32-1	900	19010.93	25919.57	21.12	28.8
10	2-Nonanol	821-55-6	3	50.08	64.26	16.69	21.42
11	Methyl salicylate	119-36-8	40	5.18	846.46	<1	21.16
12	2-Nonanone	821-55-6	32	615.39	626.93	19.23	19.59
13	2-Heptanol	100-41-4	3	9.41	37.24	3.14	12.41
14	1-Octen-3-ol	542-30-3	6.12	31.64	60.58	5.17	9.9
15	Benzoic acid, ethyl ester	93-89-0	20	125.67	184.75	6.28	9.24
16	Benzoic acid, methyl ester	93-58-3	73	27.55	622	<1	8.52
17	Acetic acid, octyl ester	112-14-1	800	3757	5170.33	4.7	6.46
18	Butanedioic acid, diethyl ester	27829-71-6	790	139.14	3318.44	<1	4.2
19	Geraniol	106-24-1	40	27.34	132.24	<1	3.31
20	Ethyl 9-decenoate	67233-91-4	100	7622.85	290.55	76.23	2.91
21	2,6-Octadien-1-ol, 3,7-dimethyl-, (Z)-	103-36-6	80	96.03	231.92	1.2	2.9
22	Butanoic acid, 2-methyl-, ethyl ester	7452-79-1	18	28.12	47.26	1.56	2.63
23	2-Heptanone	151301-57-4	140	11.21	363.76	<1	2.6
24	Ethyl trans-4-decenoate	76649-16-6	112.29	7630.66	290.91	67.95	2.59
25	3-Hexen-1-ol, acetate, (Z)-	3681-71-8	31	8.5	74.85	<1	2.41
26	Decanoic acid ethyl ester	110-38-3	1500	7622.91	2685.09	5.08	1.79
27	Butanoic acid ethyl ester	105-54-4	400	271.51	534.78	<1	1.34
28	2-Ethylcaproic acid	149-57-5	230	1092.49	290.12	4.75	1.26
29	Dodecanoic acid, ethyl ester	106-33-2	400	798.82	451.17	2	1.13
30	Heptanoic acid, ethyl ester	106-30-9	400	1092.43	289.98	2.73	<1

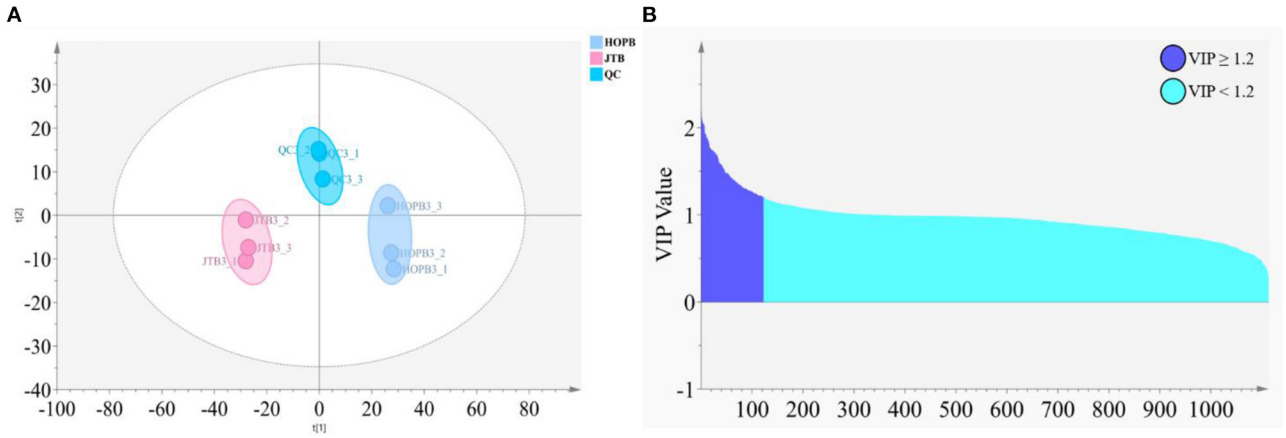

FIGURE 4
Analysis of differential metabolites in different beers. **(A)** PCA score plot; **(B)** PLS-DA S-plot of HOPB vs. JTB (purple: VIP ≥ 1.2, blue: VIP < 1.2).

3.3.3. Analysis of major odor-active compounds

The relative odor activity value (ROAV) (41) was used to identify the contributions made by the 75 key volatiles to the overall flavor of the beers, finding 30 substances with ROAV ≥1 (Table 3), of which 22 were found in HOPB and 29 in JTB. The major contributors to the overall flavor of HOPB were linalool, ethyl 9-decenoate, 1-decanol, hexanoic acid ethyl ester and octanoic acid ethyl ester (ROAV 82.35, 76.23, 67.95, 32.19, and 21.12, respectively). The major contributors to the overall flavor of JTB were linalool, methyl anthranilate, 3-methyl-1-butyl acetate, 1-decanol, and hexanoic acid ethyl ester (ROAV 368.52, 73.85, 45.76, 44.77, and 43.61, respectively). Linalool, 1-decanol, and hexanoic acid ethyl ester were all relatively high in JTB and HOPB and contributed strongly to their aromas.

Methyl anthranilate and ethyl 9-decenoate were the components with the second highest ROAV values in JTB and HOPB, respectively, and both these compounds differed markedly between the two beers. This appears to be related to the different ingredients; methyl anthranilate is a key aroma component of jasmine tea (42, 43), and ethyl 9-decenoate is a key aroma component of hops (44). Linalool is the main contributor to the overall flavor of both beers (largest ROAV) and is a key flavor component of late hopped beers and teas; it provides a floral flavor to beer (45). Hexanoic acid ethyl ester and 1-decanol are volatile compounds produced during fermentation, which can provide floral and fruity aromas, respectively (20, 46).

3.4. Metabolomic analysis of non-volatile beer components by LC-MS

After LC-MS data preprocessing, a total of 1,113 compound ion features were obtained from univariate and multivariate analysis. The QC samples were closely grouped in the PCA scores plot, indicating that the metabolomic analysis was reliable (Figure 4A). The JTB and HOPB samples were both closely grouped, but the two beer type groups were well separated, i.e., LC-MS analysis could clearly distinguish the two beer types. The criterion of PLS-DA VIP value ≥1.2 (Figure 4B) was used to screen for compounds that significantly differed between the two beers, and identified 123 differential compounds (Figure 4B, purple).

The 123 compounds were initially identified on the basis of their exact molecular masses and fragmentation spectra. Thirty-nine differential compounds were identified by comparing with the HMDB database (http://www.hmdb.ca/), laboratory standard libraries and previous reports (Table 4), namely, six bitter acids and derivatives, three amino acids, five phenolic acids, five organic acids, seven dimeric catechins, nine flavone/flavonol glycosides, and four others. Overall, JTE addition resulted in significant changes in metabolic profile.

A heatmap was plotted to visualize the differential metabolites resulting from JTE addition (Figure 5). The content of phenolic acids, amino acids, dimeric catechins and flavone/flavonol glycosides in JTB was significantly higher than that in HOPB, whereas bitter acid and some organic acids were less abundant in JTB. These differences are consistent with the substitution of late hopping with the addition of JTE, as amino acids, dimeric catechins, flavone/flavonol glycosides and phenolic acids are abundant in tea, whereas bitter acids are only found in hops (47–50). Dimeric catechins, amino acids and flavone/flavonol glycosides from the JTE would give the beer a tea-like flavor, especially the theanine, which has an umami taste (51). The high content of iso-alpha-acids is the main reason for the bitterness of beer (52), which is consistent with the sensory evaluation results (see below). HOPB had a higher bitterness intensity.

3.5. Sensory evaluation

Taste, flavor and other sensory attributes are the main determinants of beer quality (53). The appearance, foam, aroma, taste, and overall acceptability of the two beers were compared by sensory evaluation (Figure 6). There were differences in flavor intensity between the beers, with HOPB having a higher bitterness intensity and JTB having a higher floral and light fresh-scent

TABLE 4 Forty tentatively identified metabolites between two groups of beer sample (in negative mode).

	Compound	Rt (min)	*m/z* [M−H]$^-$	Fragments *m/z*	Molecular formula
1	Gluconic acid	0.87	195.05003	129.018, 75.008, 99.008	$C_6H_{12}O_7$
2	Ribonic acid	0.88	165.0396	75.008, 129.018, 147.029	$C_5H_{10}O_6$
3	Maltotetraose	0.9	665.2151	161.054, 179.056, 101.023	$C_{24}H_{42}O_{21}$
4	Theanine	1.21	173.09214	85.028, 129.018	$C_7H_{14}N_2O_3$
5	Citramalic acid	1.56	147.02878	87.008, 85.028, 129.018	$C_5H_6K_2O_5$
6	Inosine	1.67	267.07369	135.03	$C_{10}H_{12}N_4O_5$
7	Glucogallin	1.85	331.06715	169.014, 211.025, 128.0340	$C_{13}H_{16}O_{10}$
8	Gallic acid	2.03	169.01328	125.096, 126.100	$C_7H_6O_5$
9	Xanthosine	2.03	283.06854	151.025	$C_{10}H_{12}N_4O_6$
10	(+)-Gallocatechin	3.7	305.06667	125.023, 167.035, 175.035	$C_{15}H_{14}O_7$
11	Chlorogenic acid	4.38	353.08804	191.056, 192.059, 161.024	$C_{16}H_{18}O_9$
12	5′-Methylthioadenosine	4.53	296.08232	134.046	$C_{11}H_{15}N_5O_3S$
13	EGC	4.932	305.06668	125.023, 179.034, 167.035	$C_{15}H_{14}O_7$
14	2-Isopropylmalic acid	5	175.06039	115.039, 113.060, 85.065	$C_7H_{12}O_5$
15	Procyanidin B1	5.03	577.13589	125.032, 289.072, 407.079, 161.024	$C_{30}H_{26}O_{12}$
16	C	5.2	289.07184	245.082, 109.029.125.023	$C_{\{1\}\{5\}}H_{\{1\}\{4\}}O_{\{6\}}$
17	Neochlorogenic acid	5.31	353.08799	191.056, 179.034, 135.044	$C_{16}H_{18}O_9$
18	Procyanidin B2	5.41	577.13589	125.032, 289.072, 407.079, 161.024	$C_{30}H_{26}O_{12}$
19	caffenic acid	5.61	179.03417	135.044, 179.034	$C_9H_8O_4$
20	EC	5.77	289.07183	245.082, 109.029.203.071	$C_{15}H_{14}O_6$
21	Epigallocatechin gallate	5.83	457.07799	169.013, 125.023, 305.067	$C_{22}H_{18}O_{11}$
22	3-O-p-Coumaroylquinic acid	5.877	337.09307	173.045	$C_{16}H_{18}O_8$
23	GCG	6.01	457.07799	169.013, 125.023, 305.067	$C_{22}H_{18}O_{11}$
24	Apigenin 6-C-glucoside 8-C-arabinoside	6.03	563.14115	353.068, 383.078, 443.089, 473.110	$C_{26}H_{28}O_{14}$
25	N-Acetyl-L-leucine	6.26	172.0971	130.088	$C_8H_{15}NO_3$
26	4-Coumaric acid	6.47	163.03927	119.0049	$C_9H_8O_3$
27	Rutin	6.47	609.14655	300.028, 301.033, 302.039	$C_{27}H_{30}O_{16}$
28	Isoquercitrin	6.63	463.06504	169.013, 125.023, 300.028	$C_{21}H_{20}O_{12}$
29	ECG	6.65	441.08292	169.013, 289.092.125.023	$C_{22}H_{18}O_{10}$
30	N-Acetyl-DL-tryptophan	6.79	245.09317	230.082, 74.024, 116.034	$C_{13}H_{14}N_2O_3$
31	Kaempferol-3-O-D-galactoside	7.09	447.09369	284.033, 285.044, 488.097	$C_{21}H_{20}O_{11}$
32	Kaempferol	8.7	285.04057	285.041	$C_{15}H_{10}O_6$
33	Isoxanthohumol	8.95	353.1467	119.0493, 233.817, 59.0127	$C_{21}H_{22}O_5$
34	Cohumulone	9.9	347.1863	235.134	$C_{20}H_{28}O_5$
35	ad-humulone	10.131	361.20211	235.134, 36.137, 125.060	$C_{21}H_{30}O_5$
36	iso-Cohumulone	10.19	347.18629	181.050, 251.129, 233.118	$C_{20}H_{28}O_5$
37	iso-Cohumulone	10.394	347.18631	251.129, 181.050, 233.118	$C_{20}H_{28}O_5$
38	iso-n/ad-humulone	10.466	361.20209	195.066, 265.145, 247.134	$C_{21}H_{30}O_5$
39	Cohumulone	10.53	347.1863	278.116, 181.050, 251.129	$C_{20}H_{28}O_5$
40	N-humulone	10.69	361.20214	292.133	$C_{21}H_{30}O_5$

intensity (Figure 6A); the aroma score for JTB was 8.8, 31.0% higher than that of HOPB. The aroma differences are consistent with the relative volatile profiles of the beers (section 3.2), i.e., JTB contained higher concentrations of linalool, α-terpineol and citronellol. The score for taste of JTB was 7.8, 32.5% higher than that of HOPB, whereas HOPB scored higher for bitterness. JTB had a richer, whiter and finer foam, with a score of 7.7, compared with 7.0 for HOPB. However, JTB scored lower for appearance than HOPB, because JTB was a little more turbid than HOPB. Overall, JTB had a higher organoleptic rating than HOPB. The taste of JTB was mellower, softer and with a pleasing tea flavor (Figure 6B). JTB had a higher aroma score than HOPB ($p < 0.05$), apparently because of the abundant floral and fresh fragrances released from JTE (54, 55). HOPB had a lower taste score and higher bitterness score than JTB, probably resulting from the late hopping of HOPB; late hopping enhances the bitterness of beer (56). The study of Oladokun et al. (57) showed a significant effect of polyphenol content on the perceived intensity and characteristics of bitterness, with higher polyphenol content resulting in stronger bitterness and poorer bitterness characteristics expression in beer. It is noteworthy that although the beer with tea extract added in this study had higher polyphenol content, the bitterness intensity of JTB did not become stronger.

3.6. Antioxidant capacity

The antioxidant capacity influences the functional properties and the oxidation resistance of the beer during storage (30). The DPPH and ABTS+ radical scavenging capacities, and ferric reducing antioxidant power (FRAP) were determined to compare the antioxidant capacity of the beers (Figure 7). The DPPH, ABTS+, and FRAP capacities of JTB were 80.9, 42.3, and 50.3 mg/L, respectively, 52.6, 28.8, and 47.7% higher ($p < 0.05$) than those of HOPB, respectively.

The higher antioxidant capacities of JTB are consistent with its 1.6-fold higher phenolic content than HOPB; polyphenols, flavonoids, and flavonols account for the antioxidant capacity of beer (58, 59). Similarly, addition of fresh fruits during beer fermentation significantly enriched the content of phenolic compounds and increased the antioxidant capacity of the beer (60). Increased antioxidant capacity improves the storage stability of beer (36).

3.7. α-Amylase and α-glucosidase inhibition

α-Glucosidase and α-amylase are the key enzymes in the digestive system that hydrolyze dietary carbohydrates. Inhibition the two amylase can reduce and control postprandial blood glucose spikes, delaying hydrolysis of carbohydrates and suppressing postprandial hyperglycemia in prediabetes, diabetes, and obesity patients (61). The inhibitory effect on these digestive enzymes of the beers was determined (Figure 8); both beers inhibited α-amylase activity by 42.5 ± 1.5% (HOPB) and 72.1 ± 1.0% (JTB). α-Amylase inhibition by JTB was 30.5% higher than that of HOPB, probably because of its higher phenolic content; tea catechins strongly inhibit

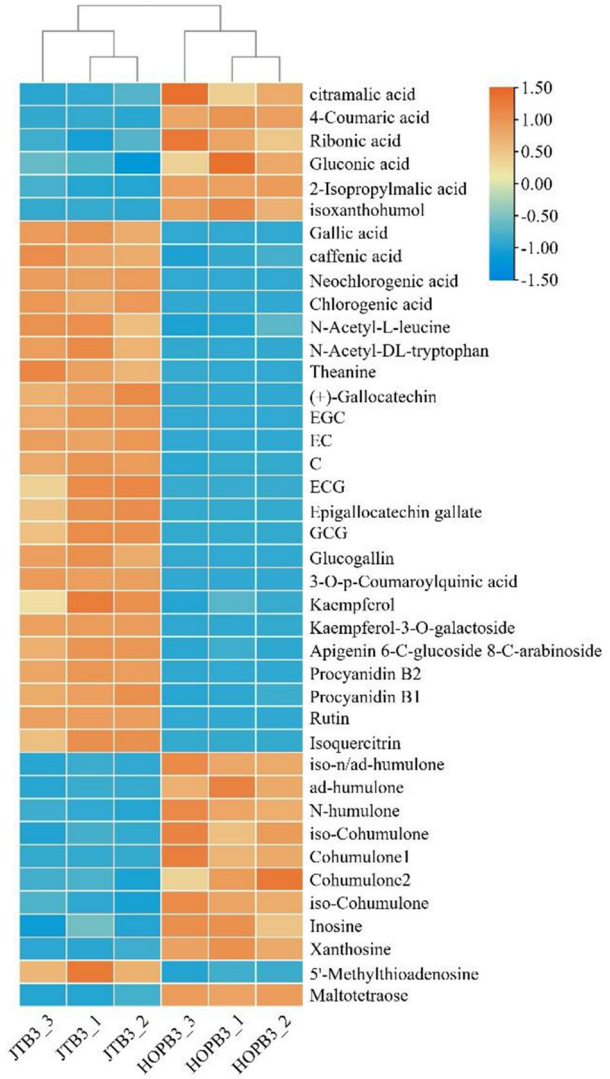

FIGURE 5
Heatmap analysis of critical metabolites in two beer samples. A color-coded scale grading from blue to orange corresponds to the content of critical metabolite shifting from low to high.

α-amylase activity (62, 63) and gallocatechin gallate is the strongest inhibitor among the catechins (61). HOPB inhibited α-glucosidase by 50.3%, whereas JTB had no significant effect. The characteristic compounds in hops inhibit both α-amylase (64) and α-glucosidase activity (65–67), which is consistent with the inhibition of both enzymes by HOPB.

4. Conclusion

In this study, beer was brewed with the addition of jasmine tea extract instead of hops at the late hopping stage. In general, the differences in physicochemical parameters between JTB and HOPB were not significant except for organic acid content and foam stability, but the overall sensory score of JTB was higher

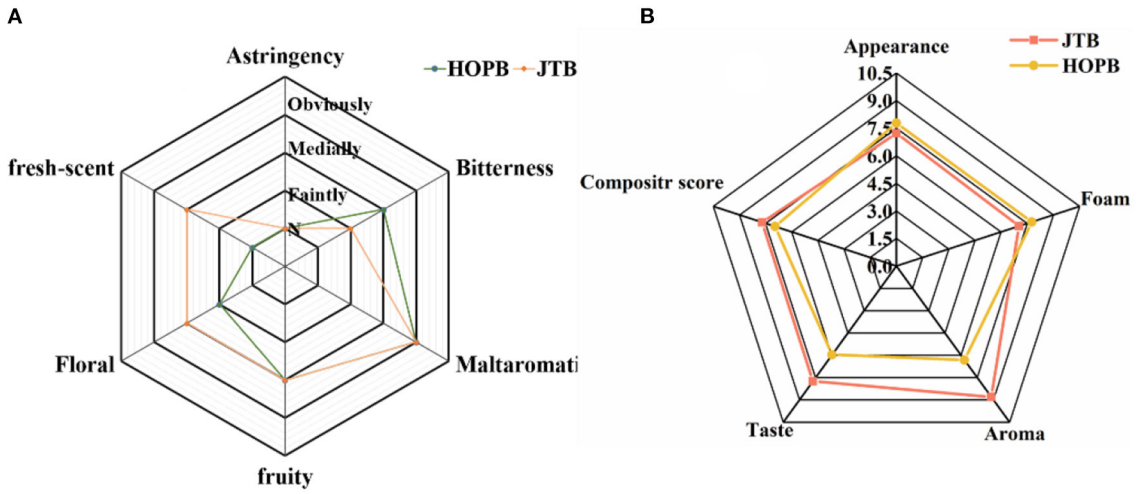

FIGURE 6
Results of the sensory profiling of the beer samples. **(A)** Sensory evaluation of beer flavor. **(B)** Rating evaluation of flavor intensity of beer characteristics.

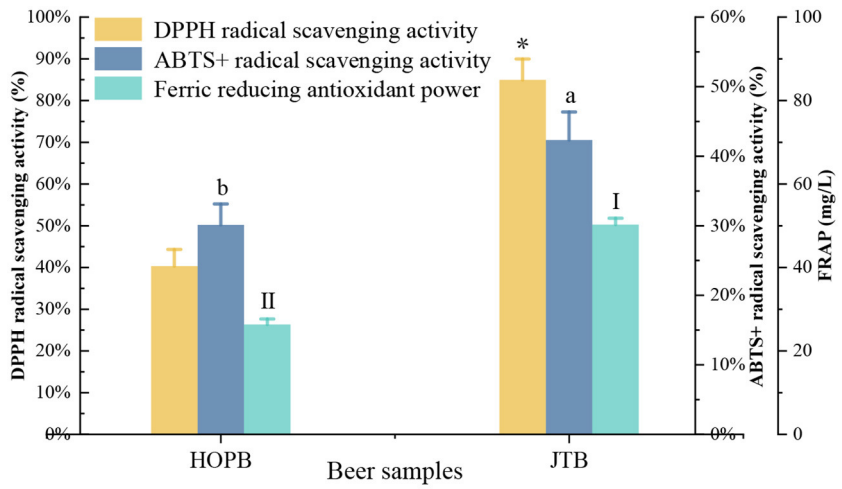

FIGURE 7
Antioxidant activity and polyphenol content. "a, b, I, II" and "*" Different letters in the same indexes indicate significant differences between mean values ($p < 0.05$). ABTS, 2,2′-azino-bis (3-ethylbenzothiazoline-6-sulphonic acid); DPPH, 2,2-diphenyl-1-picrylhydrazyl; FRAP, ferric reducing antioxidant power.

than that of HOPB and JTB had higher antioxidant capacity and polyphenol content.

The flavor volatiles in JTB and HOPB were distinctive; HOPB contained more abundant floral and fresh aroma compounds (e.g., nerol and methyl salicylate), whereas JTB contained more abundant green/grassy aroma compounds (e.g., hexanal). The differential compounds that distinguished the two beers were dimeric catechins, flavone/flavonol glycosides, and bitter acids and derivatives, which account for differences in sensory attributes and antioxidant capacity.

The overall sensory acceptability of JTB was higher than that of HOPB; JTB had a pleasant floral and fresh-scent aroma and softer taste, with a pleasant tea flavor and a taste. JTB had higher DPPH, ABTS and FRAP antioxidant capacities, which should result in better storage stability.

JTB has a stronger inhibitory effect on α-amylase activity than HOPB and is better able to regulate blood sugar levels. The consumption of this type of beer may therefore have a slowing effect on obesity.

Overall, adding jasmine tea extract instead of hops improved the overall sensory acceptability, foam stability and antioxidant capacity of the beer, as well as conferring a unique taste and flavor. This process modification has the potential to develop a novel application for tea in craft beer and compensate for the scarcity of aromatic hops in China.

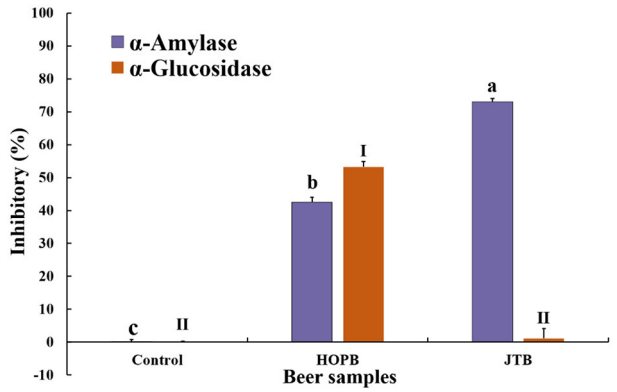

FIGURE 8
α-amylase and α-Glucosidase inhibitory effects by the two beers. "a, b, c, and I, II" Different letters in the same indexes indicate significant differences between mean values ($p < 0.05$).

Data availability statement

The original contributions presented in the study are included in the article/supplementary material, further inquiries can be directed to the corresponding author/s.

Ethics statement

The studies involving human participants were reviewed and approved by Zhejiang Gongshang University Human Ethics Committee. The patients/participants provided their writen informed consent to participate in this study.

Author contributions

Y-QX and CZ: conceived and designed the experiments. D-QC, CZ, Y-BH, and XZ: performed the experiments. D-QC, CZ, and Y-QX: analyzed the data. D-QC, CZ, Y-QX, PC, and J-FY: wrote and revised the paper. All authors have read and agreed to the published version of the manuscript.

Funding

This research was supported by the Key Research and Development Program of Zhejiang (2022C02033), the Key Research and Development Program of Guangdong (2022B0202040002), the China Agriculture Research System of MOF and MARA (CARS-19), and the Innovation Project for the Chinese Academy of Agricultural Sciences.

Acknowledgments

We are grateful to the School of Food and Biological Engineering, Zhejiang University of Technology and Industry (Hangzhou, China) for providing us with brewing equipment; to Han-Yu Zheng, Yi-Qing Zheng, Hao-Ying Han, and Yu Zheng for their help during the brewing process; and to Jian-Xin Chen, Fang Wang, Qing-Qing Cao, Jie-Qiong Wang, Shuang Liang, Ru-Yi Li, Lin Zeng, Si-Han Deng, Yu-Yi Liu, and Yi-Zhou Gao for acting as our sensory reviewers. We would also like to thank the Instrumental Analysis Center in Tea Research Institute Chinese Academy of Agricultural Sciences.

Conflict of interest

The authors declare that the research was conducted in the absence of any commercial or financial relationships that could be construed as a potential conflict of interest.

Publisher's note

All claims expressed in this article are solely those of the authors and do not necessarily represent those of their affiliated organizations, or those of the publisher, the editors and the reviewers. Any product that may be evaluated in this article, or claim that may be made by its manufacturer, is not guaranteed or endorsed by the publisher.

References

1. Gasiński A, Kawa RJ, Mikulski D, Kłosowski G, Głowacki A. Application of white grape pomace in the brewing technology and its impact on the concentration of esters and alcohols, physicochemical parameteres and antioxidative properties of the beer. *Food Chem.* (2022) 367:130646. doi: 10.1016/j.foodchem.2021.130646

2. Baiano A. Craft beer: an overview. *Compr Rev Food Sci Food Saf.* (2021) 20:1829–56. doi: 10.1111/1541-4337.12693

3. Villacreces S, Blanco CA, Caballero I. Developments and characteristics of craft beer production processes. *Food Biosci.* (2022) 45:101495. doi: 10.1016/j.fbio.2021.101495

4. Gordon R, Power A, Chapman J, Chandra S, Cozzolino D. A review on the source of lipids and their interactions during beer fermentation that affect beer quality. *Fermentation.* (2018) 4:89. doi: 10.3390/fermentation4040089

5. Gutiérrez A, Boekhout T, Gojkovic Z, Katz M. Evaluation of non- *Saccharomyces* yeasts in the fermentation of wine, beer and cider for the development of new beverages. *J Inst Brew.* (2018) 124:389–402. doi: 10.1002/jib.512

6. Rodman AD, Gerogiorgis DI. Dynamic simulation and visualisation of fermentation: effect of process conditions on beer quality. *IFAC-PapersOnLine.* (2016) 49:615–20. doi: 10.1016/j.ifacol.2016.07.236

7. Hiralal L, Olaniran AO, Pillay B. Aroma-active ester profile of ale beer produced under different fermentation and nutritional conditions. *J Biosci Bioeng.* (2014) 117:57–64. doi: 10.1016/j.jbiosc.2013.06.002

8. Hopfer H, McDowell EH, Nielsen LE, Hayes JE. Preferred beer styles influence both perceptual maps and semantic descriptions of dry hops. *Food Qual Prefer.* (2021) 94:104337. doi: 10.1016/j.foodqual.2021.104337

9. Sharp D, Qian Y, Clawson, Shellhammer TH. An exploratory study toward describing hop aroma in beer made with American and European Hop Cultivars. *Brew Sci.* (2016) 69:112–22.

10. Takoi K, Koie K, Itoga Y, Katayama Y, Shimase M, Nakayama Y, et al. Biotransformation of hop-derived monoterpene alcohols by lager yeast and their contribution to the flavor of hopped beer. *J Agric Food Chem.* (2010) 58:5050–8. doi: 10.1021/jf1000524

11. Castro R, Díaz AB, Durán-Guerrero E, Lasanta C. Influence of different fermentation conditions on the analytical and sensory properties of craft beers: hopping, fermentation temperature and yeast strain. *J Food Compos Anal.* (2022) 106:104278. doi: 10.1016/j.jfca.2021.104278

12. Dietz C, Cook D, Wilson C, Oliveira P, Ford R. Exploring the multisensory perception of terpene alcohol and sesquiterpene rich hop extracts in lager style beer. *Food Res Int.* (2021) 148:110598. doi: 10.1016/j.foodres.2021.110598

13. Dean GH. *The Extraction Efficiency of Hop Bitter Acids and Volatiles During Dry-Hopping* [Master's thesis]. Corvallis: Oregon State University

14. Michael D, Tatiana P, FilipVO, Ann VH, Jan VN. From wort to beer: the evolution of hoppy aroma of single hop beers produced by early kettle hopping, late kettle hopping and dry hopping. In: *Proc. 34th EBC Congress, 2013*, *Luxembourg*, Luxemburg.

15. Jaskula B, Syryn E, Goiris K, Rouck G, van Opstaele F, Clippeleer J de, et al. Hopping technology in relation to beer bitterness consistency and flavor stability. *J Am Soc Brew Chem.* (2007) 65:38–46. doi: 10.1094/ASBCJ-2007-0112-03

16. Gerhards S, Talaverano MI, Andrés AI, Sánchez VC, Lozano J, García LC, et al. Different dry hopping and fermentation methods: influence on beer nutritional quality. *J Sci Food Agric.* (2021) 101:2828–35. doi: 10.1002/jsfa.10912

17. Kiyoshi T, Keita T, Ayako S, Yoshiharu U. Varietal difference of hop-derived flavour compounds in late-hopped/dry-hopped beers. *Brew Sci.* (2016) 69:1–7.

18. Martínez A, Vegara S, Martí N, Valero M, Saura D. Physicochemical characterization of special persimmon fruit beers using bohemian pilsner malt as a base. *J Inst Brew.* (2017) 123:319–27. doi: 10.1002/jib.434

19. Gasiński A, Kawa RJ, Paszkot J, Pietrzak W, Sniegowska J, Szumny A. Second life of hops: analysis of beer hopped with hop pellets previously used to dry-hop a beer. *LWT.* (2022) 159:113186. doi: 10.1016/j.lwt.2022.113186

20. Rong L, Peng LJ, Ho CT, Yan SH, Meurens M, Zhang ZZ, et al. Brewing and volatiles analysis of three tea beers indicate a potential interaction between tea components and lager yeast. *Food Chem.* (2016) 197:161–7. doi: 10.1016/j.foodchem.2015.10.088

21. Guglielmotti M, Passaghe P, Buiatti S. Use of olive (*Olea europaea* L) leaves as beer ingredient, and their influence on beer chemical composition and antioxidant activity. *Food Sci.* (2020) 85:2278–85. doi: 10.1111/1750-3841.15318

22. Hao J, Dong J, Yin H, Yan P, Ting PL Li Q, et al. Optimum method of analyzing hop derived aroma compounds in beer by headspace solid-phase microextraction (SPME) with GC/MS and their evolutions during chinese lager brewing process. *J Am Soc Brew Chem.* (2014) 72:261–70. doi: 10.1094/ASBCJ-2014-1021-01

23. Seo S-H, Kim E-J, Park S-E, Park D-H, Park KM, Na C-S, et al. GC/MS-based metabolomics study to investigate differential metabolites between ale and lager beers. *Food Bioscience.* (2020) 36:100671. doi: 10.1016/j.fbio.2020.100671

24. Dennenlöhr J, Thörner S, Manowski A, Rettberg N. Analysis of selected hop aroma compounds in commercial lager and craft beers using HS-SPME-GC-MS/MS. *J Am Soc Brew Chem.* (2020) 78:16–31. doi: 10.1080/03610470.2019.1668223

25. Gao Y, Cao QQ, Chen Y-H, Granato D, Wang JQ, Yin JF, et al. Effects of the baking process on the chemical composition, sensory quality, and bioactivity of Tieguanyin oolong tea. *Front Nutr.* (2022) 9:881865. doi: 10.3389/fnut.2022.881865

26. Intelmann D, Haseleu G, Dunkel A, Lagemann A, Stephan A, Hofmann T. Comprehensive sensomics analysis of hop-derived bitter compounds during storage of beer. *J Agric Food Chem.* (2011) 59:1939–53. doi: 10.1021/jf104392y

27. Salviati E, Sommella E, Carrizzo A, Di Sarno V, Bertamino A, Venturini E. et al. Characterization of phase I and phase II metabolites of hop (*Humulus lupulus* L) bitter acids: *in vitro* and *in vivo* metabolic profiling by UHPLC-Q-Orbitrap. *J Pharm Biomed Anal.* (2021) 201:114107. doi: 10.1016/j.jpba.2021.114107

28. Paszkot J, Kawa-Rygielska J, Anioł M. Properties of dry hopped dark beers with high xanthohumol content. *Antioxidant.* (2021) 10:763. doi: 10.3390/antiox10050763

29. Leitao C, Marchioni E, Bergaentzlé M, Zhao M, Didierjean L, Taidi B, et al. Effects of processing steps on the phenolic content and antioxidant activity of beer. *J Agric Food Chem.* (2011) 59:1249–55. doi: 10.1021/jf104094c

30. Habschied K, Lončarić A, Mastanjević K. Screening of polyphenols and antioxidative activity in industrial beers. *Foods.* (2020) 9:238. doi: 10.3390/foods9020238

31. Gasiński A, Kawa-Rygielska J, Szumny A, Gasior J, Głowacki A. Assessment of volatiles and polyphenol content, physicochemical parameters and antioxidant activity in beers with dotted hawthorn (*Crataegus punctata*). *Foods.* (2020) 9:775. doi: 10.3390/foods9060775

32. He J, Dong Y, Liu X, Wan Y, Gu T, Zhou X, et al. Comparison of chemical compositions, antioxidant, and anti-photoaging activities of *Paeonia suffruticosa* flowers at different flowering stages. *Antioxidants.* (2019) 8:345. doi: 10.3390/antiox8090345

33. Thilagam E, Parimaladevi B, Kumarappan C, Mandal SC. α-Glucosidase and α-amylase inhibitory activity of *Senna surattensis*. *J Acupunct Meridian Stud.* (2013) 6:24–30. doi: 10.1016/j.jams.2012.10.005

34. Sheng Z, Dai H, Pan S, Wang H, Hu Y, Ma W. Isolation and characterization of an α-glucosidase inhibitor from *Musa* spp. (Baxijiao) flowers. *Molecules.* (2014) 19:10563–73. doi: 10.3390/molecules190710563

35. Da Santos MA, Ribeiro PV, Andrade CP, Machado AR, Souza PG de. Kirsch Ld. Physicochemical and sensory analysis of craft beer made with soursop (*Annona muricata* L). *Acta Sci Pol Technol Aliment.* (2021) 20:103–12. doi: 10.17306/J.AFS.2021.0845

36. Francesco G de, Bravi E, Sanarica E, Marconi O, Cappelletti F, Perretti G. Effect of addition of different phenolic-rich extracts on beer flavour stability. *Foods.* (2020) 9:638. doi: 10.3390/foods9111638

37. Salanţă LC, Coldea TE, Ignat MV, Pop CR, Tofană M, Mudura E, et al. Non-alcoholic and craft beer production and challenges. *Processes.* (2020) 8:1382. doi: 10.3390/pr8111382

38. Li g, Liu F. Changes in organic acids during beer fermentation. *J Am Soc Brew Chem.* (2015) 73:275–9. doi: 10.1094/ASBCJ-2015-0509-01

39. Olaniran AO, Hiralal L, Mokoena MP, Pillay B. Flavour-active volatile compounds in beer: production, regulation and control. *J Inst Brew.* (2017) 123:13–23. doi: 10.1002/jib.389

40. Neiens SD, Steinhaus M. Investigations on the impact of the special flavor hop variety huell melon on the odor-active compounds in late hopped and dry hopped beers. *J Agric Food Chem.* (2019) 67:364–71. doi: 10.1021/acs.jafc.8b05663

41. Zeng L, Fu YQ, Huang JS, Wang JR, Jin S, Xu YQ, et al. Comparative analysis of volatile compounds in Tieguanyin with different types based on HS–SPME–GC–MS. *Foods.* (2022) 11:1530. doi: 10.3390/foods11111530

42. Lin J, Chen Y, Zhang P, Ren M, Xu H, Wang X. A novel quality evaluation index and strategies to identify scenting quality of jasmine tea based on headspace volatiles analysis. *Food Sci Biotechnol.* (2013) 22:331–40. doi: 10.1007/s10068-013-0085-x

43. An H, Ou X, Zhang Y, Li S, Xiong Y, Li Q, et al. Study on the key volatile compounds and aroma quality of jasmine tea with different scenting technology. *Food Chem.* (2022) 385:132718. doi: 10.1016/j.foodchem.2022.132718

44. Liana CS. Optimization of ITEX/GC-MS method for beer wort volatile compounds characterisation. *J Agroaliment Proc Technol.* (2012) 18:229–35.

45. Tomasz P, Joanna H. New methods of hopping (dryhopping) and their impact on sensory properties of beer. *Acta Innovations.* (2016) 118:81–8.

46. Yin H, Liu LP, Yang M, Ding XT, Jia SR, Dong JJ, et al. Enhancing medium-chain fatty acid ethyl ester production during beer fermentation through EEB1 and ETR1 overexpression in *Saccharomyces pastorianus*. *J Agric Food Chem.* (2019) 67:5607–13. doi: 10.1021/acs.jafc.9b00128

47. Rutnik K, Knez HM, JoŽe KI. Hop essential oil: chemical composition, extraction, analysis, and applications. *Food Rev Int.* (2021) 38:529–51. doi: 10.1080/87559129.2021.1874413

48. Steenackers B, Cooman L, Vos D. Chemical transformations of characteristic hop secondary metabolites in relation to beer properties and the brewing process: a review. *Food Chem.* (2015) 172:742–56. doi: 10.1016/j.foodchem.2014.09.139

49. Wang S, Zhao F, Wu W, Wang P, Ye N. Comparison of volatiles in different jasmine tea grade samples using electronic nose and automatic thermal desorption-gas chromatography-mass spectrometry followed by multivariate statistical analysis. *Molecules.* (2020) 25:380. doi: 10.3390/molecules25020380

50. Chen DQ Ji WB, Granato D, Zou C, Yin JF, Chen JX, et al. Effects of dynamic extraction conditions on the chemical composition and sensory quality traits of green tea. *LWT.* (2022) 169:113972. doi: 10.1016/j.lwt.2022.113972

51. Das PR, Kim Y, Hong S-J, Eun J-B. Profiling of volatile and non-phenolic metabolites-amino acids, organic acids, and sugars of green tea extracts obtained by different extraction techniques. *Food Chem.* (2019) 296:69–77. doi: 10.1016/j.foodchem.2019.05.194

52. Zhao H. Effects of processing stages on the profile of phenolic compounds in beer. In: Zhao H, editor. *Processing and Impact on Active Components in Food*. Amsterdam: Elsevier (2015), p. 533–9. doi: 10.1016/B978-0-12-404699-3.00064-0

53. Ocvirk M, Mlinarič NK, Košir IJ. Comparison of sensory and chemical evaluation of lager beer aroma by gas chromatography and gas chromatography/mass spectrometry. *J Sci Food Agric.* (2018) 98:3627–35. doi: 10.1002/jsfa.8840

54. Zhang Y, Xiong Y, An H, Li J, Li Q, Huang J, et al. Analysis of volatile components of jasmine and jasmine tea during scenting process. *Molecules.* (2022) 27:479. doi: 10.3390/molecules27020479

55. Ye JH, Ye Y, Yin JF, Jin J, Liang YR, Xu YQ, et al. Bitterness and astringency of tea leaves and products: formation mechanism and reducing strategies. *Trends Food Sci Tech.* (2022) 123:130–43. doi: 10.1016/j.tifs.2022.02.031

56. Oladokun O, James S, Cowley T, Dehrmann F, Smart K, Hort J, et al. Perceived bitterness character of beer in relation to hop variety and the impact

of hop aroma. *Food Chem.* (2017) 230:215–24. doi: 10.1016/j.foodchem.2017.03.031

57. Oladokun O, Tarrega A, James S, Smart K, Hort J, Cook D. The impact of hop bitter acid and polyphenol profiles on the perceived bitterness of beer. *Food Chem.* (2016) 205:212–20. doi: 10.1016/j.foodchem.2016.03.023

58. Martinez GA, Caballero I, Blanco CA. Phenols and melanoidins as natural antioxidants in beer. structure, reactivity and antioxidant activity. *Biomolecules.* (2020) 10:400. doi: 10.3390/biom10030400

59. Mudura E, Coldea T. Hop-derived prenylflavonoids and their importance in brewing technology – a review. *Bull UASVM Food Sci Technol.* (2015) 72:1–10. doi: 10.15835/buasvmcn-fst:11198

60. Nardini M, Garaguso I. Characterization of bioactive compounds and antioxidant activity of fruit beers. *Food Chem.* (2020) 305:125437. doi: 10.1016/j.foodchem.2019.125437

61. Liu S, Ai Z, Qu F, Chen Y, Ni D. Effect of steeping temperature on antioxidant and inhibitory activities of green tea extracts against α-amylase, α-glucosidase and intestinal glucose uptake. *Food Chem.* (2017) 234:168–73. doi: 10.1016/j.foodchem.2017.04.151

62. Hua F, Zhou P, Wu HY, Chu G-X, Xie ZW, Bao GH. Inhibition of α-glucosidase and α-amylase by flavonoid glycosides from Lu'an GuaPian tea: molecular docking and interaction mechanism. *Food Funct.* (2018) 9:4173–83. doi: 10.1039/C8FO00562A

63. Xu P, Chen L, Wang Y. Effect of storage time on antioxidant activity and inhibition on α-amylase and α-glucosidase of white tea. *Food Sci Nutr.* (2019) 7:636–44. doi: 10.1002/fsn3.899

64. Yilmazer-Musa M, Griffith AM, Michels AJ, Schneider E, Frei B. Grape seed and tea extracts and catechin 3-gallates are potent inhibitors of α-amylase and α-glucosidase activity. *J Agric Food Chem.* (2012) 60:8924–9. doi: 10.1021/jf301147n

65. Keskin S, Sirin Y, Çakir HE. Keskin M. An investigation of *Humulus lupulus* L: phenolic composition, antioxidant capacity and inhibition properties of clinically important enzymes. *S Afr J Bot.* (2019) 120:170–4. doi: 10.1016/j.sajb.2018.04.017

66. Wang L, Zhang Y, Johnpaul IA, Hong K, Song Y, Yang X. et al. Exploring two types of prenylated bitter compounds from hop plant (*Humulus lupulus* L) against α-glucosidase *in vitro* and *in silico*. *Food Chem.* (2022) 370:130979. doi: 10.1016/j.foodchem.2021.130979

67. Liu M, Yin H, Liu G, Dong J, Qian Z, Miao J. Xanthohumol, a prenylated chalcone from beer hops, acts as an α-glucosidase inhibitor *in vitro*. *J Agric Food Chem.* (2014) 62:5548–54. doi: 10.1021/jf500426z

frontiers | Frontiers in Nutrition

TYPE Review
PUBLISHED 16 March 2023
DOI 10.3389/fnut.2023.1145862

OPEN ACCESS

EDITED BY
Wenjiang Dong,
Chinese Academy of Tropical Agricultural Sciences, China

REVIEWED BY
Liana Claudia Salanta,
University of Agricultural Sciences and Veterinary Medicine Cluj-Napoca, Romania
Wenchao Cai,
Shihezi University, China

*CORRESPONDENCE
Gan-Lin Chen
✉ ganlin-chen@gxaas.net
Li-Fang Yang
✉ yanglf1990@163.com

†These authors have contributed equally to this work

SPECIALTY SECTION
This article was submitted to Food Chemistry, a section of the journal Frontiers in Nutrition

RECEIVED 16 January 2023
ACCEPTED 17 February 2023
PUBLISHED 16 March 2023

CITATION
Chen G-L, Zheng F-J, Lin B, Yang Y-X, Fang X-C, Verma KK and Yang L-F (2023) Vinegar: A potential source of healthy and functional food with special reference to sugarcane vinegar. *Front. Nutr.* 10:1145862. doi: 10.3389/fnut.2023.1145862

Vinegar: A potential source of healthy and functional food with special reference to sugarcane vinegar

Gan-Lin Chen[1,2,3*†], Feng-Jin Zheng[2,3†], Bo Lin[2,3], Yu-Xia Yang[2,3], Xiao-Chun Fang[2,3], Krishan K. Verma[4,5,6] and Li-Fang Yang[1*]

[1]School of Chemistry and Chemical Engineering, Guangxi Minzu University, Nanning, Guangxi, China, [2]Institute of Agro-Products Processing Science and Technology, Guangxi Academy of Agricultural Sciences, Nanning, Guangxi, China, [3]Guangxi Key Laboratory of Fruits and Vegetables Storage-Processing Technology, Nanning, China, [4]Key Laboratory of Sugarcane Biotechnology and Genetic Improvement (Guangxi), Ministry of Agriculture and Rural Affairs, Nanning, Guangxi, China, [5]Guangxi Key Laboratory of Sugarcane Genetic Improvement, Nanning, Guangxi, China, [6]Sugarcane Research Institute, Guangxi Academy of Agricultural Sciences, Nanning, Guangxi, China

Vinegar is one of the most widely used acidic condiments. Recently, rapid advances have been made in the area of vinegar research. Different types of traditional vinegar are available around the globe and have many applications. Vinegar can be made either naturally, through alcoholic and then acetic acid fermentation, or artificially, in laboratories. Vinegar is the product of acetic acid fermentation of dilute alcoholic solutions, manufactured by a two-step process. The first step is the production of ethanol from a carbohydrate source such as glucose, which is carried out by yeasts. The second step is the oxidation of ethanol to acetic acid, which is carried out by acetic acid bacteria. Acetic acid bacteria are not only producers of certain foods and drinks, such as vinegar, but they can also spoil other products such as wine, beer, soft drinks, and fruits. Various renewable substrates are used for the efficient biological production of acetic acid, including agro and food, dairy, and kitchen wastes. Numerous reports on the health advantages associated with vinegar ingredients have been presented. Fresh sugarcane juice was fermented with wine yeast and LB acetate bacteria to develop a high-quality original sugarcane vinegar beverage. To facilitate the current study, the bibliometric analysis method was adopted to visualize the knowledge map of vinegar research based on literature data. The present review article will help scientists discern the dynamic era of vinegar research and highlight areas for future research.

KEYWORDS

fatty acid, fermentation processes, health benefits, VOCs, phytochemistry, production approaches, *Saccharum* spp., vinegar

Introduction

Rapid development in the food supply chain has led to an increased interest in quality in the food sector. Human health and food safety have become essential in the last few decades. Health problems are highly related to diet and nutritional habits. The connection between nutrition and the development of various health problems is even more noticeable when close attention is given to every age group. As regards the chemical composition of foods, a large number of bioactive compounds present in plants, fruits, vegetables, dairy products, meat, and fish are currently known. Bioactive compounds from

food play an important role in disease prevention (1, 2). Vinegar has antibacterial properties, antioxidant activity, anti-diabetic and anti-tumor effects, and the ability to prevent cardiovascular disorders. Additionally, due to its medicinal properties, it has long been applied in traditional ancient medicine (3, 4). Every nation or location in the world has varieties of vinegar with distinctive aromas and flavors derived from the raw ingredients, microorganisms, and vinegar manufacturing processes (3, 5, 6). In addition to being used as a flavoring agent, vinegar is a functional food and beverage since it contains some healthy ingredients, particularly in the older varieties (7, 8).

Globalization and the rapid expansion of food production have resulted in new consumer expectations regarding food and balanced diets. However, due to the significant increase in life expectancy, there is an urgent need for specific foods that meet all nutritional requirements and help us maintain a healthy diet, which is essential for maintaining human health (9–11). Therefore, food industries must keep up with consumers' interests and needs while developing novel products. Additionally, health experts, food technologists, biologists, healthcare companies, and consumers tend to highlight a great deal of interest in disease prevention. Functional foods are classified as nutritious foods, medicinal foods, regulatory foods, fortified foods, nutraceuticals, and pharmacological foods. Functional foods contain nutrients that have the potential to improve human life or reduce the risk of certain abnormalities (11–13).

Fruit is a well-known source of nutrients with functional qualities. Fruit contains flavors, colors, and aromas in addition to phytochemicals with antioxidant activities. Due to their capacity to scavenge and suppress free radicals formed during the oxidative metabolism that have detrimental effects on human health, antioxidants found in fruits have already been linked to nutritional advantages (14, 15). As a result, there is great interest in developing approaches for delivering these nutrients, and vinegar represents a promising possibility for establishing an improved functional food. In addition to being used as a food condiment, vinegar is a key component in the formulation of several drinks. Consequently, it was estimated that the market for products related to vinegar and the demand for genuine, high-quality fruit vinegar products will increase (2, 16). Fruit vinegar designation is also valid for products that mix juice with vinegar. However, establishing the types of vinegar made from fruits is crucial to provide a final product with natural fruit properties, given consumers' interest in high-quality and good food products (16).

Vinegar is an acidic condiment produced from various raw materials, including grains, fruits, and vegetables, and is manufactured worldwide. Cider vinegar and regular vinegar are the two varieties. Cider vinegar is made from fruit juices. It is a highly advantageous beverage, as it helps to promote various types of beneficial effects to consumers. Additionally, cider vinegar has been reported to have the potential to balance pH levels in the body if taken regularly. Regular vinegar is manufactured from unprocessed plant materials, i.e., grains, apples, grapes, or sugarcane (17–19). Depending on the ingredients used in their production, the fermentation processes, and the microorganisms participating in the process, different kinds of vinegar exhibit unique characteristics, flavors, and tastes (19). Numerous studies have already shown how effective the production process is concerning the final aroma characteristic of vinegar and its organoleptic properties (20, 21). Other than the production process, other factors affect the proportion of specific compounds, such as volatile and phenolic compounds, which is essential for the determination of vinegar quality (22). Recent studies on fruit vinegar production have focused on the isolation of specific acetic acid bacteria and the vinegars' phenolic and aromatic profiles to manage and improve vinegar quality (23). The ability of various bacterial strains to produce vinegar at high acetic acid concentrations has been tested (24).

Sugarcane is the world's largest source of sugar, and the main crop in many regions, and as a C_4 plant with high energy efficiency, it is more important than other crops in terms of renewable energy utilization rate and crop production capacity. It has wide adaptability, stress tolerance, a high net energy ratio, and yield potential. Crop growth characteristics, widely planted in tropical and subtropical regions, not only as the main raw material for the sugar industry but also as a vital energy crop, the average annual biomass production is 180–200 t/ha, the yield as raw material, and ethanol production are significant due to other crops. The use of commercial promoters to initiate acetic fermentation or the implementation of cutting-edge techniques to produce high-quality sugarcane vinegar is an interesting research area discussed in this article with key importance given to the production process of sugarcane vinegar.

History and current status of vinegar

Vinegar is used as a condiment or preservative in salad dressings, ketchups, and sauces or mixed with water for use as a beverage (22). Interestingly, vinegar was once thought to be a culinary byproduct produced when wine deteriorated from exposure to air. The first known use of vinegar was over 10,000 years ago (25, 26). French chemist Durande succeeded in creating glacial acetic acid by concentrating vinegar in the 18th century. A technique for making vinegar known as the generator process, invented by German scientist Schutzenbach in the 19th century, allowed vinegar to be produced in 7 days. German inventor Hromatka developed submerged acetification, an improved vinegar-making process that uses better aeration and stirring to develop vinegar in a shorter period (25).

In Europe, America, and Africa, fruit vinegar is usually manufactured and used as a spice (3, 5, 6, 8). Fruit vinegar is made from various fruits, including grapes, apples, pineapples, mangoes, jujubes, and bananas (16). There are many well-known traditional fruit vinegarsthroughout the world, including traditional balsamic vinegar (TBV), balsamic vinegar (BV), and sherry vinegar (SV), all of which are PGI products in Europe (27). The ancient Egyptians, Sumerians, and Babylonians are believed to have developed, prepared, and utilized fruit vinegar first, according to historical records (5, 6).

Around 1,000 BC, China produced cereal vinegar, the most widely used vinegar in China, Japan, Korea, and other Asian nations (28). Seaweed salad, sushi, boiled and steamed fish, and other dishes are frequently seasoned with cereal vinegar (3, 5, 6). Sorghum,

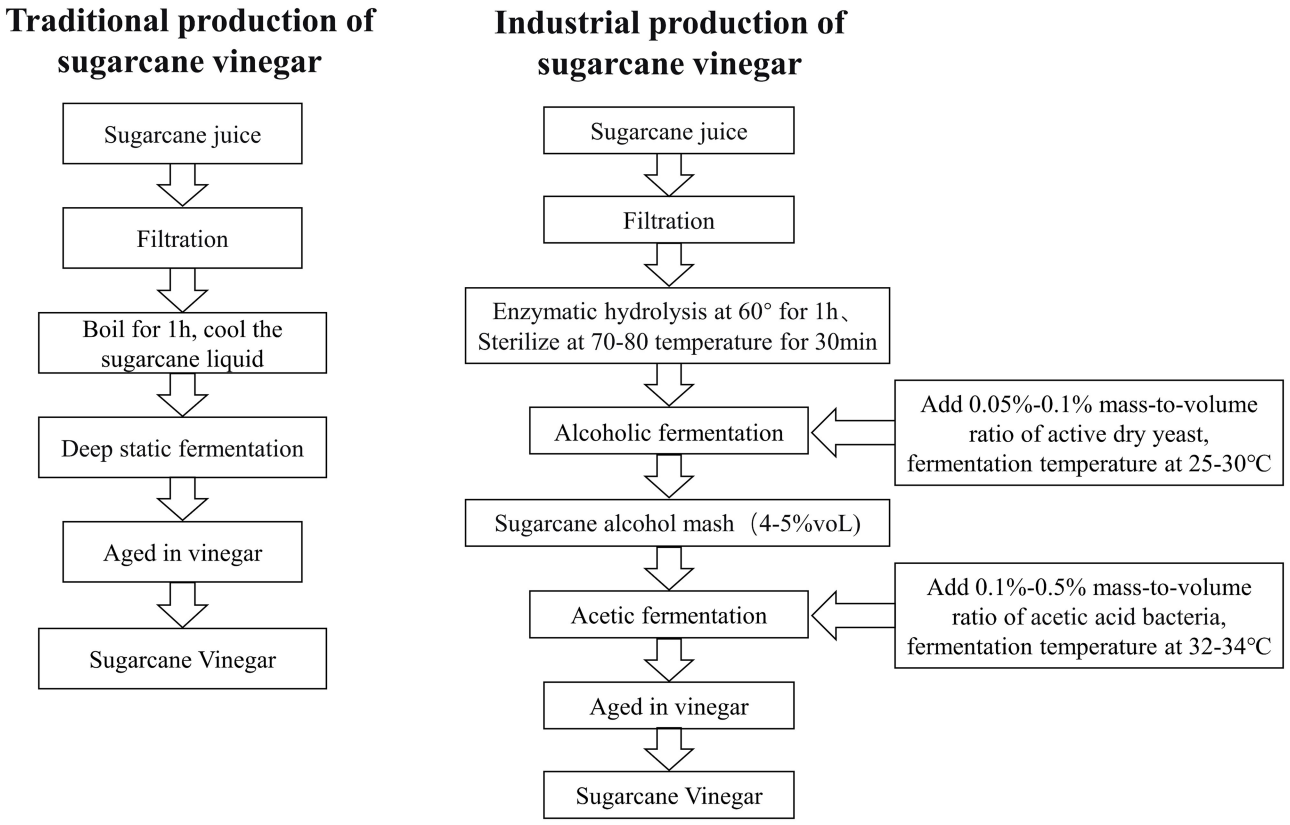

FIGURE 1
Simplified production flow diagram of sugarcane vinegar.

rice, wheat, corn, barley, and other starch-rich ingredients are the primary raw materials for cereal vinegar (3, 5, 6, 8).

Due to vinegar's nutritional properties directly affecting consumers' health, more than 3.2 million liters of vinegar is consumed daily in China. The quality of vinegar has received significant attention from the Chinese government (19). As regards Chinese sugar crops, i.e., sugarcane and sugar beet, more than 85% of the perennial sugar plantation area is sugarcane, which accounts for more than 90% of the total sugar production capacity. Since 1992, Guangxi, China, has become a sugarcane cultivation and sugar production area with extensive planting and production capacity. Sugarcane planting and sucrose production account for more than 60% of the Guangxi's land use. According to the statistics of the China Sugar Industry Association, the harvest area of sugarcane in the whole region was 729,600 ha, the total sugarcane output was 49,213,200 tons, sugar production was approximately 6,287,800 tons, and total sugar production was 10.67 MMT in the country during the 2020/2021 crushing season. Guangxi has become China's leading province for sugar. It is the second-largest sugar-producing province after São Paulo, Brazil. In addition, Guangxi is also the most prominent fruit-cane-producing area in China, with an annual fruit cane planting area of more than 30,000 ha, a yield of 105–150 t/ha, and a total yearly output of over 3 million tons, most of which are sold to North (29).

The high-quality fermented product processed from sugarcane juice is more significant in promoting the sugarcane industry's development in Guangxi, China, and around the globe. The sugarcane vinegar production and quality standard system in China dramatically promotes the development of China's sugarcane processing and fermented vinegar industries and enhances the influence of sugarcane vinegar standardization. Because of the high cost of raw material processing, long duration fermentation cycle, low efficiency, and unknown product efficacy, the government of the Guangxi region developed measures to promote the secondary entrepreneurship of the sugar industry. Sugarcane raw vinegar was selected as a breakthrough point to conduct technical analysis on non-sugar-diversified products with high economic value and overcome the major bottleneck of the lack of diversified processing technologies and developments in the cane industries.

Sugarcane juice is a common indigenous drink, largely and economically consumed worldwide (14). Sugarcane original vinegar (SOV) developed a complete set of advanced technologies for continuous and efficient processing of original sugarcane vinegar with high efficiency of whole-stem cane juice, developed advanced equipment for different types of automatic intelligent vinegar brewing machines, and built vats for storing sugarcane brewed by immobilized microorganisms. Compared with conventional technology, the fermentation period of raw vinegar takes approximately 13–18 days, efficiency is increased up to 42.5–52.2%, and the cost is reduced by 30%, which solves the problems of the high processing cost of sugarcane raw materials and the long fermentation period. To our knowledge, this is the first time we have shown the effective retention of sugarcane original vinegar's properties and functional components during

fermentation, revealing its essential biological functions (Figure 1). Different kinds of organic acids, such as amino acids, sugar, volatile components, and active ingredients of polyphenols, were assessed (Table 1). It has been confirmed that original sugarcane vinegar has the functions of lowering blood fat, improving anti-oxidative stress, reducing body weight, and enlarging organs to developing diversified new products derived from available sugarcane raw vinegar (30, 32).

The chemical variations in the original sugarcane vinegar produce acetic acid with two carbon atoms by the action of *Saccharomycetes* and acetic acid bacteria (catalytic enzymes) containing 12 carbon atoms of sucrose (Figure 2). The main component of raw sugarcane juice is sucrose, which is a highly suitable source of carbon for the growth of microbial activities and, thus, may be directly involved as a fermentation medium (14, 33).

Research and development on vinegar

Identification of yeast fermentation

The final vinegar depends on the yeast strains applied during the fermentation process. Different yeast strains can produce varying concentrations of volatile substances and alcohol. It implies that other kinds of vinegar will be produced based on the strains employed with reference to the aroma, alcohol level, and acetic acid content. The strain *S. cerevisiae* r. *bayanus* and the cider strain *S. cerevisiae* r. *cerevisiae* give rise to ciders with similar characteristics. Noteworthy in both strains is the low production of acetic acid and secondary fermentation compounds, as well as the fact that they give rise to ciders with a high concentration of glycerol and succinic acid (34). There are different methods for alcoholic fermentation, including spontaneous fermentation and inoculation with *S. cerevisiae* yeast. When compared to spontaneous fermentation, it was revealed that alcoholic fermentation with yeast could result in higher alcohol content (35). Yeast is essential in producing wines that contain higher alcohol (36).

In the analysis of wine's fermentation properties, special yeast for the alcohol fermentation of sugarcane vinegar was screened from three dry yeasts, such as wine high-activity dry yeast, high-temperature-resistant high-activity dry yeast, and highly active dry yeast for wine. According to the yeast growth curve, the delay period of three yeasts is 0–4 h, logarithmic growth period is 4–18 h, stable period is 18–28 h, which then declines after 28 h. The growth stability of yeast is determined as wine high-activity dry yeast > high-temperature-resistant high-activity dry yeast > highly active dry yeast for wine. The F coagulation value of the three yeasts was <20%, non-cohesive. Before fermentation (48 h), the CO_2 weight loss of the three yeasts changed, indicating that the fermentation speed was fast at this stage, the yeasts were in the vigorous reproductive stage, showed strong fermentation capacity, and displayed specific difference between the fermentation time and the frequency. The acidifying ability values changed during the 3–6 days and gradually rose to a stable level during 6–8 days of fermentation. Observing the acidifying efficiency of the three yeasts in the final fermentation stage, it was determined that wine high-activity dry yeast is superior to high-temperature-resistant high-activity dry yeast (14, 37).

Screening of acetic acid bacteria

This screening method uses sugarcane alcohol mash as raw material, through liquid submerged fermentation, LB-active acetic acid bacteria. LB-active acetic acid bacteria were selected from five acetic acid bacteria, such as bacterium and raw meal acetic acid bacteria, which are more suitable for brewing sugarcane original vinegar. The pH range between 5.5 and 6.3 is suitable for the growth of acetic acid bacteria. While some strains have been isolated from aerated media with a pH as low as 2.0, numerous investigations have demonstrated that acetic acid bacteria can still survive at pH 3.0. Three distinct strain types, known as acetophilic strains (grow at pH 3.5), acetotolerant strains (grow at pH 3.5 to 6.5), and acetophobic strains (grow at pH levels >6.5), can be explored in the production of vinegar (38). The optimal temperature for the growth of acetic acid bacteria ranged between 25 and 30°C. However, according to Raspor and Goravonic (38), acetic acid bacteria are still active at 10°C but develop more slowly.

Acetic acid is the main organic acid present in vinegar and is one of the most important functional ingredients. Acetic acid bacteria mainly produce it during fermentation. Lactic acid, which shows the highest content among nonvolatile organic acids in vinegar, is mainly produced during alcoholic fermentation. Propionic acid, tartaric acid, malic acid, citric acid, and other organic acids in vinegar are produced throughout the whole fermentation process. Moreover, the fermentation conditions also influence the contents of organic acids (7, 39). Five types of acetic acid bacteria were produced under the same situation, the acid production ability of the raw vinegar was relatively normal, and the acid production of the other four types of acetic acid bacteria showed a significant increase in the process of acetic acid fermentation (40).

Acid production and sensory quality

Vinegar is notable for its unique aromas and flavors, mainly derived from its raw materials, microbial communities, and process technologies (3, 5, 6, 20). Because some VVOCs can emerge from one of the three sources—raw materials, microbes, and processes—or two or three of them, it is exceedingly challenging to pinpoint exactly where they originate. Additionally, VVOCs alter dynamically throughout the entire production process of vinegar. The fruit vinegar fermented by LB-active acetic acid bacteria has a sweet and sour taste, outstanding aroma, and bright color. It has the highest sensory score, which is significantly higher than those of other strains. Compared with pH, the initial alcohol content, inoculum amount, sucrose addition amount, and temperature significantly affect the acetic acid fermentation process through single-factor experiments.

Process of alcohol fermentation

Saccharomyces cerevisiae, which is present in all varieties of vinegar, among the numerous microbial strains, was identified during the alcoholic fermentation process (AFP) of vinegar (3). According to Wang et al. (41), *S. cerevisiae* was the predominant

TABLE 1 Summarizing aroma compounds, organic and free amino acids in sugarcane vinegar (30, 31).

Volatile compounds	Relative content (%)	Volatile compounds	Relative content (%)	Volatile compounds	Relative content (%)	Volatile compounds	Relative content (%)	Amino acids (mg/100 ml)	Amino acids (mg/100 ml)	Amino acids (mg/100 ml)	Phenolic acids	Alcoholic fermentation (mg/L)	Acetic acid fermentation (mg/L)
Ethyl acetate	14.163 ± 0.09	3-penten-2-one	0.274 ± 0.013	Ethyl lactate	0.099 ± 0.000	Methyl benzoate	0.0385 ± 0.000	Aspartic acid (Asp)	45.10 ± 0.09	Isoleucine (Ile)	21.60 ± 0.004	Benzoic acid	1.002 ± 0.021	1.027 ± 0.070
Ethyl lactate	43.640 ± 1.263	Isoamyl alcohol	3.703 ± 0.009	N-hexanol	0.018 ± 0.000	Valeric acid	0.217 ± 0.003	Threonine (Thr)	24.30 ± 0.05	Leucine (Leu)	30.20 ± 0.004	Ferulic acid	0.205 ± 0.010	1.124 ± 0.061
Octamethyl-cyclotetra-siloxane	0.016 ± 0.001	Ethyl caproate	0.0785 ± 0.001	2-acetoxy-tetradecane	0.020 ± 0.000	Phenyl-ethanol	0.876 ± 0.013	Serine (Ser)	19.90 ± 0.02	Tyrosine (Tyr)	11.70 ± 0.003	Quinic acid	0.074 ± 0.010	0.031 ± 0.01
Isobutyl acetate	0.068 ± 0.009	4-ethoxy-2-pentanone	0.051 ± 0.000	Nonanal	0.157 ± 0.008	N-octanoic acid	0.187 ± 0.009	Glutamic acid (Glu)	38.50 ± 0.011	Phenylalanine (Phe)	20.00 ± 0.005	Chlorogenic acid	1.635 ± 0.059	1.217 ± 0.053
Ethyl Isovalerate	0.017 ± 0.005	Octanal	0.025 ± 0.003	1,3-Di-tert-butyl-benzene	0.689 ± 0.09	4-vinyl-2-methoxy-phenol	0.005 ± 0.000	Proline (Pro)	9.39 ± 0.001	Lysine (Lys)	35.40 ± 0.003	Apigenin	99200.83 ± 3956	3510.88 ± 44.08
N-hexanal	0.056 ± 0.001	3-hydroxy-2-butanone	0.093 ± 0.001	Ethyl caprylate	0.413 ± 0.10	2-hydroxy-cinnamic acid	0.014 ± 0.000	Glycine (Gly)	29.60 ± 0.003	Histidine (His)	10.80 ± 0.006	Kaempferol	336133.64 ± 7892	3399.10 ± 104
Decane	0.049 ± 0.001	Trans-2-heptenal	0.0285 ± 0.002	Acetic acid	27.445 ± 0.401	5-hydroxy-methyl furfural	0.036 ± 0.003	Alanine (Ala)	24.90 ± 0.009	Arginine (Arg)	15.60 ± 0.002	Caffeic acid	4926.56 ± 120	4715.54 ± 213
Isobutanol	0.575 ± 0.021	2-heptanol	0.013 ± 0.001	Decanal	0.118 ± 0.019	-	-	Cystine (Cys)	1.074 ± 0.001	Total amino acids (TAA)	365.77 ± 0.019	Luteolin	327692.20 ± 12384	5312.13 ± 898
Isoamyl acetate	0.496 ± 0.009	Methyl-heptenone	0.0065 ± 0.000	Propionic acid	0.0505 ± 0.005	-	-	Valine (Val)	25.40 ± 0.006	Essential amino acid (EAA)	159.21 ± 0.014	p-coumaric acid	15289.45 ± 1018	26600.51 ± 1159
-	-	-	-	-	-	-	-	Methionine (Met)	2.31 ± 0.002	Non-essential amino acids (NAA)	206.56 ± 0.009	-	-	-

Data are represented as mean ± SE for three ($n = 3$) biological replicates.

10.3389/fnut.2023.1145862

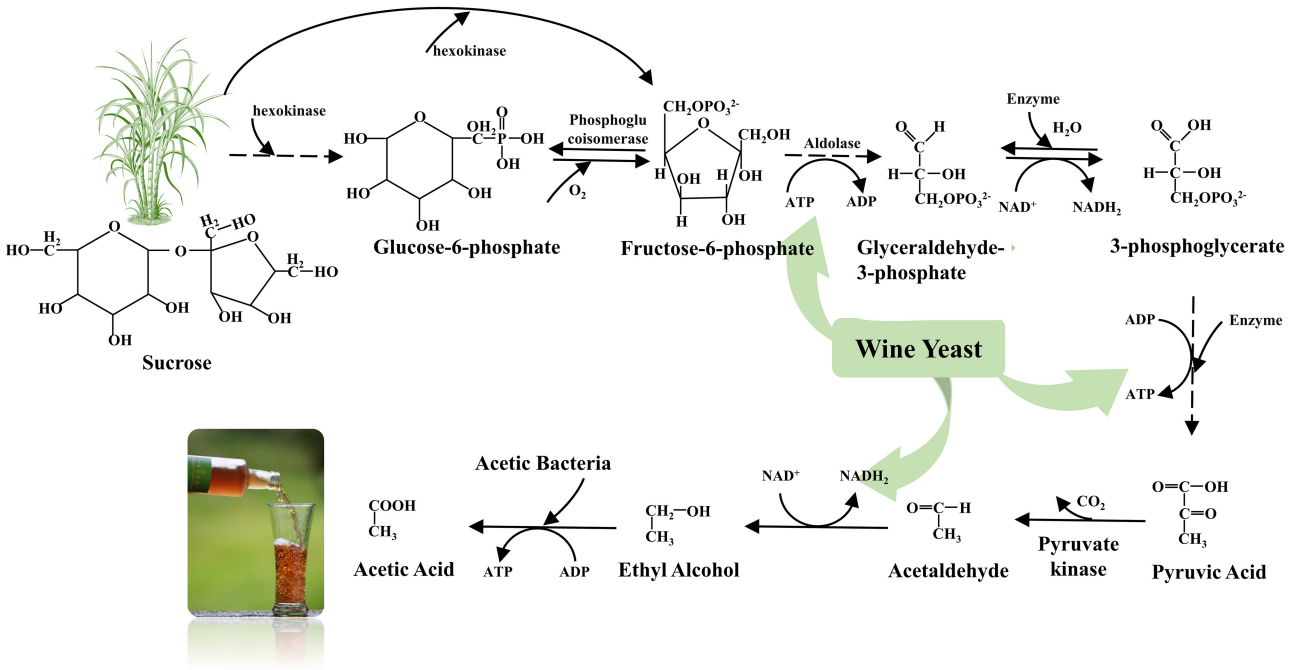

FIGURE 2
Conversion of sugarcane raw juice to acetic acid reaction.

yeast species in the AFP of fruit vinegar. Since *S. cerevisiae* strains grow better than other yeast species in the high-sugar environment of AFP (42). In addition to *S. cerevisiae*, LAB frequently appear in AFP and significantly contribute to the synthesis of vinegar volatile organic compounds, as do non-*Saccharomyces* like *Candida* spp., *Cryptococcus* spp., and *Debaryomyces* spp. (41, 43).

The sucrose in sugarcane raw juice was divided into glycogen for direct microaerobic fermentation. The optimal parameters were 0.1% yeast addition, 20°C fermentation temperature, 280-mL/(kg·d) oxygen flow, and 15 alcohol content of fermented mash. The sugar content of the fermented liquid with the added amount of 0.1% yeast is the highest (18.49 g/100 mL) but with a low alcohol content (14.3% vol); the apparent sugar content of the fermented liquid with the added amount of 0.2% yeast. Yeast additions of 0.15 and 0.2% bring about a faster fermentation rate. After 4 days of fermentation, the utilization rate of apparent sugar content consumption was not high and not conducive to the formation of post-fermentation sugarcane flavor. Considering the time period for fermentation comprehensively, the optimal amount of yeast was added to ferment low-alcohol sugarcane fruit wine (0.1%) (44). The amount of residual sugar in fruit wine is related to the alcohol content and the initial apparent sugar content utilization rate in the early fermentation process. Moderate residual sugar can improve the taste of fruit wine during aging and enrich the flavor of sugarcane fruit wine (14, 44).

Acetic acid fermentation process

Acetobacter spp., *Komagataeibacter* spp., *Gluconobacter* spp., and *Gluconacetobacter* spp. are the dominant microorganisms in the acetic acid fermentation process of vinegar, but other bacteria, mainly *Lactobacillus* spp., *Pediococcus* spp., *Bacillus* spp., *Acinetobacter* spp., and *Staphylococcus* (8, 45, 46). These bacteria, can generate aldehydes, ketone VVOCs, and acidic VVOCs. The acidic VVOCs can be utilized as substrates to produce additional VVOCs, such as ester-like VVOCs. The primary AAB strains used to develop fruit and cereal vinegar by liquid-state and solid-state fermentation, respectively, originate from the genera *Acetobacter* and *Komagataeibacter* (5, 8).

Using sugarcane, fruit wine is prepared by fermentation of sugarcane juice as raw material through liquid-submerged fermentation. The acetic acid fermentation strains preparing sugarcane fruit vinegar from sugarcane fruit wine were screened out. The acetic acid fermentation process of sugarcane fruit wine was studied using response surface methodology (RSM). Through optimization, the optimal process parameters obtained were as follows: the initial alcohol content (5%) of sugarcane fruit wine, the inoculation amount of LB-active acetic acid bacteria (0.5%), the addition of sucrose (4%), and a fermentation temperature of 26°C. Under these conditions, the acid production of 15.05 g/100 mL was observed.

The optimum process for rapid fermentation of acetic acid bacteria was immobilized in alcoholic mash: LB-active acetic acid bacteria were used as fermentation bacteria to study the effects of initial alcohol content, inoculum size, fermentation temperature, sucrose addition, and initial pH on acetic acid fermentation and determine the most suitable LB. The initial alcohol content of active acetic acid bacteria fermentation was found to be 5% (vol), inoculum size was 0.5%, fermentation temperature was 26°C, the amount of sucrose was 4%, and initial pH was 3.6. Under these conditions, the acid production reaches 15.05 g/100 mL. The sugarcane fruit vinegar fermented by this process is amber in

color, crystal clear, clear in sugarcane fragrance, and sweet and sour (40).

The interaction between initial alcohol content and inoculum volume had the most significant effect on acid production. Through regression analysis, combined with the convenience of actual operation, the processing conditions of sugarcane fruit vinegar fermented by LB-active acetic acid bacteria were determined, such as the initial alcohol content of sugarcane fruit wine was 5% vol and the inoculation amount of LB-active acetic acid bacteria was 0.5%. Compared with the predicted value of 15.57 g/100 mL, the theoretical significance and the expected value do not have a big difference, and the test results are promising, which shows that it is feasible to optimize the process conditions of fermented sugarcane fruit vinegar by response surface analysis (40).

Organic acids and volatile compounds of vinegar

The fermentation of acetic acid is primarily responsible for vinegar's distinctive flavor and aroma. Because acetic acid is present, vinegar has a strong aroma and flavor. However, in addition to acetic acid, vinegar fermentation products, such as organic acids, esters, ketones, and aldehydes, give vinegar its unique taste (47) (Table 1). Acetic acid is a precursor for synthesizing these chemicals, produced throughout the fermentation and aging process (48). The initial raw materials utilized, the techniques for making vinegar, and the length of acetification could all impact these volatile compounds (49).

A total of 61 and 38 volatile compounds were identified in the traditional and industrial vinegar samples, according to Ozturk et al. (47), which assessed the volatile compounds present in Turkish traditional homemade vinegar and industrial vinegar. The two most volatile compounds in the conventional vinegar were α-terpineol (25%) and ethyl acetate (15%), among the other identified volatile compounds. It is interesting to note that ethyl acetate predominates in grape vinegar, but α-terpineol is undetectable from all samples of grape vinegar. Octanoic acid (15.6%) and isoamyl acetate (18.6%), or "banana odor", were determined to be the principal volatile components in grape and pomegranate vinegar in the industrial samples (47).

According to Su and Chien (50), acetic acid (the vinegar odor), 2/3-methylbutanoic acid (sweaty odor), phenethyl acetate (sweet, honey odor), 2-phenyl ethanol (rosy, sweet odor), octanoic acid (sweaty odor), eugenol (clove odor), and phenylacetic acid were the most significant aroma-active compounds in the vinegar produced (overall floral odor). Some substances, including linalool (floral, cut grass odor), 2,3-butanedione (buttery odor), (E,Z)-2,6-nonadienal (cucumber odor), ethyl butanoate (apple, fruity odor), low concentrations or not detected by GC-MS.

A study on the volatile compounds in 56 balsamic vinegar samples, old traditional balsamic vinegar, and regular vinegar from Modena and Reggio Emilia, Italy, was conducted by Del Signore (51). Traditional balsamic vinegar contains less propionic acid and more esters than common balsamic vinegar. 2,3-Butanediol diacetate is found in higher concentrations in traditional balsamic vinegar. Conventional balsamic vinegar had higher concentrations of diacetyl, hexanal, and heptanal than balsamic, common, and other vinegar types (five times smaller in quantity). In terms of alcohol, traditional balsamic vinegar showed higher levels of octanol, whereas balsamic vinegar contained higher levels of 1-propanol, isobutyl alcohol, isoamyl alcohol, and 1-hexanol. 2-propanol and ethanol were more common in regular vinegar (51).

The maturation of the vinegar has a considerable impact on the organic acids (lactic, acetic, and succinic) and volatile substances (2-butanol, 2-propen-1-ol, 4-ethylguaiacol, and eugenol) of vinegar (17). These chemicals were discovered to be more prevalent in vinegar with increasing maturation levels. When compared to inoculated fermentation, spontaneous fermentation produces significantly higher amounts of esters during alcoholic fermentation (35).

Using HPLC-DAD technology to analyze the sugarcane original vinegar and its derivative products, sugarcane vinegar beverage is rich in phenolic substances, such as vanillin, coumarin, chlorogenic acid, caffeic acid, ferulic acid, p-coumaric acid, 10 types of luteolin in celery, cinnamic acid, and kaempferol, among which the contents of vanillin, coumarin, chlorogenic acid, and caffeic acid are relatively high (original sugarcane vinegar>5 ppm, sugarcane vinegar drink>2 ppm), the contents of apigenin, luteolin, cinnamic acid, and kaempferol are low (sugarcane original vinegar<33.99 ppm, sugarcane vinegar drink<0.1 ppm), and the total phenolic content of sugarcane vinegar was found to be higher (Table 1). The beverage types and content of polyphenols in sugarcane vinegar beverages were 2.5 times and five times higher than those of commercially available apple cider vinegar beverages and significantly higher than those of similar commercially available vinegar beverage products (52). The main components of organic acids in original sugarcane vinegar were identified by HPLC-UV, i.e., oxalic acid, tartaric acid, acetic acid, and succinic acid.

Sugarcane fruit wine and sugarcane vinegar were fermented with sugarcane mixed juice as raw materials. The automatic amino acid analyzer determined the types and content changes of amino acids in sugarcane juice, sugarcane fruit wine, and sugarcane vinegar. The nutritional and taste intensity values (TAVs) were used to compare fermented sugarcane products. It was found that sugarcane juice, sugarcane fruit wine, and sugarcane vinegar all contained different types of amino acids (such as glycine, leucine, methionine, tyrosine, histidine, threonine, alanine, isoleucine, and tryptophan acids,/lysine, aspartic acid, valine, phenylalanine, proline, serine, glutamic acid, and arginine), total amino acids (TAA), essential amino acids (EAA), and flavor amino acids, which were significantly different. Methionine and cysteine were the first limiting amino acids in sugarcane vinegar (Table 1). The ratio of EAA in sugarcane wine and sugarcane vinegar tended to be more reasonable than in sugarcane juice. Glutamic acid is the main flavor-contributing amino acid of sugarcane juice, sugarcane cider, and sugarcane vinegar, and its TAV was found to be between 1.3 and 2.4. Considering the ratio of essential amino acids, sugarcane fruit wine and sugarcane vinegar tend to be more reasonable, which can be prepared and eaten with other drinks or by developing new products to increase the biological nutritional value of the product (32).

The main sugar components (sucrose, fructose, and glucose) in original sugarcane vinegar identified by HPLC-UV make it clear that sucrose is the leading sugar source for active yeast and acetic acid bacteria to produce original sugarcane vinegar. The aroma

components of original sugarcane vinegar were determined by GC-MS, such as 5 alcohols (5.19%), 9 esters (59.01%), 5 aldehydes (0.42%), and 5 acids (27.92%). Four types of ketones (0.43%), 1 type of phenol (0.01%), 3 types of hydrocarbons (0.09%), and 1 type of other heterocycle (0.69%), of which ethyl lactate, iso-acetate, isoamyl alcohol, ethyl n-caproate, ethyl octanoate, acetic acid, n-octanoic acid, etc., are the aroma substances of sugarcane original vinegar (30) (Table 1).

Biological functions

With the help of *in vitro* and *in vivo* activity assessment, it was confirmed that the original sugarcane vinegar has biological functions, i.e., lowering blood lipid, improving anti-oxidative stress, reducing body weight, and organ enlargement. Sugarcane fruit wine and raw vinegar had a strong scavenging effect on DPPH and OH, which gradually increased with the increment of sample volume. The scavenging rate was higher than those of the control of Vc and gallic acid, among which was sugarcane raw vinegar. It may be related to the antioxidant components, such as polyphenols in the fermentation product, and the specific mechanism needs further exploration. Sugarcane fruit wine and original sugarcane vinegar have specific scavenging effects on NO_2 and strong chelating effects on metal ions, original sugarcane vinegar is better than sugarcane fruit wine. It can be seen that original sugarcane vinegar has good health effects. Using sugarcane juice to ferment and process new products can improve sugarcane utilization value and provide an advanced way to develop diversified high-value-added products (53).

By establishing a high-fat diet-induced hyperlipidemia mouse model, the effects of sugarcane raw vinegar on blood lipids, liver lipids, and redox capacity were studied in high-fat diet-induced lipid metabolism disorders. It was found that compared with the high-fat control group, administration of original sugarcane vinegar can significantly reduce the plasma levels of total cholesterol (TC), triglyceride (TG), and low-density lipoprotein cholesterol (LDL-C) in high-fat mice, increase high-density lipoprotein (HDL-C) level, effectively reduce amylase activity, increase lipase activity, and reduce blood sugar concentration and fat accumulation; sugarcane raw vinegar can also increase the activity of superoxide dismutase (SOD) and glutathione peroxide (GSH-Px) in plasma and the liver and reduce the activity of nitric oxide synthase (NOS), and lipid peroxidation reaction products in liver malondialdehyde (MDA) content can enhance the anti-oxidative stress level (54). The differences in body weight, organ coefficients, and serum biochemical indicators between mice fed high-fat sugarcane vinegar and the model group were analyzed. It was found that the weight gain of mice fed a high-fat diet was significantly higher than that of mice in the control group. Compared with the model group, there were very significant differences. The high-concentration of sugarcane original vinegar could effectively reduce the body weight of high-fat mice; with the exception of the lung being significantly increased, other organs had no significant difference between the sugarcane original vinegar and the other groups. Sugarcane original vinegar can substantially control the body weight of mice fed a high-fat diet. A high concentration of original sugarcane vinegar can effectively reduce body weight and lower blood lipid levels and does not affect the organ index of mice. The recent experimental findings showed that original sugarcane vinegar regulates blood lipids, improves anti-oxidative stress, reduces body weight and organ enlargement, and helps to inhibit the development of hyperlipidemia, obesity, and complications (12, 31, 55).

Social and economic benefits

Original sugarcane vinegar plays an essential role in promoting the transformation and upgradation of the cane sugar industry, stimulating the enthusiasm for sugarcane planting in China's "sea of sugarcane" and "sugar capital", and doubling the income of sugarcane farmers. At the same time, increased employment opportunities for related industry workers in Guangxi sugarcane areas extended the sugarcane industry chain and stimulated local social and economic development. The economic and social benefits of the project are remarkable, which has promoted the development of the traditional brewing industry to standardized intelligent manufacturing and significantly promoted the upgradation of the China cane sugar industry and the process of secondary entrepreneurship around the globe.

Conclusion and future directions

Although numerous types of volatile organic compounds (VOCs) in various kinds of vinegar, particularly in the well-known and traditional vinegar products, have been studied, the VOCs can be derived from their primary raw materials, associated microorganisms, heating, aging, or other processes. In addition, the majority of VOCs dynamically change during the vinegar-making process; therefore, it is highly challenging to explain the production processes of VOCs. Future research should at least focus on the following factors to better understand and investigate VOCs. Metagenomics, metaproteomics, and metabolomics are examples of multi-omics technologies that could be used to understand better how microbes make VOCs and how various bacteria contribute to VOC production.

Author contributions

G-LC, F-JZ, and BL contributed to the conceptualization, methodology, investigation, resources, software, writing, and editing of the review, as well as project administration, and funding acquisition. Y-XY, X-CF, KV, and L-FY contributed to the resources, software, and data processing. All authors have read and approved the article for publication.

Funding

This study received funding from the Guangxi Major Science and Technology Program (Grant no. GK-AA22117002), Xixiangtang Science and Technology Program of Nanning, Guangxi (Grant no. 2020032101), the Project of Guangxi Agricultural Science and Technology Innovation Alliance (Grant

no. GNKM202315), and Guangxi Academy of Agricultural Sciences Basic Research Business Project (Grant no. GNK2021YT117).

Acknowledgments

The authors would like to thank the Guangxi Academy of Agricultural Sciences, Nanning, Guangxi, China, for providing the necessary facilities for this study.

Conflict of interest

The authors declare that the research was conducted in the absence of any commercial or financial relationships that could be construed as a potential conflict of interest.

Publisher's note

All claims expressed in this article are solely those of the authors and do not necessarily represent those of their affiliated organizations, or those of the publisher, the editors and the reviewers. Any product that may be evaluated in this article, or claim that may be made by its manufacturer, is not guaranteed or endorsed by the publisher.

References

1. Lobo V, Patil A, Phatak A, Chandra N. Free radicals, antioxidants and functional foods: impact on human health. *Pharmacogn Rev.* (2010) 4:118–26. doi: 10.4103/0973-7847.70902

2. Coelho E, Genisheva Z, Oliveira JM, Teixeira JA, Domingues L. Vinegar production from fruit concentrates: effect on volatile composition and antioxidant activity. *J Food Sci Technol.* (2017) 54:4112–22. doi: 10.1007/s13197-017-2783-5

3. Solieri L, Giudici P. *Vinegars of the World*. Germany: Springer. (2009) p. 1–16. doi: 10.1007/978-88-470-0866-3_1

4. Budak NH, Aykin E, Seydim AC, Greene AK, Guzel-Seydim ZB. Functional properties of vinegar. *J Food Sci.* (2014) 79:757–64. doi: 10.1111/1750-3841.12434

5. Matsushita K, Toyama H, Tonouchi N, Okamoto-Kainuma A. *Acetic Acid Bacteria. Ecology and Physiology*. Japan: Springer. (2016). doi: 10.1007/978-4-431-55933-7

6. Sengun IY. *Acetic Acid Bacteria: Fundamentals and Food Applications*. (2017). Boca Raton, FL: CRC Press. doi: 10.1201/9781315153490

7. Chen H, Chen T, Giudici P, Chen F. Vinegar functions on health: constituents, sources, formation mechanisms. *Compr Rev Food Sci.* (2016) F15, 1124–38. doi: 10.1111/1541-4337.12228

8. Xie Z, Koysomboon C, Zhang H, Lu Z, Zhang X, Chen F. Vinegar volatile organic compounds: analytical methods, constituents, and formation processes. *Front Microbiol.* (2022) 13:907883. doi: 10.3389/fmicb.2022.907883

9. Farcas AC, Socaci SA, Mudura E, Dulf FV, Vodnar DC, Tofana M, et al. Exploitation of brewing industry wastes to produce functional ingredients. In: Kanauchi M, editor. *Brewing Technology Rijeka*. Croatia: InTech. (2017) 137–56. doi: 10.5772/intechopen.69231

10. Hong YC. After the end of chronic disease. In: Hong YC, editor. *The Changing Era of Diseases*. London, UK: Academic Press. (2019) p. 145–74. doi: 10.1016/B978-0-12-816439-6.00005-3

11. Salanta LC, Uifalean A, Iuga CA, Tofana M, Cropotova J, Pop OL, et al. (2020). Valuable food molecules with potential benefits for human health. In: *The Health Benefits of Foods–Current Knowledge and Further Development*. London, UK: IntechOpen. (2020)

12. Mahabir S. Methodological challenges conducting epidemiological research on nutraceuticals in health and disease. *Pharma Nutr.* (2014) 2:120–5. doi: 10.1016/j.phanu.2013.06.002

13. Khedkar S, Carraresi L, Bröring S. Food or pharmaceuticals? Consumers' perception of health-related borderline products. *Pharma Nutr.* (2017) 5:133–40. doi: 10.1016/j.phanu.2017.10.002

14. Oliveira ER, Caliari M, Soares MSS, Oliveira AR, Duarte RCM, Boas EVdeBV. Assessment of chemical and sensory quality of sugarcane alcoholic fermented beverage. *Food Sci Technol.* (2018) 55:72–81. doi: 10.1007/s13197-017-2792-4

15. Gulcin I. Antioxidant activity of food constituents: an overview. *Arch Toxicol.* (2012) 86:345. doi: 10.1007/s00204-011-0774-2

16. Chang R, Lee H, Ou S. Investigation of the physicochemical properties of concentrated fruit vinegar. *J Food Drug Anal.* (2005) 13:348–56. doi: 10.38212/2224-6614.2559

17. Madrera RR, Lobo AP, Alonso JJM. Effect of cider maturation on the chemical and sensory characteristics of fresh cider spirits. *Food Res Int.* (2010) 43:70–8. doi: 10.1016/j.foodres.2009.08.014

18. Junior MMS, Silva LOB, Leao DJ, Ferreira SLC. Analytical strategies for determination of cadmium in Brazilian vinegar samples using ET AAS. *Food Chem.* (2014) 160:209–13. doi: 10.1016/j.foodchem.2014.03.090

19. Ho CW, Lazim AM, Fazry S, Zaki UKHH, Lim SJ. Varieties, production, composition and health benefits of vinegars: a review. *Food Chem.* (2017) 221:1621–30. doi: 10.1016/j.foodchem.2016.10.128

20. Morales ML, González GA, Casas JA, Troncoso AM. Multivariate analysis of commercial and laboratory produced Sherry wine vinegars: Influence of acetification and aging. *Eur Food Res Technol.* (2001) 212:676–82. doi: 10.1007/s002170100301

21. Callejon RM, Tesfaye W, Torija MJ, Mas A, Troncoso AM, Morales ML, et al. Volatile compounds in red wine vinegars obtained by submerged and surface acetification in different woods. *Food Chem.* (2009) 113:1252–9. doi: 10.1016/j.foodchem.2008.08.027

22. Tesfaye W, Morales ML. Garcia-Parrilla MC, Troncoso AM. Wine vinegar: technology, authenticity and quality evaluation. *Trends Food Sci Technol.* (2002) 13:12–21. doi: 10.1016/S0924-2244(02)00023-7

23. Lu S, Cao Y, Yang Y, Jin Z, Luo X. Effect of fermentation modes on nutritional and volatile compounds of Huyou vinegar. *J Food Sci Technol.* (2018) 55:2631–40. doi: 10.1007/s13197-018-3184-0

24. Vegas C, Mateo E, González Á, Jara C, Guillamón JM, Poblet M, et al. Population dynamics of acetic acid bacteria during traditional wine vinegar production. *Int J Food Microbiol.* (2010) 138:130–6. doi: 10.1016/j.ijfoodmicro.2010.01.006

25. Tan SC. *Vinegar Fermentation [M.Sc. Thesis]*. Baton Rouge: Louisiana State University. Department of Food Science. (2005).

26. Johnston CS, Gaas CA. Vinegar: medicinal uses and antiglycemic effect. *Medscape General Med.* (2006) 8:61.

27. Marrufo-Curtido A, Cejudo-Bastante MJ, Durán-Guerrero E, Castro-Mejías R, Natera-Marín R, Chinnici F, et al. (2012). Characterization and differentiation of high-quality vinegars by stir bar sorptive extraction coupled to gas chromatography-mass spectrometry (SBSE-GC-MS). *LWT.* (2012) 47:332–341. doi: 10.1016/j.lwt.2012.01.028

28. Chen F, Li L, Qu J, Chen C. Cereal vinegars made by solid-state fermentation in China. In: Solieri L, Giudici P, editors.Vinegars of the World. (Milan: Springer). (2009) p. 243–59. doi: 10.1007/978-88-470-0866-3_15

29. Li YR, Yang LT. Research and development priorities for sugar industry of China: recent research highlights. *Sugar Tech.* (2014) 17:9–12. doi: 10.1007/s12355-014-0329-y

30. Chen GL, Zheng FJ, Lin B, Lao SB, He J, Huang Z, et al. Phenolic and volatile compounds in the production of sugarcane vinegar. *ACS Omega.* (2020) 5:30587–95. doi: 10.1021/acsomega.0c04524

31. Lin Bo, Zheng F, Fang X, Chen G. Comparison of amino acids and analysis of nutrition and flavor on sugarcane fermentation products. *Farm Prod Process.* (2022) 15:64–9. doi: 10.16693/j.cnki.1671-9646(X)2022.08.015

32. Chen GL, Zheng FJ, Sun J, Li ZC, Lin B, Li Y. R., et al. Production and characteristics of high quality vinegar from sugarcane juice. *Sugar Tech.* (2015) 17:89–93. doi: 10.1007/s12355-014-0352-z

33. Nualsria C, Reungsang A, Plangklang P. Biochemical hydrogen and methane potential of sugarcane syrup using a two-stage anaerobic fermentation process. *Ind Crops Prod.* (2016) 82:88–99. doi: 10.1016/j.indcrop.2015.12.002

34. Valles BS, Bedrinana RP, Tascon NF, Garcia AG, Madrera RR. Analytical differentiation of cider inoculated with yeast (*Saccharomyces cerevisiae*) isolated from Asturian (Spain) apple juice. *LWT - Food Sci Technol.* (2005) 38:455–61. doi: 10.1016/j.lwt.2004.07.008

35. Ubeda C, Callejón RM, Hidalgo C, Torija MJ, Troncoso AM, Morales ML, et al. Employment of different processes for the production of strawberry vinegars: Effects on antioxidant activity, total phenols and monomeric anthocyanins. *LWT – Food Sci Technol.* (2013) 52:139–45. doi: 10.1016/j.lwt.2012.04.021

36. Ibarz MJ, Hernandez-Orte P, Cacho J, Ferreira V. Kinetic study, production of volatile compounds and sensorial analysis in the fermentation of airen and merlot musts inoculated with three commercial strains of *Sacharomyces cerevisiae*. *Recent Res Develop Agric Food Chem.* (2005) 6:55.

37. Chen GL, Zheng FJ, Lin B, Wang TS, Li YR. Preparation characteristics of sugarcane low alcoholic drink by submerged alcoholic fermentation. *Sugar Tech.* (2013) 15:412–6. doi: 10.1007/s12355-013-0248-3

38. Raspor P, Goranovic D. Biotechnological applications of acetic acid bacteria. *Crit Rev Biotechnol.* (2008) 28:101–24. doi: 10.1080/07388550802046749

39. Xu QP. *The Vinegar Production Technology*. Beijing: Chemical Industry Press (2008).

40. Zheng F, Chen GL, Fang X, Sun J, Lin B, Liu G, et al. of acetic acid bacteria on acetic acid fermentation of sugarcane fruit wine. *Food Fermentation Indust.* (2016) 48:101–7.

41. Wang Z, Lu Z, Shi J, Xu Z. Exploring flavour-producing core microbiota in multispecies solid-state fermentation of traditional Chinese vinegar. *Sci Rep.* (2016) 6:1–10. doi: 10.1038/srep26818

42. Rainieri S, Zambonelli C. Organisms associated with acetic acid bacteria in vinegar production. In: Solieri L, Giudici P, editors. Vinegars of the World. (Milan: Springer). (2009) p. 73–95. doi: 10.1007/978-88-470-0866-3_5

43. Li S, Li P, Feng F, Luo L. Microbial diversity and their roles in the vinegar fermentation process. *Appl Microbiol Biotechnol.* (2015) 99:1–28. doi: 10.1007/s00253-015-6659-1

44. Chen GL, Lin B, Sun J, Li YR. Alcohol fermentation from sugarcane juice with fruit wine yeast. *Food Ferm Indust.* (2011) 37:32. doi: 10.13995/j.cnki.11-1802/ts.2011.05.042

45. Zhu Y, Zhang F, Zhang C, Yang L, Fan G, Xu Y, et al. Dynamic microbial succession of Shanxi aged vinegar and its correlation with favor metabolites during different stages of acetic acid fermentation. *Sci Rep.* (2018) 8:1–10. doi: 10.1038/s41598-018-26787-6

46. Jiang Y, Lv X, Zhang C, Zheng Y, Zheng B, Duan X, et al. Microbial dynamics and flavor formation during the traditional brewing of Monascus vinegar. *Food Res Int.* (2019) 125:1–10. doi: 10.1016/j.foodres.2019.108531

47. Ozturk I, Caliskan O, Tornuk F, Ozcan N, Yalcin H, Baslar M, et al. Antioxidant, antimicrobial, mineral, volatile, physicochemical and microbiological characteristics of traditional home-made Turkish vinegars. *LWT - Food Sci Technol.* (2015) 63:144–51. doi: 10.1016/j.lwt.2015.03.003

48. Yu YJ, Lu ZM, Yu NH, Xu W, Li GQ, Shi JS, et al. HS-SPME/GC-MS and chemometrics for volatile composition of Chinese traditional aromatic vinegar in the Zhenjiang region. *J Inst Brewing.* (2012) 118:133–41. doi: 10.1002/jib.20

49. Pizarro C, Esteban-Díez I, Sáenz-González C, González-Sáiz JM. Vinegar classification based on feature extraction and selection from headspace solid-phase microextraction/gas chromatography volatile analyses: a feasibility study. *Anal Chim Acta.* (2008) 608:38–47. doi: 10.1016/j.aca.2007.12.006

50. Su MS, Chien PJ. Antioxidant activity, anthocyanins and phenolics of rabbiteye blueberry (*Vaccinium ashei*) fluid products as affected by fermentation. *Food Chem.* (2007) 104:182–7. doi: 10.1016/j.foodchem.2006.11.021

51. Del Signore A. Chemometric analysis and volatile compounds of traditional balsamic vinegars from Modena. *J Food Eng.* (2001) 50:77–90. doi: 10.1016/S0260-8774(00)00195-3

52. He J, Lao S, Lin B, Zheng F, Chen GL. Simultaneous detection of 11 phenolic substances in apple cider vinegar and sugarcane vinegar by high performance liquid chromatography-diode array technology. *Food Industry Sci Technol.* (2017) 38:210–31. doi: 10.13386/j.issn1002-0306.2017.23.039

53. Zheng F, Chen GL, Meng Y, et al. Analysis of antioxidant capacity of sugarcane juice fermentation products. *Southern Agric J.* (2015) 46:475–9.

54. Li ZC, Chen GL, Zheng FJ, Sun J, Lin B, Khoo HE, et al. Effects of sugarcane vinegar supplementation on oxidative stress and weight reduction in hyperlipidaemic mice. *Int Food Res J.* (2020) 27:1121–31.

55. Cejudo-Bastante MJ, Duran E, Castro R. Rodriguez-Dodero MC, Natera R, Garciá-Barroso C. Study of the volatile composition and sensory characteristics of new Sherry vinegar-derived products by maceration with fruits. *LWT Food Sci Technol.* (2013) 50:469–79. doi: 10.1016/j.lwt.2012.08.022

frontiers | Frontiers in Nutrition

TYPE Brief Research Report
PUBLISHED 27 March 2023
DOI 10.3389/fnut.2023.1142971

OPEN ACCESS

EDITED BY
Mustafa Abdullah Yilmaz,
Dicle University,
Türkiye

REVIEWED BY
Ziyin Yang,
South China Botanical Garden,
Chinese Academy of Sciences (CAS),
China
Branca M. Silva,
University of Beira Interior,
Portugal

*CORRESPONDENCE
Yong-Quan Xu
✉ yqx33@126.com
Jun-Feng Yin
✉ yinjf@tricaas.com

SPECIALTY SECTION
This article was submitted to Food Chemistry, a section of the journal Frontiers in Nutrition

RECEIVED 12 January 2023
ACCEPTED 08 March 2023
PUBLISHED 27 March 2023

CITATION
Gao Y, Han Z, Xu Y-Q and Yin J-F (2023) Chemical composition and anti-cholesterol activity of tea (*Camellia sinensis*) flowers from albino cultivars.
Front. Nutr. 10:1142971.
doi: 10.3389/fnut.2023.1142971

Chemical composition and anti-cholesterol activity of tea (*Camellia sinensis*) flowers from albino cultivars

Ying Gao[1], Zhen Han[2], Yong-Quan Xu[1]* and Jun-Feng Yin[1]*

[1]Key Laboratory of Tea Biology and Resources Utilization, Tea Research Institute Chinese Academy of Agricultural Sciences, National Engineering Research Center for Tea Processing, Hangzhou, China, [2]Agro-Technical Extension Station of Ningbo City, Ningbo, China

Albino tea cultivars are mutant tea plants with altered metabolisms. Current studies focus on the leaves while little is known about the flowers. To evaluate tea flowers from different albino cultivars, the chemical composition and anti-cholesterol activity of tea flowers from three albino cultivars (i.e., Baiye No.1, Huangjinya, and Yujinxiang) were compared. According to the results, tea flowers from Yujinxiang had more amino acids but less polyphenols than tea flowers from the other two albino cultivars. A reduced content of procyanidins and a high chakasaponins/floratheasaponins ratio were characteristics of tea flowers from Yujinxiang. *In vitro* anti-cholesterol activity assays revealed that tea flowers from Yujinxiang exhibited stronger activity in decreasing the micellar cholesterol solubility, but not in cholesterol esterase inhibition and bile salt binding. It was noteworthy that there were no specific differences on the chemical composition and anti-cholesterol activity between tea flowers from albino cultivars and from Jiukeng (a non-albino cultivar). These results increase our knowledges on tea flowers from different albino cultivars and help food manufacturers in the cultivar selection of tea flowers for use.

KEYWORDS

tea flowers, albino cultivars, chemical composition, anti-cholesterol, polyphenols, amino acids, saponins

1. Introduction

Camellia sinensis is a flowering plant in the Theaceae family. Its leaves have been used to produce tea, a globally popular beverage, for centuries. Therefore, *Camellia sinensis* is regarded as an important economic plant and widely cultivated. Tea flowers are reproductive organs of *Camellia sinensis*, usually white in color, blooming from September to December. The yield of tea flowers in matured tea gardens is about 2.86–4.29 tons/acre (1). Unlike tea leaves, tea flowers were under-evaluated in the past and mostly discarded as wastes. Recent researches have revealed that multiple bioactive compounds in tea leaves also exist in tea flowers (2). Compared with tea leaves, tea flowers contain more soluble sugars, but less polyphenols and caffeine (3). Evidences indicate that tea flowers display various bioactivities (2). Anti-cholesterol activity is a featuring activity of tea flowers. Cholesterol is a type of lipid which acts as an essential structural component of animal cell membranes and serves as precursor for bile acids, vitamin D, and steroid hormones (e.g., estrogen and testosterone) (4). However, too much cholesterol is harmful to the body, which is associated with the

increased incidence of coronary artery diseases. Deng and Huang found that tea flowers exhibited anti-cholesterol activity *in vitro* (5). Ling et al. proved that oral administration of tea flowers significantly reduced the levels of serum total cholesterols and low density lipoproteins in high-fat diet-fed rats (6). Due to the excellent bioactivity and safety, tea flowers were approved as novel food components by the National Health Commission of the People's Republic of China in 2013, which permitted the legal application of tea flowers in commercial foods. By now, tea flowers have been used in beverages and snacks to improve the health-beneficial function (7, 8).

The health-beneficial function of tea flowers is determined by the chemical components. It has been reported that the chemical components in tea flowers are affected by the floral organ, flowering stage, growth area, and cultivar (3, 9–11). The cultivar not only has an impact on the levels of general components (e.g., catechins), but also on the presence of specific components (e.g., anthocyanins) (12).

Albino tea cultivars are mutant tea plants whose leaves are notably lighter in color compared with non-albino tea leaves due to the lack of chlorophylls (13). The balance of carbon and nitrogen metabolism is hampered in albino leaves, resulting in the accumulation of free amino acids and the shortage of polyphenols (14), which makes albino tea taste less bitter and astringent than non-albino tea. The synthesis of volatiles in albino tea leaves is also altered, leading to a more ethereal smell (15). Currently, more attentions are paid on studying the leaves than flowers of albino tea plants. Little is known about tea flowers from albino cultivars. In this study, the chemical composition and anti-cholesterol activity of tea flowers from three albino cultivars (i.e., Baiye No. 1, Huangjinya, and Yujinxiang) and one traditional non-albino cultivar (i.e., Jiukeng) were investigated. The results will enhance our knowledge on tea flowers from different cultivars and guide food producers choose the proper tea flowers for applications.

2. Materials and methods

2.1. Tea flower samples and reagents

Dried tea flower samples were provided by Yuyao Sichuangyan Tea Co. Ltd (Zhejiang, China). The tea flowers were collected at the half-open period from the same tea garden in Yuyao City, Zhejiang Province, China, in November. Tea flowers were withered for 4 h, dried by hot air at 40°C for 1 h (Hot air dryer, Product No. 6CHZ-9B, Fujian Jiayou tea machinery Co., Ltd., Fujian, China), cooled for 30 min, dried by hot air at 55°C for 1 h and at 70°C for 1 h to obtain dried tea flowers. The weight of fresh tea flowers in each batch was 50 kg. Three batches of samples were prepared for each cultivar.

Sodium cholate, sodium taurocholate, sodium glycocholate, and sodium chloride were purchased from Shanghai Macklin Biochemical Technology Co., Ltd (Shanghai, China). Cholesterol, cholesterol esterase, 4-nitrophenyl butyrate, cholestyramine, and epigallocatechin gallate (EGCG) were purchased from Shanghai Yuanye Bio-Technology Co., Ltd (Shanghai, China). Oleic acid was purchased from Sigma-Aldrich (Shanghai) Trading Co., Ltd (Shanghai, China).

2.2. Chemical composition analysis

Each tea flower sample was ground and filtered through a 60 Tyler mesh sieve. The tea flower powder was extracted with distilled water (3:500 w/v) at 100°C for 40 min and centrifuged at 8,000 g for 10 min to remove powder residues. The supernatant was used for analysis.

The total phenolic content was measured according to the national standard GB/T 8313–2008. The contents of eight monomeric catechins were measured using a published HPLC method (16). The content of free amino acids was measured according to the national standard GB/T 8314–2013. The composition of free amino acids was measured by an amino acid analyzer (Sykam S433-D, Eresing, Germany) using a previous method (17). Detailed description of each method was presented in the supplementary material.

The content of soluble sugars was measured using anthrone-sulfuric acid method. In brief, 1 mL sample solution was mixed with 4 mL anthrone-sulfuric acid, incubated at 100°C for 10 min, cooled to room temperature, and then measured the absorbance at 620 nm. To measure the soluble polysaccharide content, the polysaccharide was precipitated by mixing the sample solution with ethanol at a ratio of 1:5, cooled at 4°C overnight, and centrifuged at 8,500 g for 10 min. The precipitate was re-dissolved with distilled water to prepare the solution for the anthrone-sulfuric acid assay. The contents of sucrose, fructose, and glucose were determined using corresponding commercial kits (Beijing Solarbio Science & Technology Co., Ltd., Products No. BC2465, BC2455, and BC2500, Beijing, China).

The content of saponins was measured using the vanillin-sulfuric acid method. A 100 μL sample solution was mixed with 0.5 mL 8% vanillin-alcohol solution and 3 mL 70% sulfuric acid, incubated at 60°C for 10 min, cooled to room temperature, and read the absorbance at 540 nm.

Ultrahigh performance liquid chromatography-Q Exactive-Orbitrap-mass spectrometry (UPLC-QE-Orbitrap-MS) was used to determine the composition of procyanidins, organic acids, flavonols, methylxanthines, and saponins, based on published methods with modifications (11, 18). The separation was performed on an ACQUITY UPLC BEH C18 column (1.7 μm, 2.1 mm × 100 mm, Waters, Milford, MA, United States) using a Dionex Ultimate 3,000 RS system. A 0.1% formic acid in water and acetonitrile was used as mobile phases A and B. To determine procyanidins, methylxanthines, and organic acids, the gradient changes of mobile phases were 0–1 min, 5% B; 1–2 min, 5–10% B; 2–6 min, 10–35% B; 6–8.5 min, 35–100% B; 8.5–9.5 min, 100% B; 9.5–10 min, 100–5% B; and 10–12 min, 5% B. To determine saponins, the gradient changes of mobile phases were 0–5 min, 25–35% B; 5–6 min, 35–37% B; 6–15 min, 37–45% B; 15–18 min, 45–100% B; 18–19 min, 100% B; 19–20 min, 100–25% B; and 20–22 min, 25% B. To determine flavonols, the gradient changes of mobile phases were 0–6 min, 10–30% B; 6–9.5 min, 30–100% B; 9.5–10 min, 100–10% B; 10–12 min, 10% B. The total flow rate was 0.3 mL/min. The column temperature was 40°C. The MS analysis was conducted using the QE-Orbitrap mass spectrometer (Thermo Scientific, United States) with electrospray ionization (ESI), operating in the positive and negative ionization full scan modes. Auxiliary gas and sheath gas flow rates were 10 and 45 (arbitrary units), respectively. The auxiliary gas heater temperature was 300°C. The capillary temperature was 320°C. The spray voltage was 3.1 kV and the S-lens RF level was 50 V. The normalized collision energy (NCE) was 30 eV. The resolution of the

full scan and ddMS2 were 70,000 and 35,000, respectively. The full MS scan ranges were set from m/z 100 to 1,500. Data were acquired and processed using ThermoXcalibur 3.0 software (Thermo Scientific, United States). Tentative identification was based on comparing retention time, m/z values, and MS/MS fragments with standards or data from databases (e.g., MzCloud) when standards were unavailable (Detailed information is provided in Supplementary Table S1 and Supplementary Figure S1). Relative quantitation was calculated by comparing the relative intensities of the parent ions among samples and presented in a heat map after converting to Z-scores of the rows.

2.3. Micellar cholesterol solubility assay

The assay was conducted based on a previously published method (19). The micellar cholesterol solution consisted of 2 mmol/L cholesterol, 10 mmol/L sodium taurocholate, 5 mmol/L oleic acid, 132 mmol/L sodium chloride, and 15 mmol/L phosphate buffered saline (0.1 mol/L, pH = 7.4). One hundred microliter tea flower solution (or distilled water as the control) was mixed with 900 μL micellar cholesterol solution. One hundred microliter tea flower solution was mixed with 900 μL distilled water as the sample control. The mixture was incubated at 37°C for 1 h and centrifuged at 15,000 g for 20 min. The cholesterol concentration of the supernatant was measured using a total cholesterol assay kit (Nanjing Jiancheng Bioengineering Institute, Product No. A111-1-1, Nanjing, China). The remaining cholesterol (%) was calculated as follows.

$$\text{Remaining cholesterol}(\%) = \frac{A_{\text{sample}} - A_{\text{sample control}}}{A_{\text{control}}} \times 100\%$$

2.4. Cholesterol esterase inhibition assay

The assay was conducted based on a previously published method (20). One milliliter phosphate buffered saline (0.1 mol/L, pH = 7.0) containing 5.16 mmol/L sodium taurocholate and 0.1 mol/L sodium chloride was mixed with 50 μL cholesterol esterase (5 mU/mL), 20 μL 4 mmol/L 4-nitrophenyl butyrate, and 50 μL tea flower infusion (or 50 μL distilled water as the control). One milliliter phosphate buffered saline was mixed with 50 μL distilled water, 20 μL 4 mmol/L 4-nitrophenyl butyrate, and 50 μL tea flower infusion as the sample control. The mixture was incubated at 25°C for 30 min. The absorbance at 405 nm was measured and recorded as A_{sample} (or $A_{control}$). The inhibition rate was calculated using the following formula.

$$\text{Inhibition}(\%) = \frac{A_{\text{control}} - \left(A_{\text{sample}} - A_{\text{sample control}}\right)}{A_{\text{control}}} \times 100\%$$

2.5. Bile salt binding assay

The assay was conducted based on a previously published method (5) with some modifications. One hundred microliter tea flower infusion (or distilled water as the control) was mixed with 400 μL 0.5 mmol/L bile salt (sodium cholate, sodium taurocholate, or sodium glycocholate). One hundred microliter tea flower infusion was mixed with 400 μL distilled water as the sample control. and incubated at 37°C for 1 h. The mixture was centrifuged at 4,000 g for 20 min to obtain the supernatant. Two hundred microliter supernatant was mixed with 600 μL 60% sulfuric acid, incubated at 70°C for 20 min. After cooling to room temperature, the absorbance at 387 nm was determined. The bile salt binding rate was calculated as follows.

$$\text{Bile salt binding rate}(\%) = \frac{A_{\text{control}} - \left(A_{\text{sample}} - A_{\text{sample control}}\right)}{A_{\text{control}}} \times 100\%$$

2.6. Statistical analysis

The data are presented as the mean ± standard error of the mean (SEM). All experiments were carried out in triplicate and repeated in three independent sets of experiments. The results were analyzed with SPSS Version 18.0 for Windows using the one-way analysis of variance with *post hoc* test (2-sided Dunnett's test). The difference was deemed significant if the value of p was less than 0.05. Partial least squares regression was performed using the SIMCA 13.0 software.

3. Results and discussion

3.1. Chemical composition

General chemical analysis (Table 1) revealed that soluble sugars were the most abundant component in tea flowers, accounting for about 40%. Saponins were the second most abundant component, occupying over 10%. Polyphenols listed the third.

The content of soluble sugars was insignificantly different among the four samples, ranging from 400.74 to 449.30 mg/g. Xu et al. revealed that the content of soluble sugars in Longjing No.43 (a non-albino cultivar) tea flowers from Zhejiang Province was 422.73 mg/g (21). It provided more evidence that the content of soluble sugars was similar among cultivars. Sucrose, fructose, and glucose were major soluble sugars in tea flowers (Table 2), which was consistent with a previous study (21). The three small molecular sugars together made up about 70% of total soluble sugars. Baiye No.1, a temperature-sensitive albino cultivar., contained the least sucrose but the most glucose among the four samples. Though both belonging to light-sensitive albino cultivars, Yujinxiang had a higher glucose content than Huangjinya. The content of fructose was insignificantly different. Soluble polysaccharides, which were macromolecules contributing to the thick taste of tea infusions and displayed multiple bioactivities such as antioxidant and α-glucosidase inhibitory activity (18, 22), were observed in tea flowers, ranging from 12.4 to 16.2 mg/g (Table 1). Yujinxiang had a higher content of soluble polysaccharides compared with the other three. Huang et al. previously demonstrated that the content of soluble polysaccharides in tea flowers from non-albino cultivars ranged from 1.54 to 2.34% (23), most of which were higher than our results. It implied that the content of soluble polysaccharides was affected by the cultivar.

TABLE 1 The chemical compositions of four tea flowers.

Content (mg/g)	Baiye No.1	Huangjinya	Yujinxiang	Jiukeng
Free amino acids	27.74 ± 0.44^{b}	24.10 ± 0.95^{c}	36.35 ± 0.32^{a}	36.14 ± 0.44^{a}
Polyphenols	78.03 ± 1.17^{b}	83.21 ± 2.55^{a}	70.90 ± 0.56^{c}	77.03 ± 0.22^{b}
Soluble sugars	414.95 ± 31.19^{a}	400.74 ± 16.11^{a}	449.30 ± 16.87^{a}	436.37 ± 22.31^{a}
Soluble polysaccharides	14.23 ± 0.12^{b}	13.17 ± 0.51^{b}	16.19 ± 1.21^{a}	12.40 ± 0.68^{b}
Saponins	122.11 ± 2.37^{ab}	135.02 ± 4.83^{a}	115.76 ± 3.35^{b}	120.84 ± 2.44^{ab}

The same letter within each row indicates no significant difference ($p > 0.05$).

The content of saponins was varied among the four samples, ranging from 115.76 to 135.02 mg/g (Table 1). Huangjinya had the highest, while Yujinxiang had the least. The content of saponins in tea flowers was comparable to that in *Panax ginseng C. A. Meyer* flowers (24) and in *Panax Notoginseng* flowers (25), two plants which were abundant in saponins, indicating that tea flowers might be a good source of plant-derived saponins. UPLC-QE-Orbitrap-MS analysis revealed that the composition of saponins was distinct, especially between Yujinxiang and the other three samples (Figure 1A). The contents of chakasaponins I, II, and III were highest in Yujinxiang while lowest in Huangjinya. In contrast, the content of floratheasaponins was lowest in Yujinxiang. Floratheasaponins B, E, and F were accumulated in Huangjinya. Floratheasaponins A, D, and H were accumulated in Baiye No.1. A previous study indicated that distinct regional difference was observed with respect to the content of chakasaponins and floratheasaponins. The content of chakasaponins was higher in the extracts of tea flowers from Fujian and Sichuan provinces, China than those from Japan, Taiwan, and India (26). Shen et al. found that floratheasaponins were more abundant than chakasaponins in tea flowers from Jiaming No.1, Longjing No.43, and Baiye No.1 (11). On the contrary, chakasaponins were more abundant than floratheasaponins in tea flowers from Yingshuang and Fudingdabai. Our results confirmed that the abundances of floratheasaponins and chakasaponins in tea flowers were affected by the cultivar. Previous studies indicated that the activity of each saponin monomer was not the same. For example, floratheasaponins A-F, particularly floratheasaponins B & E, displayed strong anti-allergic activity by inhibiting the release of β-hexosaminidase from RBL-2H3 cells (27). Chakasaponins I-III inhibited the increase of plasma triglycerides and glucose partially by preventing gastric emptying (28). It was possible that the differential composition and content of saponins might lead to differential bioactivity among cultivars.

The content of polyphenols ranged from 70.90 to 83.21 mg/g among the four samples, with the lowest content found in Yujinxiang (Table 1). Previous studies showed that the content of polyphenols in tea flowers from non-albino cultivars collected in Guangxi and Yunnan Province ranged from 9.17 to 13.56% (29, 30), which was much higher than that we observed in tea flowers from albino cultivars. However, in our study, the content of polyphenols in tea flowers from Jiukeng was not higher than that from Baiye No.1 and Huangjinya. The inconsistency might be caused by the fact that not only the cultivar but also the region affected the content of polyphenols (29, 30).

Eight monomeric catechins were observed in tea flowers. EGCG, ECG, and EC were the three most abundant ones. The monomeric catechin composition of the four tea flower samples was distinguishable (Table 2). Yujinxiang had the highest EGCG and GCG contents among them. Compared with Yujinxiang, the GC and C levels were higher in Huangjinya. Baiye No.1 had a higher EC level than the others. Besides monomeric catechins, procyanidin B1 and B2, belonging to dimeric catechins, were observed in tea flowers (Table 2). Procyanidin B2 was the predominant one, ranging from 1.50 to 7.51 mg/g, while the content of procyanidin B1 ranged from 0.28 to 2.19 mg/g. Tea flowers from Huangjinya had more procyanidin B2 and B1 than the others. The procyanidin B2 content in Huangjinya was five times as much as that in Yujinxiang. As for procyanidin B1, the level in Huangjinya was about 8.1-fold of that in Yujinxiang. The results demonstrated that the contents of dimeric catechins were quite different among the four samples. A similar trend was observed in the content of procyanidin C1 (Table 2). Monomeric catechins and procyanidins are star molecules in plants. As secondary metabolites, they protect the plants from microbial infection and high intensity light-induced stress (31, 32). As well-known health-beneficial components, they not only possess excellent antioxidant activity, but also are involved in the regulations of energy metabolisms, immunity, and gut microbiota (33). The differences on monomeric catechins and procyanidins among the four samples might lead to the differences on the bioactivity. Besides, monomeric catechins and procyanidins are typical astringent compounds, which play important roles in the taste of grape wine and tea (34, 35), implying that they may affect the taste of tea flowers as well.

Based on previous findings and our results (29, 30), the ratio of catechins/polyphenols in tea flowers was much lower than that in tea leaves, suggesting the presence of other categories of polyphenols. Flavonols are a class of flavonoids that have the 3-hydroxyflavone backbone. Many of them possess antioxidant capacity, anti-inflammatory activity, and antimicrobial activity (36). A former study revealed that flavonols mainly existed in the forms of monoglycosides, diglycosides, and triglycosides in tea flowers, with quercetin, myricetin, and kaempferol as the main aglycones (37). In this study, five quercetin glycosides, three myricetin glycosides, and five kaempferol glycosides were observed in tea flowers (Figure 1B). Compared with the other three cultivars, Baiye No.1 contained higher contents of quercetin, quercetin glucoside, quercetin rutinoside, myricetin, myricetin galactoside, and myricetin rutinoside, but less kaempferol and derivatives. Yujinxiang contained less quercetin and derivatives, while Huangjinya contained less myricetin and myricetin galactoside. The above results revealed that the composition of flavonols in tea flowers was cultivar-specific, which was in accordance with the previous findings in tea flowers from non-albino cultivars (12).

Amino acids participate in extensive biochemical process in the body (38). Accumulated amino acids is a typical characteristic of

10.3389/fnut.2023.1142971

TABLE 2 The contents of soluble sugars, monomeric catechins, procyanidins, free amino acids, organic acids, and methylxanthines in four tea flowers.

Contents	Baiye No.1	Huangjinya	Yujinxiang	Jiukeng
Soluble sugars (mg/g)				
Sucrose	88.38 ± 4.77^{c}	107.32 ± 7.17^{b}	114.90 ± 9.53^{b}	137.63 ± 1.09^{a}
Fructose	104.67 ± 5.09^{a}	96.15 ± 8.17^{a}	125.24 ± 24.14^{a}	90.15 ± 10.67^{a}
Glucose	89.62 ± 2.04^{a}	75.30 ± 3.66^{b}	90.43 ± 1.69^{a}	79.08 ± 0.94^{b}
Monomeric catechins (mg/g)				
Gallocatehin (GC)	1.91 ± 0.11^{d}	4.75 ± 0.12^{a}	3.07 ± 0.03^{c}	4.06 ± 0.04^{b}
Epigallocatechin (EGC)	1.82 ± 0.14^{a}	1.39 ± 0.04^{a}	1.46 ± 0.06^{a}	1.10 ± 0.02^{b}
Catechin (C)	0.99 ± 0.14^{a}	1.15 ± 0.04^{a}	0.15 ± 0.02^{c}	0.80 ± 0.03^{b}
Epigallocatechin gallate (EGCG)	8.89 ± 0.35^{c}	7.11 ± 0.17^{d}	12.96 ± 0.14^{a}	9.81 ± 0.09^{b}
Epicatechin (EC)	4.89 ± 0.18^{a}	4.17 ± 0.19^{b}	2.57 ± 0.31^{d}	3.61 ± 0.05^{c}
Gallocatechin gallate (GCG)	1.93 ± 0.09^{c}	1.30 ± 0.03^{d}	2.30 ± 0.03^{a}	2.09 ± 0.04^{b}
Epicatechin gallate (ECG)	4.05 ± 0.10^{b}	5.19 ± 0.12^{a}	5.01 ± 0.04^{a}	5.01 ± 0.05^{a}
Catechin gallate (CG)	0.37 ± 0.01^{c}	0.48 ± 0.02^{b}	0.51 ± 0.02^{b}	0.56 ± 0.01^{a}
Total monomeric catechins	24.85 ± 1.03^{c}	25.53 ± 0.70^{bc}	28.02 ± 0.44^{a}	27.03 ± 0.20^{ab}
Procyanidins (mg/g)				
Procyanidin B1	1.36 ± 0.01^{c}	2.19 ± 0.01^{a}	0.28 ± 0.01^{d}	1.49 ± 0.03^{b}
Procyanidin B2	5.10 ± 0.08^{b}	7.51 ± 0.06^{a}	1.50 ± 0.08^{d}	4.56 ± 0.19^{c}
Procyanidin C1	0.54 ± 0.03^{b}	0.82 ± 0.05^{a}	0.33 ± 0.02^{c}	0.48 ± 0.04^{b}
Free amino acids (μg/g)				
Aspartate	112.7 ± 4.2^{a}	55.9 ± 1.6^{c}	46.8 ± 3.3^{d}	63.7 ± 1.8^{b}
Threonine	163.4 ± 4.0^{b}	90.9 ± 6.9^{d}	189.1 ± 7.3^{a}	117.4 ± 9.0^{c}
Serine	799.6 ± 4.9^{a}	373.7 ± 1.1^{d}	605.6 ± 12.0^{b}	456.7 ± 19.2^{c}
Asparagine	181.4 ± 8.1^{a}	130.3 ± 4.3^{b}	135.2 ± 3.0^{b}	171.9 ± 8.1^{a}
Glutamic acid	707.2 ± 14.7^{a}	462.9 ± 8.6^{c}	428.9 ± 14.7^{d}	494.1 ± 7.2^{b}
Theanine	2914.4 ± 50.1^{c}	1339.8 ± 11.4^{d}	4124.5 ± 125.7^{b}	5357.4 ± 158.3^{a}
Proline	1124.8 ± 25.7^{b}	1173.2 ± 38.2^{b}	1580.9 ± 21.2^{a}	1503.7 ± 64.3^{a}
Glycine	42.3 ± 2.4^{a}	<LOQ^{c}	29.7 ± 2.8^{b}	23.2 ± 4.6^{b}
Alanine	1000.7 ± 15.9^{a}	595.6 ± 7.3^{c}	677.0 ± 29.3^{b}	580.2 ± 12.7^{c}
Valine	187.2 ± 36.9^{a}	126.6 ± 7.1^{a}	105.5 ± 8.2^{a}	155.1 ± 21.2^{a}
Methionine	179.5 ± 6.9^{b}	263.0 ± 3.3^{ab}	271.8 ± 13.1^{ab}	362.2 ± 21.8^{a}
Isoleucine	69.7 ± 7.3^{a}	40.0 ± 2.2^{b}	49.5 ± 4.7^{ab}	42.5 ± 0.5^{ab}
Leucine	41.9 ± 4.4^{a}	30.7 ± 2.4^{a}	19.1 ± 1.3^{a}	31.9 ± 3.2^{a}
γ-Aminobutyric acid	340.9 ± 10.1^{a}	288.6 ± 7.7^{b}	218.3 ± 12.6^{c}	338.4 ± 0.9^{a}
Histidine	64.3 ± 1.4^{c}	66.3 ± 1.3^{bc}	70.7 ± 1.4^{b}	99.8 ± 4.3^{a}
Ornithine	27.9 ± 5.3^{a}	35.0 ± 3.2^{a}	31.4 ± 2.4^{a}	31.4 ± 4.6^{a}
Lysine	48.3 ± 1.2^{a}	54.4 ± 6.6^{a}	44.0 ± 2.2^{b}	51.1 ± 4.2^{a}
Arginine	150.2 ± 3.3^{b}	358.1 ± 8.6^{a}	348.8 ± 8.8^{a}	440.1 ± 33.4^{a}
Organic acids (mg/g)				
Quinic acid	2.18 ± 0.02^{a}	1.69 ± 0.27^{b}	1.05 ± 0.03^{c}	1.59 ± 0.02^{b}
Gallic acid	4.95 ± 0.36^{a}	2.83 ± 0.15^{b}	4.23 ± 0.26^{a}	3.93 ± 0.21^{a}
Citric acid	15.16 ± 0.72^{a}	9.99 ± 0.32^{c}	12.25 ± 0.91^{b}	14.55 ± 0.40^{a}
Malic acid	8.40 ± 0.29^{a}	7.46 ± 0.47^{b}	7.37 ± 0.15^{b}	7.52 ± 0.16^{b}
Succnic acid	1.13 ± 0.01^{c}	1.70 ± 0.04^{a}	1.70 ± 0.05^{a}	1.51 ± 0.09^{b}
Methylxanthines (μg/g)				
Caffeine	4966.9 ± 124.3^{a}	4453.5 ± 122.4^{b}	3291.7 ± 69.8^{d}	4022.5 ± 20.1^{c}
Theobromine	157.7 ± 6.5^{a}	55.7 ± 4.4^{d}	84.8 ± 3.3^{c}	97.4 ± 4.2^{b}
Theophylline	9.3 ± 0.8^{a}	10.4 ± 1.0^{a}	4.5 ± 0.5^{b}	5.2 ± 0.2^{b}

The same letter within each row indicates no significant difference ($p > 0.05$). LOQ is short for the limit of quantification.

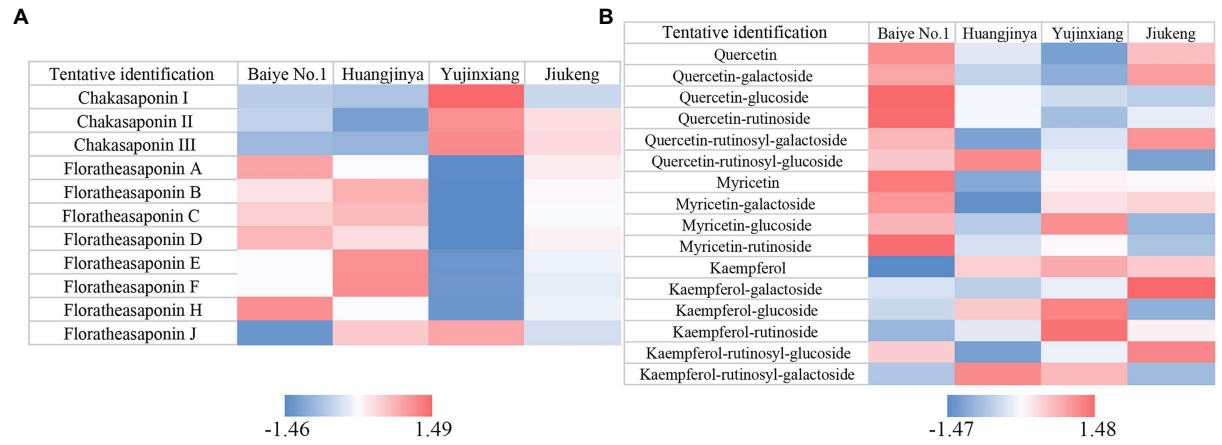

FIGURE 1
Heatmaps of Z-score normalized relative abundances of **(A)** saponins and **(B)** flavonols identified by UPLC-QE-Orbitrap-MS.

albino tea leaves (14). Enhanced theanine synthesis and reduced amino acid transport are found in albino tea leaves (39). In this study, 18 amino acids were observed in tea flowers, including 15 proteinogenic amino acids and 3 non-protein amino acids (i.e., theanine, γ-aminobutyric acid, and ornithine) (Table 2). Six of them belonged to essential amino acids, including threonine, valine, methionine, isoleucine, leucine, and lysine. These essential amino acids accounted for about 7.4–11.0% of total amino acids in the four tea flower samples. The percentage of essential amino acids in tea flowers from Huangjinya was higher than that in other three samples. Besides the nutritional value, some amino acids play dual roles in the taste and health benefits. For example, theanine is the key umami compound in tea and shows potentials in regulating the nervous system and multiple metabolisms (40). Theanine was the most abundant amino acids in tea flowers. It was unexpected that tea flowers from Jiukeng had a higher theanine content than the other three, implying that the theanine metabolism was not abnormal in tea flowers from albino cultivars. Among the three albino samples, the theanine content in Yujinxiang was three times as much as that in Huangjinya. Proline was the second most abundant amino acid. Tea flowers from Yujinxiang had about 40% more proline than that from Baiye No.1 and Huangjinya.

Citric acid, malic acid, gallic acid, quinic acid, and succinic acid were organic acids observed in tea flowers (Table 2), all of which were taste compounds. Citric acid, malic acid, and succinic acid have sour taste and are widely used as food ingredients to modify the flavor. Gallic acid and quinic acid have astringent taste. Compared with tea leaves (41), the levels of organic acids in tea flowers were much lower. Among the four samples, tea flowers from Baiye No.1 had a higher level of organic acids than others. The organic acid composition of each tea flower sample was varied, indicating the cultivar-specificity.

Methylxanthines are secondary metabolites derived from purine nucleotides and widely distributed in plants such as *Camellia sinensis* (42). Caffeine plays a role in plant defenses against abiotic and biotic stresses (43). In animals and humans, caffeine acts as a central nervous system stimulant, theobromine is used as a mild cardiac stimulant and vasodilator, and theophylline is used as a bronchodilator. The three methylxanthines were observed in these flower samples. Among them, caffeine was the major one, ranging from 3.29 to 4.97 mg/g. Yujinxiang possessed the lowest caffeine content, while Baiye No.1 had the highest. Compared with tea leaves, the caffeine content in tea flowers was much lower, indicating that tea flowers might be suitable for caffeine-sensitive consumers. Theobromine was the second abundant methylxanthine, ranging from 55.7 to 157.7 μg/g. The theobromine content in Huangjinya was almost three times as much as that in Baiye No.1. A trace of theophylline was also detected. A previous research indicated that the caffeine and theobromine contents in tea flowers from non-albino cultivars collected in Chongqing city were 1.89 to 4.94 mg/g and 103.0 to 169.9 μg/g, respectively (44). It implied that the cultivar rather than the region might have a more profound impact on the caffeine and theobromine contents.

These data suggested that the differences of tea flowers between albino cultivars and Jiukeng (a normal cultivar) on the chemical composition were not as much as expected. Reduction of polyphenols and accumulation of amino acids, which were representative characteristics of albino tea leaves, were not obvious in tea flowers from albino cultivars. Nevertheless, the content and composition of saponins, catechins, procyanidins, flavonols, amino acids, organic acids, and methylxanthines in tea flowers were varied among albino cultivars, which might lead to differential health-beneficial functions.

3.2. Anti-cholesterol activity

Previous researches demonstrated the effectiveness of tea flowers on anti-cholesterol activity *in vitro* and *in vivo* (5, 6). Absorption of dietary cholesterol is an important part of cholesterol homeostasis (45). It has been proved that the rate of intestinal cholesterol absorption is related to pancreatic cholesterol esterase activity (46). Inhibition of pancreatic cholesterol esterase effectively reduces cholesterol absorption *in vivo* (47). Bile salts not only protect cholesterol esterase against proteolytic inactivation (48), but also promote the emulsification of cholesterol in the intestinal lumen and increase the absorption of cholesterol by forming micelles (49). Bile salts are produced in hepatocytes by converting cholesterol, stored in the gallbladder, and released to the duodenum *via* bile ducts. The majority of bile salts are reabsorbed from the intestine and pass back to the liver. When the process is interrupted, the liver consumes more

cholesterol to compensate the loss. Cholestyramine, a medication used to treat hyperlipidemia, lowers the serum cholesterol level by forming nonabsorbable complex with bile salts in the intestinal lumen and disturbing the enterohepatic circulation of bile salts, which promotes hepatocytes convert more cholesterol to produce bile salts. In this study, three *in vitro* assays were conducted to compare the anti-cholesterol activity of the four samples.

All the four tea flower samples dose-dependently decreased the cholesterol solubility in a micellar solution. Among them, tea flowers from Yujinxiang were more capable than the other three (Figure 2A). The remaining cholesterol concentration in the solution exposed to Yujinxiang tea flower infusion was the lowest. The ability of the other three tea flower samples on decreasing the cholesterol solubility were comparable. It was previously revealed that tea polyphenols and polysaccharides decreased micellar cholesterol solubility (50, 51), while saponins enhanced it due to the surface activity (52). Although tea flowers from Yujinxiang contained less polyphenols, they contained less saponins and more polysaccharides, which might be advantageous to the decrease of micellar cholesterol solubility.

All the four tea flowers dose-dependently inhibited the activity of cholesterol esterase. However, the inhibitory effects of the four samples were insignificantly different (Figure 2B). It was reported that gallic acid, quercetin, and monomeric catechins were pancreatic cholesterol esterase inhibitors (53, 54). Compared with EGCG, the half maximal inhibitory concentration of quercetin was smaller (54). According to chemical analysis, tea flowers from Yujinxiang contained more monomeric catechins, while tea flowers from Baiye No.1 contained more quercetin. The presence of multiple compounds with differential cholesterol esterase inhibitory activity and their differed contents among samples might lead to the indifferent cholesterol esterase inhibitory activity.

The binding activity of tea flowers with three primary bile salts, i.e., sodium taurocholate, sodium glycocholate, and sodium cholate, was investigated. Each tea flower sample exhibited bile salt binding activity. The binding efficiency of tea flowers to each bile salt was

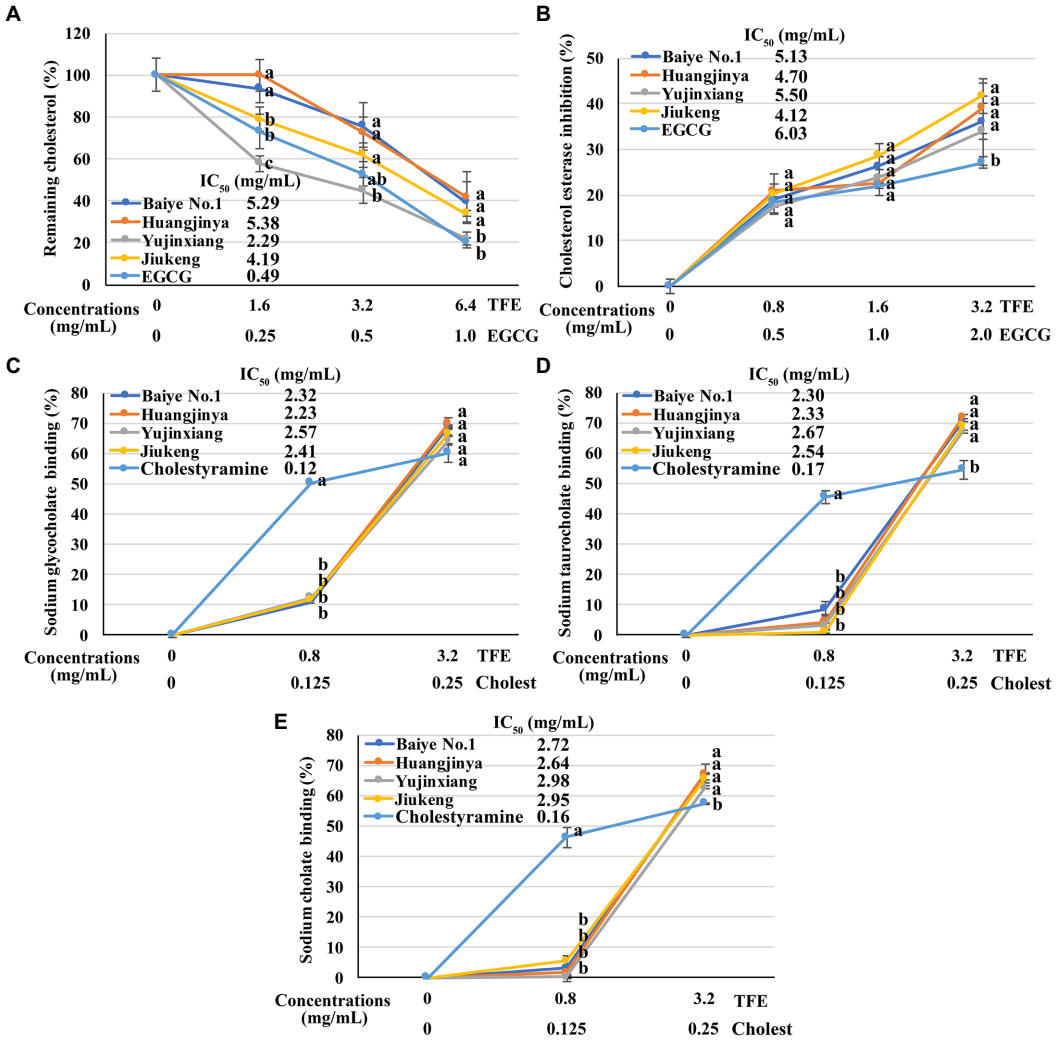

FIGURE 2
The *in vitro* anti-cholesterol activities of four tea flowers. **(A)** The activity of decreasing the micellar cholesterol solubility. **(B)** The cholesterol esterase inhibitory activity. **(C–E)** The sodium glycocholate **(C)**, sodium taurocholate **(D)**, sodium cholate **(E)**, and binding activity. Epigallocatechin gallate (EGCG) was used as the positive control for the micellar cholesterol solubility assay and cholesterol esterase inhibitory assay. Cholestyramine (Cholest) was used as the positive control for the bile salt binding assays. TFE is short for the tea flower extract. IC_{50} is short for the half maximal inhibitory concentration. The same letter within each row indicates no significant difference ($p>0.05$).

similar and the binding activity of each tea flower sample to the same bile salt was not significantly different (Figures 2C–E). Deng et al. found that the bile salt binding activity of tea flowers was correlated to the total polyphenol content (5). Further study revealed that not only polyphenols, but also polysaccharides and caffeine had bile salt binding activity. The bile salt binding activity of polyphenols was stronger than that of polysaccharides and caffeine (55). Soluble proteins in tea flowers had affinity to three primary bile salts and showed the potential of anti-cholesterol activity *in vitro* (56). A recent research suggested that some saponins also had bile salt binding activity (57). In this study, insignificant differences on the bile salt binding activity of the four tea flowers were observed, probably due to the differences on the content and composition of active bile salt binding components in each tea flower sample.

The above results demonstrated that tea flowers from Yujinxiang exhibited better activity in decreasing micellar cholesterol solubility, while the four samples showed no significant differences on the cholesterol esterase inhibition and bile salt binding.

To figure out the relationship between chemical composition and anti-cholesterol activity, partial least squares regression analysis was performed. The contents of 45 compounds were set as X variables, while the cholesterol reduction (%), cholesterol esterase inhibition (%), and the binding rates of three bile salts were set as Y variables. According to the results (Supplementary Figure S2), 21 compounds with variable importance in projection (VIP) >1 were screened out. Among them, 7 compounds, including EGCG and chakasaponins I-III, were positively correlated to the anti-cholesterol activity. While 14 compounds, including several floratheasaponins, were negatively correlated. It was interesting that different types of saponins showed opposite correlations to the anti-cholesterol activity. More experiments are needed to study their actual effects on anti-cholesterol and the possible underlying mechanisms.

4. Conclusion

The research investigated and compared the chemical composition and anti-cholesterol activity of tea flowers from three albino cultivars and one non-albino cultivar. Unlike tea leaves, the content of free amino acids in tea flowers from albino cultivars was not significantly higher than that in tea flowers from the non-albino Jiukeng cultivar and the content of polyphenols was not lower. Among the three albino samples, tea flowers from Yujinxiang had the highest free amino acids, but lowest polyphenols, especially procyanidins. On the contrary, tea flowers from Huangjinya had the highest polyphenols and saponins, but lowest free amino acids. *In vitro* anti-cholesterol activity assays revealed that tea flowers from Yujinxiang exhibited stronger activity in decreasing the micellar cholesterol solubility, while the cholesterol esterase inhibitory activity and bile salt binding activity of the four samples were insignificantly different. Future studies on the investigation of key active anti-cholesterol compounds can be conducted.

Data availability statement

The data presented in the study are deposited in the MetaboLights repository, accession number MTBLS7012.

Author contributions

YG, ZH, Y-QX, and J-FY conceived, designed the experiments, and wrote the paper. YG performed the experiments and analyzed the data. All authors contributed to the article and approved the submitted version.

Funding

This research was supported by the National Natural Science Foundation of China (32202114), China Agriculture Research System of MOF and MARA (CARS-19), and the Innovation Project for the Chinese Academy of Agricultural Sciences.

Conflict of interest

The authors declare that the research was conducted in the absence of any commercial or financial relationships that could be construed as a potential conflict of interest.

Publisher's note

Supplementary material

The Supplementary material for this article can be found online at: https://www.frontiersin.org/articles/10.3389/fnut.2023.1142971/full#supplementary-material

References

1. Wang LL. *Study on Aroma Components of tea (Camellia sinensis)*. Hangzhou: Zhejiang Gongshang University (2008).

2. Chen D, Chen G, Sun Y, Zeng X, Ye H. Physiological genetics, chemical composition, health benefits and toxicology of tea (Camellia sinensis L.) flower: a review. *Food Res Int*. (2020) 137:109584. doi: 10.1016/j.foodres.2020.109584

3. Yang PX, Liu XX, Li WJ. Analysis on main biochemical components in the flowers of tea (*camellia Sinensis*). *China Tea*. (2009) 7:24–5.

4. Jesch ED, Carr TP. Food ingredients that inhibit cholesterol absorption. *Prev Nutr Food Sci*. (2017) 22:67–80. doi: 10.3746/pnf.2017.22.2.67

5. Deng ZH, Huang HH. Bile salt-binding capacity and lipid-lowering mechanisms of water extracts from fresh tea leaves and tea flowers. *Food Sci*. (2011) 32:96–9.

6. Ling ZJ, Xiong CY, Han Q, He PM. Study on preventive effect of tea plant flower on obesity and hyperlipidemia of rats. *J Chinese Inst Food Sci. Technol*. (2011) 11:50–4. doi: 10.16429/j.1009-7848.2011.07.005

7. Yang YH, Zhang J, Zheng BD, Li DT, Wang FQ. A study on the brewing technique of Wuyi rock tea flower yellow rice wine. *J Wuyi Univ*. (2018) 37:18–22. doi: 10.14155/j.cnki.35-1293/g4.2018.03.004

8. Zhang WJ, Liu C, Lin S, Ji AB, Zheng TT, Ma L, et al. Processing of tea flower jelly drops. *China Food Safety Mag*. (2016) 27:146–8. doi: 10.16043/j.cnki.cfs.2016.27.114

9. Liu D. *Study on the Changes of Ingredients in the Growth Process of Tea Blossom and the Development of Tea Blossom Fu*. China: Hunan Agricultural University (2019).

10. Morikawa T, Lee IJ, Okugawa S, Miyake S, Miki Y, Ninomiya K, et al. Quantitative analysis of catechin, flavonoid, and saponin constituents in "tea flower", the flower buds of Camellia sinensis, from different regions in Taiwan. *Nat Prod Commun*. (2013) 8:1553–7.

11. Shen X, Shi LZ, Pan HB, Li B, Wu YY, Tu YY. Identification of triterpenoid saponins in flowers of four *camellia Sinensis* cultivars from Zhejiang province: differences between cultivars, developmental stages, and tissues. *Ind Crop Prod*. (2017) 95:140–7. doi: 10.1016/j.indcrop.2016.10.008

12. Zhou C, Mei X, Rothenberg DO, Yang Z, Zhang W, Wan S, et al. Metabolome and transcriptome analysis reveals putative genes involved in anthocyanin accumulation and coloration in white and pink tea (Camellia sinensis) flower. *Molecules*. (2020) 25:190. doi: 10.3390/molecules25010190

13. Shin YH, Yang R, Shi YL, Li XM, Fu QY, Lu JL, et al. Light-sensitive albino tea plants and their characterization. *HortScience*. (2018) 53:144–7. doi: 10.21273/HORTSCI12633-17

14. Lu M, Han J, Zhu B, Jia H, Yang T, Wang R, et al. Significantly increased amino acid accumulation in a novel albino branch of the tea plant (Camellia sinensis). *Planta*. (2019) 249:363–76. doi: 10.1007/s00425-018-3007-6

15. Dong F, Zeng L, Yu Z, Li J, Tang J, Su X, et al. Differential accumulation of aroma compounds in Normal green and albino-induced yellow tea (Camellia sinensis) leaves. *Molecules*. (2018) 23:2677. doi: 10.3390/molecules23102677

16. Xu YQ, Hu XF, Tang P, Jiang YW, Yuan HB, Du QZ, et al. The major factors influencing the formation of sediments in reconstituted green tea infusion. *Food Chem*. (2015) 172:831–5. doi: 10.1016/j.foodchem.2014.09.143

17. Liu PP, Yin JF, Chen GS, Wang F, Xu YQ. Flavor characteristics and chemical compositions of oolong tea processed using different semi-fermentation times. *J Food Sci Technol*. (2018) 55:1185–95. doi: 10.1007/s13197-018-3034-0

18. Gao Y, Cao QQ, Chen YH, Granato D, Wang JQ, Yin JF, et al. Effects of the baking process on the chemical composition, sensory quality, and bioactivity of Tieguanyin oolong tea. *Front Nutr*. (2022) 9:881865. doi: 10.3389/fnut.2022.881865

19. Vasquez-Villanueva R, Plaza M, Garcia MC, Turner C, Marina ML. A sustainable approach for the extraction of cholesterol-lowering compounds from an olive by-product based on CO(2)-expanded ethyl acetate. *Anal Bioanal Chem*. (2019) 411:5885–96. doi: 10.1007/s00216-019-01970-4

20. Ji HH, Zhu CP. Study on the extraction and composition of pomegranate peel polysaccharide and hypolipidemic activity *in vitro*. *Food Fermentation Indus*. (2023) 49:161–168. doi: 10.13995/j.cnki.11-1802/ts.029430

21. Xu RJ, Wang L, Wang CM, Ye H, Tu YY, Zeng XX. Determination of soluble sugars, catechins and free amino acids in tea flowres by high performance liquid chromatography. *Food Sci*. (2012) 33:246–50.

22. Wang Y, Yang Z, Wei X. Sugar compositions, alpha-glucosidase inhibitory and amylase inhibitory activities of polysaccharides from leaves and flowers of Camellia sinensis obtained by different extraction methods. *Int J Biol Macromol*. (2010) 47:534–9. doi: 10.1016/j.ijbiomac.2010.07.007

23. Huang AG, Dong RJ, Wei H. Identification and analysis of major bioactive compounds in tea flower. *Food Sci*. (2007) 28:400–3.

24. Wang M, Zhao ZX, Lei R, Duan JP, Liu YL, Feng L. Quantifications of six saponins *Panax ginseng C. A. Mey* leaves and flowers using the UPLC method. *J Chinese Med Mater*. (2018) 41:2623–6. doi: 10.13863/j.issn1001-4454.2018.11.029

25. Wei L, Du Y, Zhou H. Content determination of total saponin and monomer saponin of *Panax Notoginseng* flower bud in different habitats and growth ages. *Shanghai J Tradit Chinese Med*. (2008) 42:76–8. doi: 10.16305/j.1007-1334.2008.04.032

26. Morikawa T, Miyake S, Miki Y, Ninomiya K, Yoshikawa M, Muraoka O. Quantitative analysis of acylated oleanane-type triterpene saponins, chakasaponins I-III and floratheasaponins A-F, in the flower buds of Camellia sinensis from different regional origins. *J Nat Med*. (2012) 66:608–13. doi: 10.1007/s11418-012-0627-1

27. Yoshikawa M, Nakamura S, Kato Y, Matsuhira K, Matsuda H. Medicinal flowers. XIV New acylated oleanane-type triterpene oligoglycosides with antiallergic activity from flower buds of chinese tea plant (Camellia sinensis). *Chem Pharm Bull (Tokyo)*. (2007) 55:598–605. doi: 10.1248/cpb.55.598

28. Matsuda H, Hamao M, Nakamura S, Kon'i H, Murata M, Yoshikawa M, et al. Anti-hyperlipidemic and anti-hyperglycemic effects of chakasaponins I-III and structure of chakasaponin IV from flower buds of Chinese tea plant (Camellia sinensis). *Chem Pharm Bull (Tokyo)*. (2012) 60:674–80. doi: 10.1248/cpb.60.674

29. Ma R, Yang KF, Liu Y, Teng CQ, Yang QF. Analysis of the main quality characteristics and biochemical components of tea flower. *Agricul Res Appl*. (2018) 31:12–8.

30. Shi MN, Peng Y, Zhang J, Xiong CY. Biochemical components and *in vitro* antioxidant activities of large-leaf species tea flowers in Yunnan. *Sci Technol Food Ind*. (2022) 43:298–306. doi: 10.13386/j.issn1002-0306.2021110135

31. Ullah C, Unsicker SB, Reichelt M, Gershenzon J, Hammerbacher A. Accumulation of Catechin and Proanthocyanidins in black poplar stems after infection by Plectosphaerella populi: hormonal regulation, biosynthesis and antifungal activity. *Front Plant Sci*. (2019) 10:1441. doi: 10.3389/fpls.2019.01441

32. Xiang P, Zhu Q, Tukhvatshin M, Cheng B, Tan M, Liu J, et al. Light control of catechin accumulation is mediated by photosynthetic capacity in tea plant (Camellia sinensis). *BMC Plant Biol*. (2021) 21:478. doi: 10.1186/s12870-021-03260-7

33. Rue EA, Rush MD, Breemen RB. Procyanidins: a comprehensive review encompassing structure elucidation via mass spectrometry. *Phytochem Rev*. (2018) 17:1–16. doi: 10.1007/s11101-017-9507-3

34. Sasaki Y, Ito S, Zhang Z, Lyu X, Takizawa SY, Kubota R, et al. Supramolecular sensor for astringent Procyanidin C1: fluorescent artificial tongue for wine components. *Chemistry*. (2020) 26:16236–40. doi: 10.1002/chem.202002262

35. Zhang YN, Yin JF, Chen JX, Wang F, Du QZ, Jiang YW, et al. Improving the sweet aftertaste of green tea infusion with tannase. *Food Chem*. (2016) 192:470–6. doi: 10.1016/j.foodchem.2015.07.046

36. Barreca D, Trombetta D, Smeriglio A, Mandalari G, Romeo O, Felice MR, et al. Food flavonols: nutraceuticals with complex health benefits and functionalities. *Trends Food Sci Technol*. (2021) 117:194–204. doi: 10.1016/j.tifs.2021.03.030

37. Li J, Chen LF, Jin EH, Li B, Tu YY. Research on flavonoid glycosides of tea flower in different tea plant cultivars. *J Zhejiang Univ (Agric Life Sci)*. (2019) 45:707–14.

38. Rose AJ. Amino acid nutrition and metabolism in health and disease. *Nutrients*. (2019) 11:2623. doi: 10.3390/nu11112623

39. Shen ZG, He Y, Li YY, Yang TY, Xu XN, Jiang CJ. Insights into the profiling changes of amino acid content in an albino mutant (*Camellia sinensis cv. Huangshanbaicha*) during the albinostic stage. *Sci Hortic*. (2020) 260:108732. doi: 10.1016/j.scienta.2019.108732

40. Lin L, Zeng L, Liu A, Peng Y, Yuan D, Zhang S, et al. L-Theanine regulates glucose, lipid, and protein metabolism via insulin and AMP-activated protein kinase signaling pathways. *Food Funct*. (2020) 11:1798–809. doi: 10.1039/C9FO02451D

41. Tian YJ, Liu TR, Fan FY, Gong SY, Song CJ. Optimization of HPLC method for determination of organic acid and its application in organic acids detection of white tea. *J Chinese Inst Food Sci Technol*. (2021) 21:320–327. doi: 10.16429/j.1009-7848.2021.07.039

42. Ashihara H, Suzuki T. Distribution and biosynthesis of caffeine in plants. *Front Biosci*. (2004) 9:1864–76.

43. Kim YS, Choi YE, Sano H. Plant vaccination: stimulation of defense system by caffeine production in planta. *Plant Signal Behav*. (2010) 5:489–93. doi: 10.4161/psb.11087

44. Dai LF. *Research on biochemical components in tea flower petals (Camellia sinensis) and cell wall disruption processess of tea tree pollen*. China: Southwest University (2020).

45. Lu K, Lee MH, Patel SB. Dietary cholesterol absorption; more than just bile. *Trends Endocrinol Metab*. (2001) 12:314–20.

46. Lopez-Candales A, Grosjlos J, Sasser T, Buddhiraju C, Scherrer D, Lange LG, et al. Dietary induction of pancreatic cholesterol esterase: a regulatory cycle for the intestinal absorption of cholesterol. *Biochem Cell Biol*. (1996) 74:257–64.

47. Heidrich JE, Contos LM, Hunsaker LA, Deck LM, Vander Jagt DL. Inhibition of pancreatic cholesterol esterase reduces cholesterol absorption in the hamster. *BMC Pharmacol*. (2004) 4:5. doi: 10.1186/1471-2210-4-5

48. Vahouny GV, Weersing S, Treadwell CR. Taurocholate protection of cholesterol esterase against proteolytic inactivation. *Biochem Biophys Res Commun*. (1964) 15:224–9. doi: 10.1016/0006-291X(64)90150-0

49. Westergaard H, Dietschy JM. The mechanism whereby bile acid micelles increase the rate of fatty acid and cholesterol uptake into the intestinal mucosal cell. *J Clin Invest*. (1976) 58:97–108. doi: 10.1172/JCI108465

50. Sakakibara T, Sawada Y, Wang J, Nagaoka S, Yanase E. Molecular mechanism by which tea Catechins decrease the micellar solubility of cholesterol. *J Agric Food Chem*. (2019) 67:7128–35. doi: 10.1021/acs.jafc.9b02265

51. Silva IMV, Machado F, Moreno MJ, Nunes C, Coimbra MA, Coreta-Gomes F. Polysaccharide structures and their Hypocholesterolemic potential. *Molecules*. (2021) 26:4559. doi: 10.3390/molecules26154559

52. Mitra S, Dungan SR. Cholesterol solubilization in aqueous micellar solutions of quillaja saponin, bile salts, or nonionic surfactants. *J Agric Food Chem*. (2001) 49:384–94. doi: 10.1021/jf000568r

53. Ngamukote S, Makynen K, Thilawech T, Adisakwattana S. Cholesterol-lowering activity of the major polyphenols in grape seed. *Molecules*. (2011) 16:5054–61. doi: 10.3390/molecules16065054

54. Su JH, Ma ZY, Yang L, Wang HX, Gao CZ, Nie RJ. Study on the cholesterol esterase and micellar cholesterol inhibitiory activities of quercetin and EGCG. *Sci Technol Food Ind*. (2015) 36:346–9. doi: 10.13386/j.issn1002-0306.2015.11.062

55. Deng X, Huang HH. Effects of tea flower water extract and funtional components on the binding of bile salts. *Food Sci Technol*. (2013) 38:199–205. doi: 10.13684/j.cnki.spkj.2013.01.064

56. Deng X, Huang HH. *In vitro* binding of bile salts by water-soluble protein extract from tea flower. *Mod Food Sci Technol*. (2013) 29:63–7. doi: 10.13982/j.mfst.1673-9078.2013.01.040

57. Gee JM, Johnson IT. Interactions between hemolytic saponins, bile salts and small intestinal mucosa in the rat. *J Nutr*. (1988) 118:1391–7. doi: 10.1093/jn/118.11.1391

frontiers | Frontiers in Nutrition

TYPE Original Research
PUBLISHED 27 March 2023
DOI 10.3389/fnut.2023.1138783

OPEN ACCESS

EDITED BY
Ye Liu,
Beijing Technology and Business University, China

REVIEWED BY
Yong-Quan Xu,
Tea Research Institute (CAAS), China
Dongguang Xiao,
Tianjin University of Science and Technology, China

*CORRESPONDENCE
Lunzhao Yi
✉ yilunzhao@kust.edu.cn
Wenjiang Dong
✉ dongwenjiang.123@163.com

SPECIALTY SECTION
This article was submitted to Food Chemistry, a section of the journal Frontiers in Nutrition

RECEIVED 06 January 2023
ACCEPTED 07 March 2023
PUBLISHED 27 March 2023

CITATION
Zheng Y, Zhang C, Ren D, Bai R, Li W, Wang J, Shan Z, Dong W and Yi L (2023) Headspace solid-phase microextraction coupled with gas chromatography-mass spectrometry (HS-SPME-GC-MS) and odor activity value (OAV) to reveal the flavor characteristics of ripened Pu-erh tea by co-fermentation. *Front. Nutr.* 10:1138783. doi: 10.3389/fnut.2023.1138783

Headspace solid-phase microextraction coupled with gas chromatography-mass spectrometry (HS-SPME-GC-MS) and odor activity value (OAV) to reveal the flavor characteristics of ripened Pu-erh tea by co-fermentation

Yaru Zheng[1], Chunhua Zhang[2], Dabing Ren[1], Ruoxue Bai[1], Wenting Li[1], Jintao Wang[1], Zhiguo Shan[2], Wenjiang Dong[3]* and Lunzhao Yi[1]*

[1]Faculty of Food Science and Engineering, Kunming University of Science and Technology, Kunming, Yunnan, China, [2]College of Agriculture and Forestry, Pu'er University, Pu'er, Yunnan, China, [3]Spice and Beverage Research Institute, Chinese Academy of Tropical Agricultural Sciences, Wanning, China

Introduction: Pu-erh tea is a geographical indication product of China. The characteristic flavor compounds produced during the fermentation of ripened Pu-erh tea have an important impact on its quality.

Methods: Headspace solid-phase microextraction coupled with gas chromatography-mass spectrometry (HS-SPME-GC-MS) and odor activity value (OAV) is used for flavor analysis.

Results: A total of 135 volatile compounds were annotated, of which the highest content was alcohols (54.26%), followed by esters (16.73%), and methoxybenzenes (12.69%). Alcohols in ripened Pu-erh tea mainly contribute flower and fruit sweet flavors, while methoxybenzenes mainly contribute musty and stale flavors. The ripened Pu-erh tea fermented by *Saccharomyces*: *Rhizopus*: *Aspergillus niger* mixed in the ratio of 1:1:1 presented the remarkable flavor characteristics of flower and fruit sweet flavor, and having better coordination with musty and stale flavor.

Discussion: This study demonstrated the content changes of ripened Pu-erh tea's flavor compounds in the fermentation process, and revealed the optimal fermentation time. This will be helpful to further understand the formation mechanism of the characteristic flavor of ripened Pu-erh tea and guide the optimization of the fermentation process of ripened Pu-erh tea.

KEYWORDS

ripened Pu-erh tea, flavor, mixed fermentation, HS-SPME-GC-MS, OAV

1. Introduction

As a beverage with health function, tea is widely welcomed. According to the degree of fermentation, tea is generally divided into green tea, yellow tea, white tea, oolong tea, black tea, and dark tea (1, 2). Ripened Pu-erh tea is one of the most popular dark teas (3). In recent years, many studies have demonstrated that Pu-erh tea produces unique flavor through microbial activities in the process of pile fermentation (4–9), which is considered as a key factor affecting the quality of dark tea (10).

The special sensory quality of ripened Pu-erh tea is one of the most important indicators of its market price. Some previous studies explored the main volatile compounds of ripened Pu-erh tea, and the results showed that the main flavors were 1,2,3-trimethoxybenzene, 1,2,4-trimethoxybenzene, hexadecanoic acid, dihydroactinidiolide, and so on, having stale, waxy or fruit flavor (4, 11, 12). And it was reported that during the pile fermentation, the compounds with flower flavor, such as phenylethyl alcohol, oxidized linalool, and linalool gradually decreased, and compounds with stale flavor, such as 1,2,3-trimethoxybenzene and 1,2,4-trimethoxybenzene gradually increased (13, 14). This makes the ripened Pu-erh tea exhibit a typical "aged fragrance."

The dominant microorganisms are the key factors in the pile fermentation process of ripened Pu-erh tea. Previous studies have shown that the dominant species of ripened Pu-erh tea are mainly *Aspergillus*, *Penicillium*, and *Pseudolambica* (7, 15, 16). *Aspergillus* has been identified as the main flavor-producing microorganism (17). Studies have confirmed that specific microorganisms, such as *Aspergillus niger*, can improve the sensory quality of the tea by fermentation (18, 19). And there are studies on pile fermentation by inoculation of crown *Eurotium cristatum*, *Aspergillus niger*, and *Rhizopus* to affect volatile compounds and produce unique flower and fruit flavors (20, 21). So far, most of the existing studies focus on a few flavors and the content changes before and after fermentation, while systematic studies on various types of flavors in the fermentation process of ripened Pu-erh tea are rarely reported.

Headspace solid-phase microextraction (HS-SPME) coupled with gas chromatography-mass spectrometry (GC-MS) is a powerful technology to characterize the volatile compounds of tea (22, 23). HS-SPME-GC-MS is valuable for the characterization of tea flavor and allows a more comprehensive annotation of various volatile compounds in tea (24). However, the contribution of different volatile compounds to the flavor is very different, the annotation of volatile compounds is far from enough to reveal the flavor components in tea. Odor activity value (OAV) is the ratio of the concentration of flavor active compound to their flavor threshold value, which can help to identify the key flavor compounds in ripened Pu-erh tea (25). In general, compounds with OAV > 1 are considered as the main contributors to flavor (26–28).

In this study, Yunnan big-leaf sun-dried green tea (SGT) was fermented by 6 mixed strains, respectively, to obtain the ripened Pu-erh tea with flavor characteristics of flower and fruit sweet flavor. HS-SPME-GC-MS combined with OAV was employed to detect and reveal the flavor compounds of the ripened Pu-erh teas during the fermentation process. This study will help to reveal the changes of flavor compounds of ripened Pu-erh tea during fermentation, and provide valuable information for the optimization of ripened Pu-erh tea processing technology.

2. Materials and methods

2.1. Chemicals

N-alkanes, chromatographic pure grade (C_8–C_{40}) (o2si smart solutions Corporation)[1]. Decanoic acid ethyl ester, 98% purity (Sigma-Aldrich[2]).

2.2. Preparation of tea samples

Yunnan big-leaf sun-dried green tea (SGT) is used as the raw material for the pile fermentation of ripened Pu-erh tea. Each pile is stacked with 300 kg of SGT at 40% tide. Adding different proportions of beneficial strains to each pile of SGT, with 0.1% (w/w) of receiving bacteria. Group A, *Saccharomyces*: *Rhizopus* = 1:2; Group B, *Saccharomyces*: *Aspergillus niger* = 1:2; Group C, *Saccharomyces*: *Aspergillus oryzae* = 1:2; Group D, *Saccharomyces*: *Rhizopus*: *Aspergillus oryzae* = 1:1:1; Group E, *Saccharomyces*: *Rhizopus*: *Aspergillus niger* = 1:1:1; Group F, *Saccharomyces*: *Rhizopus*: *Aspergillus niger*: *Aspergillus oryzae* = 1:1:1:1. During the fermentation process, the pile was turned at the right time according to the changes in temperature, and humidity of the fermentation pile as well as the fermentation environment. The temperature, humidity, and pH of the tea pile were recorded at three time periods each day: 9:00 a.m., 15:00 p.m., and 21:30 p.m. Then the tea samples were taken on the 7th, 14th, 21st, 28th, and 35th days of fermentation, respectively, using the five-point sampling method, and the fermentation samples from the upper (10 cm thick), middle (30 cm thick), and lower (5 cm above the ground) parts were combined into one mixed sample. A total of 30 samples were collected in different mixed strains and different fermentation times in the pile (**Supplementary Table 1**). All samples collected are dried, ground into powder, placed in sealed bags (labeled with weight, time, and type), and stored in a −20°C refrigerator.

2.3. Extraction of volatile compounds in Pu-erh tea samples by HS-SPME

Headspace solid-phase microextraction was used to extract and enrich the volatile compounds in samples. The extraction fiber head type was 50/30 μm DVB/CAR/PDMS (SPME-GC Jeong-Jung Analytical Instruments Co). Accurately weigh 0.5 g of tea powder into a 20 mL headspace flask, 1.8 g of NaCl was added, and 10 μL of decanoic acid ethyl ester (0.2 mg/mL) was added as an internal standard. The headspace flask was sealed immediately after adding 5 mL of boiling water and the extraction fiber was inserted at 80°C for 40 min. After the extraction was completed, the solid-phase microextraction fiber needle was removed, and then inserted into the GC injection port for desorption (5 min, 260°C). To prevent

1 http://www.vicbio.com/Index/show/catid/22/id/403.html

2 https://www.sigmaaldrich.cn/CN/zh/campaigns/promotion/proclin-preservatives?utm_campaign=Brand%20Zone%20-%20China&utm_medium=Sigma-Aldrich_brandzone&utm_source=baidu&utm_content=headline&utm_term=proclin-preservatives

contamination, the extracted fibers need to be aged at 270°C for 1 h at the GC-MS inlet before using. The above operation was repeated for each sample to minimize errors.

2.4. GC-MS analysis of volatile compounds

A combination of GC-MS (QP2010 Shimadzu, Japan) and HP-5MS quartz capillary column (30 m × 0.25 mm × 0.25 μm) was used. The inlet temperature was 260°C. The carrier gas was high purity helium (>99.999%) at a flow rate of 1 mL/min. The samples were taken in a split-flow injection with a split ratio of 5:1. The column temperature was set at 50°C and increased (ramped) at a rate of 10°C/min to 80°C; then increased at a rate of 3°C/min to 90°C for 3 min; then increased at a rate of 3°C/min to 120°C for 3 min; continued at a rate of 3°C/min to 170°C; and finally increased at a rate of 15°C/min to 230°C for 4 min.

Mass spectrometry (MS) conditions: The ion source was an EI source with an electron ionization energy of 70 eV. The interface temperature was 260°C and the ion source temperature was 230°C. And the mass range was 30–540 atomic mass unit (amu), solvent delay time of 3.0 min, full scan mode. The retention indices (RIs) was determined using a mixture of n-alkanes (C_8–C_{40}) running under the same conditions.

2.5. Qualitative and quantitative analysis of volatile compounds

2.5.1. Qualitative analysis

The National Library of Standards and Technology (NIST) spectral library was used to search for compounds with >80% similarity, combined with C_8–C_{40} n-alkanes to calculate RIs, and finally compared with the online database NIST Chemistry WebBook.[3] The formula for calculating the retention indices is as follows,

$$RIs = 100n + \frac{100\,(t_i - t_n)}{t_{n+1} - t_n}$$

Where t_i is the retention time of the compound to be measured, t_n and t_{n+1} are the retention times of the mixture of n-alkane standards with n and n+1 carbon atoms, respectively, ($t_n < t_i < t_{n+1}$) (29).

2.5.2. Quantitative analysis

Semi-quantitative analysis was performed using decanoic acid ethyl ester as an internal standard with the following formula,

$$W_i = \frac{A_i}{A_s} W_s$$

Where W_i is the content of the compound to be measured (μg/kg), A_i is the peak area of the compound to be measured, A_s is the peak area of the internal standard in the sample, and W_s is the concentration of the internal standard (μg/kg) (30).

3 https://webbook.nist.gov/chemistry/name-ser/

2.6. Odor activity values calculation

The thresholds of different volatile compounds in water (μg/kg) were obtained from the literatures (**Supplementary Table 3**), and then the OAV of each compound were calculated based on the quantitative results. The OAV calculated from the relative concentrations of the internal standard, which we define as relative odor activity values (rOAVs). The specific calculation formula is rOAVs = C_i/OT_i, where C_i is the relative content of the compound by internal standard and OT_i is its odor threshold in water. When rOAVs ≥ 1, it means that the compound has a large contribution to the flavor of the sample (31–33).

2.7. Statistical analysis

The experimental data were imported into the website for PCA analysis[4] to distinguish between different mixed strains and the variability of volatile compounds during pile fermentation. Flavor characteristics of volatile compounds in Pu-erh tea were determined by literatures and websites,[5] and to construct radar maps for compounds with rOAVs > 1 by Origin2022.

3. Results and discussion

3.1. Analysis of volatile components in ripened Pu-erh tea fermented by mixed strains

In this study, volatile compounds were detected by HS-SPME-GC-MS. A total of 135 compounds were annotated with the help of similarity research of online databases NIST Chemistry WebBook, and retention indices. As shown in **Figure 1A**, which were mainly divided into nine categories, including 34 alcohols (54.34%), 17 esters (16.68%), 14 ketones (2.62%), 11 aldehydes (4.88%), 6 phenols (0.76%), 14 methoxybenzenes (12.64%), 4 acids (0.84%), 9 alkenes (2.11%), 3 nitrogenous compounds (3.42%), and 23 others (1.69%). The number of volatile compounds detected in different samples is shown in the **Supplementary Table 2**, and the types and contents are shown in the **Supplementary Table 3**. The total contents of volatile compounds in Group D, E, and F reached 6,999.26 μg/kg, 5,132.07 μg/kg, and 7,264.87 μg/kg, respectively, when the fermentation proceeded to the 21st day, which was significantly higher than those in Group A, B, and C. This may be due to the increase in the abundance of fermentation strains. On the 35th day of pile fermentation, the content of total volatile compounds increased significantly compared to SGT, increasing 70.26, 52.71, 66.13, 82.17, 86.35, and 106.15% for the six groups, respectively. The results indicated that the type and total content of volatile compounds increased with the increasing of the diversity of mixed strains. **Figure 1B** shows that the total content of methoxybenzene, which has a stale and musty flavor, increased in ripened Pu-erh tea, which increased with the fermentation time and

4 https://www.metaboanalyst.ca/

5 http://www.thegoodscentscompany.com/search3.php

10.3389/fnut.2023.1138783

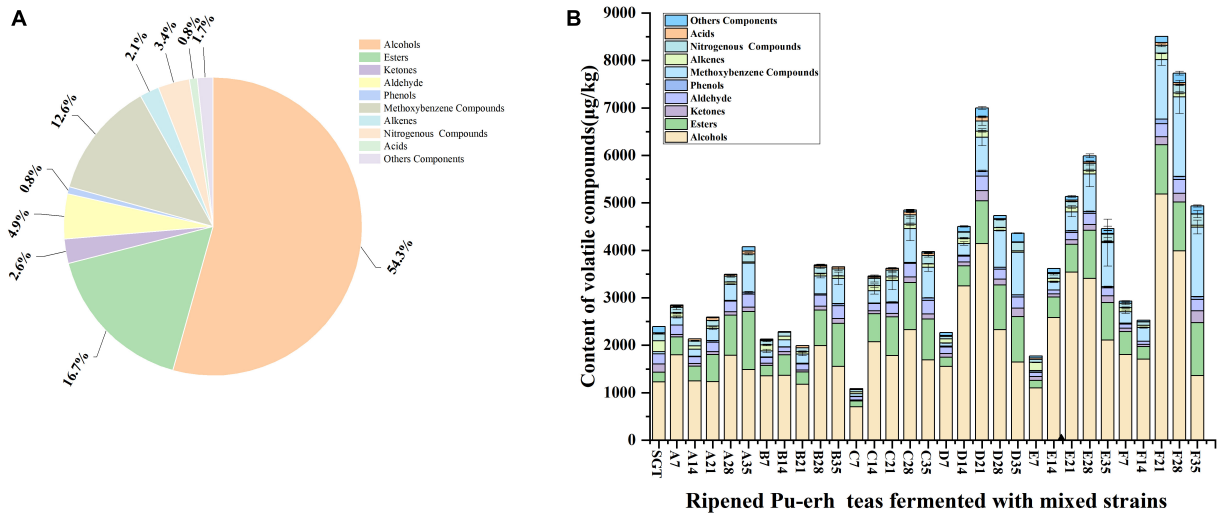

FIGURE 1
Contents of various volatile compounds. **(A)** Average percentage of various volatile compounds during the fermentation by different mixed strains; **(B)** flavor compounds of ripened Pu-erh tea during the fermentation of different mixed strains. A total of 7, 14, 21, 28, and 35 represent the fermentation time. SGT is the sun-dried green tea, A for *Saccharomyces*: *Rhizopus* = 1:2, B for *Saccharomyces*: *Aspergillus niger* = 1:2, C for *Saccharomyces*: *Aspergillus oryzae* = 1:2, D for *Saccharomyces*: *Rhizopus*: *Aspergillus oryzae* = 1:1:1, E for *Saccharomyces*: *Rhizopus*: *Aspergillus niger* = 1:1:1, F for *Saccharomyces*: *Rhizopus*: *Aspergillus niger*: *Aspergillus oryzae* = 1:1:1:1.

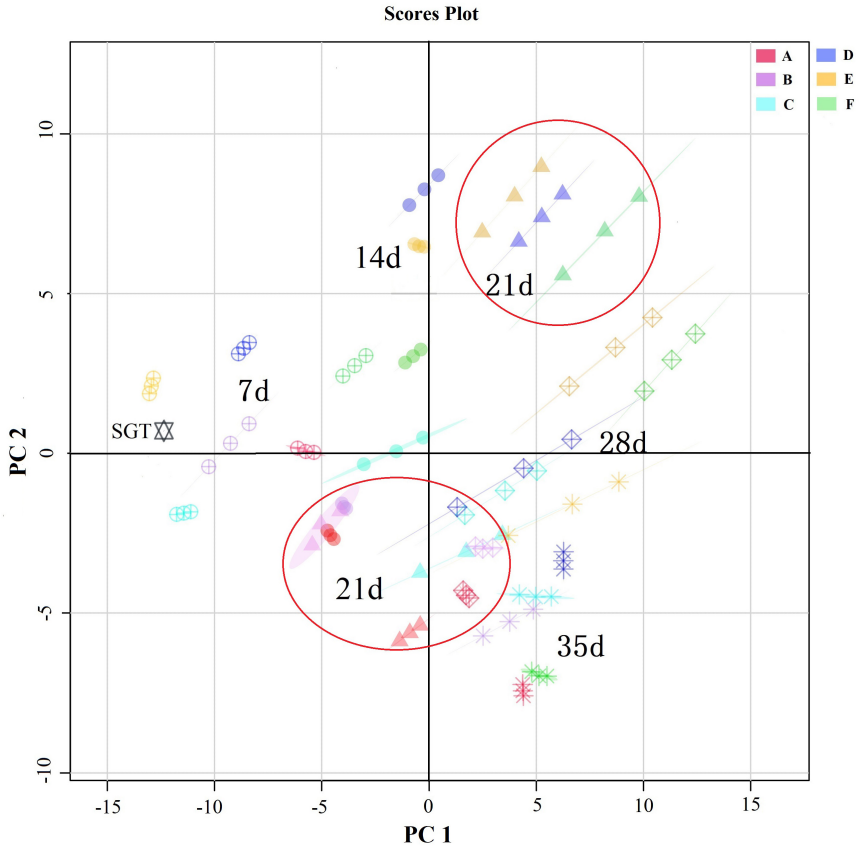

FIGURE 2
Comparison of the dynamics of ripened Pu-erh teas' volatile compounds during mixed fermentation with different strains by PCA analysis. A total of 7 days, 14 days, 21 days, 28 days, and 35 days represents the fermentation time. SGT is the sun-dried green tea. A for *Saccharomyces*: *Rhizopus* = 1:2, B for *Saccharomyces*: *Aspergillus niger* = 1:2, C for *Saccharomyces*: *Aspergillus oryzae* = 1:2, D for *Saccharomyces*: *Rhizopus*: *Aspergillus oryzae* = 1:1:1, E for *Saccharomyces*: *Rhizopus*: *Aspergillus niger* = 1:1:1, F for *Saccharomyces*: *Rhizopus*: *Aspergillus niger*: *Aspergillus oryzae* = 1:1:1:1.

10.3389/fnut.2023.1138783

TABLE 1 Flavor compounds' rOAVs of ripened Pu-erh teas fermented by mixed strains.

No.	Flavor compound	OT (μg/kg)[a]	Odor description[b]	rOAVs										
				SGT	A7	A14	A21	A28	A35	B7	B14	B21	B28	B35
1	1-Octen-3-ol	1	Grass	158.89	25.77	15.88	10.55	17.99	13.39	23.81	14.74	14.62	14.05	13.81
2	Linalool oxide I	60	Flower	1.12	2.61	3.23	3.27	5.26	5.10	1.88	3.51	3.01	5.87	4.51
3	Linalool	6	Flower, Fruit, and Sweet	52.56	54.31	17.16	16.74	22.15	12.17	42.65	30.23	21.75	28.08	13.29
4	Phenylethyl alcohol	4	Flower	30.57	120.31	77.94	66.89	105.67	93.38	85.48	72.38	61.00	119.94	91.22
5	Linalool oxide II	320	Flower	0.08	0.28	0.41	0.59	0.74	0.70	0.12	0.43	0.44	0.76	0.91
6	Terpinen-4-ol	0.2	Woody	71.75	55.58	27.36	*n.d.*	32.61	*n.d.*	57.93	36.90	30.38	39.59	*n.d.*
7	α-Terpineol	350	Sweet	0.48	0.72	0.33	0.30	0.40	0.33	0.57	0.45	0.36	0.52	0.36
8	Geraniol	7.5	Flower, Fruit, and Sweet	9.52	9.35	2.90	3.46	4.97	3.09	7.69	4.28	3.58	3.75	2.28
9	Methyl salicylate	40	Peppermint	0.56	0.43	0.58	0.54	0.94	0.83	0.42	0.46	0.39	1.33	1.03
10	6-methyl-5-Hepten-2-one	68	Fruit	1.04	0.15	0.09	0.10	0.15	0.17	0.14	0.09	0.09	0.22	0.24
11	3,5-Octadien-2-one	0.5	Fruit and Fat	34.77	*n.d.*	10.49	23.31	20.28	33.49	*n.d.*	*n.d.*	*n.d.*	24.04	24.02
12	α-Ionone	0.4	Flower	10.75	6.18	3.73	*n.d.*	*n.d.*	*n.d.*	*n.d.*	*n.d.*	*n.d.*	*n.d.*	*n.d.*
13	β-Ionone	0.2	Flower, Fruit, and Woody	164.58	79.27	55.69	78.12	70.73	79.32	82.41	74.62	61.24	71.34	70.67
14	2-Heptenal	20	–	0.85	0.48	0.37	*n.d.*	0.65	*n.d.*	*n.d.*	*n.d.*	0.38	*n.d.*	*n.d.*
15	2,4-Heptadienal	2.56	Fat	8.97	5.10	5.46	14.10	12.30	21.29	4.65	4.29	4.92	10.47	15.38
16	Benzeneacetaldehyde	4	Flower and Sweet	5.72	5.42	3.81	5.88	5.65	5.66	4.11	3.40	3.95	6.37	4.94
17	1H-Pyrrole-2-carboxaldehyde,1-ethyl	2	Roast	39.38	57.18	39.85	40.17	48.85	56.84	38.25	27.37	28.19	61.18	64.03
18	2-Octenal	3	Fat	2.52	1.10	*n.d.*	1.31	*n.d.*	2.93	*n.d.*	*n.d.*	*n.d.*	1.26	2.00
19	Nonanal	1	Fruit, Flower, and Fat	n.d.	*n.d.*	*n.d.*	18.02	17.92	18.65	*n.d.*	*n.d.*	13.68	15.77	16.08
20	2,6-Nonadienal	0.1	Fruit and Flower	n.d.	*n.d.*	*n.d.*	*n.d.*	*n.d.*	99.24	*n.d.*	*n.d.*	*n.d.*	*n.d.*	78.89
21	Decanal	0.1	Sweet and Fruit	26.37	19.93	21.77	44.82	26.65	48.83	19.86	*n.d.*	16.31	19.57	24.00
22	Benzene, 1,2-dimethoxy	3.17	Sweet and Musty	5.30	10.16	10.30	18.20	22.89	32.12	6.66	11.95	11.49	24.91	22.42
23	1,2,3-Trimethoxybenzene	0.75	Stale and Musty	29.04	91.31	57.42	147.39	153.96	318.89	64.45	69.32	92.85	194.74	322.33
24	1,2,4-Trimethoxybenzene	3.06	Stale and Medicinal	2.75	20.64	19.87	29.68	47.96	67.85	9.68	13.48	27.39	47.86	68.94
25	β-Myrcene	13	Woody, Fruit, and Peppermint	2.99	1.24	1.62	0.83	0.65	0.63	2.78	0.81	0.66	0.72	0.70
26	D-Limonene	10	Sweet and Fruit	10.38	3.87	3.18	2.81	2.45	*n.d.*	4.63	3.99	2.81	2.94	3.15
27	Nonanoic acid	1.5	Fat and Sweet	17.34	13.89	11.66	21.50	10.74	18.36	8.24	5.95	13.87	10.75	14.36
No.	Compound	OT (μg/kg)[a]	Odor description[b]	rOAVs										
				C7	C14	C21	C28	C35	D7	D14	D21	D28	D35	
1	1-Octen-3-ol	1	Grass	8.23	22.06	28.83	19.01	15.12	45.26	21.94	47.27	18.65	24.36	
2	Linalool oxide I	60	Flower	0.97	4.82	4.79	6.98	5.35	2.70	8.18	14.36	8.61	8.44	
3	Linalool	6	Flower, Fruit, and Sweet	19.82	51.72	29.19	39.19	20.64	46.35	84.06	99.86	35.56	14.71	
4	Phenylethyl alcohol	4	Flower	48.96	118.30	96.40	112.84	80.66	111.36	152.51	128.11	93.81	42.52	
5	Linalool oxide II	320	Flower	0.08	0.57	0.76	0.96	0.92	0.16	0.65	1.36	0.94	0.54	
6	Terpinen-4-ol	0.2	Woody	23.75	62.87	35.16	50.32	*n.d.*	53.06	97.66	105.45	50.93	37.21	

(Continued)

10.3389/fnut.2023.1138783

TABLE 1 (Continued)

No.	Compound	OT (μg/kg)[a]	Odor description[b]	rOAVs									
				C7	C14	C21	C28	C35	D7	D14	D21	D28	D35
7	α-Terpineol	350	Sweet	0.28	0.67	0.52	0.74	0.44	0.46	1.00	1.07	0.62	0.45
8	Geraniol	7.5	Flower, Fruit, and Sweet	4.94	8.34	3.32	4.55	2.61	6.72	14.38	15.68	3.86	2.61
9	Methyl salicylate	40	Peppermint	0.22	0.52	1.07	0.96	1.12	1.19	1.65	4.31	1.77	1.08
10	6-methyl-5-Hepten-2-one	68	Fruit	0.05	0.15	0.13	0.16	0.16	0.26	0.24	0.55	0.21	0.29
11	3,5-Octadien-2-one	0.5	Fruit, Fat	*n.d.*	*n.d.*	13.06	21.25	21.18	14.43	23.87	54.63	43.09	60.88
12	α-Ionone	0.4	Flower	2.70	7.35	*n.d.*	8.97	*n.d.*	8.80	11.84	15.34	8.91	8.59
13	β-Ionone	0.2	Flower, Fruit, and Woody	37.58	94.34	*n.d.*	108.00	86.95	96.36	95.50	197.75	109.95	104.79
14	2-Heptenal	20	–	*n.d.*	*n.d.*	0.69	0.70	0.63	1.01	0.63	1.56	0.80	0.79
15	2,4-Heptadienal	2.56	Fat	1.97	5.99	10.34	12.28	13.93	8.54	7.11	27.96	19.38	27.83
16	Benzeneacetaldehyde	4	Flower and Sweet	1.96	4.91	4.82	6.09	5.46	4.57	3.96	6.09	4.68	3.19
17	1H-Pyrrole-2-carboxaldehyde,1-ethyl	2	Roast	21.18	44.48	53.18	65.68	68.18	15.76	26.94	57.51	33.39	31.28
18	2-Octenal	3	Fat	0.49	*n.d.*	1.88	1.46	1.66	2.96	*n.d.*	4.77	3.24	2.61
19	Nonanal	1	Fruit, Flower, and Fat	*n.d.*	*n.d.*	14.84	19.82	16.23	*n.d.*	*n.d.*	*n.d.*	16.69	17.95
20	2,6-Nonadienal	0.1	Fruit and Flower	*n.d.*	*n.d.*	*n.d.*	*n.d.*	*n.d.*	*n.d.*	*n.d.*	*n.d.*	0.00	*n.d.*
21	Decanal	0.1	Sweet and Fruit	*n.d.*	*n.d.*	21.55	31.37	24.85	17.50	*n.d.*	50.97	0.00	*n.d.*
22	Benzene, 1,2-dimethoxy	3.17	Sweet and Musty	3.69	24.17	24.23	37.16	32.49	7.82	31.28	83.38	62.19	79.99
23	1,2,3-Trimethoxybenzene	0.75	Stale and Musty	25.21	158.20	285.84	479.80	420.69	23.64	71.53	238.80	326.31	412.44
24	1,2,4-Trimethoxybenzene	3.06	Stale and Medicinal	5.91	19.00	47.81	70.16	63.57	2.31	10.59	56.30	70.05	75.56
25	β-Myrcene	13	Woody, Fruit, and Peppermint	0.61	1.33	0.89	1.01	0.81	0.92	1.59	1.90	0.77	0.52
26	D-Limonene	10	Sweet and Fruit	2.17	5.73	4.08	5.15	4.64	3.18	4.35	5.64	3.24	*n.d.*
27	Nonanoic acid	1.5	Fat and Sweet	8.23	12.19	10.44	12.66	10.53	6.00	*n.d.*	22.80	0.00	*n.d.*
No.	Compound	OT (μg/kg)[a]	Odor description[b]	rOAVs									
				C7	C14	C21	C28	C35	D7	D14	D21	D28	D35
1	1-Octen-3-ol	1	Grass	49.45	17.76	23.80	16.99	15.69	29.85	12.28	37.47	19.36	28.61
2	Linalool oxide I	60	Flower	2.36	7.45	12.37	13.27	8.89	4.51	5.18	17.82	16.67	7.72
3	Linalool	6	Flower, Fruit, and Sweet	40.41	76.09	80.60	68.49	33.63	51.65	39.10	113.65	74.73	16.04
4	Phenylethyl alcohol	4	Flower	41.67	106.35	137.66	113.38	58.31	104.49	85.24	177.96	121.42	26.49
5	Linalool oxide II	320	Flower	0.10	0.60	1.05	1.35	0.87	0.43	0.55	2.14	1.64	0.26
6	Terpinen-4-ol	0.2	Woody	52.98	67.05	80.86	*n.d.*	53.10	54.30	41.42	103.00	65.90	32.06
7	α-Terpineol	350	Sweet	0.33	0.81	1.01	0.92	0.59	0.49	0.47	1.33	1.04	0.31
8	Geraniol	7.5	Flower, Fruit, and Sweet	5.95	13.11	12.73	9.95	3.90	4.96	4.97	18.16	9.02	1.35
9	Methyl salicylate	40	Peppermint	1.20	1.60	3.35	3.54	1.18	0.78	0.57	5.35	3.94	1.57
10	6-methyl-5-Hepten-2-one	68	Fruit	0.33	0.16	0.35	0.26	0.19	0.18	0.09	0.42	0.28	0.45
11	3,5-Octadien-2-one	0.5	Fruit and Fat	17.06	16.18	22.10	28.98	42.51	13.11	12.66	39.18	52.85	84.76
12	α-Ionone	0.4	Flower	9.27	7.83	9.31	12.16	8.34	10.11	4.68	19.61	12.24	7.97
13	β-Ionone	0.2	Flower, Fruit, and Woody	101.92	75.95	84.77	91.89	79.74	84.74	49.00	167.99	159.72	121.76
14	2-Heptenal	20	–	0.53	0.42	0.75	0.65	0.44	0.51	0.28	0.96	0.62	0.75

(Continued)

TABLE 1 (Continued)

No.	Compound	OT (μg/kg)[a]	Odor description[b]	rOAVs									
				C7	C14	C21	C28	C35	D7	D14	D21	D28	D35
15	2,4-Heptadienal	2.56	Fat	7.85	5.58	10.94	17.65	17.41	6.22	4.30	18.85	25.00	33.38
16	Benzeneacetaldehyde	4	Flower and Sweet	3.82	2.67	3.11	3.82	3.30	*n.d.*	1.64	5.06	4.57	3.25
17	1H-Pyrrole-2-carboxaldehyde,1-ethyl	2	Roast	3.89	17.46	32.64	46.03	24.80	15.72	14.01	67.92	55.22	25.46
18	2-Octenal	3	Fat	1.90	*n.d.*	2.32	2.82	2.26	1.60	0.73	3.45	3.33	3.42
19	Nonanal	1	Fruit, Flower, and Fat	*n.d.*	*n.d.*	*n.d.*	17.36	15.02	*n.d.*	*n.d.*	0.00	23.38	*n.d.*
20	2,6-Nonadienal	0.1	Fruit and Flower	*n.d.*	*n.d.*	*n.d.*	123.73	*n.d.*	*n.d.*	*n.d.*	0.00	142.07	119.20
21	Decanal	0.1	Sweet and Fruit	*n.d.*	*n.d.*	*n.d.*	*n.d.*	38.07	*n.d.*	*n.d.*	70.08	49.99	29.92
22	1,2-dimethoxybenzene	3.17	Sweet and Musty	4.66	24.66	51.07	81.21	83.33	27.88	32.23	109.81	123.86	106.39
23	1,2,3-Trimethoxybenzene	0.75	Stale and Musty	14.92	49.81	136.58	342.72	440.54	89.52	112.41	711.75	1025.16	814.02
24	1,2,4-Trimethoxybenzene	3.06	Stale and Medicinal	1.28	4.83	23.70	60.90	71.30	8.63	13.01	71.87	115.13	110.59
25	β-Myrcene	13	Woody, Fruit, and Peppermint	1.97	1.12	1.28	1.04	0.72	1.18	0.62	2.45	1.03	0.44
26	D-Limonene	10	Sweet and Fruit	4.30	3.28	4.41	3.94	*n.d.*	3.55	2.42	6.27	4.89	*n.d.*
27	Nonanoic acid	1.5	Fat and Sweet	12.80	6.54	12.50	11.32	*n.d.*	*n.d.*	*n.d.*	24.72	16.63	*n.d.*

OT, odor threshold; n.d., not detected; 7, 14, 21, 28, and 35, fermentation time; SGT, sun-dried green tea.

[a]Threshold value of different volatile compounds in water (μg/kg).

[b]Odor description for the volatile compounds.

A for *Saccharomyces*: *Rhizopus* = 1:2; B for *Saccharomyces*: *Aspergillus niger* = 1:2; C for *Saccharomyces*: *Aspergillus oryzae* = 1:2; D for *Saccharomyces*: *Rhizopus*: *Aspergillus oryzae* = 1:1:1; E for *Saccharomyces*: *Rhizopus*: *Aspergillus niger* = 1:1:1; F for *Saccharomyces*: *Rhizopus*: *Aspergillus niger*: *Aspergillus oryzae* = 1:1:1:1.

the abundance of fermenting mixed strains. Alcohol compounds were significantly higher in groups D, E, and F than in groups A, B, and C when fermented to the 21st day. Ester compounds increased significantly in their content with the increase of fermentation time. These differences in volatile compounds may be due to the differences in fermentation strains. During the pile-fermentation process, microorganisms secrete large amounts of peroxidases, cellulase, pectinase, lipase, and various hydrolases, which are involved in the oxidation, degradation, and molecular modification of catechins, gallic acid, and other aromatic precursors (3).

As shown in **Figure 2**, the results of principal component analysis (PCA) showed that the differences in volatile compounds increased with the increasing of fermentation time. The differences in volatile compounds at adjacent fermentation times were small. When fermentation proceeded to the 21st day, groups D, E, and F were mainly distributed in the first quadrant and groups A, B, and C were mainly distributed in the third quadrant, and their differences were significant. There were significant differences in the volatile compounds of the samples fermented with different mixed strains in the same fermentation time.

3.2. Flavor characteristics of ripened Pu-erh tea fermented with mixed strains

The contribution of volatile compound to tea flavor is not only related to the compound content but also to the odor threshold. Currently, OAV is commonly used to evaluate the contribution of volatile compounds to tea flavor, and it is generally believed that the larger the OAV, the greater contribution to the flavor, and compounds with OAV > 1 are usually considered as important flavor compounds in tea (34, 35). rOAVs values of volatile compounds of ripened Pu-erh tea fermented with mixed strains were shown in **Table 1**. There were 27 compounds with rOAVs > 1, including 8 alcohols, 1 ester, 4 ketones, 8 aldehydes, 3 methoxybenzenes, 2 alkenes, and 1 acid, such as linalool and its oxidation, geraniol, 6-methyl-5-hepten-2-one, 3,5-octadiene-2-ketone, 1,2,3-trimethoxybenzene, β-myrcene, limonene, and so on. In order to reveal the flavor characteristics of ripened Pu-erh teas, radar plots were constructed with the aroma characteristics of the 27 compounds (**Figure 3**). Radar plots of samples in the pile fermentation process from 7 to 35 days were shown in **Supplementary Figure 1**. At the end of fermentation on the 35th day, the ripened Pu-erh teas fermented with different mix strains was obtained. **Figure 3** indicated that ripened Pu-erh teas of Group A, B, and C presented the flavor characteristics of flower and sweet, compared with SGT. Compared with Group A, B, and C, the flavor characteristics of Group E were more prominent. These ripened Pu-erh teas (Group A, B, C, and E) present typical flower, fruit, and sweet flavor (**Figure 3**), which was defined as flower and fruit sweet flavor. The flower intensity of group D was similar to that of groups A, B, and C but the musty, stale and medicinal flavors were stronger than those of the three groups (**Figure 3D**, 35 days). F was significantly different from the first five groups, and this group had significantly higher musty and stale flavors than the other groups after 35 days of fermentation, and the flower flavor was significantly weaker than that other groups. This group of ripened Pu-erh tea presented typical stale and musty flavor (**Figure 3F**, 35 days). Previous studies (12)

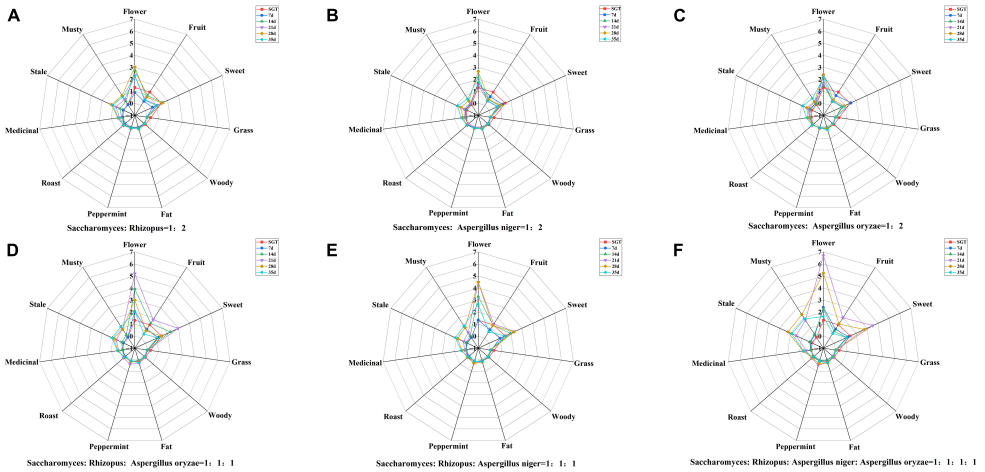

FIGURE 3
Radar plots of flavor characteristics of ripened Pu-erh teas during mixed fermentation with different strains (rOAVs > 1). **(A)** *Saccharomyces*: *Rhizopus* = 1:2; **(B)** *Saccharomyces*: *Aspergillus niger* = 1:2; **(C)** *Saccharomyces*: *Aspergillus oryzae* = 1:2; **(D)** *Saccharomyces*: *Rhizopus*: *Aspergillus oryzae* = 1:1:1; **(E)** *Saccharomyces*: *Rhizopus*: *Aspergillus niger* = 1:1:1; **(F)** *Saccharomyces*: *Rhizopus*: *Aspergillus niger*: *Aspergillus oryzae* = 1:1:1:1.

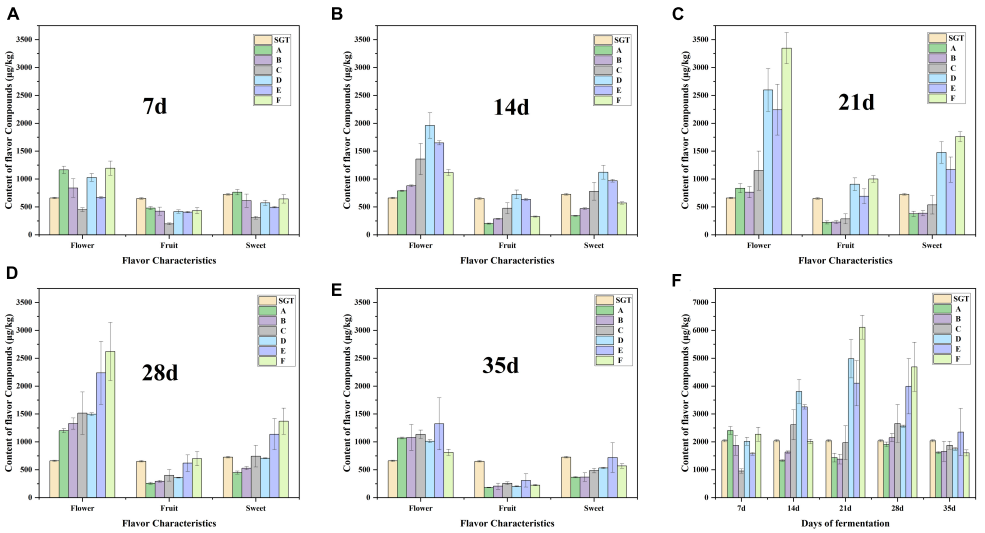

FIGURE 4
Content changes of the 17 volatile compounds with flower, fruit or sweet flavor during the fermentation process. Panels **(A–E)** are the content changes from 7 to 35 days, respectively. Panel **(F)** is the change in total content of the 17 compounds.

have indicated that *Aspergillus* is the main glucosidase-producing genus, and the fermentation treatment by microorganisms can effectively increase terpene alcohols from glycosides and linalool oxides through oxidation, and the increasing in the content of these compounds contributes to the formation of ripened Pu-erh tea with flower and fruit sweet flavor.

3.3. Changes of flower and fruit sweet flavor chemicals during fermentation process

Here we focus on the changes of chemicals with flower and fruit sweet flavor in Group D, E, and F. This research can help us find the suitable fermentation time of Pu-erh tea with pleasant flavor. There are 17 compounds having flower and fruit sweet flavor, including linalool, geraniol, 6-methyl-5-hepten-2-one, 3,5-octadien-2-one, limonene, linalool oxide, phenylethyl alcohol, α-Ionone, β-Ionone, benzeneacetaldehyde, nonanal, 2,6-nonadienal, decanal, β-myrcene, nonanoic acid, α-terpineol. Linalool presents flower, sweet, and fruit flavors (35, 36). Compounds that have a fruit flavor mainly include 6-methyl-5-hepten-2-one, 3,5-octadien-2-one, and limonene, the sweet compounds are mainly benzeneacetaldehyde, and the compounds that are mostly flower flavor are linalool oxide, geraniol, phenylethyl alcohol, and α-Ionone (26, 35–38). β-Ionone is a key aromatic compound in tea and contributes flower and fruit flavor (35, 37, 38). Nonanal and 2,6-nonadienal have fruit and flower flavor. Nonanoic acid and α-terpineol have

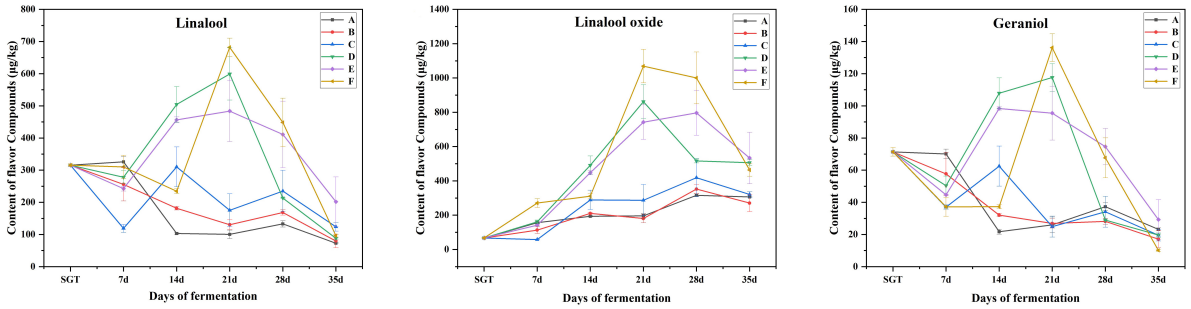

FIGURE 5
Content changes of linalool, linalool oxide, and geraniol with flower flavor during the fermentation process. A for *Saccharomyces*: *Rhizopus* = 1:2, B for *Saccharomyces*: *Aspergillus niger* = 1:2, C for *Saccharomyces*: *Aspergillus oryzae* = 1:2, D for *Saccharomyces*: *Rhizopus*: *Aspergillus oryzae* = 1:1:1, E for *Saccharomyces*: *Rhizopus*: *Aspergillus niger* = 1:1:1, F for *Saccharomyces*: *Rhizopus*: *Aspergillus niger*: *Aspergillus oryzae* = 1:1:1:1.

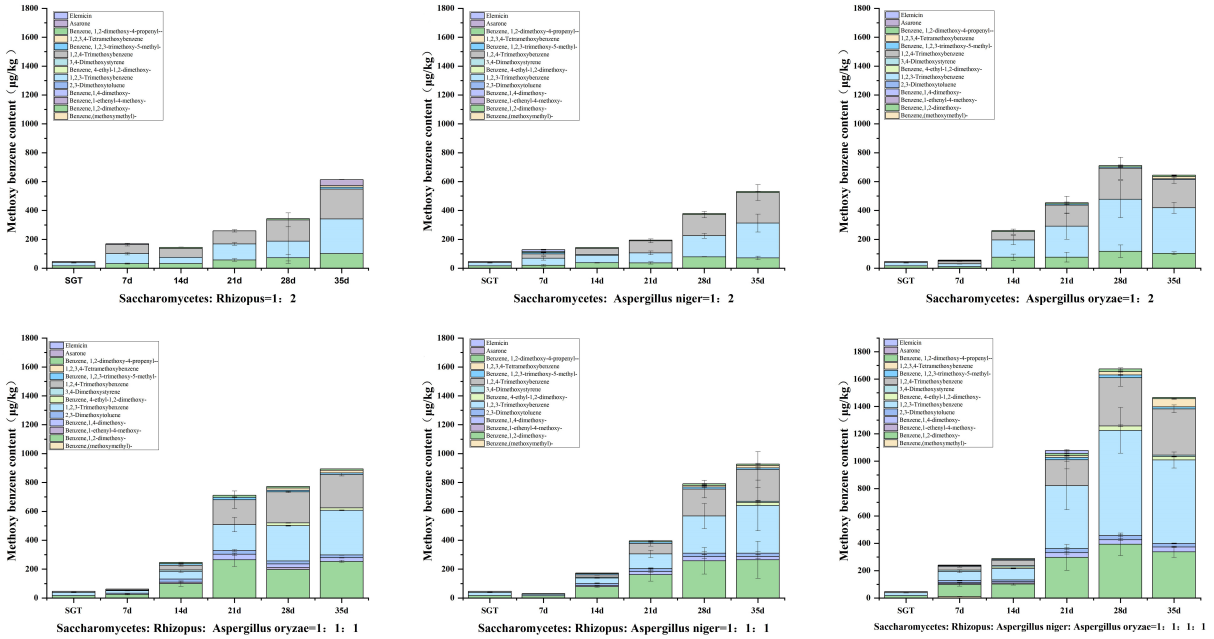

FIGURE 6
Content changes of 14 methoxybenzenes during the fermentation process.

sweet flavor. Decanal and β-myrcene have sweet and fruity flavor. The flavor profiles of these compounds were checked from http://www.thegoodscentscompany.com/search3.php. The total contents of these flavor compounds reached its maximum on the 21st day (**Figure 4F**), especially the flower flavor compounds (**Figure 4C**). The flower and fruit sweet flavor of Group D, E, and F increased significantly at the 21st day compared with the sun-dried green tea, by 144.27, 101.20, and 199.59%, respectively. When the fermentation continued to 35 days, the flower and fruit sweet flavor of Group E was stronger than that of SGT, increasing by 15.36%, decreasing 20.70, 18.80, 7.87, 14.33, and 21.32% in Group A, B, C, D, and F, respectively (**Figure 4**).

The three main flower flavor compounds mainly include linalool, linalool oxide, and geraniol, all increased significantly when the fermentation proceeded to the 21st day, then gradually deceased (**Figure 5**). Microorganisms can release β-primeverosides and β-glucopyranosides through enzymatic hydrolysis, and then biosynthesize linalool, and its oxides. It can increase the content of linalool and its oxides in this way (12). In summary, in this study, the flower and fruit sweet flavor of the ripened Pu-erh tea fermented for 21 days is the most remarkable, which is fermented by *Saccharomyces*: *Rhizopus*: *Aspergillus niger* mixed in the ratio of 1:1:1 (Group E).

3.4. Characterization of methoxybenzenes in ripened Pu-erh tea fermented by mixed strains

Methoxybenzenes are typical flavor compounds in ripened Pu-erh tea, which present stale flavor (39, 40). However, high contents

of methoxybenzenes usually have stale and musty flavor (9, 25, 41, 42, 43).

The total of 14 methoxybenzenes were annotated in this study, including 1,2-dimethoxybenzene, 1,2,3-trimethoxybenzene, 1,2,4-trimethoxybenzene, 1,4-dimethoxybenzene, 2,3-dimethoxytoluene, 3,4,5-trimethoxytoluene, 1,2,3,4-tetramethoxybenzene, 1,2-dimethoxy-4-propenyl-benzene, elemicin, asarone, et al. It was found that the types and contents of methoxyphenols produced in Group A, B, and C were lower than those in Group D, E, and F (**Figure 6**). The total content of methoxybenzenes reached to 613.60 μg/kg, 531.66 μg/kg, and 644.44 μg/kg in Group A, B, and C at the 35th day of fermentation, respectively. The total content of methoxybenzenes reached to 893.42 μg/kg and 927.88 μg/kg for Group D and E, respectively, by 35 days of fermentation. Group E had better coordination between flower and fruit sweet flavor and musty and stale flavor, compared with Group D. The total content of methoxybenzenes in group F reached 1,466.20 μg/kg by 35 days of fermentation, which was significantly higher than the other groups. In this study, it was found that the contents of methoxybenzenes increased with the prolongation of fermentation time, and the species and contents increased with the increase of strain richness, as shown in **Figure 6**. It is noteworthy that many reports described the odor of methoxybenzenes such as 1,2,3-trimethoxybenzene and 1,2,4-trimethoxybenzene as musty and stale, which may make methoxybenzenes contribute musty and stale flavor to the ripened Pu-erh tea (39). Furthermore, previous investigation showed that microorganisms can increase the content of gallic acid (GA) by degrading epigallocatechin gallate (EGCG) and hydrolyzing tannins during the fermentation of ripened Pu-erh tea in a hot and humid environment. Microorganisms such as *Aspergillus niger* can replace the hydrogen atoms of hydroxyl radicals in GA with methyl groups, resulting in methoxybenzenes, and compounds with similar structures (8, 12). Similar to our results, the pile fermentation process may contribute to the accumulation of methoxybenzenes.

4. Conclusion

In this study, ripened Pu-erh tea with flower and fruit sweet flavor was obtained by *Saccharomyces*, *Rhizopus,* and *Aspergillus niger* co-fermentation, using Yunnan big-leaf sun-dried green tea as fermentation raw materials. With the help of HS-SPME-GC-MS, a total of 135 volatile compounds were annotated, and due to the different strains and fermentation time, the ripened Pu-erh teas' volatile compounds varied greatly. OAV analysis illustrated that there were 17 volatile compounds presenting flower and fruit sweet flavor. The total content of these compounds increased until the 21th day and then decreased, which indicated that the 21th day was an important time point for the fermentation of ripened Pu-erh tea with flower and fruit sweet flavor. There were 14 volatile compounds showing musty and stale flavor. The content of these compounds increased with the extension of fermentation time, and the types and contents increased with the abundance of the strains. The flavor of ripened Pu-erh tea is the result of the synergistic effect of different flavor compounds. In this study, the flavor characteristics and content changes of volatile components in ripened Pu-erh tea during fermentation were demonstrated in detail. This will help us to further understand the formation mechanism of the characteristic flavor of ripened Pu-erh tea, so as to guide the optimization of the fermentation process of ripened Pu-erh tea.

Data availability statement

The original contributions presented in this study are included in the article/**Supplementary material**, further inquiries can be directed to the corresponding authors.

Author contributions

LY was responsible for methodology, writing—review, commentary editing, supervision, resources, and funding acquisition. WD was responsible for resources, supervision, methodology, and writing—review. YZ was responsible for writing—original draft, experimentation, formal analysis, and methodology. CZ and ZS were responsible for resources. DR was responsible for the formal analysis. RB, WL, and JW were responsible for investigation. All authors contributed to the article and approved the submitted version.

Funding

This research was supported by Yunnan Major Scientific and Technological Projects (Grant No. 202202AG050009).

Conflict of interest

The authors declare that the research was conducted in the absence of any commercial or financial relationships that could be construed as a potential conflict of interest.

Publisher's note

All claims expressed in this article are solely those of the authors and do not necessarily represent those of their affiliated organizations, or those of the publisher, the editors and the reviewers. Any product that may be evaluated in this article, or claim that may be made by its manufacturer, is not guaranteed or endorsed by the publisher.

Supplementary material

The Supplementary Material for this article can be found online at: https://www.frontiersin.org/articles/10.3389/fnut.2023.1138783/full#supplementary-material

References

1. Jiang L, Zheng KA. rapid classification method of tea products utilizing X-ray photoelectron spectroscopy: relationship derived from correlation analysis, modeling, and quantum chemical calculation. *Food Res Int.* (2022) 160:111689. doi: 10.1016/j.foodres.2022.111689

2. Li Y, Bai R, Wang J, Li Y, Hu Y, Ren D, et al. Pear polyphenol oxidase enhances theaflavins in green tea soup through the enzymatic oxidation reaction. *eFood.* (2022) 3:e35. doi: 10.1002/efd2.35

3. Ma W, Zhu Y, Shi J, Wang J, Wang M, Shao C, et al. Insight into the volatile profiles of four types of dark teas obtained from the same dark raw tea material. *Food Chem.* (2021) 346:128906. doi: 10.1016/j.foodchem.2020.128906

4. Zhang W, Cao J, Li Z, Li Q, Lai X, Sun L, et al. and GC/MS volatile component analysis of Yinghong No. 9 dark tea during the pile fermentation process. *Food Chem.* (2021) 357:129654. doi: 10.1016/j.foodchem.2021.129654

5. Zhang L, Zhang Z, Zhou Y, Ling T, Wan X. Chinese dark teas: postfermentation, chemistry and biological activities. *Food Res Int.* (2013) 53:600–7. doi: 10.1016/j.foodres.2013.01.016

6. Lu H, Yue P, Wang Y, Fu R, Jiang J, Gao X. Optimization of submerged fermentation parameters for instant dark tea production by *Eurotium cristatum*. *J Food Process Preservat.* (2016) 40:1134–44. doi: 10.1111/jfpp.12694

7. Xu J, Wei Y, Li F, Weng X, Wei X. Regulation of fungal community and the quality formation and safety control of Pu-erh tea. *Comp Rev Food Sci Food Safety.* (2022) 21:4546–72. doi: 10.1111/1541-4337.13051

8. Lv H, Zhong Q, Lin Z, Wang L, Tan J, Guo L. Aroma characterisation of Pu-erh tea using headspace-solid phase microextraction combined with GC/MS and GC–olfactometry. *Food Chem.* (2012) 130:1074–81. doi: 10.1016/j.foodchem.2011.07.135

9. Li Z, Feng C, Luo X, Yao H, Zhang D, Zhang T. Revealing the influence of microbiota on the quality of Pu-erh tea during fermentation process by shotgun metagenomic and metabolomic analysis. *Food Microbiol.* (2018) 76:405–15. doi: 10.1016/j.fm.2018.07.001

10. Zhu M, Li N, Zhou F, Ouyang J, Lu D, Xu W, et al. Microbial bioconversion of the chemical components in dark tea. *Food Chem.* (2020) 312:126043. doi: 10.1016/j.foodchem.2019.126043

11. Lv S, Wu Y, Li C, Xu Y, Liu L, Meng Q. Comparative analysis of Pu-erh and Fuzhuan teas by fully automatic headspace solid-phase microextraction coupled with gas chromatography-mass spectrometry and chemometric method. *J Agricultural Food Chem.* (2014) 62:1810. doi: 10.1021/jf405237u

12. Deng X, Huang G, Tu Q, Zhou H, Li Y, Shi H, et al. Evolution analysis of flavor-active compounds during artificial fermentation of Pu-erh tea. *Food Chem.* (2021) 357:129783. doi: 10.1016/j.foodchem.2021.129783

13. Hu S, He C, Li Y, Yu Z, Chen Y, Wang Y, et al. Changes of fungal community and non-volatile metabolites during pile-fermentation of dark green tea. *Food Res Int.* (2021) 147:110472. doi: 10.1016/j.foodres.2021.110472

14. Li Y, Hao J, Zhou J, He C, Yu Z, Chen S, et al. Pile-fermentation of dark tea: conditions optimization and quality formation mechanism. *LWT.* (2022) 166:113753. doi: 10.1016/j.lwt.2022.113753

15. Zhao M, Zhang D, Su X, Duan S, Wan J, Yuan WX, et al. An integrated metagenomics/metaproteomics investigation of the microbial communities and enzymes in solid-state fermentation of Pu-erh tea. *Sci Rep.* (2015) 5:10117. doi: 10.1038/srep10117

16. Li Q, Chai S, Li Y, Huang J, Luo Y, Xiao L, et al. Biochemical components associated with microbial community shift during the pile-fermentation of primary dark Tea. *Front Microbiol.* (2018) 9:1509. doi: 10.3389/fmicb.2018.01509

17. Ma Y, Ling T, Su X, Jiang B, Nian B, Chen L, et al. Integrated proteomics and metabolomics analysis of tea leaves fermented by *Aspergillus niger*, *Aspergillus tamarii* and *Aspergillus fumigatus*. *Food Chem.* (2021) 334:127560. doi: 10.1016/j.foodchem.2020.127560

18. Xu X, Yan M, Zhu Y. Influence of fungal fermentation on the development of volatile compounds in the puer tea manufacturing process. *Eng Life Sci.* (2005) 5:382–6. doi: 10.1002/elsc.200520083

19. Abe M, Takaoka N, Idemoto Y, Takagi C, Imai T, Nakasaki K. Characteristic fungi observed in the fermentation process for Puer tea. *Int J Food Microbiol.* (2008) 124:199–203. doi: 10.1016/j.ijfoodmicro.2008.03.008

20. Cao L, Guo X, Liu G, Song Y, Ho C, Hou R, et al. A comparative analysis for the volatile compounds of various Chinese dark teas using combinatory metabolomics and fungal solid-state fermentation. *J Food Drug Anal.* (2018) 26:112–23. doi: 10.1016/j.jfda.2016.11.020

21. Han X, Zhao Y, Hu B, Yang H, Peng Q, Tian R. Influence of different yeast strains on the quality of fermented greengage (*Prunus mume*) alcoholic beverage and the optimization of fermentation conditions. *LWT.* (2020) 126:109292. doi: 10.1016/j.lwt.2020.109292

22. Du L, Li J, Li W, Li Y, Li T, Xiao D. Characterization of volatile compounds of pu-erh tea using solid-phase microextraction and simultaneous distillation-extraction coupled with gas chromatography-mass spectrometry. *Food Res Int.* (2014) 57:61–70.

23. Zhang H, Wang J, Zhang D, Zeng L, Liu Y, Zhu W, et al. Aged fragrance formed during the post-fermentation process of dark tea at an industrial scale. *Food Chem.* (2020) 342:128175. doi: 10.1016/j.foodchem.2020.128175

24. Wang L, Lee J, Chung J, Baik J, So S, Park S. Discrimination of teas with different degrees of fermentation by SPME–GC analysis of the characteristic volatile flavour compounds. *Food Chem.* (2008) 109:196–206. doi: 10.1016/j.foodchem.2007.12.054

25. Wang B, Meng Q, Xiao L, Li R, Peng C, Liao X, et al. Characterization of aroma compounds of Ripened Pu-erh tea using solvent assisted flavor evaporation coupled with gas chromatography-mass spectrometry and gas chromatography-olfactometry. *Food Sci Hum Wellness.* (2022) 11:618–26. doi: 10.1016/j.fshw.2021.12.018

26. Tan F, Wang P, Zhan P, Tian H. Characterization of key aroma compounds in flat peach juice based on gas chromatography-mass spectrometry-olfactometry (GC-MS-O), odor activity value (OAV), aroma recombination, and omission experiments. *Food Chem.* (2021) 366:130604. doi: 10.1016/j.foodchem.2021.130604

27. Chen J, Yang Y, Deng Y, Liu Z, Shen S, Zhu J, et al. Characterization of the key differential volatile components in different grades of Dianhong Congou tea infusions by the combination of sensory evaluation, comprehensive two-dimensional gas chromatography-time-of-flight mass spectrometry, and odor activity value. *LWT.* (2022) 165:113755. doi: 10.1016/j.lwt.2022.113755

28. Gonzalez A, Benfodda Z, Bénimélis D, Fontaine J, Molinié R, Meffre P. Extraction and identification of volatile organic compounds in scentless flowers of 14 *Tillandsia species* using HS-SPME/GC-MS. *Metabolites.* (2022) 12:628. doi: 10.3390/metabo12070628

29. Van Den Dool H, Dec Kratz PA. generalization of the retention index system including linear temperature programmed gasâ"liquid partition chromatography. *J Chromatography A.* (1963) 11:463–71. doi: 10.1016/S0021-9673(01)80947-X

30. Fan X, Chen N, Cai F, Ren F, Zhong J, Wang D, et al. Effects of manufacturing on the volatile composition of raw Pu-erh tea with a focus on de-enzyming and autoclaving–compressing treatments. *LWT.* (2020) 137:110461. doi: 10.1016/j.lwt.2020.110461

31. Zhu J, Niu Y, Xiao Z. Characterization of the key aroma compounds in Laoshan green teas by application of odour activity value (OAV), gas chromatography-mass spectrometry-olfactometry (GC-MS-O) and comprehensive two-dimensional gas chromatography mass spectrometry (GC×GC-qMS). *Food Chem.* (2021) 339:128136. doi: 10.1016/j.foodchem.2020.128136

32. Hu W, Wang G, Lin S, Liu Z, Wang P, Li J, et al. Digital evaluation of aroma intensity and odor characteristics of tea with different types-based on OAV-Splitting method. *Foods.* (2022) 11:2204. doi: 10.3390/foods11152204

33. Ma L, Gao M, Zhang L, Qiao Y, Li J, Du L, et al. Characterization of the key aroma-active compounds in high-grade Dianhong tea using GC-MS and GC-O combined with sensory-directed flavor analysis. *Food Chem.* (2022) 378:132058. doi: 10.1016/j.foodchem.2022.132058

34. Usami A, Kashima Y, Marumoto S, Miyazawa M. Characterization of aroma-active compounds in dry flower of *Malva sylvestris* L. by GC-MS-O analysis and OAV calculations. *J Oleo Sci.* (2013) 62:563–70. doi: 10.5650/jos.62.563

35. Xiao Z, Wang H, Niu Y, Zhu J, Ma N. Analysis of aroma components in four Chinese congou black teas by odor active values and aroma extract dilution analysis coupled with partial least squares regression. *Food Sci.* (2018) 39:242–9. doi: 10.7506/spkx1002-6630-201810037

36. Joshi R, Gulati A. Fractionation and identification of minor and aroma-active constituents in Kangra orthodox black tea. *Food Chem.* (2015) 167:290–8. doi: 10.1016/j.foodchem.2014.06.112

37. Lv S, Meng Q, Xu Y, Liu S. Recent progress in aroma analysis methods and aroma active compounds in Pu-erh tea. *Food Sci.* (2014) 35:292–8. doi: 10.7506/spkx1002-6630-201411058

38. Wang M, Ma W, Shi J, Zhu Y, Lin Z, Lv H. Characterization of the key aroma compounds in Longjing tea using stir bar sorptive extraction (SBSE) combined with gas chromatography-mass spectrometry (GC-MS), gas chromatography-olfactometry (GC-O), odor activity value (OAV), and aroma recombination. *Food Res Int.* (2020) 130:108908. doi: 10.1016/j.foodres.2019.108908

39. Zhu J, Chen F, Wang L, Niu Y, Xiao Z. Evaluation of the synergism among volatile compounds in Oolong tea infusion by odour threshold with sensory analysis and E-nose. *Food Chem.* (2017) 221:1484–90. doi: 10.1016/j.foodchem.2016.11.002

40. Wang J, Zhang X, Xiao Q, Chu Z, Lu C. Analysis of volatile substances in different grades of Pu'erh ripe tea. *Food Industry Sci Technol.* (2022) 43:319–28. doi: 10.13386/j.issn1002-0306.2022010069

41. Xie J, Zhang W, Chen X, Zhao Y, Zhu X. Analysis of aroma changes during storage of ripe Pu'er tea. *Food Sci.* (2015) 36:154–7.

42. Tong W. *Study on the Characteristic Aroma Compounds of Pu-erh Tea*. China: Tianjin University of Science and Technology (2020). doi: 10.27359/d.cnki.gtqgu.202n.d.0376

43. Yamauchi H, doi MO-. Methylation of 2, 6-Dimethoxy-4-methylphenol by *Aspergillus glaucus* and their possible contribution to katsuobushi flavor. *Biosci Biotechnol Biochem.* (1997) 61:1386–7. doi: 10.1271/bbb.61.1386

frontiers | Frontiers in Nutrition

TYPE Original Research
PUBLISHED 22 June 2023
DOI 10.3389/fnut.2023.1160954

OPEN ACCESS

EDITED BY
Predrag Putnik,
University North, Croatia

REVIEWED BY
Krishan K. Verma,
Guangxi Academy of Agricultural Sciences, China
Fuping Zheng,
Beijing Technology and Business University, China

*CORRESPONDENCE
Huaixiang Tian
✉ tianhx@sit.edu.cn

RECEIVED 07 February 2023
ACCEPTED 30 May 2023
PUBLISHED 22 June 2023

CITATION
Yu H, Li Q, Guo W, Ai L, Chen C and Tian H (2023) Unraveling the difference in flavor characteristics of *Huangjiu* fermented with different rice varieties using dynamic sensory evaluation and comprehensive two-dimensional gas chromatography–quadrupole mass spectrometry.
Front. Nutr. 10:1160954.
doi: 10.3389/fnut.2023.1160954

Unraveling the difference in flavor characteristics of *Huangjiu* fermented with different rice varieties using dynamic sensory evaluation and comprehensive two-dimensional gas chromatography–quadrupole mass spectrometry

Haiyan Yu[1], Qiaowei Li[1], Wei Guo[1], Lianzhong Ai[2], Chen Chen[1] and Huaixiang Tian[1]*

[1]Department of Food Science and Technology, Shanghai Institute of Technology, Shanghai, China, [2]School of Medical Instrument and Food Engineering, University of Shanghai for Science and Technology, Shanghai, China

To investigate the specific differences in flavor characteristics of *Huangjiu* fermented with different rice varieties, dynamic sensory evaluation, comprehensive two-dimensional gas chromatography-quadrupole mass spectrometry (GC×GC–qMS) and multivariate statistical analysis were employed. Dynamic sensory evaluation methods including temporal dominance of sensations (TDS) and temporal check all that apply (TCATA) were applied to explore the differences and variations in sensory attributes. The sensory results showed that the intensity of astringency and post-bitterness in the *Huangjiu* fermented with glutinous rice was weaker while ester and alcoholic aroma were more prominent than the one fermented with japonica rice. The results of free amino acids and aroma compounds analysis indicated that the amino acids were mainly sweet and bitter amino acids, and some key aroma compounds were predominant in the *Huangjiu* fermented with glutinous rice, such as ethyl butyrate (OAV: 38–59), 3–methylthiopropionaldehyde (OAV: 47–96), ethyl caprylate (OAV: 30–38), while nonanal, phenyl acetaldehyde and vanillin contributed significantly to the *Huangjiu* fermented with japonica rice. The multivariate statistical analysis further confirmed that 17 compounds (VIP>1 and $p<0.05$) could be supposed to be the key compouns that cause significant flavor differences in *Huangjiu* samples fermented with different brewing rice. Moreover, partial least-squares analysis revealed that most compounds (ethyl butyrate, 3-penten-2-one, isoamyl acetate, and so on) correlated with ester and alcoholic aroma. The results could provide basic data and theoretical basis for the selection of raw materials in *Huangjiu*.

KEYWORDS

***Huangjiu* (Chinese rice wine), rice varieties, flavor characteristics, dynamic sensory evaluation, comprehensive two-dimensional gas chromatography–mass spectrometry**

1. Introduction

Huangjiu (Chinese rice wine), with a strong ester aroma and taste of rich and full-bodied, is one of the oldest fermented alcoholic beverages in the world and popular among consumers in East Asia (1). It is typically fermented with unique raw materials (brewing rice, brewing water and saccharification starter). The main rice varieties used in *Huangjiu* are glutinous rice and japonica rice, and their differences in amylopectin, protein and fat will affect the flavor quality of *Huangjiu*. The flavors of different *Huangjiu* brewed from indica glutinous rice, japonica glutinous rice and daily rice were compared and analyzed, and found that the content of volatile flavor compounds such as ethyl esters in *Huangjiu* brewed from japonica glutinous rice was significantly higher than that of the other two kinds of rice (2). In addition, there were significant differences in the concentrations of sweet, bitter, fresh and astringent amino acids in Chinese rice wine brewed from different rice varieties (3). The old saying that "rice is the flesh of Shaoxing *Huangjiu*" intuitively further reveals the importance of brewing rice to *Huangjiu*.

The unique raw materials and fermentation process endowed *Huangjiu* in Shaoxing region with the taste characteristics of fresh, sweet, mellow, and refreshing (4). At present, the taste evaluation of *Huangjiu* was mainly based on descriptive sensory analysis, which focused on static judgment of the sensory attributes or intensity of the sample within a given time (5), ignoring that the perception of sensory attributes may change with the residence time in the mouth (6). Dynamic sensory evaluation techniques represented by temporal dominance of sensation (TDS) and temporal check-all-that-apply (TCATA) can clearly captured the dynamic changes of various taste attributes and simultaneously compared and analyzed multiple taste attributes. Therefore, dynamic sensory evaluation techniques have been applied in the taste evaluation of beverages and wines (7, 8). Comparative analysis on the differences in physicochemical indexes and flavor characteristics of *Huangjiu* brewed with different rice varieties were studied (9, 10). Descriptive analysis is the main sensory evaluation method to reveal the flavor characteristics of *Huangjiu*. To our knowledge, there is no research on the flavor characteristics of *Huangjiu* brewed with different rice using dynamic sensory evaluation method.

Alcohols, esters, acids, aldehydes and ketones are the main volatile aroma compounds of *Huangjiu*, which has been extensively studied by researchers using gas chromatography–mass spectrometry (11, 12). However, due to the low resolution, sensitivity and insufficient separation ability of one-dimensional GC–MS (13), the actual flavor components were more abundant than those detected. Comprehensive two-dimensional gas chromatography (GC × GC) can overcome the defects with the advantages of high selectivity and sensitivity, large peak capacity and higher recognition ability. Two-dimensional gas chromatography is widely combined with rapid scanning quadrupole mass spectrometry (qMS) and time-of-flight mass spectrometry (TOF-MS) to analyze the aroma compounds in wine (14, 15). In our previous study, GC × GC-qMS was used to analyze the aroma characteristics of *Huangjiu* in Shaoxing region with different vintage (16) and different brewing water (17). The conclusions of these researches showed that the coverage of aroma compounds of GC × GC-qMS was much higher than that of GC–MS. However, current research mainly applied GC–MS to compare and analyze the aroma compounds of *Huangjiu* brewed by different rice varieties, the identification of aroma component involving GC × GC-qMS analysis are still insufficient.

The objectives of this study are (1) to evaluate the differences in taste and aroma characteristics of *Huangjiu* fermented with different brewing rice by using quantitative description sensory analysis and dynamic sensory evaluation techniques (TDS and TCATA) combined with electronic tongue; (2) to reveal the molecular difference of flavor compounds among the samples by using GC × GC-qMS and high performance liquid chromatography (HPLC), respectively; and (3) to further clarify the difference of aroma characteristics by multivariate statistical analysis, and to analyze the influence of brewing rice on the flavor characteristics by analyzing the correlation between the aroma-active compounds and sensory attributes among the samples. This study would improve the understanding of the influence of the brewing rice on the flavor compounds and provide a scientific basis for the selection of rice varieties to brew high-quality *Huangjiu*.

2. Materials and methods

2.1. Samples and chemicals

Huangjiu samples in Shaoxing region (S1, S2) fermented by glutinous rice and japonica rice, respectively, were provided by Zhejiang Pagoda Brand Shaoxing Rice Wine Co., Ltd., Shaoxing City, Zhejiang Province, China. The samples were brewed using the same Jianhu water, wheat *Qu* (a saccharification starter) and *Jiuyao* (a fermentation starter) with the same ratio. And the same brewing technique including soaking and steaming rice, fermentation (primary fermentation at 28°C for 3–5 days, then secondary fermentation at medium-low temperatures for about 90 days), filtration, pressing, clarification and storage was applied. All of the samples were stored at 4°C and they were analyzed within 1 month after being transferred to the laboratory.

The regents, aspartate, leucine, lysine, proline, histidine, arginine, 2-octanol (internal standard) and *n*-alkane standards (C_5–C_{30}) of chromatographic grade and purity ≥98.0% were obtained from Sigma Aldrich (Shanghai, China).

2.2. Sensory evaluation

The training and sensory analyzes were performed in a professional sensory laboratory at 20°C following ISO 8586-1:2012. Ten sensory panelists (5 males and 5 females, 23–27 years old) were selected from 40 candidates (20 males and 20 females, 23–30 years old) from the School of Perfume and Aroma Technology, Shanghai Institute of Technology (Shanghai, China). The taste sensory evaluation training was conducted for using the taste reference solution and Shaoxing *Huangjiu* samples for 4 weeks (1 h each time and 3 times a week). The panelists were specially trained to use taste description attributes and interval scale of 10 points for evaluation. During the taste sensory evaluation, *Huangjiu* sample (20 mL) was placed in a covered and odorless glass cup vial marked with a random three-digit code. The taste attributes included acidity (stated as the taste of citric acid aqueous solution), sweet (sucrose aqueous solution), bitter (quinine sulfate aqueous solution), astringent (alum aqueous solution), and umami (sodium glutamate aqueous solution). The intensities of the taste attributes were quantitatively determined on the interval scale of 10 points, where 0 indicated none and 9 indicated very intense. The methods and procedures of dynamic sensory

evaluation including TCATA and TDS analysis were performed as described in our previous research (18).

Quantitative descriptive analysis (QDA) was similar to above taste sensory training, its methods and procedures were performed as described by our previous research (19). According to preliminary experiment discussion by the panelists, and referenced to a relevant literature (20), eight aroma attributes were selected, including sour (the aroma of acetic acid), sauce (4-ethylphenol), ester (ethyl acetate), sweet (vanillin), alcoholic (3-methylbutanol), caramel (caramel), fruit (ethyl isovalerate) and wheat (wheat *qu* aroma extract) aroma attributes. Prior to the formal sensory evaluation, the panelists were asked to smell each aroma attributes of standard reference sample and evaluated repeatedly according to the interval scale of 10 points. Additionally, for each one of the sensory evaluation indicated below, the sensory evaluation glasses used were ISO standard black glasses to eliminate the influence of sample color on the panelists. All sensory tests were conducted in triplicate, and a 10-min interval was maintained between each evaluation step.

2.3. Electronic tongue analysis

The TS-5000Z electronic tongue system (Insent Inc., Atsugi-Shi, Japan) including CAO, GL1, COO, AE1, AAE and Aftertaste-B sensors was used to collect the information of sour, sweet, bitter, astringent, fresh and post-bitter of the samples at 25°C. With tartric acid/potassium chloride solution as the reference solution, the sampling time was set to 120 s with the frequency was1 time/s, and each sample was were measured in triplicate.

2.4. Free amino acid analysis

Qualitative and quantitative analysis of 17 free amino acids in two kinds of *Huangjiu* samples was carried out by referring to QB/T 4356–2012 (National Standards of China). The C18 column (250 mm × 4.6 mm, 5 μm) was purchased from Agilent Technologies. The column temperature was maintained at 40°*C. mobile* phase A was 20 mmol/L sodium acetate buffer containing 0.05% v/v triethylamine. Mobile phase B was 80% acetonitrile and 20% water. The gradient elution procedure was as follows: 8–100% B from 0 to 33 min, 100% B from 33 to 36 min, 100–8% B from 36 to 38 min, and 8% B from 38 to 45 min. The injection volume was set to 10 μL, and the flow rate and detection wavelength were set to 1.0 mL/min and 254 nm, respectively. The amino acids in the samples were identified by comparing their retention times with those of the amino acid standards, and the concentration of each amino acid was analyzed according to the standard working curve of each amino acid standard solution.

2.5. Analysis of volatile compounds by solvent assisted flavor evaporation extraction combined with GC× GC-qMS

2.5.1. Conditions of solvent assisted flavor evaporation

SAFE analysis was performed as described in our previous research (17), *Huangjiu* sample (60 mL), 200 μL internal standards (2-octanol, 315 μg/mL) and dichloromethane (60 mL) were placed in 250 mL conical flask, and extracted for 60 min at 250 r/min (20°C) in a shaker (ME104E, Mettler Toledo Instruments Co., Ltd., Shanghai, China). The extract was collected into a centrifuge tube (50 mL), and centrifuged at 4°C for 5 min (8,000 r/min) to collect the organic phase. The procedures of extraction were duplicated three times. The collected extract (about 180 mL) was combined, dried by nhydrous sodium sulfate and separated by SAFE apparatus (Glasbläserei Bahr, Manching, Germany). Liquid nitrogen was added to the cold trap and the turbine pump was turned on. When the required pressure (approximately 3×10^{-3} Pa) was reached, the sample was slowly and evenly controlled to drop into the distillation bottle. After extraction, the extract was dried and collected by rotary evaporation. Finally, the SAFE distillate was blown to 1 mL with nitrogen and stored at −20°C.

2.5.2. Gas chromatography-quadrupole mass spectrometry analysis

The parameters and procedures for GC × GC-qMS (Shimadzu Co., Kyoto, Japan) analysis was described in our previous study (20, 21). An Agilent (Santa Clara, CA) HP-Innowax (60 m × 0.25 mm × 0.25 μm) and a Restek (Philadelphia, United States) BPX-1 (2 m × 0.1 mm × 0.1 μm) were used as column 1 and column 2, respectively. The column flow rate was 0.95 mL/min and split ratio was 20:1. The conditions were as follows: the oven temperature was held at 40°C and held for 5 min, then increased at 3°C/min to 150°C, finally increased at 4°C/min to 230°C. The temperature of column 2 was set to 5°C higher than that of column 1. And the modulation period was set to 8 s. The electron ionization energy was set to 70 eV, the ion source temperature was set at 200°C with high scanning frequency (20,000 Hz), and the total ion currents were recorded from m/z of 20 to 350. The analyzes were conducted in triplicate.

The volatile compounds were comprehensively characterized by GC-Image software (GC-Image LLC, Lincoln, NE), retention index and NIST 2014 (NIST, Gaithersburg-MD, United States) database and peak library matching factor. And the retention index was calculated based on C_5-C_{30} alkane standards (Sigma-Aldrich, St. Louis, MO, United States).

2.6. Odor activity values calculation

The contribution of a certain compound to the aroma characteristics of the samples was evaluated by its OAV (ratio of the mass concentration and the odor threshold value) (17). The odor threshold values were taken from available information in the compilation (22) and based on water or ethanol solution matrix. The characteristic aroma compounds in the samples were screened according to OAV > 1.

2.7. Statistical analysis

Sensory data were analyzed by Duncan's multiple range tests using SPSS Statistics 21 (SPSS Inc., Chicago, United States). Heat map was generated by using the pheatmap package of the R program. The multivariate analyzes were performed by SIMCA-PTM14.1 (UMetrics AB, Umea, Sweden) software.

3. Results and discussion

3.1. Taste characteristics analysis of *Huangjiu* fermented with different brewing rice

In the process of drinking, the taste attributes were not static, and the dynamic changes of tastes will also affect the judgment on the taste quality of *Huangjiu*. Therefore, the taste properties of *Huangjiu* samples fermented with different brewing rice were analyzed by dynamic sensory evaluation methods including TCATA and TDS. By collecting the citation proportion of each taste attribute of the samples within 60s, the TCATA test can intuitively reflect the dynamic changes of taste attributes of the samples with time during drinking. As shown in Figure 1, the variation trends of the taste attributes of *Huangjiu* samples fermented with different brewing rice were basically similar. Among them, the taste attributes of *Huangjiu* samples fermented with glutinous rice and japonica rice that were noted more than 50% of the time were mainly sour, bitter and astringent at the early stage, and sweet and umami in the late stage. The citation proportion of sour, bitter and astringent tastes in two kinds of *Huangjiu* samples gradually decreased after drinking, while the umami taste was the opposite, which may be related to the fact that the sauce flavor in *Huangjiu* was transformed into post-nose taste after being drunk in the mouth, thus gradually enhancing the perception of umami taste of the panelists (23). Complex oral processing can also enhance the umami taste in the middle and late stages of digestion (24). On the whole, the citation proportion of taste attributes of the *Huangjiu* fermented with japonica rice was slightly higher than that of the *Huangjiu* fermented with glutinous rice, and the taste characteristic was relatively richer. However, the taste of the former was more sour and bitter, and the citation proportion of bitter at the end of the 60s test was 19.5%, which was also significantly higher than that of S1 sample (8.9%).

Compared with TCATA, a sensory analysis method that is close to consumer testing (25), the TDS method can better reflect the influence of some dominant taste attributes on sensory attributes during drinking. The dominance rates of taste attributes of two types of *Huangjiu* samples within 60s after drinking were collected to clarify the changes of dominant taste attributes. The TDS analysis results among the *Huangjiu* samples are shown in Figure 2. The taste attributes of the two types of *Huangjiu* samples had similar dynamic trends that the order of sour, bitter and umami was maintained. At the beginning of the test (0 s), the sour taste dominated in the two types of *Huangjiu* samples. In the first 20s, with the decrease of the dominant rate of sour taste over time, the dominance of bitter taste gradually increased, which may be related to the symmetrical inhibition of sour and bitter. After 20s of the TDS test, the dominant rates of sour and bitter tastes among the samples gradually decreased, while umami taste broke through the chance level and significance level, and then occupied the dominant taste attribute. The curve above the line of chance level indicated that taste attributes can be accidentally perceived, and the significance level revealed that the cut-off above, the probability of taste attributes being selected was significantly greater than chance (26). The above feature was not only consistent with the taste characteristics of umami taste in the late stage, but also related to the inhibition of umami taste on sour and bitter taste (27). In general, although the variation trends of the taste attributes during drinking among the samples were basically similar, the bitter taste maintained shorter time and lower dominance rate in the overall drinking process of *Huangjiu* fermented with glutinous rice, indicating that the bitterness of *Huangjiu* fermented with glutinous rice was lighter and easier to dissipate than that of *Huangjiu* fermented with japonica rice, and the overall palatability was higher than that of the latter.

To further analyze the taste of *Huangjiu* samples and test the results of TCATA and TDS, the taste of two types of *Huangjiu* fermented by different brewing rice was evaluated by intelligent sensory electronic tongue technology. The taste evaluation of *Huangjiu* samples was shown in Table 1. The response values of astringency and post-bitterness taste of S1 sample were weaker than those of S2 sample ($p < 0.05$), but there were no difference in other taste attributes. Additionally, the response value of umami taste was slightly better than the latter, which was consistent with the above dynamic sensory test results. The combination of artificial sensory evaluation and

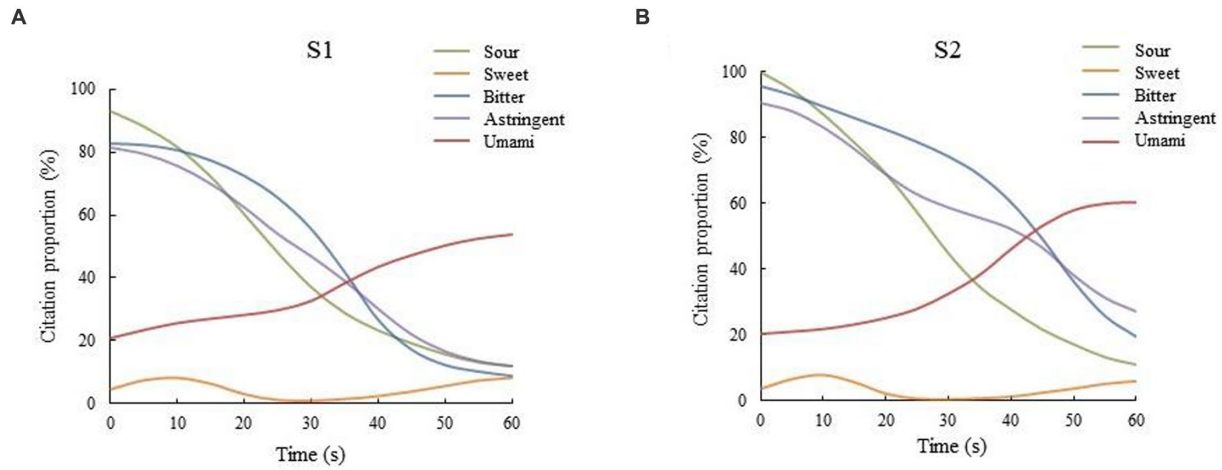

FIGURE 1
TCATA curves of the taste of the two types of *Huangjiu* samples fermented with different rice varieties (**A**,**B** represent the *Huangjiu* fermented with glutinous rice and japonica rice, respectively).

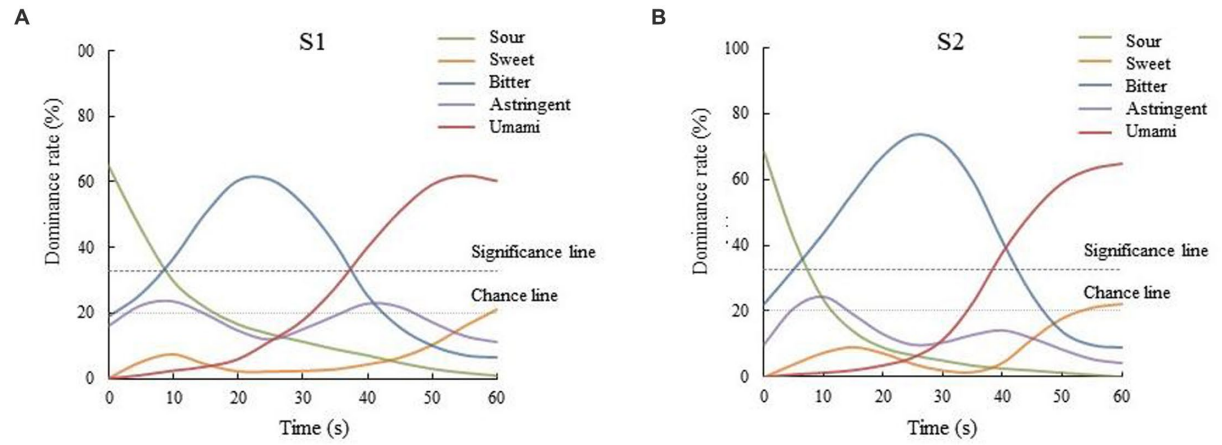

FIGURE 2
TDS curves of the taste of the two types of *Huangjiu* samples fermented with different rice varieties (A and B represent the *Huangjiu* fermented with glutinous rice and japonica rice, respectively).

TABLE 1 Taste evaluation of *Huangjiu* fermented with different rice varieties by electronic tongue.

	Sour	Sweet	Bitter	Astringent	Umami	After-bitterness
S1	6.47 ± 0.634a	−5.23 ± 0.287a	5.52 ± 0.376a	1.22 ± 0.0143b	9.61 ± 0.528a	0.609 ± 0.0275b
S2	6.64 ± 0.620a	−5.48 ± 0.241a	5.74 ± 0.289a	1.35 ± 0.0256a	9.39 ± 0.633a	0.632 ± 0.0240a

electronic tongue was conducive to fully characterize the taste evaluation of *Huangjiu*.

3.2. Free amino acids analysis of *Huangjiu* fermented with different brewing rice

Huangjiu contained a large amount of amino acids, which endowed *Huangjiu* with a rich taste level such as delicious, soft and mellow. The concentrations of free amino acids determined by high performance liquid chromatography (HPLC) in two kinds of *Huangjiu* samples are shown in Table 2. The total content of free amino acids in *Huangjiu* fermented with japonica rice (S2) was slightly higher than that in *Huangjiu* fermented with glutinous rice (S1), which was related to the higher protein content in japonica rice. The concentrations of free amino acids imparting sweet, bitter, umami, astringent and sour tastes were significantly different among the samples. The contents of aspartic acid and glutamic acid in S1 sample were higher, which played an important contribution to the umami and mellow taste. In addition, bitter amino acids were found to account for more than 40% of the total amino acids in the *Huangjiu* samples (40.2–43.9%), which was consistent with that of Liang et al. (28). Among them, the concentrations of histidine and leucine with bitter taste in S2 sample were higher than those of S1 sample, while isoleucine, phenylalanine and arginine were lower than the latter. Arginine imparted little bitter tastes, and bitterness was enhanced at high concentrations.

The umami and sweet taste of tea soup had a positive correlation, while the umami and bitter taste negatively correlated (29). The same taste interaction may also exist in *Huangjiu*, where the umami taste provided by glutamic acid and aspartic acid may enhance the perception of sweet taste and weaken the perception of bitter taste. Therefore, the perception of sweet taste in S1 sample was stronger than that of S2 sample, while the bitterness perception was weaker. The contents of sour and astringent amino acids in *Huangjiu* samples fermented with glutinous rice were significantly lower ($p < 0.05$), which was consistent with the results of electronic tongue and artificial sensory tests on the whole.

3.3. Quantitative descriptive sensory analysis of *Huangjiu* fermented with different brewing rice

To determine the aroma difference among the samples fermented with different brewing rice, quantitative descriptive analysis was analyzed and the results were shown in Figure 3. Ester, alcoholic, sauce and fruit aroma were the representative aroma in the two kinds of *Huangjiu*. Statistical analysis showed that the attributes of ester and alcoholic aroma in S1 sample were significantly higher ($p < 0.05$). Additionally, the scores of sweet, sauce, caramel and sour aroma were abundant, while there was no significant difference between these aroma attributes, which was consistent with the research of Chen et al. (19). The results of sensory evaluation indicated that *Huangjiu* fermented with glutinous rice was more prominent in ester and alcoholic aroma, and had better aroma quality.

3.4. Aroma components analysis of *Huangjiu* fermented with different brewing rice by GC×GC-qMS

The volatile characteristics of *Huangjiu* fermented with different brewing rice were systematically analyzed by GC×GC-qMS. The three-dimensional chromatograms of the volatile distribution of two

10.3389/fnut.2023.1160954

TABLE 2 Analysis of free amino acids of *Huangjiu* fermented with different rice varieties (mg/kg).

Free amino acid	S1	S2
Sweet		
Serine (Ser)	98.6 ± 1.63a	98.8 ± 1.02a
Glycine (Gly)	202 ± 2.34b	212 ± 1.66a
Threonine (Thr)	124 ± 2.04a	124 ± 1.35a
Alanine (Ala)	430 ± 4.89b	461 ± 2.04a
Proline (Pro)	499 ± 5.93b	614 ± 6.19a
Methionine (Met)	53.3 ± 3.23a	59.5 ± 3.10a
Bitter		
Histidine (His)	91.6 ± 1.15b	95.9 ± 1.09a
Arginine (Arg)	600 ± 5.51a	526 ± 4.08b
Valine (Val)	235 ± 4.49a	225 ± 1.22b
Isoleucine (Ile)	143 ± 1.87a	140 ± 2.66a
Leucine (Leu)	387 ± 4.89a	390 ± 2.55a
Phenylalanine (Phe)	235 ± 4.08a	194 ± 2.51b
Lysine (Lys)	180 ± 2.33a	167 ± 1.86b
Umami		
Aspartic acid (Asp)	277 ± 1.86a	273 ± 2.67b
Glutamate (Glu)	422 ± 3.72a	420 ± 5.31a
Astringent		
Tyrosine (Tyr)	280 ± 1.98a	313 ± 3.31b
Sour		
Cysteine (Cys)	7.93 ± 0.883a	10.3 ± 0.577b

Values with different letters (a–b) in a row are significantly different using Duncan's multiple comparison tests ($p < 0.05$).

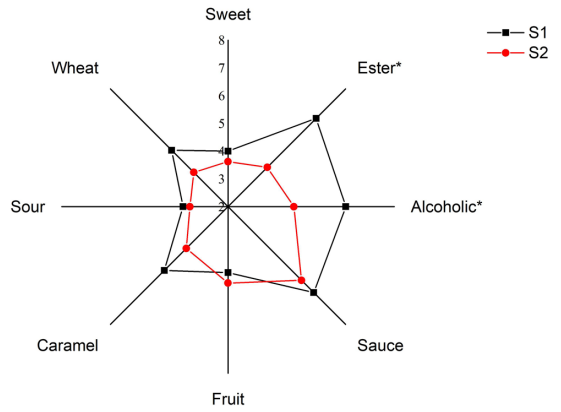

FIGURE 3
Quantitative descriptive sensory radar chart of *Huangjiu* fermented with different different rice varieties (*represents $p<0.05$, S1 and S2 correspond to the *Huangjiu* samples fermented by glutinous rice and japonica rice, respectively).

kinds of *Huangjiu* samples are shown in Figure 4. DB-INNOWAX column was used to successfully separate the volatile compounds in the first dimension, and the BPX-5 column was also successfully separated in the second dimension. The aroma components of the *Huangjiu* samples were analyzed and their results were listed in Supplementary Table S1. A total of 111 volatile compounds were identified, of which 101 and 99 were identified in S1 sample and S2 sample, respectively, which consisted of 32 esters, 20 alcohols, 12 aldehydes, 19 acids, 9 ketones, 5 phenols, 1 ether, 6 amines, 1 epoxide and 6 other compounds. Although the composition of volatile compounds in the two samples was basically similar, there were obvious differences in the concentrations of specific compounds.

The content of esters in the *Huangjiu* samples fermented with different brewing rice was abundant, and most of which were ethyl esters. Ethyl ester was mainly formed by esterification of fatty acids and ethanol (30) and endowed *Huangjiu* with fruity, sweet and floral aroma. Among the esters detected, monoethyl succinate, ethyl 3-hydroxybutyrate, diethyl succinate, ethyl butyrate, propyl nonolactone and ethyl caprylate were the major esters with the highest concentrations. Among them, the OAVs of ethyl butyrate (OAV: 38–59), ethyl caprylate (OAV: 30–38) and propyl nonolactone (OAV: 4–7) were all greater than 1. These three compounds had apple, banana and peach aroma, respectively, indicating they were important compounds that affected the aroma characteristics of *Huangjiu*. In addition, isoamyl acetate (OAV = 5) and sugar lactone (OAV = 6) with low concentrations were only indentified in S1 sample. The compound isoamyl acetate contributed to sweet and fruity aroma and was an important precursor for the formation of many aroma compounds. The compound sugar lactone was a key compound for the aroma characteristics of *Huangjiu*, which endowed *Huangjiu* with caramel aroma at low concentrations while curry aroma at high concentrations (31). This result was consistent with the scores of sweet and caramel aroma in descriptive sensory analysis. However, the compound 2-methylbutyl acetate (OAV = 14) with low concentration was only detected in S2 sample and was a characteristic aroma compound endowing *Huangjiu* with fruity aroma.

Alcohols were the important source of aroma in *Huangjiu* and were precursors of esters, which endowed *Huangjiu* with mellow and sweet. The concentrations of total alcohols in S1 sample (93.35–101.92 μg/g) were significantly higher than those in S2 sample (84.92–94.97 μg/g). This trend may be related to the higher content of amylopectin in glutinous rice, and the easy gelatinization of amylopectin, which promoted the conversion of sugars to alcohols during *Huangjiu* fermentation and thus improving the alcohol yield. Among the alcohols detected, 3-methylbutanol had the highest content, followed by phenylethanol, isobutanol, 2,3-butanediol, 3-methylthiopropanol and 1-butanol. The sum of these six alcohols accounted for 97.2–97.3% of the total alcohols among the samples. Among them, the OAVs of phenylethyl alcohol (OAV: 3–4) and 3-methylthiopropanol (1–3) were both greater than 1. The compound phenylethyl alcohol with rose and honey aromas can be synthesized by pentose phosphate or glycolytic pathway (32), and under anaerobic conditions, valine and phenylalanine can be converted into isobutanol and phenylethanol, respectively (33). The compound 3-methylthiopropanol with sweet and potato aromas may be derived from the degradation of sulfur-containing amino acids.

Aldehydes and ketones were conducive to enhancing the aroma and soft taste of *Huangjiu*. Most aldehydes were produced by the oxidation of higher alcohols or Maillard reaction during *Huangjiu* fermentation. The content of aldehydes in S1 sample was higher than that in S2 sample. The main aldehydes with high concentrations in the samples were n-hexanal, furfural and 5-methyl furfural. The concentrations of furfural and syringaldehyde with sweet taste in S1

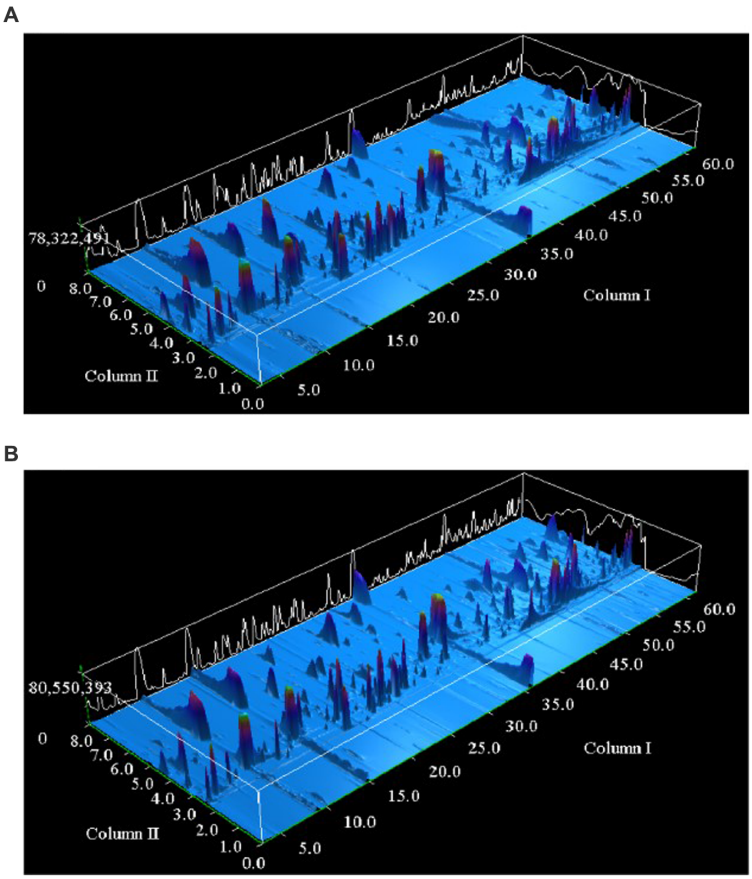

FIGURE 4
Three dimensional chromatograms of volatile components of Huangjiu fermented with **(A)** glutinous rice and **(B)** japonica rice were determined by GC×GC/qMS.

sample were higher than that in S2 sample, while nonaldehyde, benzaldehyde and phenylacetaldehyde in S2 sample were significantly higher than that in S1 sample. Among them, the compound phenylacetaldehyde (OAV = 292) with sweet and floral aroma was only detected in S2 sample, and was an important odorant in *Huangjiu* (34). In S1 sample, the compound 3-hydroxy-2-butanone with sweet and creamy aroma had the highest concentration, which was the key compound for the synthesis of 2,3-butanedione and 2,3-butanediol. Additionally, 4-ethylphenol, 4-vinyl-2-methoxyphenol and guaiacol had high relative concentrations. Among them, the compound 4-ethylphenol endowed a smoky aroma (35) and was only detected in S1 sample. And the concentration of 4-vinyl-2-methoxyphenol with clove aroma in S1 sample was much higher than that in S2 sample. The abundance of acids increased the body of *Huangjiu* and facilitated the formation of aromatic esters. Appropriate amount of acids can also increase the sweet taste and weaken the bitterness of wine, which may be the reason why *Huangjiu* fermented with glutinous rice was less bitter and astringent than *Huangjiu* fermented with japonica rice. A total of 19 acid compounds were detected in the samples. The contents of acids in S1 sample (11.31–11.34 μg/g) were significantly higher than those in S2 sample (8.31–7.49 μg/g). This may be due to the low protein content and dispersed structure in glutinous rice (36). Among them, the concentration of butyric acid was the highest, followed by acetic acid, palmitic acid and hexanoic acid. The production of these organic acids were closely related to the raw materials in *Huangjiu* brewing, including the process of alcohol fermentation or aging (37).

In conclusion, the total contents of alcohols, aldehydes, acids and characteristic flavor compounds in *Huangjiu* sample fermented with glutinous rice were higher than those of *Huangjiu* sample fermented with japonica rice. The compound ethyl butyrate, isoamyl acetate, 3–methylthiopropionaldehyde and ethyl caprylate were the characteristic flavor compounds of S1 sample, while nonanal, phenyl acetaldehyde and vanillin contributed greatly to the flavor of S2 sample.

3.5. Differences of aroma characteristics among the samples with different brewing rice

To fully explore the data of aroma compounds obtained by GC × GC-qMS, one-way ANOVA was performed on 111 identified volatile compounds. The results showed that there were significant differences in 64 compounds among the samples. Among them, 48 compounds had clear aroma descriptions, including 15 esters, 6 alcohols, 7 aldehydes, 10 acids, 2 phenols, 1 ether, 2 ketones, 4 aromatics and 1 amine compound. The correlation between the samples and the 48 important aroma compounds ($p < 0.05$) with

aroma description was visualized by heatmap, and the results were shown in Figure 5A.

The VIP values were usually used to assess the contributions of X-variables to the model, and variables with VIP > 1 were considered important variables (Figure 5B). The VIP values of 17 volatile compounds were greater than 1, including 7 acids (butyric acid, acetic acid, hexanoic acid, levulinic acid, benzoic acid, isobutyric acid and myristic acid), 4 alcohols (isobutanol, phenethyl alcohol,

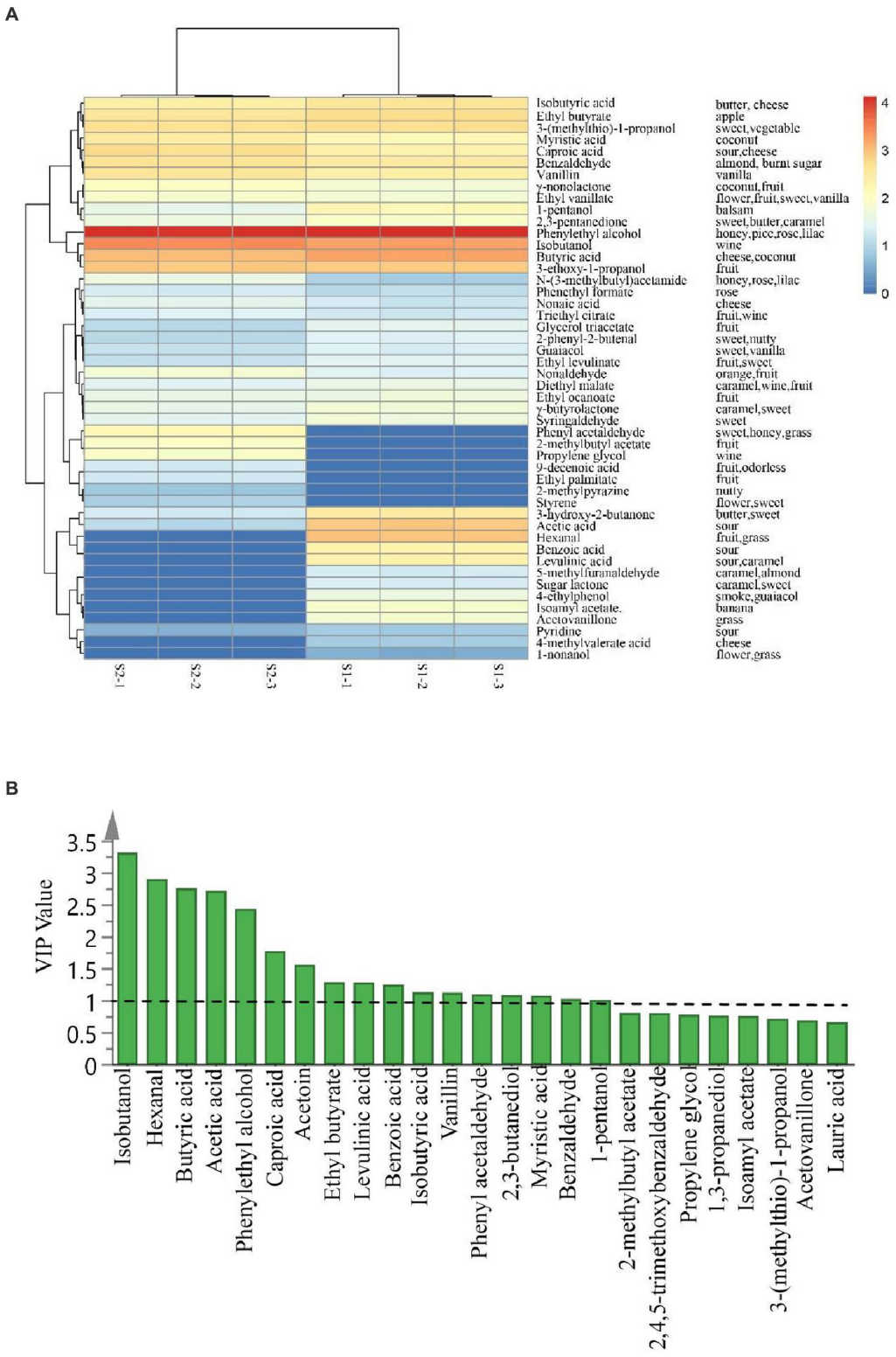

FIGURE 5
Heat map and HCA clustering results of 48 aroma compounds with a significant difference ($p<0.05$) and aroma descriptors in *Huangjiu* samples **(A)** (S1 and S2 correspond to the *Huangjiu* samples fermented by glutinous rice and japonica rice, respectively); The VIP plot of the aroma compounds based on the OPLS-DA regression model **(B)**.

2,3-butanediol and 1-pentanol), 3 aldehydes (hexanal, phenylacetaldehyde and benzaldehyde), ethyl butyrate, acetoin and vanillin. These volatile compounds could be conducive to distinguishing the *Huangjiu* samples fermented with different rice varieties.

3.6. Correlation analysis between the aroma compounds and sensory attributes in *Huangjiu* samples

To further determine the correlation between the aroma compounds and sensory attributes, and analyze their contributions to the aroma of the *Huangjiu* samples fermented with different rice varieties, PLS regression was performed and the results are shown in Figure 6. The values of cumulated R^2X (0.907) and R^2Y (0.902) corresponding to the relationships between the explanatory variables (X, aroma-active compounds) and dependent variables (Y, intensity of the aromas of the compounds) were close to 1. And the model quality ($Q^2 = 0.701$) was appropriate as $Q^2 > 0.50$, indicating that the correlation between the two variables can be well represented by PLS analysis.

S1 sample was correlated with 'ester', 'alcoholic', 'wheat', 'caramel', 'sauce', 'sweet' and 'sour' aromas, while S2 sample was correlated with 'fruit' aroma. And the volatile compounds ethyl octanoate and 2-octanone were strongly associated with 'sauce', 'caramel', 'wheat' and 'alcoholic' aromas. The 'ester' and 'alcoholic' aromas were strongly associated with most compounds, including ethyl butyrate, 3-penten-2-one, 3-(methylthio)propanal, isoamyl acetate, and so on. Collcetively, most aroma-active compounds were correlated with 'ester' aroma in *Huangjiu* sample fermented with glutinous rice, which was consistent with the results of QDA analysis.

4. Conclusion

The effect of different rice varieties on the taste and aroma characteristics of *Huangjiu* was investigated using dynamic sensory evaluation, GC × GC-qMS and multivariate statistical analysis. The results revealed that the flavor characteristics and profiles of two kinds of *Huangjiu* had remarkable differences. Compared with *Huangjiu* fermented with japonica rice, the tastes of bitter and astringency in *Huangjiu* fermented with glutinous rice were weaker, and the ester and alcoholic aromas were more prominent. Ethyl butyrate, isoamyl acetate, 3–methylthiopropionaldehyde and ethyl caprylate contributed greatly to the flavor of *Huangjiu* sample fermented with glutinous rice, while nonanal, phenyl acetaldehyde and vanillin were the characteristic flavor compounds in *Huangjiu* sample fermented with japonica rice. Furthermore, the total contents of alcohols, acids and aldehydes were higher in the *Huangjiu* sample fermented with glutinous rice, and the important aroma compounds (especially key esters) were more abundant. Correlation analysis further proved that most aroma-active compounds significantly correlated with ester and alcoholic aroma in the *Huangjiu* sample fermented with glutinous rice. The comprehensive analysis of taste and aroma characteristics showed that the *Huangjiu* fermented by glutinous rice had higher flavor quality. Our results would provide a certain guiding effect on the quality control and taste improvement of *Huangjiu*. However, the exact factors that cause the differences in aroma and taste of the two

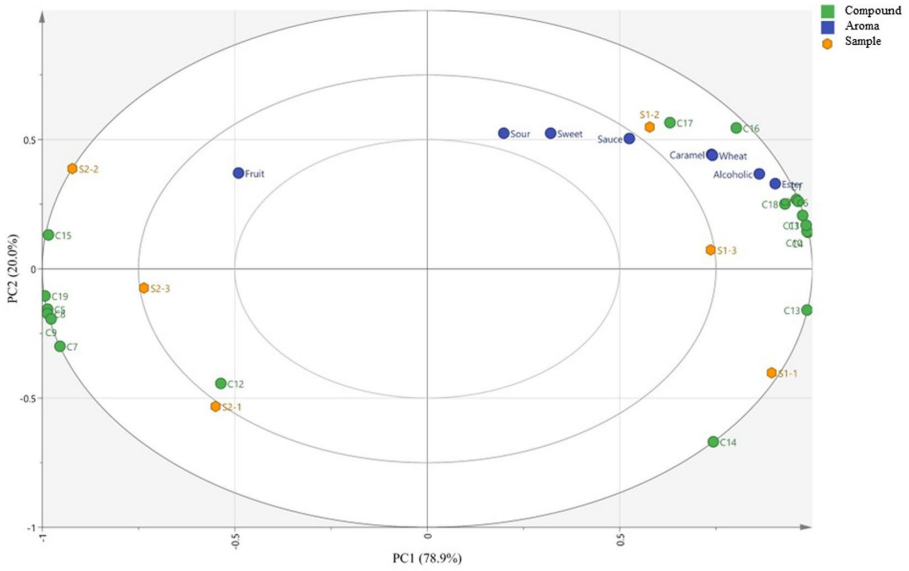

FIGURE 6
Correlation of aromas with aroma-active compounds. Yellow dots represent two *Huangjiu* samples. Blue dots represent 7 aroma attributes. Green dots represent the active-aroma compounds with OAV >1 shown in Supplementary Table S1 (C1: ethyl butyrate, C2: 3-penten-2-one, C3: isoamyl acetate, C4: 1-pentanol, C5: nonanal, C6: butyric acid, C7: γ-nonanolactone, C8: Phenyl acetaldehyde, C9: vanillin, C10: hexanal, C11: sugar lactone, C12: 3-ethoxy-1-propanol, C13: 3-(methylthio)-1-propanol. C14: phenylethyl alcohol, C15: ethyl hexanoate, C16: 2-octanone, C17: ethyl caprylate, C18: 3-(methylthio)propionaldehyde, C19: 2-methylbutyl acetate).

kinds of *Huangjiu* are still unclear, and further research from the microbial perspective is needed.

Data availability statement

The original contributions presented in the study are included in the article/Supplementary material, further inquiries can be directed to the corresponding author.

Author contributions

HY: conceptualization, methodology, formal analysis, resources, writing–original draft, and writing–review and editing. QL: methodology, formal analysis, investigation, and writing–original draft. WG: methodology and formal analysis. LA: resources and supervision. CC: resources, supervision, and project administration. HT: writing–review and editing and project administration. All authors contributed to the article and approved the submitted version.

Funding

The research was supported by the National Natural Science Foundation of China (No. 32172336) and the Capacity Project of Local Colleges and Universities of the Science and Technology Commission of Shanghai, China (No. 21010504100).

Acknowledgments

The authors would like to thank all those who contributed directly or indirectly to the project.

Conflict of interest

The authors declare that the research was conducted in the absence of any commercial or financial relationships that could be construed as a potential conflict of interest.

Publisher's note

Supplementary material

The Supplementary material for this article can be found online at: https://www.frontiersin.org/articles/10.3389/fnut.2023.1160954/full#supplementary-material

References

1. Jiao A, Xu X, Jin Z. Research progress on the brewing techniques of new-type rice wine. *Food Chem*. (2017) 215:508–15. doi: 10.1016/j.foodchem.2016.08.014

2. Ge D, Long X, Yang C, Zhan Z, Guo Z. Comparative study on flavor quality of rice wine made from different raw materials based on electronic nose and GC-MS. *Food Res Dev*. (2019) 40:137–42. doi: 10.3969/j.issn.1005-6521.2019.09.023

3. You H, Mao J, Zhou Z. Characteristics of Chinese rice wine with different varieties of rice. *J Food Sci Biotech*. (2019) 38:39–45. doi: 10.3969/j.issn.1673-1689.2019.03.006

4. Liu S, Chen Q, Zou H, Yu Y, Zhou Z, Mao J, et al. A metagenomic analysis of the relationship between microorganisms and flavor development in Shaoxing mechanized *Huangjiu* fermentation mashes. *Int J Food Microbiol*. (2019) 303:9–18. doi: 10.1016/j.ijfoodmicro.2019.05.001

5. Richter VB, De Almeida TCA, Prudencio SH, De Toledo Benassi M. Proposing a ranking descriptive sensory method. *Food Qual Prefer*. (2010) 21:611–20. doi: 10.1016/j.foodqual.2010.03.011

6. Sudre J, Pineau N, Loret C, Martin N. Comparison of methods to monitor liking of food during consumption. *Food Qual Prefer*. (2012) 24:179–89. doi: 10.1016/j.foodqual.2011.10.013

7. Frost SC, Blackman JW, Ebeler SE, Heymann H. Analysis of temporal dominance of sensation data using correspondence analysis on merlot wine with differing maceration and cap management regimes. *Food Qual Prefer*. (2018) 64:245–52. doi: 10.1016/j.foodqual.2016.11.011

8. Ma X, Sun B, Zhao X. Application of TDS combined with TI sensory evaluation method in acid-reducing mountain wine. *Food Ferment Ind*. (2018) 44:231–5. doi: 10.13995/j.cnki.11-1802/ts.017417

9. Qian M, Tang S, Zhao W, Huang M, Li B. Effects of raw rice on fermentation and γ-aminobutyric acid production of Guangdong Hakka rice wine. *Sci Tech Food Ind*. (2018) 39:15–9. doi: 10.13386/j.issn1002-0306.2018.07.004

10. Shi L, Li A, Mou F, Zhang W. Effects of different millet varieties on flavor of Chinese rice wine. *China Brew*. (2021) 40:54–63. doi: 10.11882/j.issn.0254-5071.2021.03.011

11. Zhao P, Cai J, Gu S, Qian B, Wang L, Lv F, et al. Analysis of Characteristic Flavor Substances of Traditional Shaoxing Rice Wines of Different Ages. *Food Sci*. (2020) 41:231–237. doi: 10.7506/spkx1002-6630-20191021-214

12. Yu H, Xie J, Xie T, Chen C, Ai L, Tian H. Identification of key odorants in traditional Shaoxing-jiu and evaluation of their impacts on sensory descriptors by using sensory-directed flavor analysis approaches. *J Food Meas Charact*. (2021) 15:1877–88. doi: 10.1007/s11694-020-00769-7

13. Song X, Jing S, Zhu L, Ma C, Song T, Wu J, et al. Untargeted and targeted metabolomics strategy for the classification of strong aroma-type baijiu (liquor) according to geographical origin using comprehensive two-dimensional gas chromatography-time-of-flight mass spectrometry. *Food Chem*. (2020) 314:126098. doi: 10.1016/j.foodchem.2019.126098

14. He Y, Liu Z, Qian M, Yu X, Xu Y, Chen S. Unraveling the chemosensory characteristics of strong-aroma type baijiu from different regions using comprehensive two-dimensional gas chromatography–time-of-flight mass spectrometry and descriptive sensory analysis. *Food Chem*. (2020) 331:127335. doi: 10.1016/j.foodchem.2020.127335

15. Zhou Z, Ji Z, Liu S, Han X, Zheng F, Mao J. Characterization of the volatile compounds of *Huangjiu* using comprehensive two-dimensional gas chromatography coupled to time of flight mass spectrometry (GC×GC-TOFMS). *J Food Process Preserv*. (2019) 43:e14159. doi: 10.1111/jfpp.14159

16. Yu H, Xie T, Qian X, Ai L, Chen C, Tian H. Characterization of the volatile profile of Chinese rice wine by comprehensive two-dimensional gas chromatography coupled to quadrupole mass spectrometry. *J Sci Food Agric*. (2021) 99:5444–56. doi: 10.1002/jsfa.9806

17. Yu H, Guo W, Ai L, Chen C, Tian H. Unraveling the difference in aroma characteristics of *Huangjiu* from Shaoxing region fermented with different brewing water, using descriptive sensory analysis, comprehensive two-dimensional gas chromatography–quadrupole mass spectrometry and multivariate data analysis. *Food Chem*. (2022) 372:131227. doi: 10.1016/j.foodchem.2021.131227

18. Yu H, Guo W, Xie J, Ai L, Chen C, Tian H. Evaluation of taste characteristics of chinese rice wine by quantitative description analysis, dynamic description sensory and electronic tongue. *J Food Meas Charact*. (2022) 17:824–35. doi: 10.1007/s11694-022-01637-2

19. Yu H, Xie T, Xie J, Ai L, Tian H. Characterization of key aroma compounds in Chinese rice wine using gas chromatography-mass spectrometry and gas chromatography olfactometry. *Food Chem*. (2019) 293:8–14. doi: 10.1016/j.foodchem.2019.03.071

20. Chen S, Wang D, Xu Y. Characterization of odor-active compounds in sweet-type Chinese rice wine by aroma extract dilution analysis with special emphasis on sotolon. *J Agric Food Chem*. (2013) 61:9712–8. doi: 10.1021/jf402867m

21. Zhu Y, Zhang N, Jiang S, Liu J, Liu Y. The research progress on food umami perception. *J Chinese Inst Food Sci.* Tech. 21. (2021) 21:1–16. doi: 10.16429/j.1009-7848.2021.01.001

22. Van Gemert L. *Compilations of odour threshold values in air, water and other media*. The Netherlands: Oliemans Punter and Partners (2003).

23. Jestrović I, Coyle JL, Sejdić E. Decoding human swallowing via electroencephalography: a state-of-the-art review. *J Neural Eng*. (2015) 12:051001. doi: 10.1088/1741-2560/12/5/051001

24. Poveromo AR, Hopfer H. Temporal check-all-that-apply (TCATA) reveals matrix interaction effects on flavor perception in a model wine matrix. *Foods*. (2019) 8:641. doi: 10.3390/foods8120641

25. Olegario LS, González-Mohino A, Estevez M, Madruga MS, Ventanas S. Impact of 'free-from'and 'healthy choice'labeled versions of chocolate and coffee on temporal profile (multiple-intake TDS) and liking. *Food Res Int*. (2020) 137:109342. doi: 10.1016/j.foodres.2020.109342

26. Hartley IE, Liem DG, Keast R. Umami as an 'alimentary'taste. A new perspective on taste classification. *Nutrients*. (2019) 11:182. doi: 10.3390/nu11010182

27. Liang Z, Su H, Lin X, He Z, Li W, Deng D. Microbial communities and amino acids during the fermentation of Wuyi Hong Qu Huangjiu. *LWT*. (2020) 130:109743. doi: 10.1016/j.lwt.2020.109743

28. Wang C, Chen S, Wang D, Xu Y. Development and validation of a quantitative method for key caramel aroma compound (sotolon) in Chinese rice wine and its contribution to the aroma of Chinese rice wine. *Food Ferm*. Indus. (2021) 44:246–251. doi: 10.13995/j.cnki.11-1802/ts.016909

29. Liu P, Deng Y, Yin J, Chen G, Wang F, Yuan H, et al. Study on quantification of green tea flavor and its correlation with chemical components. *J Chin Inst Food Sci Technol*. (2018) 14:173–81. doi: 10.16429/j.1009-7848.2014.12.029

30. Yu H, Guo W, Xie T, Ai L, Tian H, Chen C. Aroma characteristics of traditional *Huangjiu* produced around winter solstice revealed by sensory evaluation, gas chromatography–mass spectrometry and gas chromatography–ion mobility spectrometry. *Food Res Int*. (2021) 145:110421. doi: 10.1016/j.foodres.2021.110421

31. Wang J, Yuan C, Gao X, Kang Y, Huang M, Wu J, et al. Characterization of key aroma compounds in *Huangjiu* from northern China by sensory-directed flavor analysis. *Food Res Int*. (2020) 134:109238. doi: 10.1016/j.foodres.2020.109238

32. Huang X, Qian M, Ruan F, Li X, Bai W. Research progress of alcohols in Chinese rice wine. *Food Ind*. (2022) 43:237–40.

33. Chen S, Xu Y, Qian MC. Comparison of the aromatic profile of traditional and modern types of Huang Jiu (Chinese rice wine) by aroma extract dilution analysis and chemical analysis. *Flavour Frag J*. (2018) 33:263–71. doi: 10.1002/ffj.3440

34. Fan W, Qian MC. Headspace solid phase microextraction and gas chromatography–olfactometry dilution analysis of young and aged Chinese "Yanghe Daqu" liquors. *J Agric Food Chem*. (2005) 53:7931–8. doi: 10.1021/jf051011k

35. Mao Q, Yu G. Study on the characteristics of different varieties of rice in *Huangjiu* production. *Liquor Making*. (2010) 37:70–3. doi: 10.3969/j.issn.1002-8110.2010.04.027

36. Feng T, Hu Z, Chen L, Chen D, Wang X, Yao L, et al. Quantitative structure-activity relationships (QSAR) of aroma compounds in different aged *Huangjiu*. *J Food Sci*. (2020) 85:3273–81. doi: 10.1111/1750-3841.15421

37. Luo T, Fan W, Xu Y. Characterization of volatile and semi-volatile compounds in Chinese rice wines by headspace solid phase microextraction followed by gas chromatography-mass spectrometry. *J Inst Brew*. (2008) 114:172–9. doi: 10.1002/j.2050-0416.2008.tb00323.x

Frontiers in Nutrition

Explores what and how we eat in the context of health, sustainability and 21st century food science

A multidisciplinary journal that integrates research on dietary behavior, agronomy and 21st century food science with a focus on human health.

Discover the latest Research Topics

See more →

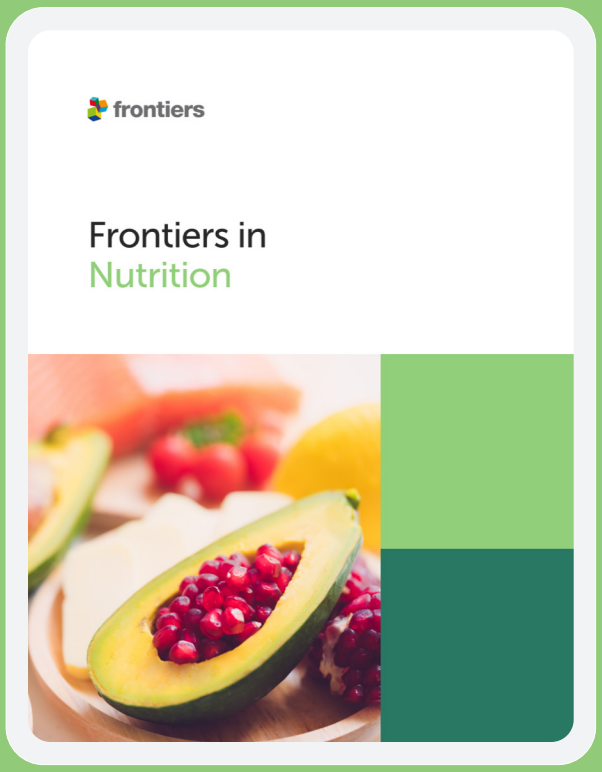

Frontiers

Avenue du Tribunal-Fédéral 34
1005 Lausanne, Switzerland
frontiersin.org

Contact us

+41 (0)21 510 17 00
frontiersin.org/about/contact